Rusty rice

–

Unravelling rice plant and microbial interactions

in the paddy soil iron cycle

Dissertation

der Mathematisch-Naturwissenschaftlichen Fakultät
der Eberhard Karls Universität Tübingen
zur Erlangung des Grades eines
Doktors der Naturwissenschaften
(Dr. rer. nat.)

vorgelegt von
M. Sc. Markus Pascal Maisch
aus Stuttgart

Tübingen
2020

"A scientist in his laboratory is not a mere technician: he is also a child confronting natural phenomena that impress him as though they were fairy tales."

– Marie Curie

Contents

Summary

Paddy fields represent one of the most important agricultural areas and serve more than half of World's population with a major food stock – rice. Iron (Fe) is one of the most abundant redox active metals in paddy soils, mostly present as reduced ferrous iron, Fe(II) or oxidized ferric iron, Fe(III). Water-logged paddy soils, typically depleted in oxygen (O_2), allow Fe to be abundant as mobile and dissolved Fe(II). Rice plants demand Fe as essential micronutrient. However, high uptake of Fe through roots can lead to a toxification and damage the photosystem. In order to control the uptake of Fe, rice plants diffusively release O_2 from their roots by radial oxygen loss (ROL) which locally oxygenates the anoxic paddy soil, oxidizes Fe(II) and forms ferric non-mobile iron plaque minerals on the root surface. The formation of iron plaque on roots not only diminishes the mobility of iron but also serves as an adsorbent for contaminants in paddy fields and can reduce the uptake into rice grains.

Besides rice plants, numerous other chemical and microbial redox processes can impact the speciation and appearance of Fe by the oxidation of Fe(II) and the reduction of Fe(III). This iron redox cycle in paddy soils is coupled to a large variety of other soil element cycles which can influence the fate and the (im)mobilization of many nutrients and contaminants. Representing the bottle neck for a translocation of soil contaminants into the food chain, it is crucial to better understand processes involved in the biogeochemical iron cycle in paddy fields. In particular microaerophilic Fe(II)-oxidizing bacteria that enzymatically couple the oxidation of Fe(II) to the reduction of O_2 under micro-oxic conditions and their role in the paddy field iron cycle remains so far poorly understood. Moreover, a holistic study that quantitatively investigated the spatiotemporal development of root iron plaque and interactions with Fe-cycling bacteria in water-logged paddy soils during plant growth is still lacking. Specifically, the consequences of microbial Fe(III) reduction for root iron plaque minerals to serve as a sink or source for contaminants are so far scarcely documented. In this PhD thesis project, we developed new approaches that allowed a dynamic non-invasive identification of geochemical rhizosphere parameters and a quantification of root iron plaque minerals forming during the growth of rice plants. Further, we derived an enumerative understanding for microbial processes impacting the paddy field iron cycle and contaminant (im)mobility (i.e. arsenic) by Fe(II) oxidation and Fe(III) reduction over the vegetative growth of rice plants.

Although microaerophilic Fe(II)-oxidizing bacteria are found in numerous environments with opposing gradients of O_2 and Fe(II), little is known about their contribution to the oxidative

side of the iron cycle. The rapid autocatalytic oxidation of Fe(II) with O_2 at neutral pH displaces these microorganisms into niches where O_2 concentrations are low enough to compete with the abiotic reaction. Concomitantly, a quantification of microbial Fe(II) oxidation rates in classical microcosms remained challenging, because abiotic and biotic Fe(II) oxidation reactions remained indecipherable so far. In particular the accumulation of ferric (bio)minerals, as a product of (a)biotic Fe(II) oxidation increases the competition by stimulating abiotic surface-catalyzed heterogeneous Fe(II) oxidation rates. In this project, we therefore developed an experimental approach that allows a quantification of microbial and abiotic Fe(II) oxidation rates in the presence or initial absence of ferric (bio)minerals. At dissolved O_2 concentrations of 20 µM O_2 and the initial absence of Fe(III) minerals, an Fe(II)-oxidizing culture (99.6% similarity to *Sideroxydans* spp.), isolated from a paddy field, contributed 40% to the total Fe(II) oxidation within approximately 26 hours and oxidized up to 3.6×10^{-15} mol Fe(II) cell^{-1} h^{-1}. We found that this culture could enzymatically compete with the abiotic Fe(II) oxidation within an optimum range from 5 to 20 µM dissolved O_2. Lower O_2 levels limited the biotic Fe(II) oxidation, while higher O_2 concentrations accelerated the abiotic Fe(II) oxidation which dominated over the microbial impact. Additionally, we could demonstrate that the initial presence of ferric (bio)minerals induced the surface-catalytic heterogeneous abiotic Fe(II) oxidation and reduced the microbial contribution to Fe(II) oxidation from 40% to only 10% at levels with 10 µM O_2. We hypothesize that this newly-developed approach can be used for a large variety of microaerophilic Fe(II)-oxidizing cultures, while the obtained results can help to better assess the impact of microaerophilic Fe(II) oxidation on the biogeochemical iron cycle in numerous environmental natural and anthropogenic settings.

Besides a microbial Fe(II) oxidation, also direct plant-mediated oxidation of Fe(II) by ROL can significantly influence numerous paddy field soil parameters and alter microbial communities. Especially the biogeochemistry of water-logged rice paddies, which are typically characterized by anoxic and reducing conditions, can dramatically be impacted by the temporal oxygenation of the rhizosphere with O_2 from ROL. The local availability of ROL-borne O_2 not only triggers the autocatalytic abiotic oxidation of Fe(II) but also provides the electron acceptor for microaerophilic Fe(II)-oxidizing bacteria. In the rice plant rhizosphere, both processes can contribute to the formation of ferric iron plaque minerals on and around the root surface. However, the identification of potential niches in the rice plant rhizosphere remained speculative so far. In this project, we temporally resolved spatial changes in ROL in the entire rice plant rhizosphere and identified the impact on the redoximorphic paddy soil biogeochemistry. By applying a series of non-invasive techniques in a transparent artificial soil, we could visualize for the first time opposing gradients of O_2 and Fe(II) that extend from

the rice root surface between 10–25 mm into the rhizosphere. This microoxic zone expanded exponentially in size throughout the entire rhizosphere creating optimum niches for microaerophilic Fe(II)-oxidizing bacteria during rice plant growth over 45 days. By non-invasively following and quantifying iron mineral formation, identifying changes in soil pH, and determining Fe(II) oxidation kinetics in the entire rhizosphere, we could demonstrate that root-related ROL induced iron redox transformations on and around the root surface which correlates to an acidification of the rhizosphere. These findings highlight the dynamic nature of roots in the rice plant rhizosphere while this newly-developed combination of methods spatiotemporally resolved their impact on iron redox chemistry and the formation of dynamic niches for microaerophilic Fe(II)-oxidizing bacteria in the rice plant rhizosphere.

Complementing the above-reported studies, we found, that while radial oxygen loss (ROL) is the main driver for rhizosphere iron oxidation, roots tips showed the highest spatio-temporal variation in ROL (<5-50µM) following diurnal patterns. Root iron plaque covered >30% of the total root surface corresponding to 60-180 mg Fe(III) per gram dried root. Moreover, we found that root iron plaque minerals gradually transformed from freshly formed low-crystalline minerals (e.g. ferrihydrite) on root tips, to >20% higher-crystalline minerals (e.g. goethite) within 40 days. A culture of Fe(III)-reducing bacteria (*Geobacter* spp.), isolated from a rice paddy, was capable of remobilizing up to 30% Fe(II) from root iron plaque by reductive dissolution, while >50% iron plaque minerals transformed to Fe(II) minerals (e.g. siderite, vivianite and Fe–S phases) or persisted by >15% as Fe(III) minerals. Based on the obtained data, we estimated that ROL-induced root iron plaque formation and microbial reductive dissolution impact more than 5% of the total rhizosphere iron budget which can severely impact the (im)mobilization of soil contaminants and nutrients.

In this context, it is generally accepted that root iron plaque on rice roots can immobilize As by sorption or coprecipitation which decreases the net uptake into the plant and diminishes its mobility in contaminated soils. However, little is known about the role of bacteria in the reduction of As-bearing Fe(III) plaque minerals or the efficiency of reduced iron plaque in As immobilization. In this project, we demonstrate the formation of secondary root iron plaque minerals (70% siderite, 30% ferrihydrite, Fh & goethite, Gt) during microbial iron plaque reduction, that can immobilize 2.5 times more As than fully oxidized iron plaque (Fh & Gt). By comparing 3 different As-loads in iron plaque minerals, we found that >1mg As per 10 mg iron plaque can negatively affect microbial reduction rates by 50%. During reductive dissolution, As was first remobilized but re-adsorbed onto secondary iron plaque minerals after 7 days. Abiotic reduction of dissolved As(V) occurred on redox-active surfaces of

secondary iron plaque minerals and produced >20% As(III) out of the initial As(V) pool. The later immobilization onto secondary iron plaque minerals was selective for As(V) and increased the relative abundance of As(III) in solution. These findings suggest that the obtained results can help to assess the role of microbial iron plaque reduction and to enumerate the consequences for the fate of As in contaminated paddy fields.

In general, the reported findings in this PhD project identified a series of yet spatio-dynamically unresolved biological mechanisms that influence the iron cycle in rice paddies using newly-developed approaches and combinations of methods. The capability to quantify so far invisible iron redox processes in the entire rice plant rhizosphere and to decipher the role of microaerophilic Fe(II)-oxidizing and Fe(III)-reducing microorganisms provides a novel vision on the paddy soil biogeochemical iron redox cycle in which highly spatio-dynamic physico-chemical features can control the (im)mobility of iron, nutrients and contaminants. Overall, this PhD project provides a tangible example that yet invisible processes can be visualized by developing and combining classical and state-of-the art techniques.

Zusammenfassung

Reisfelder stellen eines der weltweit wichtigsten Agrargebiete dar und versorgen mehr als die Hälfte der Weltbevölkerung mit einem der wichtigsten Nahrungsmittel - Reis. Eisen (Fe) ist eines der am häufigsten vorkommenden redoxaktiven Metalle in Reisfeldböden. Meist liegt es als reduziertes Eisen (Fe(II)) oder oxidiertes Eisen (Fe(III)) vor. In wassergesättigten Reisfeldböden, die typischerweise frei von Sauerstoff (O_2) sind, liegt Fe in seiner mobilen und gelösten Form als Fe(II) vor. Eisen stellt einerseits einen essentiellen Mikronährstoff für Reispflanzen dar. Eine zu hohe Eisenaufnahme über die Wurzeln kann jedoch zu einer Vergiftung führen und das Photosystem schädigen. Um die Aufnahme von Fe zu kontrollieren, können Reispflanzen O_2 über die Wurzeln abgeben an den Boden abgeben. Dieser Prozess wird Radial Oxygen Loss (ROL) genannt. Durch ROL wird der Boden mit O_2 angereichert, Fe(II) oxidiert und fällt auf der Wurzeloberfläche aus und wird als Eisen-Plaque-Minerale abgelagert. Die Bildung von Eisenplaque an den Wurzeln verringert nicht nur die Mobilität des Eisens, sondern dient auch als Adsorptionsmittel für Schadstoffe in Reisfeldern und kann deren Aufnahme in die Reiskörner verringern.

Neben Reispflanzen können zahlreiche andere chemische und mikrobielle Redox-Prozesse die Speziation von Fe durch die Oxidation von Fe(II) und die Reduktion von Fe(III) beeinflussen. Dieser Eisen-Redox-Kreislauf in Reisböden ist an eine Vielzahl anderer Bodenelementkreisläufe gekoppelt, die die (Im)mobilisierung vieler Nähr- und Schadstoffe beeinflussen können. Insbesondere mikroaerophile Fe(II)-oxidierende Bakterien, die die Oxidation von Fe(II) enzymatisch an die Reduktion von O_2 koppeln, spielen bei der Oxidation von Fe(II) eine wichtige Role. Ihr Einfluss auf den Eisenkreislauf in Reisfeldern ist bisher jeodch nur unzureichend verstanden. Darüber hinaus fehlt noch immer eine ganzheitliche Studie, die die räumlich-zeitliche Entwicklung von Eisenplaque an Reiswurzeln und die Wechselwirkungen mit Bodenbakterien in wassergesättigten Reisfeldern während des Pflanzenwachstums quantitativ untersucht. Insbesondere ist der Einfluss von mikrobieller Fe(III)-Reduktion auf die Mineralogie von Eisenplaque, welche als Senke oder Quelle für Schadstoffe fungieren kann, bisher kaum dokumentiert. In diesem Dissertationsprojekt haben wir neue Ansätze entwickelt, die eine dynamische, nicht-invasive Identifizierung von geochemischen Rhizosphärenparametern und eine Quantifizierung der Eisenminerale, die während des Wachstums von Reispflanzen gebildet werden, ermöglichen. Darüber hinaus leiteten wir Einflussgrößen mikrobieller Prozesse ab, die den Eisenkreislauf in Reisfeldböden

und die (Im)mobilisierung von Schadstoffen, wie etwa Arsen, durch Fe(II)-Oxidation und Fe(III)-Reduktion während des vegetativen Wachstums von Reispflanzen beeinflussen.

Obwohl mikroaerophile Fe(II)-oxidierende Bakterien in verschiedensten Ökogebieten, die durch entgegengesetzte Gradienten an O_2 und Fe(II) geprägt sind, identifiziert wurden, ist wenig über ihren Einfluss auf den Eisenzyklus bekannt. Die schnelle Oxidation von Fe(II) mit O_2 unter neutralen pH-Wert Bedingungen verdrängt diese Mikroorganismen in Nischen, in denen die O_2 Konzentrationen niedrig genug sind, um mit der abiotischen Reaktion zu konkurrieren. Eine Quantifizierung der mikrobiellen Fe(II)-Oxidationsraten in klassischen Mikrokosmen stellt weiterhin eine Herausforderung dar, da abiotische und biotische Fe(II)-Oxidationsreaktionen bisher nicht separat quantifizierbar waren. Insbesondere die Akkumulation von Fe(III) (Bio)mineralen als Produkt der (a)biotischen Fe(II)-Oxidation steigert den Konkurrenzdruck auf die Bakterien durch die Beschleunigung abiotischer oberflächenkatalysierter heterogener Fe(II)-Oxidationsraten. In diesem Projekt wurde daher ein experimenteller Ansatz entwickelt, der eine Quantifizierung der mikrobiellen und abiotischen Fe(II)-Oxidationsraten ermöglicht. Bei O_2 Konzentrationen von 20 µM O_2 und der anfänglichen Abwesenheit von Fe(III)-Mineralien konnten mikroaerophile Bakterien (99,6% Ähnlichkeit mit *Sideroxydans* spp.), welche aus einem Reisfeld isoliert wurden, innerhalb von etwa 26 Stunden mit bis zu 40% zur gesamten Fe(II)-Oxidation beitragen. Eine Zelle oxidierte hierbei bis zu $3{,}6 \times 10^{-15}$ mol Fe(II) pro Stunde. Bei O_2 Konzentrationen von 5 bis 20 µM war der biologische Fe(II) Umsatz am höchsten, während niedrigere O_2 Konzentrationen die biologische Fe(II)-Oxidation hemmten. Höhere O_2-Konzentrationen beschleunigten wiederum die abiotische Fe(II)-Oxidation, die ab 30 µM O_2 über die mikrobielle Fe(II)-Oxidation dominierte. Zusätzlich konnte gezeigt werden, dass Fe(III)-(Bio)minerale die oberflächenkatalytische heterogene abiotische Fe(II)-Oxidation induzieren und den mikrobiellen Einfluss auf Fe(II)-Oxidation von 40% auf nur 10% reduzieren. Dieser neu entwickelte Ansatz kann für die Kultivierung verschiedenster mikroaerophiler Kulturen Verwendung finden und dabei helfen mikrobielle Fe(II) Umsatzraten zu ermitteln. Die Ergebnisse können dann dazu beitragen, die Auswirkungen der mikroaerophilen Fe(II)-Oxidation auf den biogeochemischen Eisenzyklus in zahlreichen natürlichen und anthropogenen Ökosystemen besser einzuschätzen.

Neben der mikrobiellen Fe(II)-Oxidation kann die Reispflanze selbst durch die Oxidation von Fe(II) mittels ROL zahlreiche Bodenparameter beeinflussen und mikrobielle Gemeinschaften verändern. Die O_2 Abgabe über die Wurzeln führt nicht nur zur chemischen Oxidation von Fe(II), sondern kann auch von zum Beispiel mikroaerophilen Fe(II)-oxidierenden Bakterien als

den Elektronenakzeptor benutzt werden. In der Rhizosphäre der Reispflanze können so sowohl mikrobielle als auch chemische Prozesse zur Bildung von Eisenmineralen auf und um die Wurzeloberfläche beitragen. Die Identifikation von potentiellen Nischen für mikroaerophile Fe(II)-oxidierende Bakterien in der Rhizosphäre von Reispflanzen blieb jedoch bisher aus. Im Rahmen dieser Dissertation wurden die räumliche Ausdehnung von ROL an Reiswurzeln währen des Wachstums von Reispflanzen zeitlich hochaufgelöst quantifiziert und dessen Einfluss auf andere Bodenparameter identifiziert. Durch die Anwendung nicht-invasiver Techniken in transparenten künstlichen Böden konnte so zum ersten Mal festgestellt werden, dass sich gegengesetzte Gradienten an O_2 und Fe(II) rund um die Wurzeloberflöche ausbilden, welche sich von der Oberfläche der Reiswurzel bis zu 10-25 mm in die Rhizosphäre erstrecken. Diese mikrooxische Zone dehnte sich in der gesamten Rhizosphäre exponentiell aus und schuf optimale Nischen für mikroaerophile Fe(II)-oxidierende Bakterien. Durch die nicht-invasive Quantifizierung von Eisenmineralen, der Identifikation von Boden-pH-Wert Veränderungen und dem Bestimmen der Fe(II)-Oxidationskinetik in der gesamten Rhizosphäre, konnten abschließend festgestellt werden, dass ROL maßgeblich die Bildung von Eisenplaque und lokale pH-Wert Veränderungen steuert. Die gesammelten Ergebnisse unterstreichen die dynamischen geochemischen Wechselwirkungen an Reiswurzeln, während die neu entwickelten Methoden dazu beitragen können, den räumlich und zeitlich hoch dynamischen Eisenkreislauf in der Rhizosphäre zu verfolgen.

Ergänzend wurde festgestellt, dass Wurzelspitzen die mitunter höchste Variation an lokalen O_2 Konzentrationen aufweisen. Radial oxygen loss führte hier zu tageszeitlichen Schwankungen der O_2 Konzentrationen zwischen 5-50 µM O_2. Die gesamte Wurzelmasse wurde hierbei zu etwa 30% mit Eisenplaque bedeckt, was 60-180 mg Fe(III) pro Gramm getrockneter Wurzel entspricht. Darüber hinaus wurde festgestellt, dass sich die Mineralogie der Eisenplaqueminerale während des Pflanzenwachstums veränderte. Innerhalb von 40 Tagen wurden frisch gebildete niedrigkristalline Eisenminerale (z.B. Ferrihydrit) an den Wurzelspitzen in höherkristalline Eisenminerale (z.B. Goethit) umgewandelt. Eisen(III)-reduzierende Bakterien (*Geobacter* spp.), waren hierbei in der Lage, bis zu 30% Fe(II) durch reduktive Auflösung von Eisenplaque zu remobilisieren. Mehr als 50% der Eisenplaqueminerale haben sich in Fe(II)-Minerale (z.B. Siderit, Vivianit und Fe-S-Phasen) umgewandelt während etwa 15% als Fe(III)-Mineralien zurückblieben. Auf der Grundlage gesammelter Daten konnte abschließend quantitativ festgestellt werden, dass die ROL-induzierte Bildung von Eisenplaque an der Wurzel und die mikrobielle reduktive Auflösung mehr als 5% des gesamten Eisenhaushalts der Rhizosphäre beeinflussen, was Auswirkungen

auf die (Im-)mobilisierung von beispielsweise Bodennährstoffen und Schadstoffen haben kann.

In diesem Zusammenhang ist es allgemein anerkannt, dass die Eisenminerale auf Reiswurzeln Schadstoffe, wie beispielsweise Arsen (As) durch Sorption oder Komplexierung immobilisieren können. Das verringert nicht nur die Nettoaufnahme in die Pflanze, sondern vermindert auch deren Mobilität in kontaminierten Böden. Wenig ist jedoch über die Auswirkungen von Fe(III)-reduzierenden Bakterien auf die Schadstoff-Immobilisierungskapazität von Eisenplaque-Mineralen an Reiswurzeln bekannt. Im Rahmen dieser Dissertation wurde die Bildung von sekundär gebildeten Eisenmineralen (70% Siderit, 30% Ferrihydrit, Fh & Goethit, Gt) als Produkt der mikrobiellen Eisenplaque-Reduktion identifiziert. Diese mikrobiell reduzierten Eisenplaqueminerale immobilisierten bis zu 2,5-mal mehr As, als vollständig oxidierte Eisenplaqueminerale (Fh & Gt). Bei Untersuchungen mit 3 verschieden hohen As-Konzentrationen in Eisenplaque, wurde festgestellt, dass >1 mg As pro 10 mg Eisenplaque die mikrobielle Reduktionsrate um 50% negativ beeinflusst. Während der reduktiven Auflösung von Eisenplaque wurde As zunächst remobilisiert, aber nach etwa 7 Tagen wieder an sekundär gebildete Eisenplaqueminerale adsorbiert. Etwa 20% des ursprünglichen Arsen(V) wurden an der redoxaktiven Oberfläche der sekundären Eisenplaqueminerale zu As(III) reduziert. Die Immobilisierung auf sekundären Eisenplaquemineralen war selektiv für As(V) und erhöhte den relativen Massenanteil von As(III) in Lösung. Diese Beobachtungen helfen dabei, den Einfluss mikrobieller Fe(III)-Reduktion und deren Auswirkungen auf die Schadstoff-(Im)mobilisierung in belasteten Reisfeldböden abzuschätzen.

Ermöglicht wurden die im Rahmen dieser Doktorarbeit zusammengestellten Beobachtungen durch neu entwickelte Ansätze und Methodenkombinationen. Die Möglichkeit, bisher unsichtbare Eisen-Redox-Prozesse in der gesamten Rhizosphäre der Reispflanze zu quantifizieren und den Einfluss mikroaerophiler Fe(II)-oxidierender und Fe(III)-reduzierender Mikroorganismen zu entschlüsseln, ermöglicht eine neue Sicht auf den biogeochemischen Eisen-Redox-Zyklus in wassergesättigten Reisfeldböden. Das Wechselspiel zwischen Pflanzen, Bodenorganismen und Parametern beeinflusst nicht zuletzt die physikalisch-chemischen Eigenschaften von Eisenplaquemineralen, welche wiederum die Verfügbarkeit von Bodennährstoffen und die (Im)mobilität von Schadstoffen steuern kann.

1 Introduction

1.1 Rice plant cultivation and the impact on paddy field iron biogeochemistry.

Only around 10% of the World's surface is covered with a complex mixture of minerals, water, air, organic compounds, and endless organisms that are living on the heritage of other organisms decaying in it – soils.[1,2] Nonetheless, these 10% probably represent one of the most vulnerable parts of the Earth's surface and are therefore often referred to as Geoderma – the skin of the Earth.[3] Soil environments are the most divers ecosystems on planet Earth and can be regarded as complex and interactive bioreactors.[4] Besides minerals, organic matter and water, they consist of a huge variety of micro- and macroorganisms such as soil bacteria, soil fauna and plants. Each of these components is characterized by its own complexity and represents a complete biosystem on its own. However, the functioning of the Earth's skin does not rely on single individual components but rather works as a huge network with endless interactions between each soil compartment. These interactions need to remain intact to sustain a healthy soil environment.[2]

Humans learned to use Earth's soil to sustain their life on Earth. The development of controlled agriculture to provide food stock to billions of humans was one major step towards the evolution of modern civilizations. One of the oldest civilizations on Earth is rooted in China. Along the Yangtze and Huai rivers, the use of paddy soils for the cultivation of agricultural goods dates back more than 9,000 years.[5] But still today, the cultivation of plants on paddy soils serves more than half of World's population and covers almost 20% of the daily needs in calories for humans worldwide with a major food stock – rice.

Nowadays, the extensive cultivation of rice plants on water-logged paddy soils impacts a large variety of other environmental processes. Ranging from the emissions of greenhouse gases, such as methane or nitrous oxides,[6-10] fertilization and intensified use of modern agricultural techniques lead to significant changes in soil redox conditions.[11-13] Soil redox conditions in turn determine the speciation and bioavailability of metals and nutrients that are on the one hand essential for cultivated rice plants and the quality of produced rice grains,[14,15] On the other hand, soil redox conditions also severely impact the (im)mobility and phytotoxicity of dissolved metals and potential contaminants in paddy fields.[16,17]

In this context, iron (Fe) needs to be mentioned as one of the most abundant redox-active elements in the Earth's crust and as an essential micronutrient to all organisms living

in soils.[18,19] Iron is mainly present in soils in two redox states, as reduced iron (Fe(II)) or in its oxidized form as Fe(III).[20] Water-logged paddy soils are predominantly characterized by reducing conditions.[21] Catalyzed by iron-sulfur minerals or different types of organic compounds, Fe(III) can be abiotically reduced and persist in its more mobile form Fe(II) under anoxic conditions.[21,22] Moreover, also microbial processes are continuously fueling the pool of Fe(II) by microbial Fe(III) reduction.[23,24] Both processes typically lead to elevated concentrations of Fe(II) in these water-logged paddy fields. The bioavailability of dissolved Fe(II) is essential for rice plants and the functioning of an intact photosystem in plants.[20] However, the extensive uptake of dissolved Fe(II) through roots results in the formation of oxygen radicals in the plant tissue.[25] These radicals oxidize membrane lipids in the photosystem and degrade proteins in the leaf tissue which consequently leads to a phenomenon called leaf bronzening – a sign for a toxification of the plant.[26]

Rice plants and numerous other wetland plants have evolved a strategy to control the uptake of soil-borne Fe(II) and to reduce the toxic effect. These plants form an aerenchymatous tissue inside the stem and roots. The sponge- and channel-like structure of this aerenchymatous tissue allows gas diffusion and therefore serves as a conductor for gas exchange between the oxic atmosphere and the anoxic paddy soil.[27,28] Gas molecules, such as oxygen (O_2) from oxygenic photosynthesis or the atmosphere, can laterally diffuse through the aerenchymatous plant tissue and are exuded radially outwards trough the root surface into the anoxic soil, due to an O_2 concentration gradient between root and soil.[27] This process was observed in numerous wetland plants and has been described as radial oxygen loss (ROL) from roots.[29,30] Moreover, it was observed that ROL locally increases O_2 concentrations in the soil and raises redox conditions around the roots. Under oxic conditions and at circum-neutral pH, Fe(II) is thermodynamically instable and becomes rapidly oxidized by O_2 to form Fe(III).[31,32] Due to the low solubility of Fe(III) at circum-neutral pH conditions, Fe(III) (oxyhydr)oxides form and precipitate along the root surface as iron minerals (Figure 1).[33] The formation of thick iron-rich mineral precipitates on roots of wetland plants has been described as root iron plaque.[34-36]
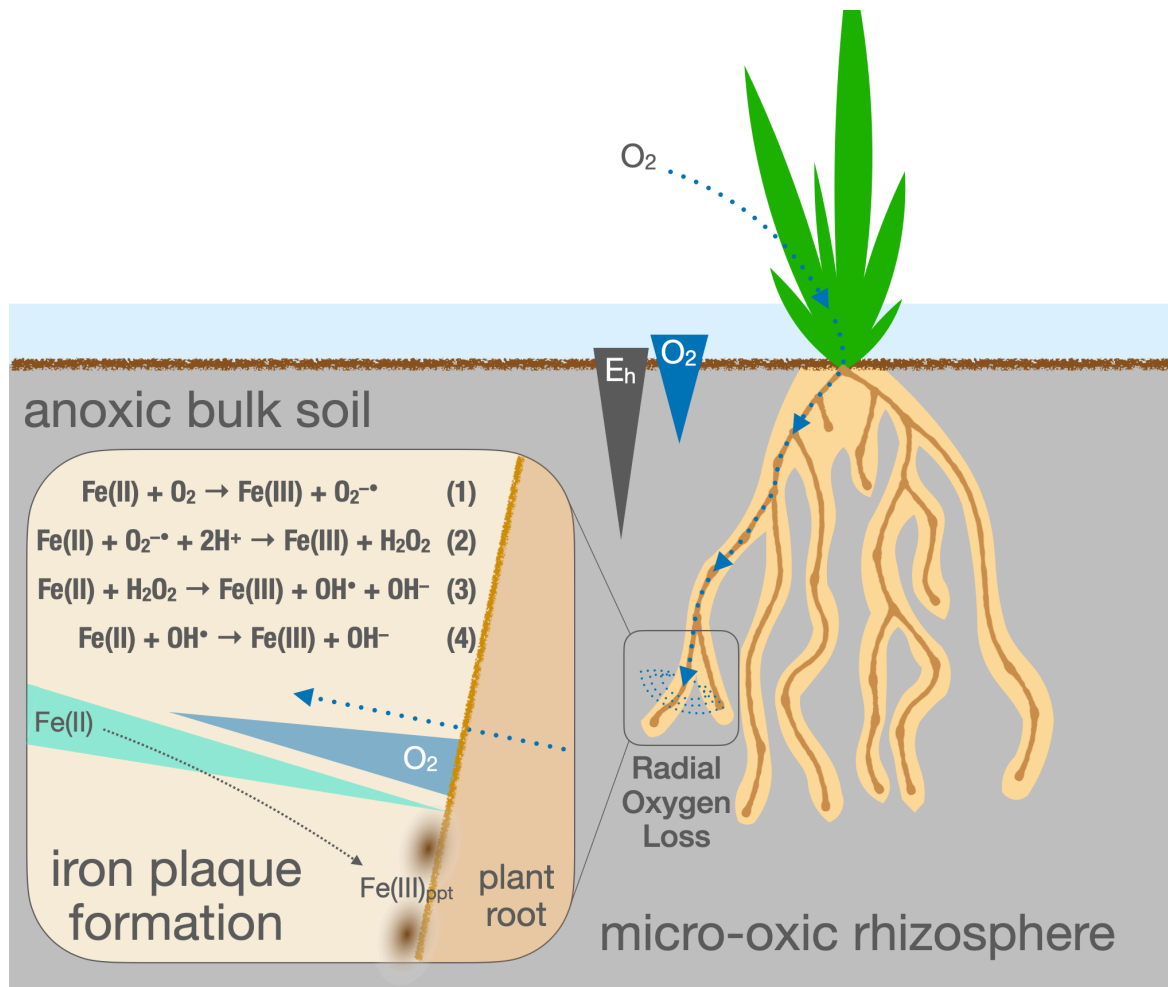
Figure 1 – Schematics on root iron plaque formation. Oxygen is passively transported through the rice plant aerenchymatous tissue and diffusively released from roots by radial oxygen loss (ROL). Under micro-oxic conditions around roots and at circum-neutral pH, soil-borne Fe(II) is rapidly oxidized by O_2 or reactive oxygen species (ROS) such as superoxide, ($O_2^{-\bullet}$), hydrogen peroxide (H_2O_2) or hydroxyl radicals ($OH^\bullet$) (eq. 1-4) which are produced during the stepwise reduction of O_2. Formed Fe(III) consequently precipitates as Fe(III) (oxyhydr)oxides on the root surface as root iron plaque.

Over the last decades, intensive fertilization and the extended use of contaminated water for paddy field irrigation resulted in a dramatic increase in concentrations of heavy metal(loid)s, such as cadmium (Cd) and arsenic (As) in paddy soils.[37,38] Especially in Southeast Asia, As from geogenic origin contaminated the groundwater which is used for paddy field irrigation.[37,39] To date, As concentrations in the soil pore water on contaminated fields exceed the guidelines of the World Health Organization (WHO) for safe limits of drinking water often by a factor of 100.[38, 40, 41] The translocation of contaminants from paddy soil to rice grains was shown to not only negatively impact the vitality of rice plants but also to possess a risk to human health.[41-43] Several studies therefore focused on the fate of As in paddy fields and potential pathways for As uptake into rice plants. In some studies, it has been evidently shown

that the formation of root iron plaque minerals can reduce the uptake of As into the plant.[44,45] Moreover, it has been demonstrated that a large variety of (heavy) metals, such as zinc (Zn), copper (Cu), lead (Pb) and even uranium (U) accumulated in the root iron plaque minerals of rice plants.[46] These studies concluded that a large number of these metal(loid)s form complexes with the iron plaque minerals or adsorb to the mineral surface and are conclusively immobilized in the rhizosphere.[16,47-49] In other words, the high specific surface area of these ferric iron plaque minerals acts as a physical barrier for contaminants, lowers the local concentration of heavy metals in the surrounding soil and suppresses their uptake into the plant roots by sorption processes. In fact, these effects were shown to lower As concentrations in rice grains growing on contaminated paddy fields, thus reducing the potential risk to human health.[50,51]

1.2   The impact of microbial activity on iron cycling in the paddy field rhizosphere.

To date, numerous microorganisms in paddy soils have been described that can influence the iron budget in soils by microbial Fe(II) oxidation or Fe(III) reduction.[22,52] Fe(III)-reducing bacteria have been found in a large variety of environments. Besides microorganisms that couple the oxidation of methane (CH_4) to the reduction of Fe(III).[53] the most prominent representatives in paddy soils were identified as *Shewanella* spp. and *Geobacter* spp.. These Fe(III)-reducing bacteria were shown to generate metabolic energy by coupling the oxidation of organic substrates such as lactate or acetate to the reduction of Fe(III) (Figure 2).[54,55] Due to the low solubility of Fe(III) at circum-neutral pH conditions,[33] these strains had to evolve strategies to enhance electron transport to their metabolic ferric substrate. These include direct electron transfer from cells that are in contact with the iron mineral surface,[56,57] the use of naturally-abundant electron-shuttling compounds like humic substances,[58,59] or the use of excreted redox-active substances.[60] Recently, also Fe(III)-reducing bacteria have been described that are capable of donating electrons to Fe(III) minerals by the extension of nano-wires or pilis.[61,62,63]

All these were shown to facilitate the cell–Fe(III) mineral electron transport and enable the cells to conserve metabolic energy.[60,64] Moreover, it has been shown that these microorganisms are able to mobilize nutrients from stable minerals by releasing protons and organic acids, which dissolve poorly-crystalline iron minerals and particles.[65] During the microbial reduction and consequent dissolution, so called reductive dissolution of Fe(III) minerals, a large quantity of dissolved Fe(II) can be remobilized into the pore water (Figure 2).[65] Dissolved Fe(II) can either remain in solution as hydrolyzed species,[31] be organically-complexed,[66] adsorbed and incorporated into remaining Fe(III) minerals and form mixed-

valent Fe(II)/Fe(III) minerals[67,68] or precipitate as newly-formed Fe(II) minerals.[23] In general, Fe(III)-reducing bacteria have been recognized as one of the main drivers for the recharge of dissolved Fe(II) in anoxic paddy fields and their activity was found to be considerably enhanced by the presence of organic substrates (e.g. fatty acids) and the availability of electron shuttling compounds such as humic substances or flavins,[69,70] both reported to be present at high concentrations and bioavailable in water-logged paddy fields.[11,54]

On the contrary, a variety of microorganisms has been identified that considerably contribute to the oxidation of the Fe(II) pool in soil systems. Under anoxic conditions, and if nitrate is present, nitrate-dependent Fe(II) oxidation was described as a dominant microbial pathway affecting the oxidative side of the paddy soil iron cycle.[71] These bacteria were found to couple the reduction of nitrate to the oxidation of Fe(II).[72] Anoxygenic phototrophic Fe(II) oxidation was hypothesized to be relevant only in the sunlit surface of water-logged paddy soil.[54] Whereas, under oxic and circum-neutral pH conditions, microaerophilic Fe(II)-oxidizing bacteria couple the reduction of O_2 to the oxidation of Fe(II) to conserve metabolic energy (Figure 2).[73] Besides *Sideroxydans* spp., *Gallionella* spp. was described as the most popular representative among microaerophilic Fe(II)-oxidizing bacteria in paddy fields.[74] However, at circum-neutral pH and atmospheric O_2 concentrations, the abiotic oxidation of dissolved Fe(II) proceeds rapidly and kinetically outcompetes aerobic microbial Fe(II) oxidation.[22,75]

Typically, these microaerophilic Fe(II)-oxidizing microorganisms find their optimum conditions in environmental niches where O_2 concentrations are sufficiently low to slow down the abiotic oxidation reaction which increases the persistence of dissolved Fe(II) and increases the availability for bacteria.[76-78] Such conditions were described in the environment in systems with opposing gradients of dissolved Fe(II) and O_2, such as in the transition zone between anoxic and oxic sediments,[79] at deep sea vents[80] or in groundwater seeps.[81] But also the rhizosphere of wetland plants was found to serve as suitable habitat for microaerophilic Fe(II)-oxidizing bacteria.[82,83] In particular, a narrow zone around the roots of wetland plants with steep opposing gradients of O_2 from ROL and Fe(II) from the soil matrix was hypothesized to represent optimum conditions for microaerophilic Fe(II)-oxidizing bacteria to compete with abiotic oxidation kinetics and successfully conserve metabolic energy (Figure 2).[84,85]
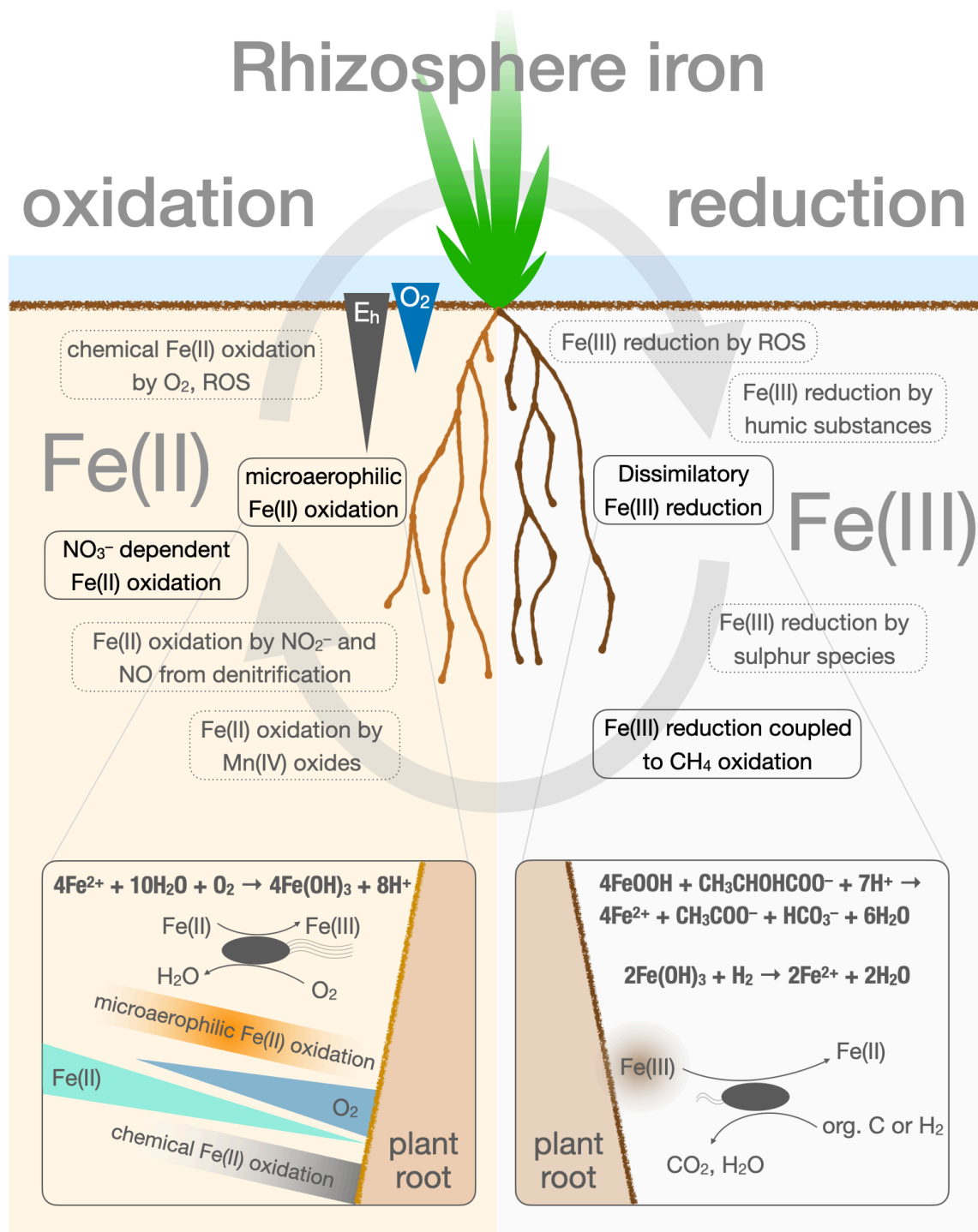
Figure 2 – Overview on chemical and microbial processes interacting with iron cycling in the rhizosphere of water-logged paddy soils. Left side represents biological (plain) and chemical (grey) processes contributing to the oxidation of Fe(II) in the rice plant rhizosphere. Microaerophilic Fe(II) oxidation (left box) is proposed to enzymatically couple the oxidation of soil Fe(II) to the reduction of O_2 from ROL, forming Fe(III) biominerals. Right side represents biological (plain) and chemical (grey) processes contributing to the reduction of Fe(III). Microbial Fe(III) reduction (right box) is proposed to couple the reduction of root Fe(III) plaque minerals to the oxidation of organic substrates or hydrogen (H_2), releasing Fe(II) from root iron plaque during reductive dissolution

1.3 Rhizosphere trinity: plant – microbes – iron minerals.

A narrow region within the soil, in which the chemistry, microbiology and numerous other biogeochemical factors are influenced by the growth, respiration and nutrient exchange of plant roots, is called the rhizosphere.[86] The biogeochemical interplay in the rhizosphere of a paddy field is governed by a complex and interacting trinity of the plant, the organisms associated with the root and physico-chemical soil parameters.[87] Rice plants exert a strong control over the local soil geochemistry within the rhizosphere.[32] The release of O_2 by ROL, formation of iron plaque, the excretion of root exudates and other chelating compounds alter soil redox conditions, influence the rhizosphere iron speciation and affect the microbial rhizosphere community.[88-90] In particular the distribution of O_2 was in the focus of numerous studies investigating rhizosphere processes with regards to iron plaque formation.[35,91,92] Often, highest rates in ROL were detected at the root tips of rice plants, hypothesized to protect sensitive root tips from reduced compounds and the formation of radicals.[32] However, root iron plaque formation only barely precipitated in this redox-active zone around the tip of roots, but rather formed around mature roots at the oxic/anoxic interface of the soil.[45] Moreover, ROL was described to be highly dynamic during the different growth stages of the plant. In particular during the vegetative stage of the growth period, the encapsulation of roots by thick iron plaque precipitates was observed to correlate with ROL from mature roots.[93,94] Towards the end of the growing cycle, however, ROL was shown to diminish and cease completely with the beginning of the flowering and ripening stage of the rice plant.[95,96]

These dynamic changes in redox conditions were expected to impact the mineralogy of iron minerals on the roots which was of a major interest to many studies, since it was generally expected that the iron plaque mineralogy ultimately affects the retention of soil contaminants.[48,97,98] Among poorly-crystalline ferrihydrite ($Fe(OH)_3$), lepidocrocite (γ-FeOOH) and higher-crystalline goethite (α-FeOOH) as pure Fe(III) minerals, also Fe(II) minerals such as siderite ($FeCO_3$) and vivianite ($Fe_3(PO_4)_2$) were found to be abundant as root iron plaque minerals as well as a variety of mixed-valent iron minerals such as magnetite (Fe_3O_4).[36,45,99,100]

From these findings, it has been concluded that the presence of Fe(II) minerals indicated the activity of Fe(III)-reducing bacteria in the paddy soil and redox interactions with root iron plaque minerals.[101] Moreover, it was hypothesized that root exudates (e.g. fatty acids) and freshly precipitated poorly crystalline iron plaque minerals represent ideal substrates to attract Fe(III) reducing bacteria in the root environment.[101-104] This hypothesis was confirmed by findings from Weiss et al., (2003) who found a significantly higher number of Fe(III)-reducing bacteria in the rhizosphere of wetland plants compared to bulk soil. Ultimately demonstrated Hori et al., (2010) that *Geobacter* species actively contribute to Fe(III)

reduction to a large extent which suggested that these bacteria are capable of root iron plaque reduction in paddy fields.[24] As a consequence, investigations shifted towards an understanding of the microbial impact on root iron plaque formation and mineral transformation during Fe(III) reduction. Also, in the context of contaminant (im)mobilization, studies found that microbial root iron plaque reduction and reductive dissolution can ultimately remobilize adsorbed contaminants into the rhizosphere.[97,101,105] diminish the functioning of root iron plaque as physical barrier for contaminants such as As and consequently facilitate the translocation of soil-borne As into rice grains.[49,96]

Over the last decades, intensive research increased the understanding of Fe(III)-reducing bacteria and their impact on the rhizosphere iron cycle.[70,106] Fe(III) reduction rates as well as the physical characterization are well described for a large variety of Fe(III)-reducing organisms in paddy soils.[24,107,108] However, their exact impact on root iron plaque mineral (trans)formation and their extent in iron and contaminant remobilization from iron plaque still remains scarcely documented.[49,97] One of the largest research gaps remains in the understanding of their role in closing the rhizosphere iron cycle between root iron plaque minerals and the pool of dissolved Fe(II) in paddy fields. So far, the knowledge about iron mineralogical transformation products during a microbial reduction of root iron plaque is lacking in an enumerative understanding of iron remobilization and iron mineral identification, which calls for further investigation.[109,110] Especially with regards to contaminant (im)mobility in paddy fields, the understanding on how contaminants in root iron plaque influence microbial Fe(III) reduction and vice versa is crucial to fully decipher the fate of metal(loid)s such as As in these systems.[38,40,49,105,109,111]

On the oxidative side of microbial interactions with the iron cycle in the paddy field rhizosphere, microaerophilic Fe(II)-oxidation was suggested to represent a potential key player in biological Fe(II) oxidation.[70,112] One of the first isolated neutrophilic microaerophilic Fe(II)-oxidizing cultures was collected from the root surface of a wetland plant almost entirely covered in iron plaque precipitates.[73,84] The postulated hypothesis, the steep gradient of ROL and soil-borne Fe(II) created favoring conditions for microaerophilic Fe(II)-oxidizing bacteria, was supported by Weiss et al., (2003). They found a significantly higher number of microaerophilic Fe(II)-oxidizers in the rhizosphere over bulk soil and suggest a microbial rhizosphere iron cycle in wetlands such as paddy fields.[70] However, only a few studies really focused on a potential contribution of microaerophilic Fe(II)-oxidizing bacteria to the formation of ferric iron minerals in the environment.[112-114] So far, only Neubauer et al. (2007) showed in a bioreactor experiment which contained microaerophilic Fe(II)-oxidizing bacteria (isolated from a wetland plant rhizosphere) that microbial Fe(II) oxidation can contribute by 18 – 35%

to the total iron oxidation in a wetland plant rhizosphere.[115] In doing so, microaerophilic Fe(II) oxidation should theoretically have the potential to contribute to root iron plaque formation on rice roots to a large extent.[83] Undoubtedly, understanding their role in iron plaque formation could also have significant implications for the retention of contaminants in polluted paddy fields.

However, the real extent in microaerophilic Fe(II) oxidation in contributing to root iron plaque formation still remains very speculative so far.[112] A large variety of microaerophilic Fe(II)-oxidizing bacteria has been isolated in gradient-based culturing techniques that resemble natural habitats.[73,77,79,116] In all these, a quantification of microbial Fe(II) oxidation rates is challenging due to the simultaneous chemical oxidation reaction that masks the biological impact.[22] Only a few numbers on microaerophilic Fe(II) oxidation rates have been reported, with a minor proportion quantifying microaerophilic Fe(II) oxidation in paddy fields.[82] The speculated hot spot for microaerophilic Fe(II)-oxidizers along the roots of rice plants has neither been identified nor followed by an investigation of spatio-temporally dynamic geochemical gradients in the rice plant rhizosphere so far.[94,117] Without that, it remains still unclear i) how microaerophilic Fe(II) oxidation can find environmental niches in an otherwise anoxic environment and ii) under which circumstances microbial oxidation can contribute to iron plaque formation.

Definitely, the roots of rice plants represent a biogeochemical and ecological hot spot in paddy soils.[54,93] In particular the spatio-temporal varying release of O_2, the formation of iron minerals and the excretion of plant exudates create a unique and highly dynamic microenvironment.[94,117] In this rhizosphere, not only geochemical conditions differ but also the relative abundance of iron-cycling bacteria is significantly higher compared to the surrounding bulk soil.[118] Within the rice plant rhizosphere as biogeochemical reaction center, microbial interactions with root iron plaque on a small scale can ultimately impact biogeochemical processes in the entire paddy field.[119] Our fundamental understanding of the physicochemical and biological interactions in paddy soils is essential for restoring and sustaining ecosystem productivity of rice paddies.[46,87] Especially the role of rice plants and iron-metabolizing rhizosphere bacteria, which are ultimately controlling the transformation, transport, fate, and toxicity of metals and metalloids in the rhizosphere, which is the bottleneck of contamination for the terrestrial food chain, deserves increasing attention.[87]

1.4 Objectives of this study.

Intensive research substantially increased our understanding about biogeochemical processes in paddy fields. In particular, the rice plant-mediated formation of iron plaque and the presence of Fe(II)-oxidizing and Fe(III)-reducing bacteria have been described by several studies over the past decades.[15,70,101] However, these investigations are still lacking a holistic study that combines the vegetative development of the rice plant and its effect on rhizosphere soil geochemistry, iron mineralogy and the influence on microbial processes with respect to the biogeochemical iron cycling. The quantitative understanding of microaerophilic Fe(II) oxidation, their contribution to the overall iron oxidation as well as the dynamic spatio-temporal identification of habitats in the rice plant rhizosphere are crucial to elucidate their role in the iron cycle of paddy fields. Following ROL-induced formation of iron minerals, the quantitative impact of iron-oxidizing and -reducing bacteria on iron plaque mineral formation, transformation and dissolution could close current research gaps in fully understanding the rhizosphere iron cycle and can ultimately have broad implications on the fate of arsenic in contaminated paddy fields. To improve our understanding on biogeochemical interactions with the iron plaque on the roots of rice plants and their impact on the iron cycle in paddy fields, the objectives of this study are:

- the isolation of microaerophilic Fe(II)-oxidizing bacteria from a paddy soil and the development of a new approach to quantify microbial Fe(II) oxidation rates under various microoxic conditions. This allows to extrapolate the contribution of neutrophilic microaerophilic Fe(II)-oxidizing bacteria to total rhizosphere iron oxidation and their impact on the iron cycle in paddy fields – **Chapter 2**.

- the spatio-temporal identification of small-scale changes of geochemical parameters, such as O_2, Fe(II), Fe(III) and pH in the rice plant rhizosphere during plant growth to identify dynamic changes in local redox properties, iron speciation and root iron plaque formation. The most urgent tasks in this field involve the correlation of geochemical, mineralogical and microbial small-scale variations as a function of plant and root development and the localization of niches for microaerophilic Fe(II)-oxidizing bacteria during plant growth – **Chapter 3**.

- based on the collected data, a quantitative estimation of biogeochemical fluxes across rhizosphere interfaces, including the impact of rice roots on iron mineral plaque formation, the extent of iron-oxidizing bacteria in affecting the rhizosphere iron cycling

and the amount of root iron plaque remobilization during microbial iron plaque reduction. These findings will help to further decipher the rhizosphere iron cycle and increase an enumerative understanding for individual processes impacting the iron budget in paddy fields – **Chapter 4.**

- the identification of a toxic effect of As-loaded root iron plaque on microbial Fe(III) reduction and the quantification of Fe(II) and As remobilization rates from iron plaque during reductive dissolution. Additionally, secondary iron plaque minerals, as a product of microbial Fe(III) reduction, will be quantitatively identified and the fate of As in setups with microbially-reduced and non-reduced iron plaque will be determined – **Chapter 5.**

1.5 References

1. Sparks, D. L.; Page, A. L.; Helmke, P. A.; Loeppert, R. H., *Methods of soil analysis, part 3: Chemical methods*. John Wiley & Sons: 2020; Vol. 14.

2. Lal, R., Soil science and the carbon civilization. *Soil Sci Soc Am J* **2007,** *71*, (5), 1425-1437.

3. Bockheim, J. G.; Gennadiyev, A. N., Soil-factorial models and earth-system science: A review. *Geoderma* **2010,** *159*, (3-4), 243-251.

4. Roth, V. N.; Lange, M.; Simon, C.; Hertkorn, N.; Bucher, S.; Goodall, T.; Griffiths, R. I.; Mellado-Vazquez, P. G.; Mommer, L.; Oram, N. J.; Weigelt, A.; Dittmar, T.; Gleixner, G., Persistence of dissolved organic matter explained by molecular changes during its passage through soil. *Nat Geosci* **2019,** *12*, (9), 755-+.

5. Normile, D., Archaeology - Yangtze seen as earliest rice site. *Science* **1997,** *275*, (5298), 309-309.

6. Conrad, R., Soil microorganisms as controllers of atmospheric trace gases (H-2, CO, CH4, OCS, N2O, and NO). *Microbiol Rev* **1996,** *60*, (4), 609-640.

7. Hou, A. X.; Chen, G. X.; Wang, Z. P.; Van Cleemput, O.; Patrick, W. H., Methane and nitrous oxide emissions from a rice field in relation to soil redox and microbiological processes. *Soil Sci Soc Am J* **2000,** *64*, (6), 2180-2186.

8. Ll, C. S., Quantifying greenhouse gas emissions from soils: Scientific basis and modeling approach. *Soil Sci Plant Nutr* **2007,** *53*, (4), 344-352.

9. Hadi, A.; Inubushi, K.; Yagi, K., Effect of water management on greenhouse gas emissions and microbial properties of paddy soils in Japan and Indonesia. *Paddy Water Environ* **2010,** *8*, (4), 319-324.

10. Carlson, K. M.; Gerber, J. S.; Mueller, N. D.; Herrero, M.; MacDonald, G. K.; Brauman, K. A.; Havlik, P.; O'Connell, C. S.; Johnson, J. A.; Saatchi, S.; West, P. C., Greenhouse gas emissions intensity of global croplands. *Nat Clim Change* **2017,** *7*, (1), 63-+.

11. Li, Z. P.; Liu, M.; Wu, X. C.; Han, F. X.; Zhang, T. L., Effects of long-term chemical fertilization and organic amendments on dynamics of soil organic C and total N in paddy soil derived from barren land in subtropical China. *Soil Till Res* **2010,** *106*, (2), 268-274.

12. Gotoh, S.; Yamashita, K., Oxidation-reduction potential of a paddy soil in in situ with special reference to the production of ferrous ikon, manganous manganese and sulfide. *Soil Sci Plant Nutr* **1966,** *12*, (6), 24-32.

13. Kalpagé, F. S. C. P., Redox potential trends in a submerged rice soil. *Plant Soil* **1965,** *23*, (1), 129-136.

14. Trolldenier, G., Mineral nutrition and reduction processes in the rhizosphere of rice. *Plant Soil* **1977,** *47*, (1), 193-202.

15. Said-Pullicino, D.; Cucu, M. A.; Sodano, M.; Birk, J. J.; Glaser, B.; Celi, L., Nitrogen immobilization in paddy soils as affected by redox conditions and rice straw incorporation. *Geoderma* **2014,** *228*, 44-53.

16. Borch, T.; Kretzschmar, R.; Kappler, A.; Van Cappellen, P.; Ginder-Vogel, M.; Voegelin, A.; Campbell, K., Biogeochemical Redox Processes and their Impact on Contaminant Dynamics. *Environ Sci Technol* **2010,** *44*, (1), 15-23.

17. Yamaguchi, N.; Ohkura, T.; Takahashi, Y.; Maejima, Y.; Arao, T., Arsenic Distribution and Speciation near Rice Roots Influenced by Iron Plaques and Redox Conditions of the Soil Matrix. *Environ Sci Technol* **2014,** *48*, (3), 1549-1556.

18. Frey, P. A.; Outten, C. E., Forging ahead: new mechanistic insights into iron biochemistry. *Curr Opin Chem Biol* **2011,** *15*, (2), 257-259.

19. Frey, P. A.; Reed, G. H., The Ubiquity of Iron. *Acs Chem Biol* **2012,** *7*, (9), 1477-1481.

20. Lindsay, W. L.; Schwab, A. P., The Chemistry of Iron in Soils and Its Availability to Plants. *J Plant Nutr* **1982,** *5*, (4-7), 821-840.

21. Gotoh, S.; Patrick, W. H., Transformation of Iron in a Waterlogged Soil as Influenced by Redox Potential and Ph. *Soil Sci Soc Am J* **1974,** *38*, (1), 66-71.

22. Ionescu, D.; Heim, C.; Polerecky, L.; Thiel, V.; De Beer, D., Biotic and abiotic oxidation and reduction of iron at circumneutral pH are inseparable processes under natural conditions. *Geomicrobiol J* **2015,** *32*, (3-4), 221-230.

23. Hansel, C. M.; Benner, S. G.; Neiss, J.; Dohnalkova, A.; Kukkadapu, R. K.; Fendorf, S., Secondary mineralization pathways induced by dissimilatory iron reduction of ferrihydrite under advective flow. *Geochim Cosmochim Ac* **2003,** *67*, (16), 2977-2992.

24. Hori, T.; Muller, A.; Igarashi, Y.; Conrad, R.; Friedrich, M. W., Identification of iron-reducing microorganisms in anoxic rice paddy soil by C-13-acetate probing. *Isme J* **2010,** *4*, (2), 267-278.

25. Miyao, M.; Ikeuchi, M.; Yamamoto, N.; Ono, T., Specific Degradation of the D1 Protein of Photosystem-Ii by Treatment with Hydrogen-Peroxide in Darkness - Implications for

the Mechanism of Degradation of the D1 Protein under Illumination. *Biochemistry-Us* **1995,** *34*, (31), 10019-10026.

26. Becker, M.; Asch, F., Iron toxicity in rice-conditions and management concepts. *Journal of Plant Nutrition and Soil Science* **2005,** *168*, (4), 558-573.

27. Kawase, M., Anatomical and Morphological Adaptation of Plants to Waterlogging. *Hortscience* **1981,** *16*, (1), 30-34.

28. Armstrong, J.; Armstrong, W., Phragmites-Australis - a Preliminary-Study of Soil-Oxidizing Sites and Internal Gas-Transport Pathways. *New Phytol* **1988,** *108*, (4), 373-382.

29. Colmer, T. D., Aerenchyma and an inducible barrier to radial oxygen loss facilitate root aeration in upland, paddy and deep-water rice (Oryza sativa L.). *Ann Bot-London* **2003,** *91*, (2), 301-309.

30. Ando, T.; Yoshida, S.; Nishiyama, I., Nature of Oxidizing Power of Rice Roots. *Plant Soil* **1983,** *72*, (1), 57-71.

31. Schwertmann, U., Solubility and Dissolution of Iron-Oxides. *Plant Soil* **1991,** *130*, (1-2), 1-25.

32. Trolldenier, G., Visualization of Oxidizing Power of Rice Roots and of Possible Participation of Bacteria in Iron Deposition. *Z Pflanz Bodenkunde* **1988,** *151*, (2), 117-121.

33. Cornell, R. M.; Schwertmann, U., *The iron oxides: structure, properties, reactions, occurrences and uses*. John Wiley & Sons: 2003.

34. Zhang, X. K.; Zhang, F. S.; Mao, D. R., Effect of iron plaque outside roots on nutrient uptake by rice (Oryza sativa L.). Zinc uptake by Fe-deficient rice. *Plant Soil* **1998,** *202*, (1), 33-39.

35. Green, M. S.; Etherington, J. R., Oxidation of Ferrous Iron by Rice (Oryza-Sativa-L) Roots - Mechanism for Waterlogging Tolerance. *J Exp Bot* **1977,** *28*, (104), 678-&.

36. Taylor, G. J.; Crowder, A. A.; Rodden, R., Formation and Morphology of an Iron Plaque on the Roots of Typha-Latifolia L Grown in Solution Culture. *Am J Bot* **1984,** *71*, (5), 666-675.

37. Nordstrom, D. K., Public health - Worldwide occurrences of arsenic in ground water. *Science* **2002,** *296*, (5576), 2143-2145.

38. Cullen, W. R.; Reimer, K. J., Arsenic Speciation in the Environment. *Chem Rev* **1989,** *89*, (4), 713-764.

39. Fendorf, S.; Michael, H. A.; van Geen, A., Spatial and Temporal Variations of Groundwater Arsenic in South and Southeast Asia. *Science* **2010,** *328*, (5982), 1123-1127.

40. Dittmar, J.; Voegelin, A.; Roberts, L. C.; Hug, S. J.; Saha, G. C.; Ali, M. A.; Badruzzaman, A. B. M.; Kretzschmar, R., Spatial distribution and temporal variability of arsenic in irrigated rice fields in Bangladesh. 2. Paddy soil. *Environ Sci Technol* **2007,** *41*, (17), 5967-5972.

41. Smith, A. H.; Lingas, E. O.; Rahman, M., Contamination of drinking-water by arsenic in Bangladesh: a public health emergency. *B World Health Organ* **2000,** *78*, (9), 1093-1103.

42. Zavala, Y. J.; Duxbury, J. M., Arsenic in rice: I. Estimating normal levels of total arsenic in rice grain. *Environ Sci Technol* **2008,** *42*, (10), 3856-3860.

43. Williams, P. N.; Islam, M. R.; Adomako, E. E.; Raab, A.; Hossain, S. A.; Zhu, Y. G.; Feldmann, J.; Meharg, A. A., Increase in rice grain arsenic for regions of Bangladesh irrigating paddies with elevated arsenic in groundwaters. *Environ Sci Technol* **2006,** *40*, (16), 4903-4908.

44. Chen, Z.; Zhu, Y. G.; Liu, W. J.; Meharg, A. A., Direct evidence showing the effect of root surface iron plaque on arsenite and arsenate uptake into rice (Oryza sativa) roots. *New Phytol* **2005,** *165*, (1), 91-97.

45. Seyfferth, A. L.; Webb, S. M.; Andrews, J. C.; Fendorf, S., Arsenic Localization, Speciation, and Co-Occurrence with Iron on Rice (Oryza sativa L.) Roots Having Variable Fe Coatings. *Environ Sci Technol* **2010,** *44*, (21), 8108-8113.

46. Shakoor, M. B.; Riaz, M.; Niazi, N. K.; Ali, S.; Rizwan, M.; Arif, M. S.; Arif, M., Recent Advances in Arsenic Accumulation in Rice. *Advances in Rice Research for Abiotic Stress Tolerance* **2019**, 385-398.

47. Xu, X. W.; Chen, C.; Wang, P.; Kretzschmar, R.; Zhao, F. J., Control of arsenic mobilization in paddy soils by manganese and iron oxides. *Environ Pollut* **2017,** *231*, 37-47.

48. Waychunas, G. A.; Rea, B. A.; Fuller, C. C.; Davis, J. A., Surface chemistry of ferrihydrite: Part 1. EXAFS studies of the geometry of coprecipitated and adsorbed arsenate. *Geochim Cosmochim Ac* **1993,** *57*, (10), 2251-2269.

49. Takahashi, Y.; Minamikawa, R.; Hattori, K. H.; Kurishima, K.; Kihou, N.; Yuita, K., Arsenic behavior in paddy fields during the cycle of flooded and non-flooded periods. *Environ Sci Technol* **2004,** *38*, (4), 1038-1044.

50. Moyer, C. E.; Tappero, R.; Bais, H.; Sparks, D. L., Role of iron plaques in immobilizing arsenic in the rice-root environment. *Abstr Pap Am Chem S* **2012,** *244*.

51. Wu, C.; Ye, Z. H.; Shu, W. S.; Zhu, Y. G.; Wong, M. H., Arsenic accumulation and speciation in rice are affected by root aeration and variation of genotypes. *J Exp Bot* **2011,** *62*, (8), 2889-2898.

52. Fredrickson, J. K.; Gorby, Y. A., Environmental processes mediated by iron-reducing bacteria. *Curr Opin Biotech* **1996,** *7*, (3), 287-294.

53. Cai, C.; Leu, A. O.; Xie, G.-J.; Guo, J.; Feng, Y.; Zhao, J.-X.; Tyson, G. W.; Yuan, Z.; Hu, S., A methanotrophic archaeon couples anaerobic oxidation of methane to Fe(III) reduction. *The ISME Journal* **2018,** *12*, (8), 1929-1939.

54. Liesack, W.; Schnell, S.; Revsbech, N. P., Microbiology of flooded rice paddies. *Fems Microbiol Rev* **2000,** *24*, (5), 625-645.

55. Lovley, D. R.; Giovannoni, S. J.; White, D. C.; Champine, J. E.; Phillips, E. J. P.; Gorby, Y. A.; Goodwin, S., Geobacter-Metallireducens Gen-Nov Sp-Nov, a Microorganism Capable of Coupling the Complete Oxidation of Organic-Compounds to the Reduction of Iron and Other Metals. *Arch Microbiol* **1993,** *159*, (4), 336-344.

56. Kato, S., Microbial extracellular electron transfer and its relevance to iron corrosion. *Microb Biotechnol* **2016,** *9*, (2), 141-148.

57. Ross, D. E.; Brantley, S. L.; Tien, M., Kinetic Characterization of OmcA and MtrC, Terminal Reductases Involved in Respiratory Electron Transfer for Dissimilatory Iron Reduction in Shewanella oneidensis MR-1. *Appl Environ Microb* **2009,** *75*, (16), 5218-5226.

58. Kappler, A.; Benz, M.; Schink, B.; Brune, A., Electron shuttling via humic acids in microbial iron(III) reduction in a freshwater sediment. *Fems Microbiol Ecol* **2004,** *47*, (1), 85-92.

59. Lovley, D. R.; Fraga, J. L.; Blunt-Harris, E. L.; Hayes, L. A.; Phillips, E. J. P.; Coates, J. D., Humic substances as a mediator for microbially catalyzed metal reduction. *Acta Hydrochimica Et Hydrobiologica* **1998,** *26*, (3), 152-157.

60.   Straub, K. L.; Schink, B., Evaluation of electron-shuttling compounds in microbial ferric iron reduction. *Fems Microbiol Lett* **2003,** *220*, (2), 229-233.

61.   Reguera, G.; McCarthy, K. D.; Mehta, T.; Nicoll, J. S.; Tuominen, M. T.; Lovley, D. R., Extracellular electron transfer via microbial nanowires. *Nature* **2005,** *435*, (7045), 1098-1101.

62.   Gorby, Y. A.; Yanina, S.; McLean, J. S.; Rosso, K. M.; Moyles, D.; Dohnalkova, A.; Beveridge, T. J.; Chang, I. S.; Kim, B. H.; Kim, K. S.; Culley, D. E.; Reed, S. B.; Romine, M. F.; Saffarini, D. A.; Hill, E. A.; Shi, L.; Elias, D. A.; Kennedy, D. W.; Pinchuk, G.; Watanabe, K.; Ishii, S.; Logan, B.; Nealson, K. H.; Fredrickson, J. K., Electrically conductive bacterial nanowires produced by Shewanella oneidensis strain MR-1 and other microorganisms. *P Natl Acad Sci USA* **2006,** *103*, (30), 11358-11363.

63.   Lovley, D. R.; Walker, D. J. F., Geobacter Protein Nanowires. *Front Microbiol* **2019,** *10*.

64.   Bird, L. J.; Bonnefoy, V.; Newman, D. K., Bioenergetic challenges of microbial iron metabolisms. *Trends Microbiol* **2011,** *19*, (7), 330-340.

65.   Benner, S. G.; Hansel, C. M.; Wielinga, B. W.; Barber, T. M.; Fendorf, S., Reductive dissolution and biomineralization of iron hydroxide under dynamic flow conditions. *Environ Sci Technol* **2002,** *36*, (8), 1705-1711.

66.   Van Den Berg, C. M. G., Evidence for Organic Complexation of Iron in Seawater. *Mar Chem* **1995,** *50*, (1-4), 139-157.

67.   Dixit, S.; Hering, J. G., Sorption of Fe(II) and As(III) on goethite in single- and dual-sorbate systems. *Chem Geol* **2006,** *228*, (1-3), 6-15.

68.   Larese-Casanova, P.; Kappler, A.; Haderlein, S. B., Heterogeneous oxidation of Fe(II) on iron oxides in aqueous systems: Identification and controls of Fe(III) product formation. *Geochim Cosmochim Ac* **2012,** *91*, 171-186.

69.   Bongoua-Devisme, A. J.; Mustin, C.; Berthelin, J., Responses of Iron-Reducing Bacteria to Salinity and Organic Matter Amendment in Paddy Soils of Thailand. *Pedosphere* **2012,** *22*, (3), 375-393.

70.   Weiss, J. V.; Emerson, D.; Backer, S. M.; Megonigal, J. P., Enumeration of Fe(II)-oxidizing and Fe(III)-reducing bacteria in the root zone of wetland plants: Implications for a rhizosphere iron cycle. *Biogeochemistry* **2003,** *64*, (1), 77-96.

71.   Ratering, S.; Schnell, S., Nitrate-dependent iron(II) oxidation in paddy soil. *Environ Microbiol* **2001,** *3*, (2), 100-109.

72.   Straub, K. L.; Benz, M.; Schink, B.; Widdel, F., Anaerobic, nitrate-dependent microbial oxidation of ferrous iron. *Appl Environ Microb* **1996,** *62*, (4), 1458-1460.

73.   Emerson, D.; Moyer, C., Isolation and characterization of novel iron-oxidizing bacteria that grow at circumneutral pH. *Appl Environ Microb* **1997,** *63*, (12), 4784-4792.

74.   Naruse, T.; Ban, Y.; Yoshida, T.; Kato, T.; Namikawa, M.; Takahashi, T.; Nishida, M.; Asakawa, S.; Watanabe, T., Community structure of microaerophilic iron-oxidizing bacteria in Japanese paddy field soils. *Soil Sci Plant Nutr* **2019,** *65*, (5), 460-470.

75.   Sung, W.; Morgan, J. J., Kinetics and Product of Ferrous Iron Oxygenation in Aqueous Systems. *Environ Sci Technol* **1980,** *14*, (5), 561-568.

76.   Sobolev, D.; Roden, E. E., Characterization of a neutrophilic, chemolithoautotrophic Fe(II)-oxidizing beta-proteobacterium from freshwater wetland sediments. *Geomicrobiol J* **2004,** *21*, (1), 1-10.

77.   Druschel, G. K.; Emerson, D.; Sutka, R.; Suchecki, P.; Luther, G. W., Low-oxygen and chemical kinetic constraints on the geochemical niche of neutrophilic iron(II) oxidizing microorganisms. *Geochim Cosmochim Ac* **2008,** *72*, (14), 3358-3370.

78.   Emerson, D.; Fleming, E. J.; McBeth, J. M., Iron-Oxidizing Bacteria: An Environmental and Genomic Perspective. *Annu Rev Microbiol* **2010,** *64*, 561-583.

79.   Laufer, K.; Nordhoff, M.; Halama, M.; Martinez, R. E.; Obst, M.; Nowak, M.; Stryhanyuk, H.; Richnow, H. H.; Kappler, A., Microaerophilic Fe(II)-Oxidizing Zetaproteobacteria Isolated from Low-Fe Marine Coastal Sediments: Physiology and Composition of Their Twisted Stalks. *Appl Environ Microb* **2017,** *83*, (8).

80.   Emerson, D.; Moyer, C. L., Neutrophilic Fe-Oxidizing bacteria are abundant at the Loihi Seamount hydrothermal vents and play a major role in Fe oxide deposition. *Appl Environ Microb* **2002,** *68*, (6), 3085-3093.

81.   Videla, H. A.; Characklis, W. G., Biofouling and Microbially Influenced Corrosion. *Int Biodeter Biodegr* **1992,** *29*, (3-4), 195-212.

82.   Weiss, J. V.; Rentz, J. A.; Plaia, T.; Neubauer, S. C.; Merrill-Floyd, M.; Lilburn, T.; Bradburne, C.; Megonigal, J. P.; Emerson, D., Characterization of neutrophilic Fe(II)-oxidizing bacteria isolated from the rhizosphere of wetland plants and description of Ferritrophicum radicicola gen. nov sp nov., and Sideroxydans paludicola sp nov. *Geomicrobiol J* **2007,** *24*, (7-8), 559-570.

83. Neubauer, S. C.; Emerson, D.; Megonigal, J. P., Life at the energetic edge: Kinetics of circumneutral iron oxidation by lithotrophic iron-oxidizing bacteria isolated from the wetland-plant rhizosphere. *Appl Environ Microb* **2002,** *68*, (8), 3988-3995.

84. Emerson, D.; Weiss, J. V.; Megonigal, J. P., Iron-oxidizing bacteria are associated with ferric hydroxide precipitates (Fe-plaque) on the roots of wetland plants. *Appl Environ Microb* **1999,** *65*, (6), 2758-2761.

85. Roden, E. E.; Sobolev, D.; Glazer, B.; Luther, G. W., Potential for microscale bacterial Fe redox cycling at the aerobic-anaerobic interface. *Geomicrobiol J* **2004,** *21*, (6), 379-391.

86. Curl, E. A.; Truelove, B., *The rhizosphere*. Springer Science & Business Media: 2012; Vol. 15.

87. Huang, P. M., Impacts of Physicochemical-Biological Interactions on Metal and Metalloid Transformations in Soils: An Overview. *Wiley-Iupac Ser Biop* **2008**, 3-52.

88. Armstrong, W., Radial Oxygen Losses from Intact Rice Roots as Affected by Distance from Apex, Respiration and Waterlogging. *Physiol Plantarum* **1971,** *25*, (2), 192-+.

89. Mendelssohn, I. A.; Kleiss, B. A.; Wakeley, J. S., Factors Controlling the Formation of Oxidized Root Channels - a Review. *Wetlands* **1995,** *15*, (1), 37-46.

90. Wang, Z. P.; Delaune, R. D.; Masscheleyn, P. H.; Patrick, W. H., Soil Redox and Ph Effects on Methane Production in a Flooded Rice Soil. *Soil Sci Soc Am J* **1993,** *57*, (2), 382-385.

91. Wu, C.; Ye, Z. H.; Li, H.; Wu, S. C.; Deng, D.; Zhu, Y. G.; Wong, M. H., Do radial oxygen loss and external aeration affect iron plaque formation and arsenic accumulation and speciation in rice? *J Exp Bot* **2012,** *63*, (8), 2961-2970.

92. Wang, X.; Yao, H. X.; Wong, M. H.; Ye, Z. H., Dynamic changes in radial oxygen loss and iron plaque formation and their effects on Cd and As accumulation in rice (Oryza sativa L.). *Environ Geochem Hlth* **2013,** *35*, (6), 779-788.

93. Flessa, H.; Fischer, W. R., Plant-Induced Changes in the Redox Potentials of Rice Rhizospheres. *Plant Soil* **1992,** *143*, (1), 55-60.

94. Schmidt, H.; Eickhorst, T.; Tippkotter, R., Monitoring of root growth and redox conditions in paddy soil rhizotrons by redox electrodes and image analysis. *Plant Soil* **2011,** *341*, (1-2), 221-232.

95. Doran, G.; Eberbach, P.; Helliwell, S., The impact of rice plant roots on the reducing conditions in flooded rice soils. *Chemosphere* **2006,** *63*, (11), 1892-1902.

96. Garnier, J. M.; Travassac, F.; Lenoble, V.; Rose, J.; Zheng, Y.; Hossain, M. S.; Chowdhury, S. H.; Biswas, A. K.; Ahmed, K. M.; Cheng, Z.; van Geen, A., Temporal variations in arsenic uptake by rice plants in Bangladesh: The role of iron plaque in paddy fields irrigated with groundwater. *Sci Total Environ* **2010,** *408*, (19), 4185-4193.

97. Yamaguchi, N.; Nakamura, T.; Dong, D.; Takahashi, Y.; Amachi, S.; Makino, T., Arsenic release from flooded paddy soils is influenced by speciation, Eh, pH, and iron dissolution. *Chemosphere* **2011,** *83*, (7), 925-932.

98. Tufano, K. J.; Reyes, C.; Saltikov, C. W.; Fendorf, S., Reductive Processes Controlling Arsenic Retention: Revealing the Relative Importance of Iron and Arsenic Reduction. *Environ Sci Technol* **2008,** *42*, (22), 8283-8289.

99. Liu, W. J.; Zhu, Y. G.; Hu, Y.; Williams, P. N.; Gault, A. G.; Meharg, A. A.; Charnock, J. M.; Smith, F. A., Arsenic sequestration in iron plaque, its accumulation and speciation in mature rice plants (Oryza sativa L.). *Environ Sci Technol* **2006,** *40*, (18), 5730-5736.

100. Nanzyo, M.; Yaginuma, H.; Sasaki, K.; Ito, K.; Aikawa, Y.; Kanno, H.; Takahashi, T., Identification of vivianite formed on the roots of paddy rice grown in pots. *Soil Sci Plant Nutr* **2010,** *56*, (3), 376-381.

101. Wang, X. J.; Chen, X. P.; Yang, J.; Wang, Z. S.; Sun, G. X., Effect of microbial mediated iron plaque reduction on arsenic mobility in paddy soil. *J Environ Sci-China* **2009,** *21*, (11), 1562-1568.

102. Bacilio-Jimenez, M.; Aguilar-Flores, S.; Ventura-Zapata, E.; Perez-Campos, E.; Bouquelet, S.; Zenteno, E., Chemical characterization of root exudates from rice (Oryza sativa) and their effects on the chemotactic response of endophytic bacteria. *Plant Soil* **2003,** *249*, (2), 271-277.

103. Lynch, J. M.; Whipps, J. M., Substrate Flow in the Rhizosphere. *Plant Soil* **1990,** *129*, (1), 1-10.

104. Kusel, K.; Chabbi, A.; Trinkwalter, T., Microbial processes associated with roots of bulbous rush coated with iron plaques. *Microbial Ecol* **2003,** *46*, (3), 302-311.

105. Bissen, M.; Frimmel, F. H., Arsenic — a Review. Part I: Occurrence, Toxicity, Speciation, Mobility. *Acta hydrochimica et hydrobiologica* **2003,** *31*, (1), 9-18.

106. Biophysico-Chemical Processes of Heavy Metals and Metalloids in Soil Environments. *Wiley-Iupac Ser Biop* **2008**, 1-659.

107. Jackel, U.; Schnell, S., Role of microbial iron reduction in paddy soil. *Non-Co2 Greenhouse Gases: Scientific Understanding, Control and Implementation* **2000**, 143-144.

108. Ding, L. J.; Su, J. Q.; Xu, H. J.; Jia, Z. J.; Zhu, Y. G., Long-term nitrogen fertilization of paddy soil shifts iron-reducing microbial community revealed by RNA-C-13-acetate probing coupled with pyrosequencing. *Isme J* **2015,** *9*, (3), 721-734.

109. Wu, S. B.; Vymazal, J.; Brix, H., Critical Review: Biogeochemical Networking of Iron in Constructed Wetlands for Wastewater Treatment. *Environ Sci Technol* **2019,** *53*, (14), 7930-7944.

110. Jacob, D. L.; Otte, M. L., Conflicting processes in the wetland plant rhizosphere: Metal retention or mobilization? *Water, Air and Soil Pollution: Focus* **2003,** *3*, (1), 91-104.

111. Babechuk, M. G.; Weisener, C. G.; Fryer, B. J.; Paktunc, D.; Maunders, C., Microbial reduction of ferrous arsenate: Biogeochemical implications for arsenic mobilization. *Appl Geochem* **2009,** *24*, (12), 2332-2341.

112. Li, X. M.; Mou, S.; Chen, Y. T.; Liu, T. X.; Dong, J.; Li, F. B., Microaerobic Fe(II) oxidation coupled to carbon assimilation processes driven by microbes from paddy soil. *Sci China Earth Sci* **2019,** *62*, (11), 1719-1729.

113. Kirby, C. S.; Thomas, H. M.; Southam, G.; Donald, R., Relative contributions of abiotic and biological factors in Fe(II) oxidation in mine drainage. *Appl Geochem* **1999,** *14*, (4), 511-530.

114. Hädrich, A.; Taillefert, M.; Akob, D. M.; Cooper, R. E.; Litzba, U.; Wagner, F. E.; Nietzsche, S.; Ciobota, V.; Rösch, P.; Popp, J.; Küsel, K., Microbial Fe(II) oxidation by Sideroxydans lithotrophicus ES-1 in the presence of Schlöppnerbrunnen fen-derived humic acids. *Fems Microbiol Ecol* **2019,** *95*, (4).

115. Neubauer, S. C.; Toledo-Duran, G. E.; Emerson, D.; Megonigal, J. P., Returning to their roots: Iron-oxidizing bacteria enhance short-term plaque formation in the wetland-plant rhizosphere. *Geomicrobiol J* **2007,** *24*, (1), 65-73.

116. Lueder, U.; Druschel, G.; Emerson, D.; Kappler, A.; Schmidt, C., Quantitative analysis of O-2 and Fe2+ profiles in gradient tubes for cultivation of microaerophilic Iron(II)-oxidizing bacteria. *Fems Microbiol Ecol* **2018,** *94*, (2).

117. Revsbech, N. P.; Pedersen, O.; Reichardt, W.; Briones, A., Microsensor analysis of oxygen and pH in the rice rhizosphere under field and laboratory conditions. *Biol Fert Soils* **1999,** *29*, (4), 379-385.

118. Cahyani, V. R.; Murase, J.; Ikeda, A.; Taki, K.; Asakawa, S.; Kimura, M., Bacterial communities in iron mottles in the plow pan layer in a Japanese rice field: Estimation using PCR-DGGE and sequencing analyses. *Soil Sci Plant Nutr* **2008,** *54*, (5), 711-717.

119. Gregory, P. J., Roots, rhizosphere and soil: the route to a better understanding of soil science? *Eur J Soil Sci* **2006,** *57*, (1), 2-12.
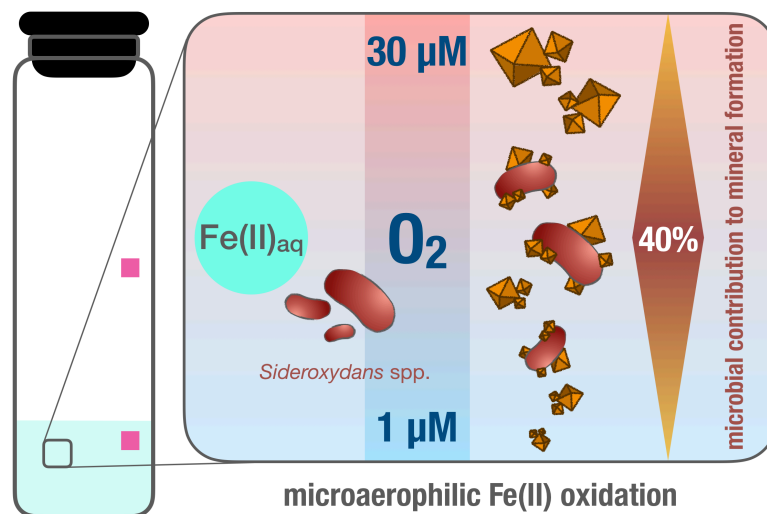
2 Contribution of Microaerophilic Iron(II)-Oxidizers to Iron(III) Mineral Formation

Markus Maisch[1], Ulf Lueder[1], Katja Laufer[2], Caroline Scholze[2], Andreas Kappler[1,2], Caroline Schmidt[1]

[1] Geomicrobiology, Center for Applied Geosciences, University of Tübingen, Germany

[2] Department for Bioscience, Aarhus University, Denmark

Chapter 2

2.1 Abstract

Neutrophilic microbial aerobic oxidation of ferrous iron (Fe(II)) is restricted to pH-circumneutral environments characterized by low oxygen where microaerophilic Fe(II)-oxidizing microorganisms successfully compete with abiotic Fe(II) oxidation. However, accumulation of ferric (bio)minerals increases competition by stimulating abiotic surface-catalyzed heterogeneous Fe(II) oxidation. Here, we present an experimental approach that allows quantification of microbial and abiotic contribution to Fe(II) oxidation in the presence or initial absence of ferric (bio)minerals. We found that at 20 µM O_2 and the initial absence of Fe(III) minerals, an iron(II)-oxidizing enrichment culture (99.6% similarity to *Sideroxydans* spp.) contributed 40% to the overall Fe(II) oxidation within approx. 26 hours and oxidized up to $3.6 \cdot 10^{-15}$ mol Fe(II) cell^{-1} h^{-1}. Optimum O_2 concentrations at which enzymatic Fe(II) oxidation can compete with abiotic Fe(II) oxidation ranged from 5-20 µM. Lower O_2 levels limited biotic Fe(II) oxidation, while at higher O_2 levels abiotic Fe(II) oxidation dominated. The presence of ferric (bio)minerals induced surface-catalytic heterogeneous abiotic Fe(II) oxidation and reduced the microbial contribution to Fe(II) oxidation from 40% to 10% at 10 µM O_2. The obtained results will help to better assess the impact of microaerophilic Fe(II) oxidation on the biogeochemical iron cycle in a variety of environmental natural and anthropogenic settings.

2.2 Introduction

Microaerophilic Fe(II) oxidation represents a biological process contributing to iron redox cycling in many environments such as lacustrine and marine sediments,[1,2] groundwater seeps,[3] the rhizosphere,[4,5] deep sea vents,[6] and on the rusty surface of ship wrecks.[7,8] Under circumneutral pH and atmospheric O_2 concentrations, the abiotic oxidation of dissolved Fe(II) proceeds rapidly, forming poorly soluble Fe(III) (oxyhydr)oxides.[9,10] Under such conditions, microbial Fe(II) oxidation is kinetically outcompeted by fast abiotic oxidation. Optimum conditions for microbial Fe(II) oxidation are thus shifted towards niches where O_2 concentrations are sufficiently low to slow down the abiotic oxidation reaction and thus increase the bioavailability of dissolved Fe(II).[11,12,13] The range in oxygen concentrations where microaerophilic Fe(II) oxidation has been observed was determined in a variety of experimental setups such as in classical cultivation gradient setups (gradient tubes),[14] bioreactors[5] or in microbial mats[15] to be in the range of 5-50 µM.[16,17]

However, the need of continuously low oxygen concentrations complicates the cultivation of microaerophilic Fe(II)-oxidizing bacteria in classical liquid microcosm culture setups.[18] Moreover, ferric iron minerals that get produced during the biotic and abiotic oxidation of

Fe(II) serve as surface catalyst for rapid abiotic heterogeneous Fe(II) oxidation.[9,15] Even under low oxygen concentrations, heterogeneous Fe(II) oxidation kinetically outcompetes microbial Fe(II) oxidation as soon as sufficient reactive ferric mineral surface is produced. This surface-catalytic effect drastically enhances abiotic Fe(II) oxidation and subsequently decreases Fe(II) availability for microaerophilic Fe(II) oxidation[19]. The contribution of microaerophilic Fe(II)-oxidizing bacteria to the Fe(II) turnover was estimated to be 50% to 80% over a wide range of micro-oxic conditions.[13,20,21] Nevertheless, most studies lack an accurate quantification of microbial cells at constantly low O_2 concentrations, the possibility to follow Fe(II) oxidation and to derive microaerophilic Fe(II) turnover rates in the presence of abiotic homogeneous and autocatalytic abiotic heterogeneous Fe(II) oxidation.

The goal of our study was to fill this research gap and to establish an experimental approach that allows to quantify i) the contribution of neutrophilic microaerophilic Fe(II)-oxidizing bacteria to the overall Fe(II) oxidation and consecutive Fe(III) mineral formation at various (1-30 µM) O_2 concentrations in a laboratory-controlled classical liquid culture. Moreover, we envisaged to ii) quantify the impact of Fe(III) mineral particles on the acceleration of the abiotic Fe(II) oxidation. For this, we incubated a microaerophilic Fe(II)-oxidizing enrichment culture (99.6% similarity to *Sideroxydans* spp., isolated from a rice paddy field (Vercelli, Italy)) in miniaturized microcosms and followed the oxidation of dissolved ferrous iron, as well as cell numbers at a range of low oxygen concentrations (1-30 µM O_2). We quantified minimum and maximum threshold O_2 concentrations for optimum microbial Fe(II) oxidation for this enrichment culture and determined the theoretical Fe(II) turnover by abiotic (homogeneous and heterogeneous) oxidation reactions in biotically incubated and abiotic control setups. With a set of experiments, we were able to decipher the extent in Fe(II) oxidation for this microaerophilic enrichment in the presence and absence of surface-reactive minerals. Moreover, the presented approach and gathered data offers the possibility to compare Fe(II) turnover rates of various microaerophilic strains and enrichment cultures[22] and allows to estimate the impact these environmentally abundant microaerophilic communities can have on the Fe(II) oxidation in the respective habitat, e.g. acid-mine drainage,[23] marine sediments[24] or wetlands.[4]

2.3 Materials and Methods

Experimental setup. Miniaturized microcosms were prepared in 20 mL glass vials (with a flat bottom), filled with 2 mL of anoxic Modified Wolfe's Mineral Medium (MWMM) containing 550-800 µM dissolved ferrous iron ($Fe(II)_{aq}$) (preparation details see supporting information) and sealed with butyl rubber stoppers. The headspace was exchanged with N_2/CO_2 (v/v; 90/10)

prior to inoculation and adjustment of O_2 concentrations. The large headspace volume allowed to maintain constantly low and stable O_2 concentrations in the medium over the course of the incubations. For abiotic control incubations, sodium azide (NaN_3, 15 mM) was added to individual microcosms[20, 25]. Setups were prepared in triplicates unless otherwise stated.
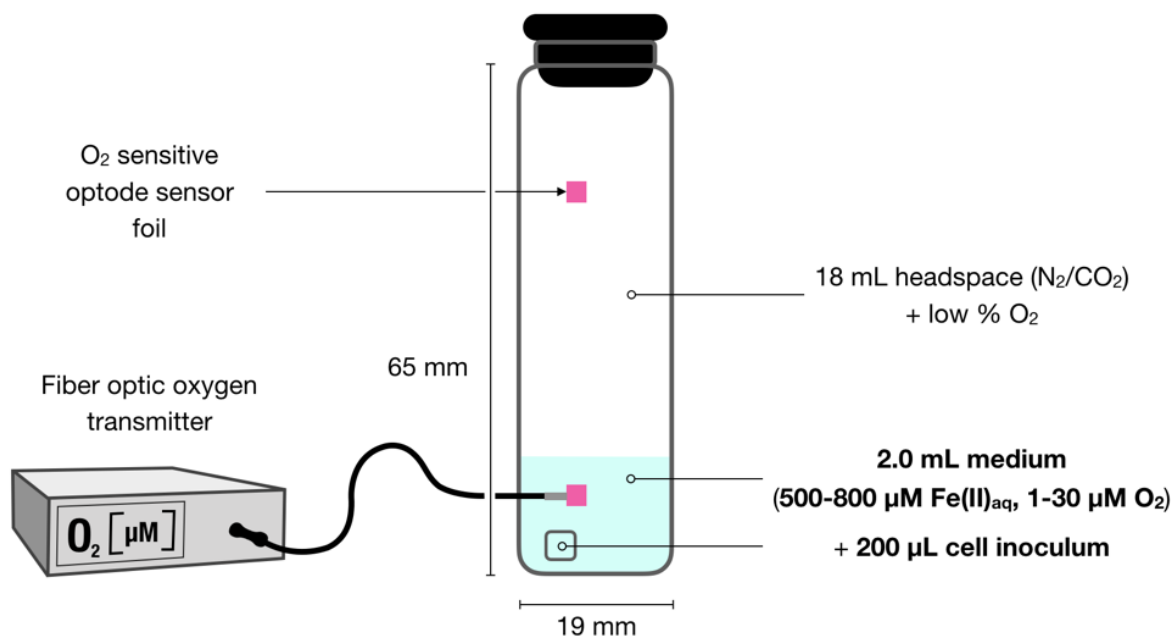
Figure 1 – Schematic representation of the miniaturized microcosm setup. 18 mL N_2/CO_2 (v/v, 90/10) atmosphere in headspace and low % O_2. 2.2 mL MWMM medium amended with $Fe(II)_{aq}$ (500-800 µM) and constant O_2 concentrations ranging from 1-30 µM O_2. In the biotic setups, 2×10^6 cells/ml of a microaerophilic Fe(II)-oxidizing enrichment culture were added and inhibited with sodium azide (15 mM) for abiotic control setups. O_2 concentrations in headspace and medium were adjusted and monitored non-invasively measuring with a fiber optic oxygen transmitter.

Inoculum. A microaerophilic Fe(II)-oxidizing enrichment culture (99.6% similarity to *Sideroxydans* spp., 97% similarity to *S. lithotrophicus* ES-1 (based on 16S rRNA)), isolated from a rice paddy field (Vercelli, Italy), was pre-cultivated on zero-valent iron (ZVI) plates[26] and harvested (SI, Culture preparation). Prior to inoculation and in order to minimize the effect of surface reactive minerals and abiotic heterogeneous Fe(II) oxidation, biomineral residues (SI, Mössbauer spectroscopy, Figure S3) from the pre-culture were removed by dissolution: cell suspensions were washed with anoxic sterile 0.1% oxalate solution for 2 minutes before washing with a bicarbonate buffer solution (10 mM, pH 6.8). Shorter oxalate washing procedures did not dissolve all mineral precipitates, while longer washing steps resulted in partial cell death. Cell viability after washing was verified by fluorescence microscopy and D/L

staining (SI, Figure S1). For each setup 0.2 mL of cell suspension were transferred into each miniaturized microcosm by needle injection through the butyl rubber stopper.

Geochemical analyses and cell quantification. Vials were equipped with optode foil sensors (4x4 mm) (PSt3, PreSens, Regensburg, Germany) glued (Silicone rubber compound RS692-542, RS Components, Northants, UK) to the inner side of the glass wall (one located at the bottom where it was covered with medium, a second one located in the headspace). Oxygen was then quantified non-invasively reading from outside the vial using a fiber optic oxygen meter (FiBox3, PreSens, Regensburg, Germany) as described in Maisch et al. (2016) (Figure 1). [27]

For $Fe(II)_{aq}$ quantification, 150 µL sample were taken and centrifuged for 10 mins at 3.600 rpm under anoxic conditions (glove box, 100% N_2). The supernatant was acidified in 1 M HCl to prevent Fe(II) oxidation outside the glovebox and was consecutively analyzed by the Ferrozine assay.[28] Due to small total sample volume, a quantification of total Fe(II) and Fe(III) was not possible and only dissolved $Fe(II)_{aq}$ was quantified. The pellet that remained after centrifugation was broken up and shaken for 10 seconds on a vortexer. A subsample was fixed in paraformaldehyde (10%; PFA) for cell quantification using constant-sheath flow cytometry (see supporting information for sample preparation). Doubling times (T_d) for cell growth were calculated for the initial incubation period of 45 h when >10% of the initially present Fe(II) was still bioavailable for energy generation and optimum growth yield conditions were expected.

Iron minerals before and after incubation were identified by Mössbauer spectroscopy (SI, Mössbauer spectroscopy, Table S1). Statistical analysis was performed as described in the supporting information (SI, Statistical treatment).

O_2 adjustment in miniaturized microcosms. In order to quantify optimum O_2 conditions at which microaerophilic Fe(II)-oxidizing bacteria successfully compete for Fe(II) with the abiotic Fe(II) oxidation, the enrichment culture was grown in FeS gradient tubes.[14] Oxygen and $Fe(II)_{aq}$ concentrations were quantified along the vertical gradient in the tube using microsensors (methods described in Lueder et al., 2018).[17] The recorded O_2 concentrations in the characteristic growth band represent the basis for the choice of the O_2 range used for the incubation in our miniaturized microcosm (SI, Growth conditions for microaerophilic Fe(II)-oxidizing enrichment culture, Figure S2). Ambient air was injected into the headspace of the miniaturized microcosms by a gas-tight syringe through a sterile filter (0.22 µm) to reach dissolved oxygen concentrations in the medium of 1, 5, 10, 20 and 30 µM O_2. Subsequently,

the microcosms were gently shaken to equilibrate O_2 between headspace and medium and to equally distribute the cells in the medium.

Quantification of Fe(II) oxidation kinetics. Abiotic (homogeneous and heterogeneous) $Fe(II)_{aq}$ oxidation rates and half-life for $Fe(II)_{aq}$ ($^{Fe(II)}t_{1/2}$) were calculated for every sampling time point in each setup. This allows to follow changes in rates and Fe(II) half-lives throughout the entire incubation at designated sampling points and to find the timeframe in which microbial Fe(II) oxidation can compete with the abiotic Fe(II) oxidation. Given that the overall Fe(II) oxidation is a combination of homogeneous and heterogeneous iron oxidation, the individual oxidation rates for each reaction pathway were calculated individually following the approach as presented in Lueder et al. (2018)[17]:

The homogeneous oxidation of $Fe(II)_{aq}$ by dissolved O_2 to Fe(III) (as Fe(III) hydroxide precipitation) is[29]

$$Fe(II)_{aq} + 0.25\,O_2 + 2.5\,H_2O \rightarrow Fe(OH)_3 + 2\,H^+ \tag{1}$$
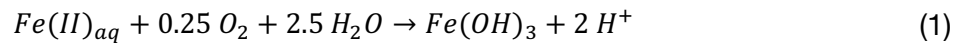
Accounting only for homogeneous $Fe(II)_{aq}$ oxidation (FeOx$_{hom}$) in the setups that contain oxalate-washed cells (no initial Fe(III) precipitates as residues from pre-cultivation), the kinetic rate law (r(FeOx$_{hom}$))

$$-\frac{d[Fe(II)_{aq}]_{hom}}{dt} = k \cdot [Fe(II)_{aq}] \tag{2}$$

with $k = k_0\,[O_2]\,[OH^-]^2$, universal rate constant for homogeneous $Fe(II)_{aq}$ oxidation by O_2, $k_0 = 2.3 \cdot 10^{14}$ mol^3 L^{-3} s^{-1} at 25°C[9], and $[Fe(II)_{aq}]$ as the measured $Fe(II)_{aq}$ concentration at time point t.

The heterogeneous oxidation of $Fe(II)_{aq}$ (FeOx$_{het}$) is described by by Fe(III) minerals that accelerate Fe(II) oxidation via the catalyzing effect of mineral surfaces[30]. In the setups with oxalate-washed cells, the amount of Fe(III) minerals is considered to be equal to the concentration of oxidized $Fe(II)_{aq}$ [9]:

$$[Fe(III)] = [Fe(II)_{aq}]_{t0} - [Fe(II)_{aq}] \tag{3}$$

The rate law of heterogeneous $Fe(II)_{aq}$ (r(FeOx$_{het}$)) oxidation can be described as

$$-\frac{\left[Fe(II)_{aq}\right]_{het}}{dt} = k' \cdot [Fe(III)] \cdot [Fe(II)_{aq}] \tag{4}$$

with $k' = \frac{k_{s,0} \cdot [O_2] \cdot K}{[H^+]}$, specific rate constant for the heterogeneous reaction, $k_{s,0}$ being 73 mol L^{-1} s^{-1} [9] and the dimensionless adsorption constant of ferrous iron on ferric hydroxide K being $10^{-4.85}$ [31]. Although this adsorption constant was empirically determined for abiogenic minerals with ideal crystal lattice properties, we consider it as an appropriate approximation for the iron mineral surfaces formed during incubation.

The combined rate equation of the total Fe(II)$_{aq}$ oxidation (r(FeOx$_{total}$)) includes both, homogeneous (FeOx$_{hom}$) and heterogeneous (FeOx$_{het}$) oxidation, is described as[30]

$$-\frac{d\left[Fe(II)_{aq}\right]}{dt} = (k + k' \cdot [Fe(III)]) \cdot [Fe(II)_{aq}] \tag{5}$$

Based on this equation, half-life for Fe(II)$_{aq}$ was calculated to be:

$$t_{\frac{1}{2},het} = \frac{\ln(2)}{k' \cdot [Fe(III)]} \tag{6}$$

The total Fe(II) oxidation rates (r(FeOx$_{total}$)) for abiotic and biotic incubation setups were calculated as follows:

$$abiotic\ setups: r(FeOx_{total}) = r(FeOx_{hom}) + r(FeOx_{het}) \tag{7}$$

$$biotic\ setups: r(FeOx_{total}) = r(FeOx_{hom}) + r(FeOx_{het}) + r(FeOx_{bio}) \tag{8}$$

Microaerophilic Fe(II) oxidation rates (r(FeOx$_{bio}$) with Fe(II)$_{aq}$ cell^{-1} hour^{-1}) within the initial incubation phase were calculated via the following equation

$$microb.\ Fe(II)\ ox.\ per\ cell = \left\{[Fe(II)_{aq}]_{tx,abio} - [Fe(II)_{aq}]_{tx,bio}\right\} \cdot t^{-1} \cdot n^{-1} \tag{9}$$

At timepoint x, with t as elapsed incubation time in hours and n as the total cell number.

Although microbial Fe(II) oxidation rates were determined for each sampling interval, the microbial contribution to the total Fe(II) oxidation (FeOx$_{total}$) was then quantified for the initial

incubation phase of 0 - 26 hours, in which approx. 50 % of the initially available Fe(II) was oxidized and differences between biotic and abiotic setups were most prominent. Within this initial incubation phase, fastest cell doubling times and highest extent in microbial Fe(II) oxidation were expected. The microbial contribution to the total Fe(II) oxidation was calculated as follows

$$biol.\, contribution.\, (\%)_t = \frac{[Fe(II)_{aq}]_{tx,abio} - [Fe(II)_{aq}]_{tx,bio}}{[Fe(II)_{aq}]_{t0,bio} - [Fe(II)_{aq}]_{tx,bio}} \cdot 100 \qquad (10)$$

2.4   Results & Discussion

Effect of O_2 concentrations on microaerophilic Fe(II) oxidation kinetics. Microaerophilic Fe(II)-oxidizing bacteria can be found where Fe(II) is bioavailable and O_2 sufficiently low that microorganisms can kinetically outcompete abiotic Fe(II) oxidation. Although a few studies performed estimations on microbial microaerophilic Fe(II) oxidation rates,[16,32-34] little is known about the microbial contribution to the overall Fe(II) oxidation at constantly low O_2 concentrations in the presence of abiotic homogeneous and autocatalytic abiotic heterogeneous Fe(II) oxidation. We therefore quantified the microbial contribution to Fe(II) oxidation and estimated biological Fe(II) turnover rates at different microoxic O_2 concentrations (10, 20 and 30 µM O_2). The cell inoculum used for this experiment was pre-washed with oxalate solution to remove any mineral residues from pre-cultivation and to suppress initially autocatalytic and rapid abiotic heterogeneous Fe(II) oxidation.

While in all setups, pre-adjusted oxygen concentrations remained constant throughout incubation (Figure S5), Fe(II)$_{aq}$ decreased rapidly by more than 50% in all biotic setups within the initial incubation phase of 26 hours. In the abiotic control, significantly less Fe(II) oxidation was observed within this initial incubation phase at 10 and 20 µM O_2 (Figure 2A) compared to biotic incubations. At 30 µM O_2, the total Fe(II) oxidation rate (incl. both biotic and abiotic Fe(II) oxidation) was highest, with a non-significant difference between Fe(II)$_{aq}$ oxidation in biotic vs. abiotic setups, which suggested that the microaerophilic Fe(II)-oxidizing bacteria did not impact nor enhance the overall Fe(II) turnover.
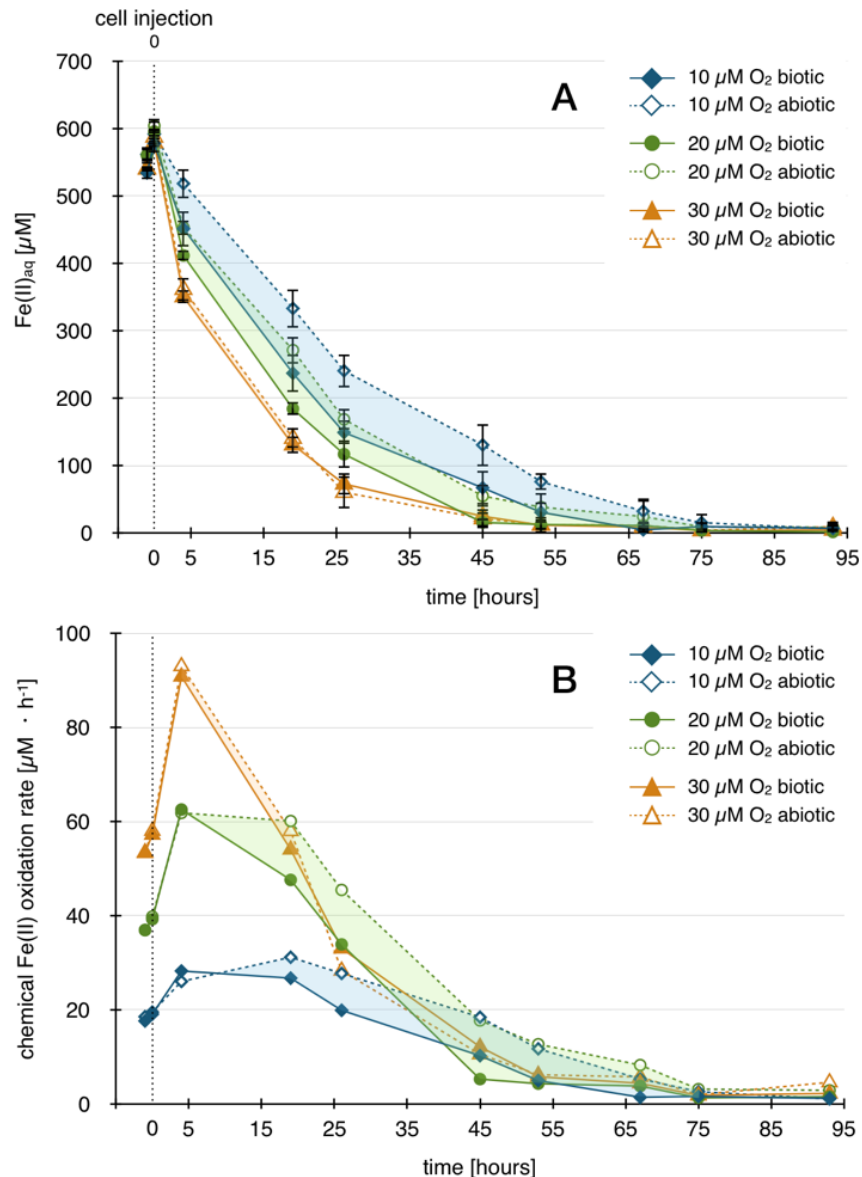
Figure 2. (A) Fe(II)$_{aq}$ concentrations in biotic and abiotic incubations with oxalate-washed cells from a microaerophilic Fe(II)-oxidizing enrichment culture at different O$_2$ concentrations; error bars represent standard deviations from experimental triplicates; shaded areas represent the difference in Fe(II) oxidation between abiotic and biotic incubations at similar O$_2$ concentrations that can be attributed to the impact of microaerophilic Fe(II)-oxidizing bacteria; (B) Calculated abiotic Fe(II)$_{aq}$ oxidation rates (homogeneous + heterogeneous Fe(II) oxidation).

The calculated half-life for Fe(II)$_{aq}$ at circumneutral pH conditions (in our experiments pH 6.8) negatively correlated with O$_2$ concentrations. While the half-life of Fe(II) in fully oxygenated water is <40 minutes, it increased to 4 and 20 hours (depending on O$_2$ and Fe(II)) under low oxygen concentrations (Table 1). Incubations at 30 µM O$_2$ suggest that the shorter the Fe(II) half-lives are, the less bioavailable Fe(II) was over time for microaerophilic Fe(II)-oxidizing bacteria. In contrast, incubations at 10 and 20 µM O$_2$ quantitatively confirmed that 2- and 5-

fold longer Fe(II) half-lives prolonged the persistence of Fe(II) and therefore increased the bioavailability for microaerophilic Fe(II)-oxidizing bacteria and the ability to compete with abiotic Fe(II) oxidation.[16]

Table 1. Half-life of Fe(II)$_{aq}$ [$^{Fe(II)}t_{1/2}$ in hours] at different O_2 concentrations in biotic and abiotic incubations with initial absence of Fe(III) minerals. Uncertainties for calculated Fe(II) half-lives are $\leq \pm 0.08$.

time	$^{Fe(II)}t_{1/2}$ 10 µM O_2		$^{Fe(II)}t_{1/2}$ 20 µM O_2		$^{Fe(II)}t_{1/2}$ 30 µM O_2	
	abiotic	biotic	abiotic	biotic	abiotic	biotic
4	40.2	**23.4**	9.8	**8.1**	4.3	**4.3**
19	11.4	**8.6**	4.5	**3.6**	2.2	**2.2**
26	8.4	**6.9**	3.4	**3.1**	1.8	**2.0**
45	6.4	**5.8**	2.7	**2.6**	1.7	**1.8**
53	5.7	**5.4**	2.6	**2.5**	1.7	**1.7**
67	5.3	**5.1**	2.5	**2.4**	1.7	**1.7**

Incubations at 30 µM O_2 showed a slight increase in cell numbers within the initial 45-hour incubation period. However, the initial cell doubling times were significantly longer compared to incubations at 10 and 20 µM O_2 (Table 2). The increase in cell numbers within the first 45 hours is reflected in the fastest doubling times at all O_2 concentrations (Table 2) that positively correlate to the highest extent in Fe(II) oxidation with only 10% of the initial Fe(II) left in all treatments. After 45 hours, cell doubling times increased around 3-fold to more than 150 hours until the end of the incubation which suggests that cells were potentially limited in Fe(II) bioavailability. At 10 and 20 µM O_2, Fe(II) half-lives were longer and total Fe(II) oxidation rates low enough to detect a biotic impact on total Fe(II) oxidation. The difference in the extent of Fe(II) consumption between abiotic and biotic setups within the initial incubation phase is attributed to microbial Fe(II) turnover.[17] Microbial contribution to Fe(II) oxidation and microbial Fe(II) turnover rates reached a maximum within the initial incubation phase of 26 hours (10 µM and 20 µM O_2: 1.1-8.5 $\cdot$ 10^{-15} and 1.7-3.0 $\cdot$ 10^{-16} mol Fe(II)$_{aq}$ $\cdot$ cell^{-1} $\cdot$ h^{-1}, respectively) (Table 2) and suggest a contribution of up to 40% by microaerophilic bacteria to the overall Fe(III) mineral formation. In agreement with these data, we measured highest cell growth and fastest doubling times (T_d 40-42 h) in setups that were incubated at 20 and 10 µM O_2 (Table 2).

Table 2. Mean cell numbers (and standard deviation) from experimental triplicates, doubling times [T_d] within the initial 45 hours and mean Fe(II)$_{aq}$ oxidation rates per cell [10^{-15} moles cell^{-1} h^{-1}] over the course of incubations at 10, 20 and 30 µM O$_2$ with the initial absence of Fe(III) minerals.

time	10 µM O$_2$			20 µM O$_2$			30 µM O$_2$		
	cell number [10^6 mL^{-1}]	T_d	microb. Fe(II)$_{aq}$ ox. rate	cell number [10^6 mL^{-1}]	T_d	microb. Fe(II)$_{aq}$ ox. rate	cell number [10^6 mL^{-1}]	T_d	microb. Fe(II)$_{aq}$ ox. rate
0	1.96 (±0.06)	41.8	–	2.03 (±0.11)	39.6	–	2.17 (±0.08)	52.1	0.12
19	2.38 (±0.13)		8.53	2.56 (±0.08)		0.31	2.87 (±0.20)		0.04
26	3.12 (±0.18)		2.12	3.46 (±0.26)		0.35	3.12 (±0.23)		*
45	4.13 (±0.48)		1.13	4.46 (±0.52)		0.17	3.95 (±0.42)		*
53	3.92 (±0.21)		0.34	5.01 (±0.41)		0.14	3.62 (±0.36)		0.07
67	4.50 (±0.26)		0.22	4.83 (±0.24)		0.11	4.43 (±0.32)		0.04
75	4.26 (±0.32)		0.09	5.87 (±0.18)		0.09	5.13 (±0.56)		0.02
93	4.48 (±0.14)		*	5.21 (±0.34)		0.15	4.88 (±0.35)		0.01

* could not be calculated due to negative rate; for comparability with table 3: initial (0-26 hours) total Fe(II) oxidation rates (^{ini}v) were calculated for abiotic and biotic setups, respectively (see supporting information).

The setup with the oxalate-washed cells had the benefit of initially decreasing the abiotic heterogeneous Fe(II) oxidation and thus prolonging the bioavailability for the microaerophilic Fe(II)-oxidizing enrichment. However, over time also in these setups Fe(III) minerals formed which initiated the surface-catalyzed reaction and enhanced the autocatalytic heterogeneous Fe(II) oxidation (Figure S6). The increase in abiotic Fe(II) oxidation rates consequently decreased Fe(II) bioavailability and thus increased the pressure on microbial Fe(II) oxidation to compete with abiotic Fe(II) oxidation reactions. These calculated abiotic (heterogeneous and homogeneous) Fe(II) oxidation rates considerably differed between the different O$_2$ treatments in both, the biotic and abiotic control setup. The total abiotic Fe(II) oxidation rate increased threefold from 10 to 30 µM O$_2$ treatments (Figure 2B) while O$_2$ concentrations remained constantly low (Figure S5). Based on equations (2), (4) and (5) for homogeneous and heterogeneous Fe(II) oxidation, homogeneous Fe(II) oxidation was calculated to be the main abiotic oxidation reaction within the first 1-5 hours, while after approx. 5 hours, heterogeneous oxidation dominated (Figure S6). After the initial 26 hours, the abiotic oxidation rates slowed down in all O$_2$ treatments, likely caused by the decrease in Fe(II) availability (the varying factor for homogeneous and heterogeneous rate calculations, see eq. (2) and (4)) (Figure 2B). The shifts in Fe(II) oxidation rates were also reflected in Fe(II) half-life that decreased drastically when Fe(II) oxidation proceeded and heterogeneous oxidation rates accelerated (Figure S6). This decrease in calculated Fe(II) half-lives correlated to increasing

abiotic Fe(II) oxidation rates. Based on these calculated abiotic rates, a maximum Fe(II) turnover of approx. 30-90 µM Fe(II) h^{-1} at O$_2$ concentrations of 10-30 µM O$_2$ can theoretically be reached, which is approx. 20% more compared to the measured data. The slower abiotic oxidation rates that were determined experimentally might be attributed to altered surface properties of the ferric precipitates formed during oxidation in the presence of microbial biomass. Freshly formed low crystalline minerals have high affinity to attach to cell surfaces and EPS,[35] resulting in the formation of mineral aggregates,[36] lowering the number of active mineral surface sites,[37,38] and thus, decreasing the reaction rate.[9]

Our data on the oxidation of Fe(II) in our biotic and abiotic incubations suggests that the microbial contribution to Fe(II)$_{aq}$ oxidation reaches a minimum at O$_2$ 30 µM (Figure 4). However, different to Krepski et al. (2013) who did not observe microbial growth at O$_2$ concentrations >29 µm O$_2$, we noted an increase in cell numbers (Figure S3) which suggests that cells were still able to grow although contribution to Fe(II) oxidation was lower compared to incubations at 10 and 20 µM O$_2$.[39] Emerson & Moyer (1997) and Neubauer et al., (2002) roughly estimated optimum O$_2$ conditions at 5-14 µM O$_2$ for a microaerophilic *Sideroxydans* spp. strain, the closest identity to the enrichment culture used in the current study (99.6% 16S rRNA sequence identity), being in agreement with our measurements that showed best growth, shortest doubling times and highest microbial Fe(II) oxidation between 10 and 20 µM O$_2$.[5,14]

The cell doubling times observed in the current study are relatively long but still comparable with reported values for *Sideroxydans* spp. by Weiss et al., (2007); Druschel et al., (2008) and Haedrich et al.,(2019).[16,40,41] That indicates that cells were potentially not growing optimally but still metabolically active to enhance Fe(II) oxidation. This in turn suggests, that the reported data on the extent of microbial Fe(II) oxidation might represent only minimal estimates on what the contribution under optimized conditions might be. However, in micro-oxic environments, where habitat parameters are often not at the physiological optimum for microbial communities, the reported Fe(II) turnover rates help to quantitatively estimate the microaerophilic contribution to Fe(II) oxidation for a wide range of micro-oxic (10-30 µM O$_2$) conditions.

In addition to the obtained information about Fe(II) oxidation rates, the developed experimental setup (Figure 1) offers the possibility to cultivate microaerophilic Fe(II)-oxidizing bacteria in a non-gradient based liquid microcosm at constantly low O$_2$ levels. The microaerophilic Fe(II)-oxidizing enrichment culture was successfully transferred for currently more than 38 transfers using the presented approach. The classical cultivation procedure using gradient tubes works perfectly well for isolation of microaerophilic Fe(II)-oxidizing

bacteria.[14,40] However, cultivation in liquid culture is essential to quantify microbial turnover rates and to assess their impact on the iron cycle under micro-oxic conditions.

Effect of mineral surfaces on Fe(II) oxidation kinetics. Several studies hypothesized and demonstrated that the surface-catalyzed heterogeneous Fe(II) oxidation can not only accelerate the abiotic Fe(II) oxidation but also decrease the relative amount of Fe(II) available for microaerophilic Fe(II)-oxidizing microorganisms.[5,9,14,33] Thus far, only a few studies attempted to quantify to which extent microbial Fe(II) oxidation can be outcompeted by the autocatalyzed abiotic heterogeneous Fe(II) oxidation in the presence of mineral surfaces.[5-17,34] The simultaneous occurrence of microbial, abiotic homogeneous and abiotic heterogeneous Fe(II) oxidation calls for a reliable experimental setup in which the individual contributions to Fe(III) mineral formation can be quantified in liquid culture. The method presented here enabled us to confirm the hypothesis that Fe(II) availability for microaerophilic Fe(II)-oxidizing bacteria can be limited due to the acceleration of the abiotic heterogeneous Fe(II) oxidation due to the presence of Fe(III) minerals.[5,15,30] Moreover, we could quantify to which extent the contribution of biotic and abiotic Fe(II) oxidation to mineral formation is controlled by i) the O_2 concentration and ii) the presence of ferric mineral catalytic surfaces. Mineral particles that were produced and associated with cells during pre-cultivation were identified as ferrihydrite (Mössbauer spectroscopy, Figure S3). In order to quantify the effect of these (bio)minerals on the overall Fe(II) oxidation kinetics, the microaerophilic Fe(II)-oxidizing enrichment culture was incubated in the initial absence and presence of ferrihydrite mineral particles at 10 µM O_2 and approx. 800 µM Fe(II)$_{aq}$. Within the initial 22-hour incubation phase, the overall extent of Fe(II) being oxidized increased significantly from less than 75% in biotic incubations with oxalate-washed cells compared to more than 80% when cells were not washed and ferrihydrite minerals from pre-cultivation were still present (Figure 3A).
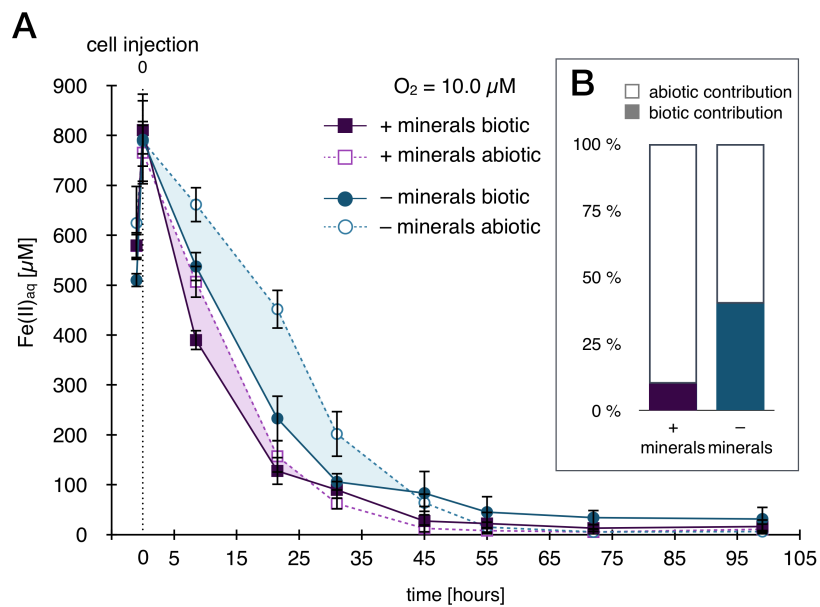
Figure 3. (A) $Fe(II)_{aq}$ oxidation in the presence and absence of initial abiogenic/biogenic ferrihydrite minerals in biotic and abiotic incubations of cells by a microaerophilic Fe(II)-oxidizing enrichment culture at 10 µM O_2; error bars represent standard deviations from experimental triplicates. (B) Relative biotic and abiotic contribution to total Fe(II) oxidation during the incubation at 10 µM O_2 in the presence and absence of initial a/biogenic ferrihydrite minerals.

Table 3. $Fe(II)_{aq}$ oxidation kinetics in biotic and abiotic incubations at 10 µM O_2 in the presence and absence of initial abiogenic/biogenic ferrihydrite minerals. ^{ini}v – Fe(II) oxidation rate, simple linear fitting results (0-22 hours) in abiotic ($^{ini}v_{abio}$) and biotic ($^{ini}v_{bio}$) incubations (r^2 – coefficient of determination).

$Fe(II)_{aq}$ oxidation [µM Fe(II) · h^{-1}]	+ minerals	– minerals
$^{ini}v_{abio}$ (r^2)	28.1 (0.83)	15.7 (0.90)
$^{ini}v_{bio}$ (r^2)	30.8 (0.85)	25.8 (0.94)

Differences in Fe(II) concentrations between biotic and abiotic incubations using non-oxalate washed cells showed only a maximum of 10% faster Fe(II) oxidation in biotic incubations within the initial 22 hours of incubation (Table 3). In contrast to that, the microbial contribution to total Fe(II) oxidation was by approx. 40% considerably higher (p<0.05) when no minerals from pre-cultivation were present compared to treatments where iron minerals were not removed prior to incubation, as already shown for the previous 10 µM O_2 setup. This is also reflected in the initial Fe(II) oxidation kinetics (Table 3), where abiotic Fe(II) oxidation rates in mineral-free treatments were slower (compared to unwashed setups) and a significantly faster

biotic Fe(II) oxidation rate. This demonstrated that the presence of ferric (oxyhydr)oxide mineral particles, as a metabolic product of microaerophilic Fe(II)-oxidizing bacteria and as a reaction product of the abiotic Fe(II) oxidation, not only most dominantly accelerated the overall (and mainly surface-catalytic) Fe(II) oxidation in biotic and abiotic setups,[31] but also decreased the microbial contribution to Fe(II) oxidation to only 10% on average within the initial 22-hour incubation phase (Figure 3B). The rate of total Fe(II)$_{aq}$ oxidation in the abiotic setup was almost 2-fold faster within these initial 22 hours in the presence of minerals compared to the abiotic treatment that was incubated with inactivated cells that did not carry any mineral residues from pre-cultivation (Table 3).

Lower oxygen threshold concentrations for microbial contribution to Fe(II) oxidation. Incubations at 1 and 5 µM O_2 with oxalate-washed cells address an open question raised in Chan et al. (2016):[13] *What is the lower O_2 concentration limit of microbial Fe oxidation?* Different from gradient-based cultivation systems, where cells seek for their ideal growth conditions, the presented method allows to adjust O_2 concentrations to a minimum that still enables them to metabolically oxidize Fe(II) under O_2-limiting conditions. The O_2 concentrations during the incubations were at the lower microoxic end, allowing Fe(II)$_{aq}$ generally to persist longer compared to incubations at higher O_2. With respect to Fe(II) oxidation, no clear distinction between abiotic and biotic Fe(II) oxidation rates were measured at 1 µM O_2 and 5 µM O_2 (Figure S7). After 30 hours mean Fe(II)$_{aq}$ concentrations were approx. 5% lower in biotic active setups incubated at 5 µM O_2 compared to abiotic controls. However, this insignificant difference suggests that microbial contribution to total Fe(II) oxidation was considerably low (<5%) at these low O_2 concentrations. Taking into account the increase in cell density within 96 hours from initially 1.11×10^6 to 4.60×10^6 mL^{-1} at 5 µM O_2 and from 1.07×10^6 to 3.97×10^6 ml^{-1} at 1 µM O_2 (Table S2), respectively indicates some microbial activity. However, cell growth and doubling times were comparatively low as against incubations at 10 and 20 µM O_2 (Table 2 & Table S2). These data suggest that cells were potentially limited in O_2 availability at such low (1-5 µM O_2) concentrations. However, the observed growth under these conditions and viable transfers from these setups imply that cells were still active and able to reproduce. At 5-10 µM O_2, microbial Fe(II) oxidation of this culture became more dominant compared to abiotic Fe(II) oxidation, allowing bacteria to contribute by up to 40% to total Fe(II) oxidation and mineral formation (Figure 4).

With the set of experiments that is presented in this study, we were able to quantify that the biotic impact on Fe(II) oxidation is less than 5% at 1 and 5 µM O_2 and micro-oxic (30 µM O_2) O_2 concentrations, it significantly increased to approx. 40% at 10 and 20 µM O_2 (Figure 4) when surface-catalyzing minerals were absent. When Fe(III) minerals were present and served

as a catalyst for heterogeneous, abiotic Fe(II) oxidation the biotic contribution strikingly decreased but still remained detectable by approx. 10% (Figure 3A/B).
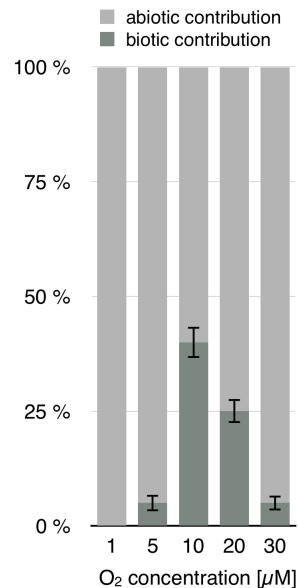
Figure 4. Relative abiotic and biotic contribution to total Fe(II)$_{aq}$ oxidation during incubations of a microaerophilic Fe(II)-oxidizing enrichment culture at an initial Fe(II)$_{aq}$ concentration of 600-800 µM and variable O$_2$ concentrations ranging from 1-30 µM in the absence of initial abiogenic or biogenic ferrihydrite minerals; error bars represent mean absolute deviations from triplicates.

Implications. The current study provides a description of an experimental setup that allows to quantify microaerophilic Fe(II) oxidation rates and to compare them to abiotic Fe(II) oxidation. The presented setup allows to grow microaerophilic Fe(II)-oxidizing bacteria in liquid culture. So far, quantitative liquid culture microcosm setups have not been successful for microaerophilic Fe(II)-oxidizing bacteria, as constantly low O$_2$ concentrations are difficult to sustain and heterogeneous Fe(II) oxidation dominated due to large cultivation volumes. Due to relatively small liquid volumes in our setups, the relatively large surface to medium area and an extensive headspace volume, O$_2$ gradients do not establish in a very defined way in the culture medium, while O$_2$ concentrations remained constant over the course of the incubations. Performing inoculation with oxalate-washed cell cultures minimizes initial heterogeneous Fe(II) oxidation and allows to distinguish between abiotic and biotic Fe(II) oxidation rates. The quantification of maximum oxidation rates for microbial Fe(II) turnover under optimized and laboratory-controlled conditions can help to understand the impact

microaerophilic bacteria can have on the environmental iron cycle. Moreover, the presented approach can be readily applied to characterize isolated and mutant strains deficient in putative genes that regulate Fe(II) oxidation or to assess the relative contribution of different members of a consortium to total Fe(II) oxidation under varying Fe(II) and O_2 concentrations. Although heterogeneous Fe(II) oxidation may be the key driver for Fe(II) oxidation in many natural habitats when O_2 is present, microaerophilic Fe(II)-oxidizing bacteria may still be able to compete for Fe(II) oxidation i) when Fe(II) is continuously formed e.g. by Fe(III)-reducing organisms that inhabit the same environmental niche[26,42] or ii) Fe(II) is constantly supplied to the open system e.g. at hydrothermal vents.[6,43] Providing a method not only to quantify the Fe(II) turnover at variable and constant O_2 conditions, our approach represents a quantitative method for a separation of biotic and abiotic Fe(II) oxidation rates, as well as for the accurate characterization of the optimum O_2 range for microaerophilic Fe(II)-oxidizing bacteria.

2.5 References

1. Melton, E. D.; Swanner, E. D.; Behrens, S.; Schmidt, C.; Kappler, A., The interplay of microbially mediated and abiotic reactions in the biogeochemical Fe cycle. *Nat Rev Microbiol* **2014,** *12*, (12), 797-808.

2. Laufer, K.; Nordhoff, M.; Halama, M.; Martinez, R. E.; Obst, M.; Nowak, M.; Stryhanyuk, H.; Richnow, H. H.; Kappler, A., Microaerophilic Fe(II)-Oxidizing Zetaproteobacteria Isolated from Low-Fe Marine Coastal Sediments: Physiology and Composition of Their Twisted Stalks. *Appl Environ Microb* **2017,** *83*, (8).

3. Roden, E. E., Microbial iron-redox cycling in subsurface environments. *Biochem Soc T* **2012,** *40*, 1249-1256.

4. Emerson, D.; Weiss, J. V.; Megonigal, J. P., Iron-oxidizing bacteria are associated with ferric hydroxide precipitates (Fe-plaque) on the roots of wetland plants. *Appl Environ Microb* **1999,** *65*, (6), 2758-2761.

5. Neubauer, S. C.; Emerson, D.; Megonigal, J. P., Life at the energetic edge: Kinetics of circumneutral iron oxidation by lithotrophic iron-oxidizing bacteria isolated from the wetland-plant rhizosphere. *Appl Environ Microb* **2002,** *68*, (8), 3988-3995.

6. Emerson, D.; Moyer, C. L., Neutrophilic Fe-Oxidizing bacteria are abundant at the Loihi Seamount hydrothermal vents and play a major role in Fe oxide deposition. *Appl Environ Microb* **2002,** *68*, (6), 3085-3093.

7. Videla, H. A.; Characklis, W. G., Biofouling and Microbially Influenced Corrosion. *Int Biodeter Biodegr* **1992,** *29*, (3-4), 195-212.

8. Ray, A. J.; Seaborn, G.; Leffler, J. W.; Wilde, S. B.; Lawson, A.; Browdy, C. L., Characterization of microbial communities in minimal-exchange, intensive aquaculture systems and the effects of suspended solids management. *Aquaculture* **2010,** *310*, (1-2), 130-138.

9. Tamura, H.; Goto, K.; Nagayama, M., The effect of ferric hydroxide on the oxygenation of ferrous ions in neutral solutions. *Corrosion Science* **1976,** *16*, (4), 197-207.

10. Cornell, R. M.; Schwertmann, U., *The iron oxides: structure, properties, reactions, occurrences and uses*. John Wiley & Sons: 2003.

11. Emerson, D.; Fleming, E. J.; McBeth, J. M., Iron-Oxidizing Bacteria: An Environmental and Genomic Perspective. *Annu Rev Microbiol* **2010,** *64*, 561-583.

12. Emerson, D.; Roden, E.; Twining, B. S., The microbial ferrous wheel: iron cycling in terrestrial, freshwater and marine environments. *Front Microbiol* **2012,** *3*.

13. Chan, C. S.; Emerson, D.; Luther, G. W., The role of microaerophilic Fe-oxidizing micro-organisms in producing banded iron formations. *Geobiology* **2016,** *14*, (5), 509-528.

14. Emerson, D.; Moyer, C., Isolation and characterization of novel iron-oxidizing bacteria that grow at circumneutral pH. *Appl Environ Microb* **1997,** *63*, (12), 4784-4792.

15. Rentz, J. A.; Kraiya, C.; Luther, G. W.; Emerson, D., Control of ferrous iron oxidation within circumneutral microbial iron mats by cellular activity and autocatalysis. *Environ Sci Technol* **2007,** *41*, (17), 6084-6089.

16. Druschel, G. K.; Emerson, D.; Sutka, R.; Suchecki, P.; Luther, G. W., Low-oxygen and chemical kinetic constraints on the geochemical niche of neutrophilic iron(II) oxidizing microorganisms. *Geochim Cosmochim Ac* **2008,** *72*, (14), 3358-3370.

17. Lueder, U.; Druschel, G.; Emerson, D.; Kappler, A.; Schmidt, C., Quantitative analysis of O-2 and Fe2+ profiles in gradient tubes for cultivation of microaerophilic Iron(II)-oxidizing bacteria. *Fems Microbiol Ecol* **2018,** *94*, (2).

18. Ionescu, D.; Heim, C.; Polerecky, L.; Thiel, V.; De Beer, D., Biotic and abiotic oxidation and reduction of iron at circumneutral pH are inseparable processes under natural conditions. *Geomicrobiol J* **2015,** *32*, (3-4), 221-230.

19. Vollrath, S.; Behrends, T.; Van Cappellen, P., Oxygen Dependency of Neutrophilic Fe(II) Oxidation by Leptothrix Differs from Abiotic Reaction. *Geomicrobiol J* **2012,** *29*, (6), 550-560.

20. Emerson, D.; Revsbech, N. P., Investigation of an Iron-Oxidizing Microbial Mat Community Located near Aarhus, Denmark - Laboratory Studies. *Appl Environ Microb* **1994,** *60*, (11), 4032-4038.

21. Sobolev, D.; Roden, E. E., Characterization of a neutrophilic, chemolithoautotrophic Fe(II)-oxidizing beta-proteobacterium from freshwater wetland sediments. *Geomicrobiol J* **2004,** *21*, (1), 1-10.

22. Ludecke, C.; Reiche, M.; Eusterhues, K.; Nietzsche, S.; Kusel, K., Acid-tolerant microaerophilic Fe(II)-oxidizing bacteria promote Fe(III)-accumulation in a fen. *Environ Microbiol* **2010,** *12*, (10), 2814-2825.

23. Muhling, M.; Poehlein, A.; Stuhr, A.; Voitel, M.; Daniel, R.; Schlomann, M., Reconstruction of the Metabolic Potential of Acidophilic Sideroxydans Strains from the Metagenome of an Microaerophilic Enrichment Culture of Acidophilic Iron-Oxidizing

Bacteria from a Pilot Plant for the Treatment of Acid Mine Drainage Reveals Metabolic Versatility and Adaptation to Life at Low pH. *Front Microbiol* **2016,** *7*.

24.   Kucera, S.; Wolfe, R. S., A selective enrichment method for Gallionella ferruginea. *J Bacteriol* **1957,** *74*, (3), 344-349.

25.   Rosson, R. A.; Tebo, B. M.; Nealson, K. H., Use of Poisons in Determination of Microbial Manganese Binding Rates in Seawater. *Appl Environ Microb* **1984,** *47*, (4), 740-745.

26.   Laufer, K.; Nordhoff, M.; Roy, H.; Schmidt, C.; Behrens, S.; Jorgensen, B. B.; Kappler, A., Coexistence of Microaerophilic, Nitrate-Reducing, and Phototrophic Fe(II) Oxidizers and Fe(III) Reducers in Coastal Marine Sediment. *Appl Environ Microb* **2016,** *82*, (5), 1433-1447.

27.   Maisch, M.; Wu, W. F.; Kappler, A.; Swanner, E. D., Laboratory Simulation of an Iron(II)-rich Precambrian Marine Upwelling System to Explore the Growth of Photosynthetic Bacteria. *Jove-J Vis Exp* **2016**, (113).

28.   Stookey, L. L., Ferrozine - a New Spectrophotometric Reagent for Iron. *Anal Chem* **1970,** *42*, (7), 779-&.

29.   Roden, E. E.; Sobolev, D.; Glazer, B.; Luther, G. W., Potential for microscale bacterial Fe redox cycling at the aerobic-anaerobic interface. *Geomicrobiol J* **2004,** *21*, (6), 379-391.

30.   Tamura, H.; Kawamura, S.; Hagayama, M., Acceleration of the Oxidation of Fe-2+ Ions by Fe(Iii)-Oxyhydroxides. *Corrosion Science* **1980,** *20*, (8-9), 963-971.

31.   Sung, W.; Morgan, J. J., Kinetics and Product of Ferrous Iron Oxygenation in Aqueous Systems. *Environ Sci Technol* **1980,** *14*, (5), 561-568.

32.   Emerson, D.; McAllister, S. M.; Chan, C.; Fleming, E.; Moyer, C., Emerging patterns in deep-sea microbial iron mats. *Geochim Cosmochim Ac* **2010,** *74*, (12), A265-A265.

33.   Chan, C. S.; Fakra, S. C.; Emerson, D.; Fleming, E. J.; Edwards, K. J., Lithotrophic iron-oxidizing bacteria produce organic stalks to control mineral growth: implications for biosignature formation. *Isme J* **2011,** *5*, (4), 717-727.

34.   Emerson, D.; Scott, J. J.; Leavitt, A.; Fleming, E.; Moyer, C., In situ estimates of iron-oxidation and accretion rates for iron-oxidizing bacterial mats at Loihi Seamount. *Deep-Sea Res Pt I* **2017,** *126*, 31-39.

35.   Hao, L. K.; Li, J. L.; Kappler, A.; Obst, M., Mapping of Heavy Metal Ion Sorption to Cell-Extracellular Polymeric Substance-Mineral Aggregates by Using Metal-Selective

Fluorescent Probes and Confocal Laser Scanning Microscopy. *Appl Environ Microb* **2013,** *79*, (21), 6524-6534.

36. Chatellier, X.; Fortin, D.; West, M. M.; Leppard, G. G.; Ferris, F. G., Effect of the presence of bacterial surfaces during the synthesis of Fe oxides by oxidation of ferrous ions. *Eur J Mineral* **2001,** *13*, (4), 705-714.

37. Hansel, C. M.; Benner, S. G.; Fendorf, S., Competing Fe(II)-induced mineralization pathways of ferrihydrite. *Environ Sci Technol* **2005,** *39*, (18), 7147-7153.

38. Mikutta, C.; Mikutta, R.; Bonneville, S.; Wagner, F.; Voegelin, A.; Christl, I.; Kretzschmar, R., Synthetic coprecipitates of exopolysaccharides and ferrihydrite. Part I: Characterization. *Geochim Cosmochim Ac* **2008,** *72*, (4), 1111-1127.

39. Krepski, S. T.; Emerson, D.; Hredzak-Showalter, P. L.; Luther, G. W.; Chan, C. S., Morphology of biogenic iron oxides records microbial physiology and environmental conditions: toward interpreting iron microfossils. *Geobiology* **2013,** *11*, (5), 457-471.

40. Weiss, J. V.; Rentz, J. A.; Plaia, T.; Neubauer, S. C.; Merrill-Floyd, M.; Lilburn, T.; Bradburne, C.; Megonigal, J. P.; Emerson, D., Characterization of neutrophilic Fe(II)-oxidizing bacteria isolated from the rhizosphere of wetland plants and description of Ferritrophicum radicicola gen. nov sp nov., and Sideroxydans paludicola sp nov. *Geomicrobiol J* **2007,** *24*, (7-8), 559-570.

41. Hädrich, A.; Taillefert, M.; Akob, D. M.; Cooper, R. E.; Litzba, U.; Wagner, F. E.; Nietzsche, S.; Ciobota, V.; Rösch, P.; Popp, J.; Küsel, K., Microbial Fe(II) oxidation by Sideroxydans lithotrophicus ES-1 in the presence of Schlöppnerbrunnen fen-derived humic acids. *Fems Microbiol Ecol* **2019,** *95*, (4).

42. Otte, J. M.; Harter, J.; Laufer, K.; Blackwell, N.; Straub, D.; Kappler, A.; Kleindienst, S., The distribution of active iron-cycling bacteria in marine and freshwater sediments is decoupled from geochemical gradients. *Environ Microbiol* **2018,** *20*, (7), 2483-2499.

43. Chan, C. S.; McAllister, S. M.; Leavitt, A. H.; Glazer, B. T.; Krepski, S. T.; Emerson, D., The Architecture of Iron Microbial Mats Reflects the Adaptation of Chemolithotrophic Iron Oxidation in Freshwater and Marine Environments. *Front Microbiol* **2016,** *7*.

2.6   Supporting Information

54

Contribution of Microaerophilic Iron(II)-Oxidizers to Iron(III) Mineral Formation

Markus Maisch[1], Ulf Lueder[1], Katja Laufer[2], Caroline Scholze[2], Andreas Kappler[1,2], Caroline Schmidt[1]

[1] Geomicrobiology, Center for Applied Geosciences, University of Tübingen, Germany

[2] Department for Bioscience, Aarhus University, Denmark

Number of tables in supporting information: 2

Number of figures in supporting information: 7

Total numbers of pages in supporting information: 13 (including cover page)

Culture preparation. A microaerophilic Fe(II)-oxidizing enrichment culture (99.6% similarity to *Sideroxydans* spp. based on 16s rRNA) was obtained from a rice paddy soil (Vercelli, Italy) following the procedure described in Laufer et al. (2017).[1] Once isolated/enriched, the culture was pre-grown on zero-valent iron (ZVI) powder[2] (200-mesh, metal basis, Alfa Aesar, Ward Hill, MA) using Modified Wolfe's Mineral Medium (MWMM) buffered at pH 6.8 with $NaHCO_3$ (22 mM) and 1 mL per liter of sterile additive solutions: vitamins (7-Vitamine solution),[3] trace elements (SL-10)[4] and selenite tungstate solution.[5] Inoculated ZVI plates were incubated in the dark at 24°C for 14 days prior to the experiment. Cells were harvested under anoxic atmosphere (100% N_2), collected in centrifuge tubes and washed with sterile and anoxic $NaHCO_3$ (10 mM) buffer solution by centrifugation at 2,100 rpm (Eppendorf MiniSpin, 12-place fixed angle rotor, rotor diameter 12 cm). We intentionally chose the rather slow centrifugation speed of 2,100 rpm to prevent shearing stress to bacteria in the presence of iron mineral particles.

Medium preparation. For the setup of the miniaturized microcosms, Modified Wolfe's Mineral Medium (MWMM) was prepared as stated above. $Fe(II)_{aq}$ concentration was adjusted to the desired range by injecting sterile anoxic 1M $Fe(II)_{aq}$ solution prepared from $FeCl_2$ (Cl_2Fe * $4H_2O$, Merck KGaA, Darmstadt, Germany). The medium was stored in dark at 4°C to allow precipitation of Fe(II) carbonate and phosphate minerals for 24 hours and consecutively filtered (0.22 µm Steritop filter unit, Merck KGaA, Darmstadt, Germany) in an anoxic glovebox (100% N_2) into sterile stock bottles. Sterile additives (stated above) were added after filtration to prevent removal of any trace metals or vitamins by filtration (removal of precipitated Fe(II) carbonate and phosphate minerals) and the headspace was exchanged to N_2/CO_2 (v/v, 90/10).

Oxalate washing and cell viability. In order to measure the influence of initially present ferric biominerals associated with inoculum on the Fe(II) oxidation kinetics, the inoculum (before washing, Fig. S1a) was washed for 2 minutes in 0.1% oxalate solution (pH 4.0) and cell viability was verified by dead-live (D/L) staining (Fig. S1b). Shorter washing duration resulted in incomplete dissolution of associated ferric biominerals (SI Figure S1c) and longer washing duration resulted in cell death (Fig. S1d). After the cell washing procedure with oxalate, small particle-like substances remained present. These particles were proven to not contain any significant amount of iron (tested by 1M HCl extraction and Ferrozine assay for Fe(total) quantification, data not shown).
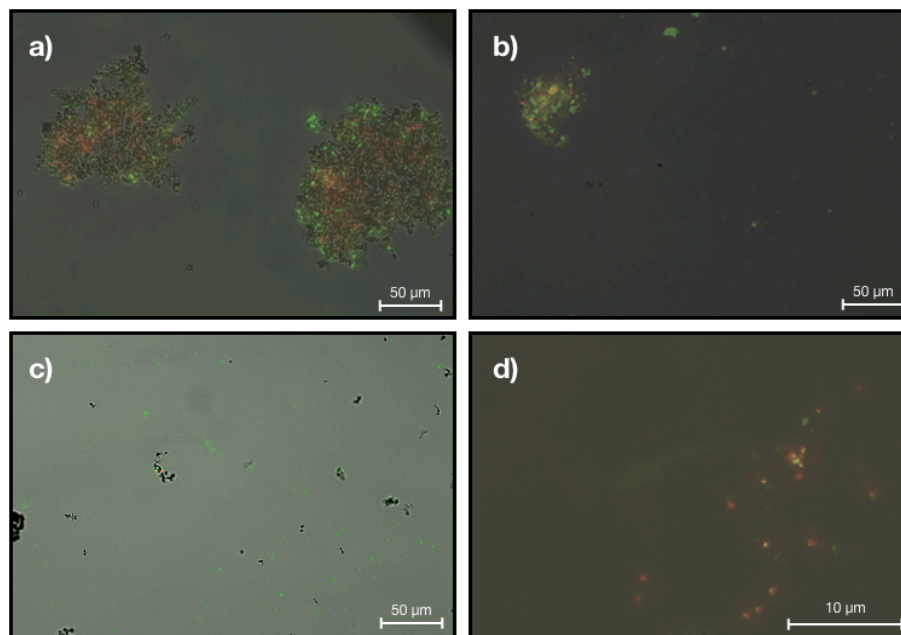
Figure S1. Fluorescence microscopy images of microaerophilic Fe(II)-oxidizing enrichment culture, taken (a) before washing procedure with 0.1% oxalate solution: cell mineral aggregates visible, (b) after 2-minutes washing: most cells viable (green) but no minerals being left (c) after 1-minute washing: cells detached but still some mineral particles left, and (d) after 3-minutes washing: cells detached but mostly dead or damaged (red).

Growth conditions for microaerophilic Fe(II)-oxidizing enrichment culture. Growth of the microaerophilic Fe(II)-oxidizing enrichment culture in FeS gradient tubes was visible after three days (Fig. S2) via a distinct growth band. The abiotic control tube showed a diffusive orange layer indicating abiotic Fe(II) oxidation. Vertical Fe(II)$_{aq}$ and O$_2$ profiles showed opposing gradients of increasing Fe(II)$_{aq}$ towards the bottom and increasing O$_2$ towards the upper part in the gradient tube. Fe(II) concentrations reached approx. 1000 µM in the position of the growth band after 2 days and stayed constant until day 6. The expansion of the growth band was constrained to a very narrow zone where concentrations of O$_2$ stayed constantly below 40 µM at the upper end of the growth band and reached lowest concentrations of 0.3 µM at the lower end. Fe(II) concentrations below 15 mm depth were considerably lower in inoculated tubes compared to the control while O$_2$ profiles did not show clear differences between active and control gradient tubes.

The measured O$_2$ concentrations in gradient tubes were considered as optimum O$_2$ concentrations and adjusted in liquid culture miniaturized microcosms. The obtained results suggested that the microaerophilic Fe(II)-oxidizing enrichment culture used in the current study had optimum O$_2$ concentrations from 10-20 µM O$_2$ where cells contributed most (up to 40%) to the overall Fe(II) oxidation.
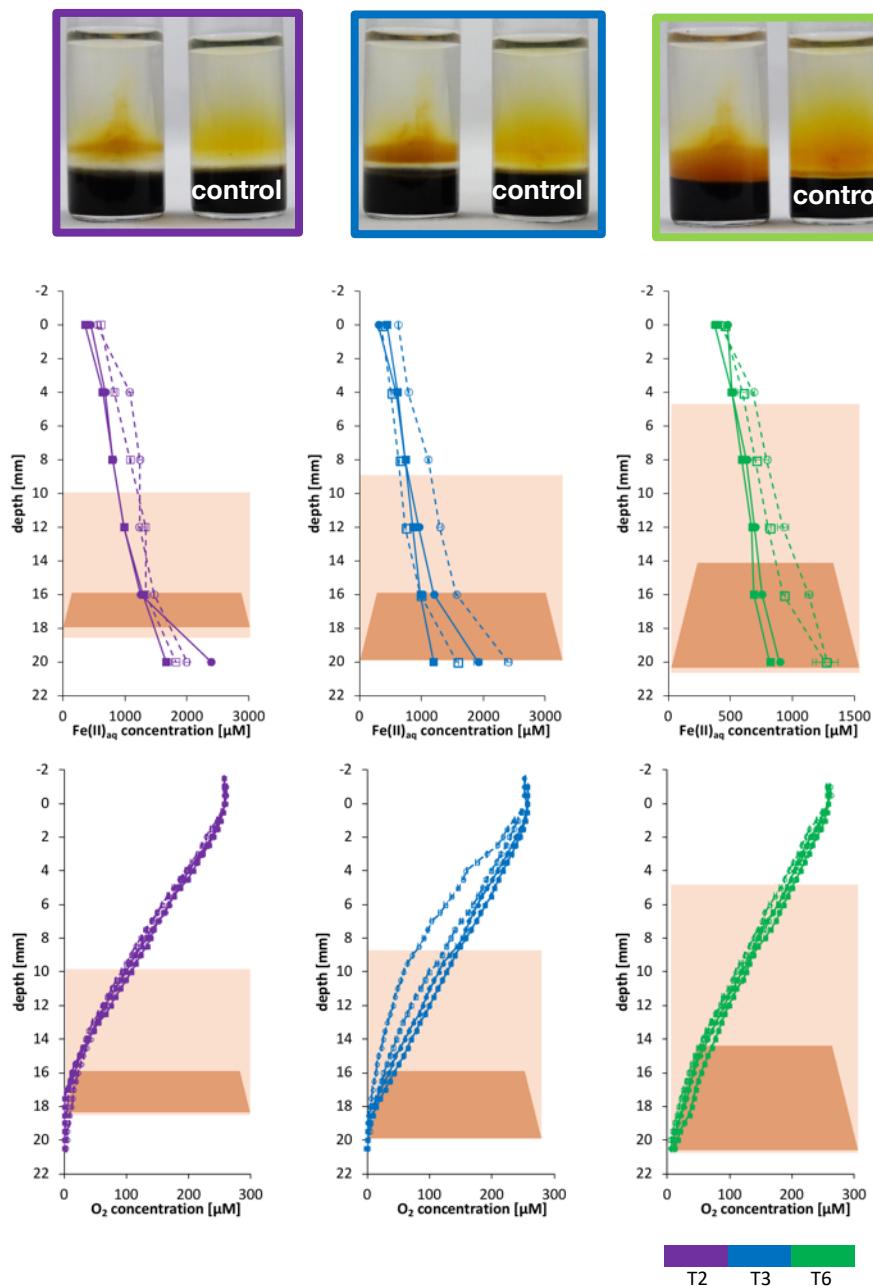
Figure S2. Microaerophilic Fe(II)-oxidizing enrichment culture growing on FeS gradient tubes, after 2 days (purple), 3 days (blue) and 6 days (green) and a control (right tube). Vertical profiles of Fe(II)$_{aq}$ and O$_2$ demonstrate diffusing opposing gradients in the tube (biotic: closed circle, straight line; control: open circle, dashed line). Growth (indicated by orange pattern) was observed in zones where O$_2$ concentrations were <40 µM and Fe(II)$_{aq}$ at approx. 1000 µM.

Mössbauer spectroscopy

Sample preparation. Iron minerals in unwashed biotic and control incubations were identified by Mössbauer spectroscopy prior and at the end of the experiment. Iron minerals in setups with oxalate-prewashed cells were identified only at the end of the incubations

(since there was not enough sample material to be analyzed prior to incubation). Under anoxic conditions (100% N_2), mineral slurries were filtered onto a cellulose filter (diam. 1 cm, mesh size 0.45 µm) and covered with Kepton tape forming a thin disc. Stored at -20 °C these samples were kept frozen before loading into a closed-cycle exchange gas cryostat (Janis cryogenics) in order to minimize mineral transformation or ripening. Transmission spectra were collected at 77 K using a constant acceleration drive system (WissEL) in transmission mode with a ^{57}Co/Rh source. All spectra were calibrated against a 7 µm thick α-^{57}Fe foil that was measured at room temperature. Analysis was carried out using Recoil (University of Ottawa) and the Voigt Based Fitting (VBF) routine[6]. The half width at half maximum (HWHM) was constrained to 0.128 mm/s during fitting.

Results. All spectra collected at 77 K were characterized by a well pronounced doublet (Db) feature (Figure S3) and a relatively dominant background noise. The best fit for all spectra using a 1-fit model resulted in compiled site properties listed in table S1. The Db feature in all samples showed very similar hyperfine field parameters with a center shift (CS) ranging from CS = 0.45 – 0.48 mm/s and a quadrupole splitting (ΔE_q) ranging from ΔE_q = 0.66 – 0.71 mm/s. These parameters can be attributed to the presence of octahedrally coordinated poorly crystalline (short range ordered) Fe(III)-(oxyhydr)oxides, similar to ferrihydrite[7]. Figure S3 shows the sample collected at the end of the incubation with oxalate-washed cells and was considered as representative for all spectra collected. The relatively dominant background noise is due to the low sample amount that could be collected for spectroscopy analyses which resulted in a low signal-to-noise ratio.
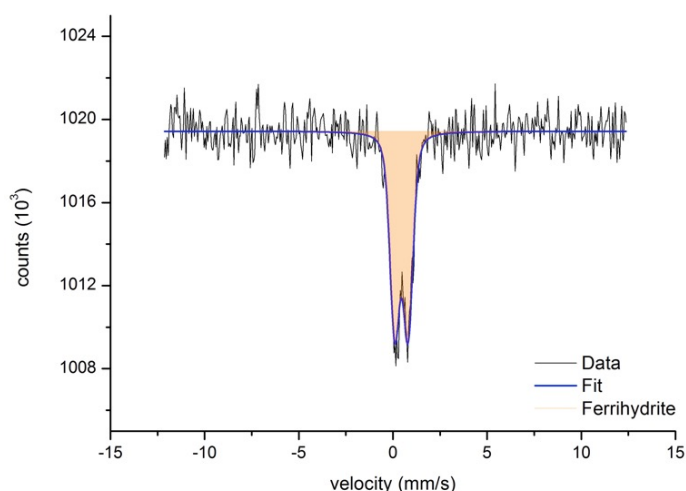
Figure S3. Mössbauer spectrum collected at 77 K from sample at the end of the incubation with oxalate-washed cells incubated at 10 µM O_2

Table S1. Hyperfine field parameters of Mössbauer spectra collected at 77 K for samples from incubations with oxalate-washed and unwashed cells incubated at 10 µM O_2

Sample	Phase	CS (mm/s)	ΔE_q (mm/s)	χ^2	Identified mineral
wash t_{end}	Db	0.48	0.71	0.5	Fh
unwash t_0	Db	0.47	0.66	0.6	Fh
unwash t_{end}	Db	0.45	0.70	0.8	Fh

wash t_{end} – samples from setups with oxalate-washed cells at the end of the incubation. unwash t_0/t_{end} – samples from setups with unwashed cells prior (t_0) and at the end (t_{end}) of the incubation. All spectra are characterized by a narrow doublet feature most likely to represent ferrihydrite. CS – Center shift, ΔEq – Quadrupole splitting, $\chi2$ – goodness of fit, Fh – ferrihydrite

Cell quantification

Cell numbers were quantified using constant-sheath flow cytometry (flow-cytometer). Cell samples were stained with 15 µL SYTO9 for quantification of total cell numbers. Sterile $NaHCO_3$ buffer solution (10 mM) was added for sample dilution prior to analysis.

Statistical treatment

Experimental incubations for each treatment (1, 5, 10, 20 and 30 µM O_2; with un/-washed cells) were set up in triplicates. Technical analyzes were performed in triplicates and standard errors were considered for data treatment. Where possible, an unpaired t-test was performed to decipher whether treatments (by means, standard deviation based on two degrees of freedom) fulfill the null hypothesis (H_0) and can be considered as statistically not different. A significance level of 5% (alpha=0.05) was set as the probability for a type I error and the rejection of the null hypothesis. If $p < 0.05$, H_0 was rejected and differences between sample means between treatments were considered as significantly different. If $p > 0.05$, H_0 was true and sample means between treatments were considered as not statistically different.

Fe(II) oxidation & cell numbers for incubations at 10, 20 and 30 µM O₂
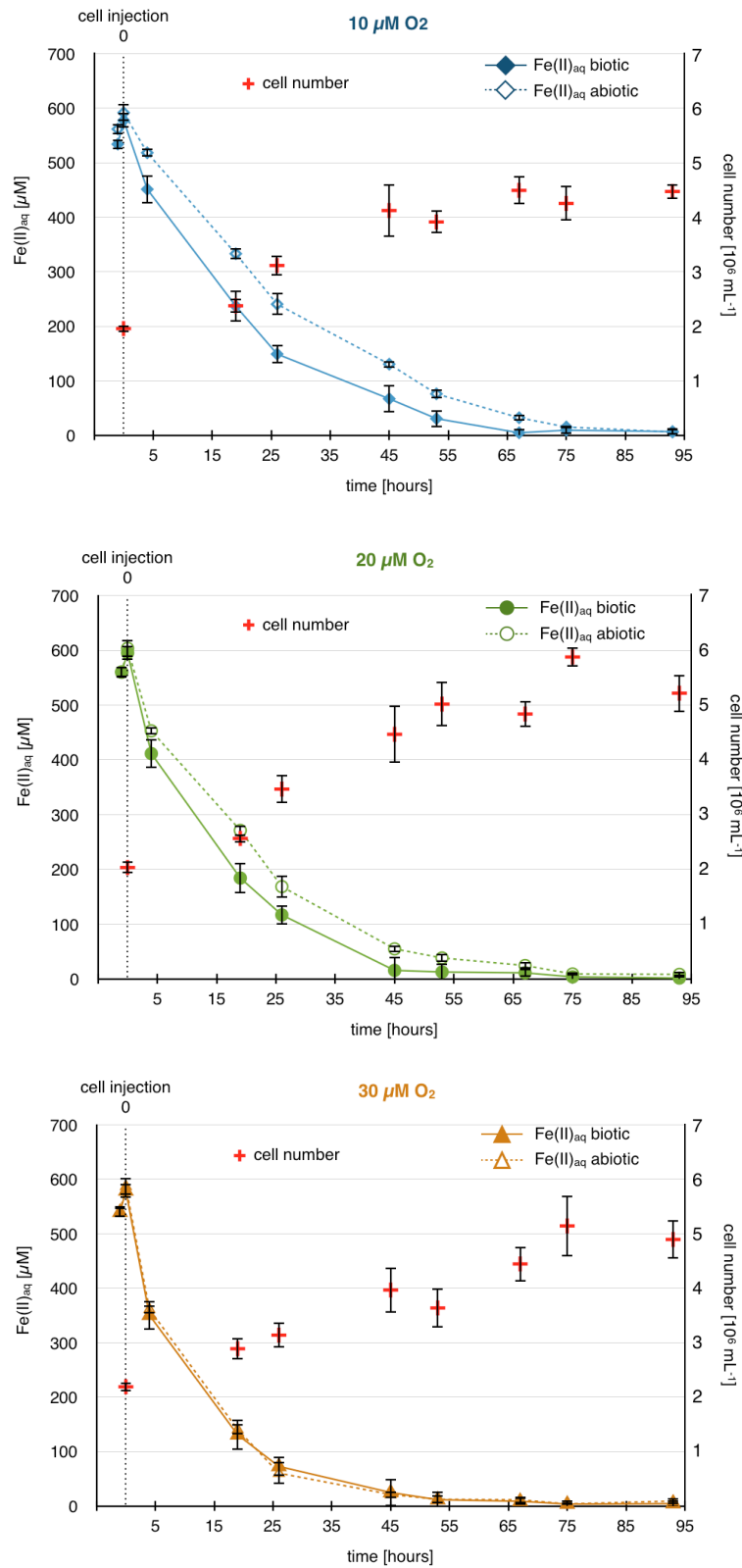
Figure S4: Microaerophilic Fe(II)-oxidizing enrichment culture – Fe(II)$_{aq}$ (in µM) and cell numbers (in 10^6 cells mL^{-1}) over the course of the incubation at 10, 20 and 30 µM O₂.

Oxygen concentrations during incubations at 10, 20 and 30 μM O$_2$

Dissolved O$_2$ was quantified non-invasively at each sampling point in one representative replicate setup each. Concentrations remained stable throughout the incubation period.
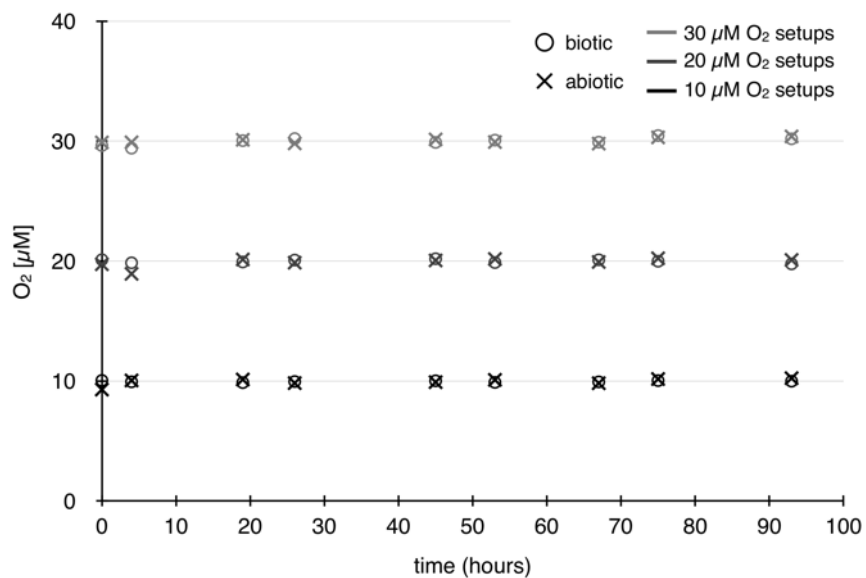
Figure S5. Oxygen concentrations in the liquid medium in setups with oxalate-washed cells incubated at 10, 20 and 30 μM O$_2$. Concentrations remained constant throughout the incubation period.

Calculated heterogeneous and homogeneous Fe(II) oxidation rates
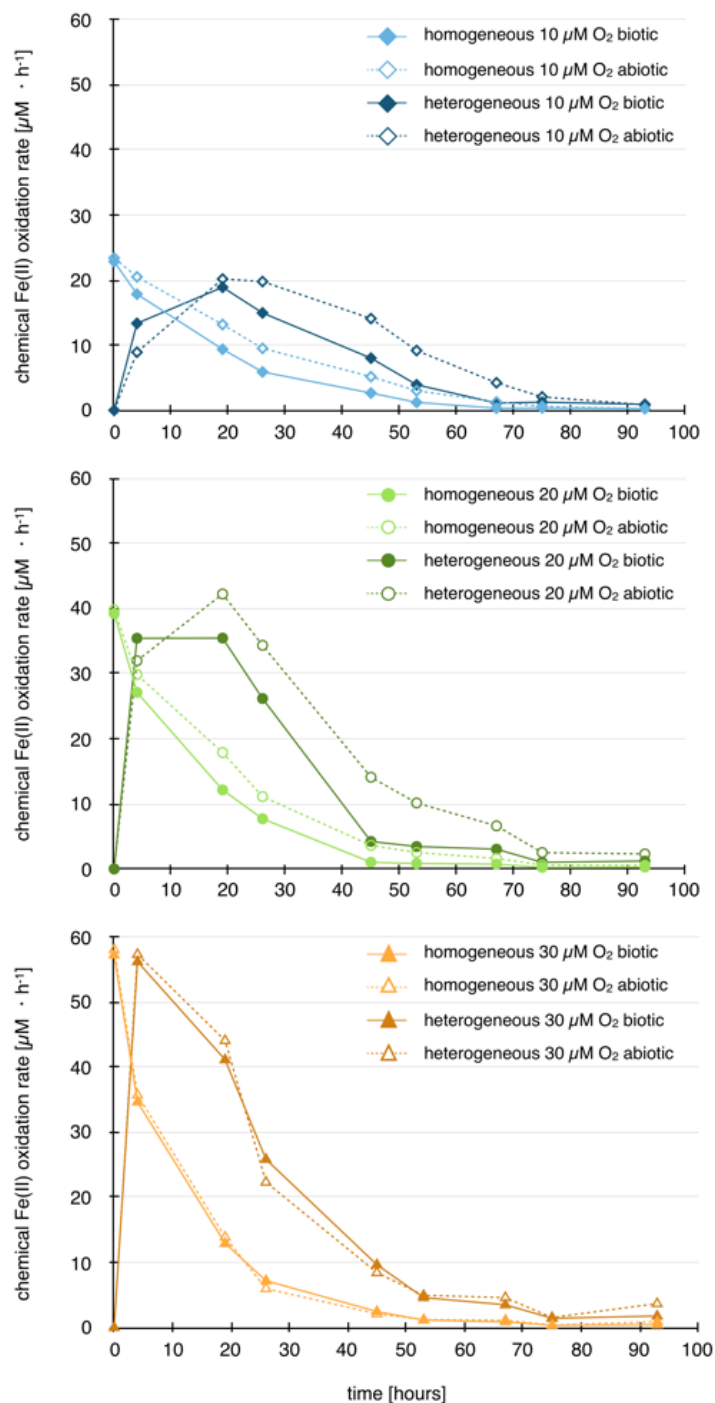
Figure S6. Abiotic homogeneous and heterogeneous Fe(II) oxidation rates in active and inhibited incubations with oxalate-washed cells at different O_2 concentrations. Based on equations (2)-(5) abiotic (hom./het.) Fe(II) oxidation rates were calculated separately based on the initial Fe(II) (600 µM) and respective O_2 concentrations.

Oxygen threshold levels for microaerophilic Fe(II) oxidation
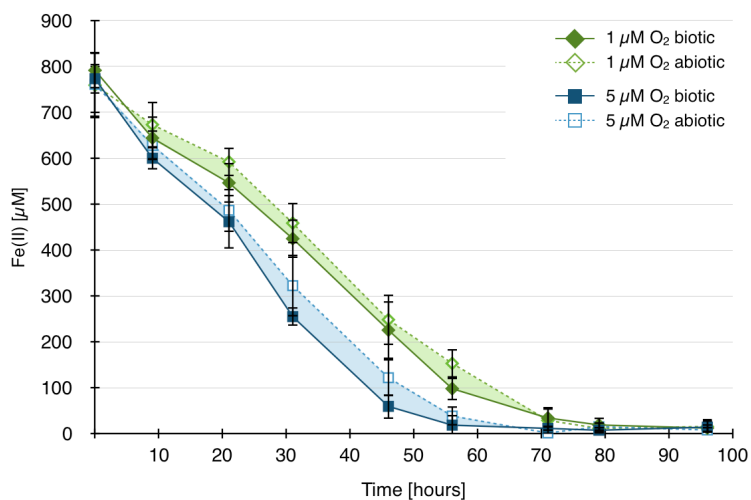
Figure S7. Fe(II)$_{aq}$ concentrations in biotic and abiotic incubations with oxalate-washed cells under O$_2$ limiting conditions at 1 and 5 μM O$_2$.

Table S2. Cell numbers [10^6 mL^{-1}] at selected time points in incubations with oxalate-washed cells under O$_2$ limiting conditions at 1 and 5 μM O$_2$ and doubling times (T$_d$) within the initial incubation phase of 46 hours.

hours of incubation	1 μM O$_2$			5 μM O$_2$		
	abiotic	biotic	T$_d$ (h)	abiotic	biotic	T$_d$ (h)
0	1.27 (±0.56)	**1.07 (±0.14)**		1.15 (±0.23)	**1.11 (±0.24)**	
46	1.05 (±0.34)	**1.85 (±0.33)**	**58.2**	1.02 (±0.44)	**2.16 (±0.53)**	**47.9**
96	0.82 (±0.37)	**3.97 (±0.35)**		0.80 (±0.24)	**4.60 (±0.54)**	

References

1.   Laufer, K.; Nordhoff, M.; Halama, M.; Martinez, R. E.; Obst, M.; Nowak, M.; Stryhanyuk, H.; Richnow, H. H.; Kappler, A., Microaerophilic Fe(II)-Oxidizing Zetaproteobacteria Isolated from Low-Fe Marine Coastal Sediments: Physiology and Composition of Their Twisted Stalks. *Appl Environ Microb* **2017,** *83*, (8), e03118-16, doi:10.1128/AEM.03118-16.

2.   McBeth, J. M.; Little, B. J.; Ray, R. I.; Farrar, K. M.; Emerson, D., Neutrophilic Iron-Oxidizing "Zetaproteobacteria" and Mild Steel Corrosion in Nearshore Marine Environments. *Appl Environ Microb* **2011,** *77*, (4), 1405-1412.

3.   Widdel, F.; Pfennig, N., Studies on Dissimilatory Sulfate-Reducing Bacteria That Decompose Fatty-Acids .1. Isolation of New Sulfate-Reducing Bacteria Enriched with Acetate from Saline Environments - Description of Desulfobacter-Postgatei Gen-Nov, Sp-Nov. *Arch Microbiol* **1981,** *129*, (5), 395-400.

4.   Tschech, A.; Pfennig, N., Growth-Yield Increase Linked to Caffeate Reduction in Acetobacterium-Woodii. *Arch Microbiol* **1984,** *137,* (2), 163-167.

5.   Widdel, F. Anaerober Abbau von Fettsaeuren und Benzoesaaeure durch neu isolierte Arten Sufat reduzierender Bakterien. 1980.

6.   Rancourt, D. G.; Ping, J. Y., Voigt-Based Methods for Arbitrary-Shape Static Hyperfine Parameter Distributions in Mossbauer-Spectroscopy. *Nucl Instrum Meth B* **1991,** *58*, (1), 85-97.

7.   Murad, E., The Mossbauer Spectrum of Well-Crystallized Ferrihydrite. *J Magn Magn Mater* **1988,** *74*, (2), 153-157.
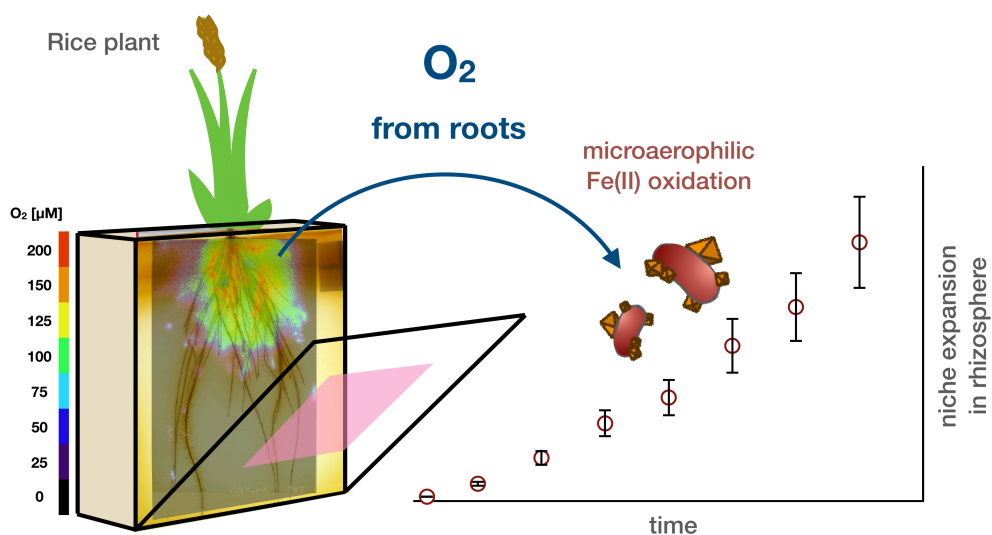
3 Iron Lung – How Rice Roots Induce Iron Redox Changes in the Rhizosphere and Create Niches for Microaerophilic Fe(II)-Oxidizing Bacteria

Markus Maisch[1], Ulf Lueder[1], Andreas Kappler[1,2], Caroline Schmidt[1]

[1] Geomicrobiology, Center for Applied Geosciences, University of Tübingen, Germany

[2] Department for Bioscience, Aarhus University, Denmark

3.1 Abstract

Although water-logged rice paddies are characterized by anoxic conditions, radial oxygen loss (ROL) from rice roots temporarily oxygenates the soil rhizosphere. ROL not only triggers the abiotic oxidation of ferrous iron (Fe(II)), but also provides the electron acceptor for microaerophilic Fe(II)-oxidizing bacteria (microFeOx). Both processes contribute to the formation of ferric (Fe(III)) iron plaque on root surfaces. Redox interactions at single roots have been studied intensively. However, temporally-resolved spatial changes of ROL in the entire rhizosphere and the impact on redoximorphic biogeochemistry are currently poorly understood. Here, we show how ROL spatio-temporally evolves and correlates with Fe-redox transformations. Applying non-invasive measurements in a transparent artificial soil, we were able to visualize opposing O_2 and Fe(II) gradients that extend from the root surface 10-25 mm into the rhizosphere. The microoxic zone expanded exponentially in size throughout the entire rhizosphere creating niches for microFeOx. Following iron mineral formation and pH, we show that root-related ROL induces iron redox transformations on and around roots, and correlates with rhizosphere acidification. These findings highlight the dynamic nature of roots in the rice plant rhizosphere and our approach spatio-temporally resolved their impact on iron redox chemistry and microbial niche formation in the rice plant rhizosphere.

3.2 Introduction

Rice paddy soils represent more than 6% of the world's cultivated and arable land surface. Traditionally cultivated under water-logged conditions, rice plants serve as an important conductor for gas-water exchange across the soil-atmosphere interface, incl. CH_4, N_2O, CO_2 and in particular O_2.[1] Oxygen from the atmosphere gets passively transported through the aerenchymatous tissue of rice plants and is released from roots as radial oxygen loss (ROL).[2] This plant-mediated oxygenation of anoxic soils strongly impacts local biogeochemistry, incl. metal speciation,[3-4] soil properties, such as porosity and pH,[5,6] microbial community structures,[7] as well as nutrient availability[8,9] and contaminant mobility.[10] In particular, ROL triggers the oxidation of Fe(II) and the formation of Fe(III) (oxyhydr)oxides that precipitate on the roots as ferric iron plaque.[11,12] There is a general agreement that ROL is the dominant driver for the formation of iron plaque.[13] However, it has been speculated that the formation of iron plaque can, at least, partly be attributed to microaerophilic Fe(II) oxidation (microFeOx). Such bacteria were found on the roots of many wetland plants and successfully isolated from rice paddy fields and numerous wetland environments.[14,15] In laboratory-controlled setups, that mimicked environmental parameters where microFeOx where isolated from,[14,16] these

bacteria have been shown to actively contribute to Fe(III) mineral precipitation by up to 40% at under microoxic conditions (5-30 µM O_2)[17] and even up to 60% on the roots of wetland plants in hydroponic culture.[15]

Although, geochemical conditions and redox processes at the root-soil interface of individual rice roots have been studied as a function of varying O_2, pH and Fe(II)/(III) conditions, a systematic spatio-temporal quantification of biogeochemical gradients in the entire rhizosphere is still lacking. Especially the remarkably high root density of rice plants with more than 20 cm root length per cm^3 surface soil (0-30 cm)[18] underline the impact rice plant roots can have on the atmospheric O_2 input into the rhizosphere of anoxic paddy soils. So far, little is known about the spatio-temporal ROL variation and its impact on the entire biogeochemical iron redox cycle in the. In the current study, we followed ROL during plant growth spatially and concluded on the extent of potential niches for microaerophilic Fe(II)-oxidizing bacteria. Different to previous studies that rely on single root measurements,[1,2,11] we hypothesize that ROL not only impacts ferric iron mineral formation at the root surface, but also in the entire soil matrix where it creates suitable microoxic niches and expands potential living space for microFeOx throughout large areas of the rhizosphere. We expect that during plant and root growth, the oxygenation of soil-borne Fe(II) and the extension of zones that provide optimum O_2 (O_2 1-30 µM) and Fe(II) concentrations for microFeOx, dynamically expand into the otherwise anoxic rice plant rhizosphere.

In order to exclude complex interactions between numerous environmental parameters, we established a transparent plexiglass rhizotron setup that allows a 2D-spatiotemporal quantification and visualization of distinct geochemical parameters in a less complex anoxic artificial Fe(II)-rich soil matrix. We conducted time-resolved high-resolution mapping of O_2, pH and dissolved Fe(II) (Fe(II)$_{aq}$) and developed a non-invasive method to spatially quantify Fe(II) and ferric iron precipitates (Fe(III)$_{ppt}$) in the entire rhizosphere. Our findings show how (i) ROL drives iron biogeochemistry in rice paddy soils, (ii) triggers iron mineral deposition on and around the root surface and (iii) reflects the importance of the entire rice plant rhizosphere as potential living space for microFeOx.

3.3   Materials & Methods

Plant growth containers. Eight rhizotrons (growth containers made of transparent plexiglass; 25 x 25 x 3 cm i.d., Figure S1) were filled under sterile and anoxic conditions with 1.73 cm^3 anoxic Hoagland solution[19] (100%, 35°C, pH 6.8) that was amended with 500 µM Fe(II)$_{aq}$ (from $FeCl_2$). Similar Fe(II)$_{aq}$ concentrations have been reported for many wetland environments where microFeOx has been observed and were documented as common Fe(II) concentrations

for water-logged rice paddy fields.[20-24] The liquid matrix was stabilized by adding 0.3% Gelrite (Carl Roth, Karlsruhe, Germany) as gelling agent forming a transparent solid artificial soil matrix at room temperature.[25] Approx. 100 mL of 20% Hoagland solution was constantly kept on top of the growth gel to prevent desiccation. The advantage of working with a transparent artificial soil matrix over real soil is to apply a suite of visual analyzing techniques that allow high spatial resolution of temporal geochemical patterns in the rice plant rhizosphere. The simplification of the natural system lacks numerous geochemical interactions substantially impacting (iron redox) geochemistry. However, the transparent setup allows to prevent interference of such processes and provides the opportunity to visually follow only specific parameters (Fe(II)/(III); O_2; pH) and to quantify the maximum impact of ROL on the iron (bio)geochemistry.

Rice seeds (*Oryza sativa* Nipponbare) were sterilized (0.1% H_2O_2 rinse, sterile ultrapure water), pre-grown on sterile Hoagland (0.5 N) solution at pH 6.8, and seedlings were transferred into rhizotrons at the three-leaf stage. Plants were grown under temperature-controlled conditions (25-27°C), at constant relative humidity (70%) and illumination conditions (high pressure sodium lamp, 10,000 – 12,000 lx) at day (14 h) - night (10 h) cycles. Rhizotrons were wrapped in opaque fabric to prevent any illumination of the roots. The front panel of the rhizotron was removable for *in-situ* microsensor measurements.

Geochemical measurements. Voltammetric microsensor measurements were applied to quantify Fe(II)$_{aq}$ in-situ in a reference rhizotron container for color referencing (see below). Cu-Au sensors with a Hg-Au alloy surface (100 µm) were constructed in the lab[26] and hooked to a potentiostat (DLK-70, Analytical Instrument Systems, Flemington, NJ, US). In order to perform in-situ microsensor measurements inside the rhizosphere, the rhizotron was positioned horizontally and the front cover was removed (lifted) under anoxic conditions. Measurements were performed as described in Supporting Information.

Oxygen and pH measurements were performed using non-invasive planar optode sensor foils (SF-RPSu4 & SF-HP5R, PreSens, Regensburg, Germany) (O_2 & pH: 15 x 9 cm) that were glued onto the inside of a plexiglass front window, a fluorescing light source (Big Area Imaging Kit, PreSens, Regensburg, Germany) and a camera detector (VisiSens TD, PreSens, Regensburg, Germany). Prior to measurements, sensor foils were calibrated using the recommended procedures given by the provider at constant temperature (25°C) in a Hoagland solution (100 %) matrix. Images were recorded at constant temperature conditions in a dark room without any light sources, except the fluorescing illumination system required for optode records. Further information on 2-dimensional O_2 and pH detection is given in the Supporting Information. Digital images of the root-zone were taken after the simulated

daylight period (14 hours) within a maximum of one hour using a camera (EOS 1200D, Canon) with constant camera and illumination settings. Potential habitable zones for microFeOx were assigned accounting for O_2 threshold concentrations of 1-30 µM O_2 (data obtained from O_2 optode sensor images using the software VisiSens, ScientifiCal (Presens, Regensburg, Germany)). The 2-dimensional extension of assigned zones was calculated using imageJ.[27] The 2-dimensional relative area (in %) for designated zones was calculated related to the total area of the artificial soil (575 cm^2).

Iron mineral analyses. Iron plaque and iron mineral formation was followed using image analysis. For image-based iron mineral identification, the rhizotron was carefully positioned horizontally and the plexiglass front window (with planar optode foil) was exchanged to a fully transparent one under anoxic and sterile conditions. Formation of orange Fe(III) (oxyhydr)oxide minerals in the gel matrix and on the root surface was followed based on color coded pixel analysis.[28,29] Image analysis was performed on the basis of color thresholding and pixel color code identity using the software Fiji (Ver.1.0, ImageJ) and a color correlation function calibrated for in-situ Fe(II) combined with identity of pixel matrices using Matlab (Supporting Information).

3.4   Results and Discussion

Rice roots as a pipeline for O_2 – creating a niche for microaerophilic Fe(II) oxidation. Rice root growth and the accompanied changes in geochemistry were monitored in transparent rhizotron cultivation chambers in order to quantify ROL and to detect niches for microFeOx on a spatio-temporal scale. Atmospheric O_2 that passively diffused through the aerenchymatous tissues was released as ROL and showed a maximum of 10-20 µM O_2 after 6-14 days after transfer (DAT) of plants in patchy patterns restricted to a narrow zone of 1-3 mm around single roots. After 15 DAT, O_2 concentrations increased, forming a constantly oxic zone (with a relative soil area of approx. 32±10.2 cm^2) with O_2 >50 µM in the upper zone where basal roots formed a dense root zone that occupied more than 5% of the total rhizosphere (Figure S2). After >35 DAT, the basal root zone was dominated by high O_2 concentrations (O_2 >100 µM) and a constantly oxygenated zone with a relative area of approx. 56.4±21.3 cm^2, which reflected approx. 10% of the total rhizosphere. Using microsensors we were able to resolve O_2 gradients around individual roots on a µm-resolution. On the surfaces of lateral roots, O_2 concentrations of more than 100 µM O_2 were detected, depleting gradually to <5 µM O_2 at a 2 mm distance away from the root into the rhizosphere (Figure S2D). The O_2

from ROL that diffuses towards soil-borne $Fe(II)_{aq}$ would rapidly oxidize $Fe(II)_{aq}$ chemically and form ferric (oxyhydr)oxides.[30] However, chemical Fe(II) oxidation negatively correlates with O_2 and slows down with decreasing O_2 concentrations[31] which are found in distance of 10-20 mm away from the roots along the O_2 diffusion gradient (Figure S3). From 5 DAT until the end of plant growth (45 DAT), we measured O_2 concentrations <30 µM O_2, in a distance of approx. 5-25 mm away from root surfaces. Under these conditions, Fe(II) half-life times were calculated to be in the range of more than 10 hours (Figure S3), which would prolong the persistence of Fe(II) and increase the bioavailability for microaerophilic Fe(II)-oxidizing bacteria.[15,16,32-34]

Previous studies suggested that these microaerophilic Fe(II)-oxidizing bacteria have their physiological niche in a micro-oxic environment with O_2 concentrations ranging from approx. 1 to <50 µM.[16,32] Recent observations showed that microaerophilic bacteria from a rice paddy field can contribute efficiently up to 40% to Fe(III) mineral under optimum O_2 conditions between 1-30 µM O_2.[17] Such bacteria were even shown to enhance iron plaque formation on roots of wetland plants.[4] We detected that areas with optimum $Fe(II)_{aq}$ and O_2 conditions for microFeOx (1-30 µM O_2) occur spontaneously especially on young rice roots (Figure 1A & 1B), while the redoximorphic transition zone from a constantly oxic bulk root zone to the anoxic rhizosphere provided a rather stable opposing gradient of >200 µM $Fe(II)_{aq}$ and <30 µM O_2. Geochemical conditions in these zones shifted drastically within 7-10 days with a significant increase in ROL creating oxygenated zones in the bulk root zone with O_2 concentrations >30 µM. The increase in O_2 concentrations was shown to enhance abiotic Fe(II) oxidation reactions by up to 30 %, favoring chemically-induced Fe(III) mineral formation (Figure S3). Thus, potential niches for microFeOx around rice roots are only short term (<7 days) and turn into oxygenated zones with rapid abiotic Fe(II) oxidation which would kinetically outcompete microaerophilic Fe(II) oxidation.[32] However, studies have demonstrated that bacteria (<2 µm, which was reported as size for microaerophilic Fe(II)-oxidizing representatives[35]) show a relatively high passive mobility (more than 10 % of total cells) within the soil porewater.[36] Additionally, the active motility of microFeOx[37] could enhance the mobility of microFeOx within the soil matrix and allow them to continue occupying the habitable niche within the rice plant rhizosphere.

Following O_2 and $Fe(II)_{aq}$ distribution patterns, we observed that during plant growth, optimal O_2 conditions for microaerophilic Fe(II)-oxidizing bacteria expanded along the O_2 diffusion gradient, away from the root surface into the rhizosphere (Figure 1C). On root surfaces, along basal roots and in the dense bulk root zone, significantly high O_2 (>100 µM O_2) and considerably low $Fe(II)_{aq}$ concentrations (<100 µM $Fe(II)_{aq}$) were detected (Figure 1A). In these zones, dominated by high O_2 concentrations, more than 60% of the $Fe(II)_{aq}$ that was

initially present were oxidized and precipitated as Fe(III) minerals. In these zones, Fe(II) half-life times were calculated to be considerably low (<5 h) which decreases the Fe(II) availability for microFeOx and thus increase the competition pressure for microbes with the chemical Fe(II) oxidation (Figure S3). Microaerophilic Fe(II)-oxidizing bacteria would find suitable conditions only along the opposing gradients of Fe(II)$_{aq}$ and O$_2$ either (i) in the redoximorphic zone between root surface (10-25 mm) and anoxic rhizosphere, or (ii) in dynamic geochemical hotspots along the roots with periodic ROL, creating temporal micro-oxic zones (Figure 1C).

The first hypothesis is strongly supported by observations made by Weiss et al., (2003)[7] who observed significantly more (3.7*10^6 g^{-1} soil) microaerophilic Fe(II)-oxidizing bacteria in the soil matrix than directly with the roots of various wetland plants (5.9*10^5 g^{-1} root). This relative 2-dimensional area in the rhizosphere, that provided suitable conditions for microFeOx, was found in the current study to expand exponentially during plant growth and increased from initially 4.8±1.3 cm^2 (<1 % of total rhizosphere) at 11 DAT to more than 32 (±11.4) cm^2 (>5 % of rhizosphere) 45 DAT (Figure S4). Such spatio-temporal fluctuations in Fe(II) and O$_2$ availability that were found throughout the entire rhizosphere not only highlight the dynamic character of the rice plant rhizosphere but might explain why microFeOx have been shown to metabolically respond very effectively to geochemical changes in highly dynamic environments like rhizosphere hot spots.[35] The substantial relative abundance of microFeOx in wetland plant rhizospheres (1-6% of total microbial community)[9,15] such as paddy soils suggests that these bacteria can widely impact the iron cycle not only around the roots of rice plants in paddy fields but around the roots of any wetland plant.[7] In addition to that, the current findings quantitatively demonstrate that ROL from roots expands the habitable niche of microFeOx throughout the entire rhizosphere which strongly increases the impact of microaerophilic Fe(II) oxidation during plant growth.
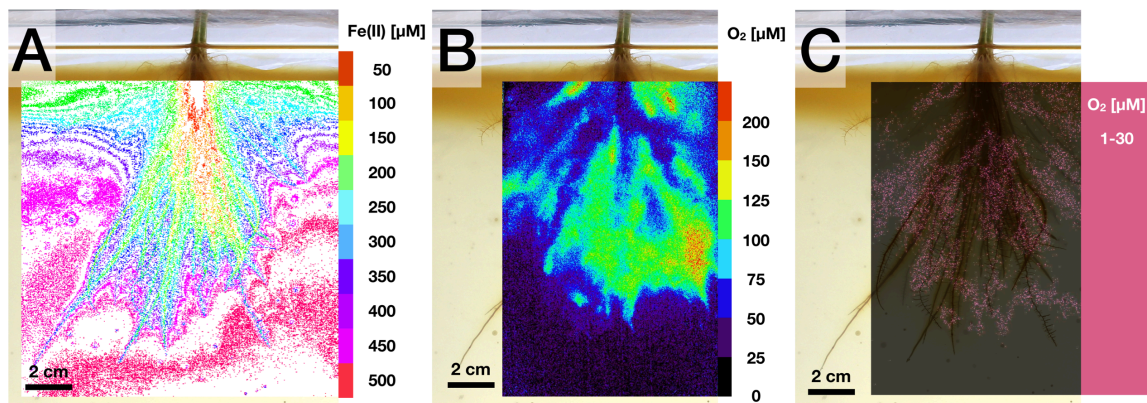
Figure 1. Rhizosphere of rice plant 28 DAT. A) Non-invasive mapping of $Fe(II)_{aq}$ in the artificial soil matrix. In the unrooted zone, $Fe(II)_{aq}$ concentrations remained high at initial $Fe(II)_{aq}$ concentrations of 500 µM. In the rhizosphere, $Fe(II)_{aq}$ concentrations decrease gradually around roots. **B)** Non-invasive mapping of O_2 in the rhizosphere. Oxygen concentrations increase in the immediate vicinity of roots and show steep gradient from high (>100 µM) to low (<25 µM) O_2 concentrations from roots to rhizosphere. **C)** Microoxic zone with O_2 concentrations (1-30 µM) providing suitable O_2 conditions for microFeOx.

Rusty Roots – Iron mineral precipitation driven by Radial Oxygen Loss. In order to spatio-dynamically correlate ROL from plant roots to iron redox chemistry, the formation of Fe(III) minerals and changes in pH were monitored non-invasively during plant growth. Within 14 DAT, fresh orange/reddish iron plaque formed on young root surfaces (shown to be ferrihydrite; Table S1 & Figure S5) in heterogenous patterns that considerably correlated with measured O_2 concentrations (Figure S6). After 16 DAT, Fe(III) mineral formation was not only limited to the surface of the roots, where highest O_2 concentrations were measured, it was also detected in a distance of up to 15 mm away from the roots where O_2 concentrations reached 30-100 µM. Based on image analysis, we quantified that the relative area that was affected by Fe(II) oxidation expanded exponentially ($R^2 = 0.95$, n = 7) from <10 cm^2 (3 DAT) to a maximum of 95±12.8 cm^2 (approx. 16.5% of total rhizosphere) on average by 45 DAT (Figure S7).
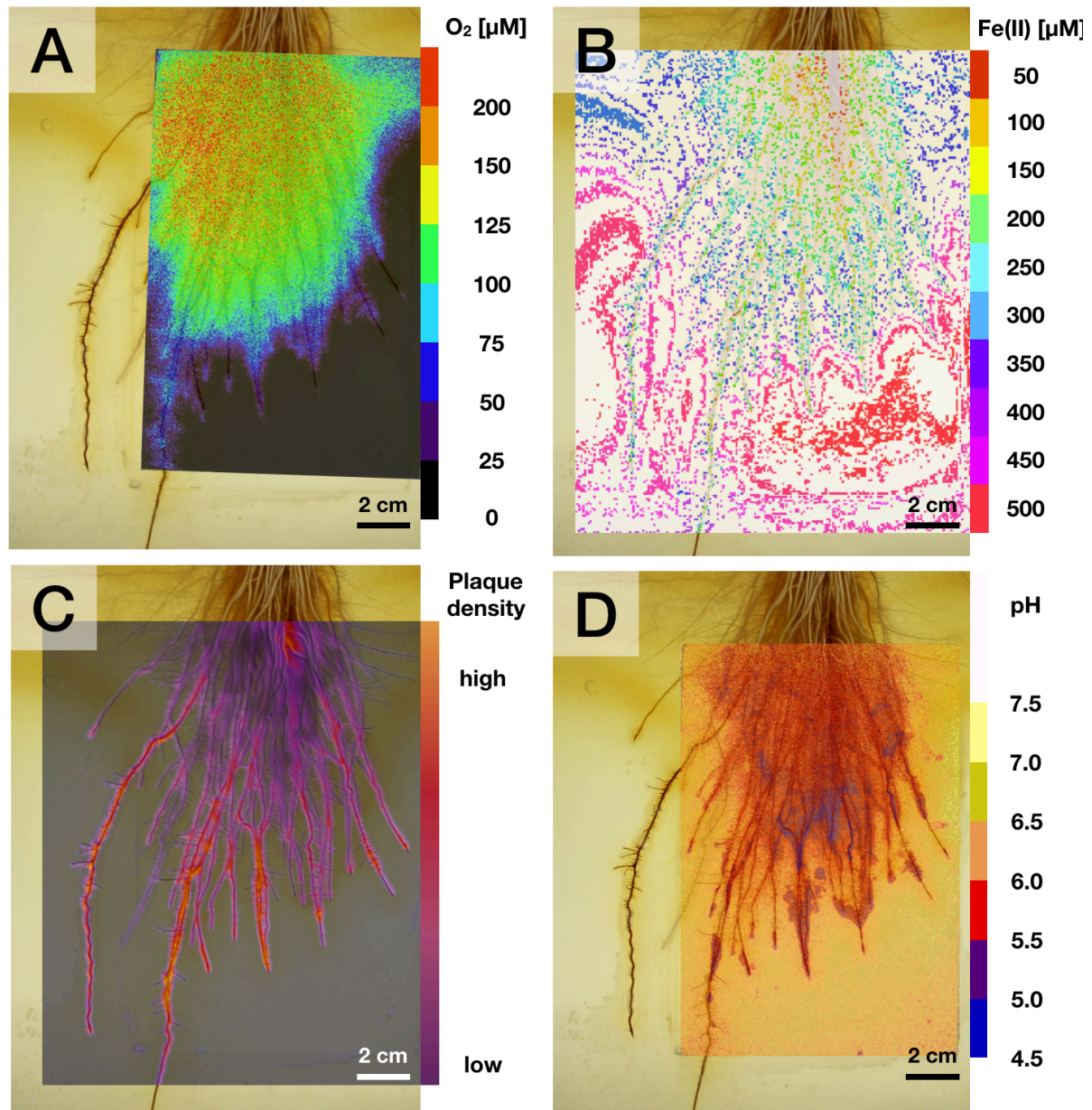
Figure 2. Rhizosphere of rice plant 45 DAT. Oxygen, Fe(II)$_{aq}$, iron plaque precipitation and pH patterns. A) Oxygen was mainly detected in the basal root zone, forming a steep gradient around from O$_2$ >200 μM in the bulk root zone to on O$_2$ <25 μM in the unrooted soil matrix. **B)** Fe(II)$_{aq}$ concentrations decrease in the bulk root zone to Fe(II)$_{aq}$ <200 μM and increase gradually toward the soil matrix to 500 μM Fe(II)$_{aq}$. **C)** Iron plaque formed dense Fe(III) (oxyhydr)oxide plaque on young roots, while basal roots showed less iron plaque. **D)** Soil matrix pH decreased around root tips, potentially due to iron plaque formation on/around root surface.

Fe(II) oxidation and consequent iron plaque formation induced a decrease in pH, which was monitored across the rhizosphere (Figure 2). After 23 DAT, pH dropped from initially 6.8 to 6.0-6.5 at the redoximorphic root-soil matrix interface (Figure S8), potentially caused by protons generated during the precipitation of Fe(III) (oxyhydr)oxides and acidification by the

74

release of plant exudates, chelating agents or plant-derived organic acid molecules[38] (found to decrease soil pH by up to 2 pH units).[39,40] The acidification of the unbuffered artificial rhizosphere proceeded until the end of the growth experiment after 45 DAT (pH 5.0-5.5; Figure S8) and significantly correlated to areas with the highest extent in Fe(III) mineral formation (Figure 2C & D). The observed pH decrease induced by ROL in our setup, has been observed in a similar manner in various wetland soils and was hypothesized to be attributed to ROL-driven Fe(II) oxidation.[40-43] These observed changes in soil pH will not only positively affect Fe(III) solubility but increase Fe(II) half-life times[28] and bioavailability for microbial Fe(II) turnover. However, in natural rice paddy soils, the soil pH buffer capacity would potentially decrease extensive changes in soil pH related to Fe(II) oxidation.

Transferability to soil rhizosphere systems. The artificial soil matrix represents a simplified rhizosphere system compared to natural settings. However, this approach not only allows to decipher the impact of ROL on iron speciation within the entire rhizosphere by visualizing geochemical gradient via imaging techniques, but facilitates the correlation of pH changes with ROL and visible Fe(III) (oxyhydr)oxide formation on and around the rice roots. The transparent soil setup used in the current study, represents a simplified rhizosphere system compared to real paddy soil. However, in this setting optimum application of imaging techniques and the quantification of a maximum impact of ROL on rhizosphere geochemistry enable to construct and predict niches for microaerophilic bacteria on an extremely high spatial and temporal resolution. Diffusion coefficients for O_2 and other gases in water-saturated rhizosphere soils ($3.2 - 8.0 * 10^{-10}$ m^2 s^{-2})[44,45] are slightly smaller compared to O_2 diffusivity in the growth gel matrix ($1.6-2.1 * 10^{-9}$ m^2 s^{-2})[46]. Thus, O_2 diffusion properties for the artificial soil are in a comparable range to real soil matrices. However, for the empirical modelling of spatio-dynamic fluxes (e.g. root-derived O_2, mobility in soil and Fe(II) oxidation) using the presented approach, differences in diffusion coefficients between the artificial soil system to real paddy soil needs to be considered. For a qualitative extrapolation of habitable niches for microFeOx from the artificial growth matrix to real paddy soils, differences in O_2 diffusivity are minor and within the natural variation of a soil matrix.[47-49]

Nevertheless, in a natural rhizosphere, not only the physical heterogeneity[50] but also a variety of aerobic and microaerophilic soil microorganisms (e.g. heterotrophs and methanotrophs) will affect O_2 mobility away from the root, compete for O_2, consequently decrease the availability for microFeOx and potentially narrow down their relative niche expansion.[51] Other reducing agents in a natural rhizosphere, such as redox-active exudates, chelating complexes such as small organic acids or reducing metal-sulfides might additionally scavenge O_2 from ROL and considerably decrease the habitable niche for microFeOx in

environmental settings. Additionally, these (plant- or microbially derived) organic molecules may trigger heterotrophic processes and or Fe(III)-reducing processes that shift redox conditions in either direction.[52] Nevertheless, the gathered data in the artificial soil replacement clearly proves the power of ROL to favor the formation of habitable niches for microFeOx in an otherwise anoxic environment.

3.5 References

1. Colmer, T. D.; Cox, M. C. H.; Voesenek, L. A. C. J., Root aeration in rice (Oryza sativa): evaluation of oxygen, carbon dioxide, and ethylene as possible regulators of root acclimatizations. New Phytol 2006, 170, 767-777.

2. Armstrong, W., Radial Oxygen Losses from Intact Rice Roots as Affected by Distance from Apex, Respiration and Waterlogging. Physiol Plantarum 1971, 25, 192-197.

3. Blossfeld, S.; Perriguey, J.; Sterckeman, T.; Morel, J. L.; Losch, R., Rhizosphere pH dynamics in trace-metal-contaminated soils, monitored with planar pH optodes. Plant Soil 2010, 330, 173-184.

4. Neubauer, S. C.; Toledo-Duran, G. E.; Emerson, D.; Megonigal, J. P., Returning to their roots: Iron-oxidizing bacteria enhance short-term plaque formation in the wetland-plant rhizosphere. Geomicrobiol J 2007, 24, 65-73.

5. Ehrenfeld, J. G.; Ravit, B.; Elgersma, K., Feedback in the plant-soil system. Annu Rev Env Resour 2005, 30, 75-115.

6. Lenzewski, N.; Mueller, P.; Meier, R. J.; Liebsch, G.; Jensen, K.; Koop-Jakobsen, K., Dynamics of oxygen and carbon dioxide in rhizospheres of Lobelia dortmanna - a planar optode study of belowground gas exchange between plants and sediment. New Phytol 2018, 218, 131-141.

7. Weiss, J. V.; Emerson, D.; Backer, S. M.; Megonigal, J. P., Enumeration of Fe(II)-oxidizing and Fe(III)-reducing bacteria in the root zone of wetland plants: Implications for a rhizosphere iron cycle. Biogeochemistry 2003, 64, 77-96.

8. Morris, J. T.; Bradley, P. M., Effects of nutrient loading on the carbon balance of coastal wetland sediments. Limnol Oceanogr 1999, 44, 699-702.

9. Bloom, A. J.; Meyerhoff, P. A.; Taylor, A. R.; Rost, T. L., Root development and absorption of ammonium and nitrate from the rhizosphere. J Plant Growth Regul 2002, 21, 416-431.

10. Borch, T.; Kretzschmar, R.; Kappler, A.; Van Cappellen, P.; Ginder-Vogel, M.; Voegelin, A.; Campbell, K., Biogeochemical Redox Processes and their Impact on Contaminant Dynamics. Environ Sci Technol 2010, 44, 15-23.

11. Wu, C.; Ye, Z. H.; Li, H.; Wu, S. C.; Deng, D.; Zhu, Y. G.; Wong, M. H., Do radial oxygen loss and external aeration affect iron plaque formation and arsenic accumulation and speciation in rice? J Exp Bot 2012, 63, 2961-2970.

12. Mendelssohn, I. A.; Kleiss, B. A.; Wakeley, J. S., Factors Controlling the Formation of Oxidized Root Channels - a Review. Wetlands 1995, 15, 37-46.

13. Stcyr, L.; Crowder, A. A., Factors Affecting Iron Plaque on the Roots of Phragmites-Australis (Cav) Trin Ex Steudel. Plant Soil 1989, 116, 85-93.

14. Emerson, D.; Weiss, J. V.; Megonigal, J. P., Iron-oxidizing bacteria are associated with ferric hydroxide precipitates (Fe-plaque) on the roots of wetland plants. Appl Environ Microb 1999, 65, 2758-2761.

15. Neubauer, S. C.; Emerson, D.; Megonigal, J. P., Life at the energetic edge: Kinetics of circumneutral iron oxidation by lithotrophic iron-oxidizing bacteria isolated from the wetland-plant rhizosphere. Appl Environ Microb 2002, 68, 3988-3995.

16. Druschel, G. K.; Emerson, D.; Sutka, R.; Suchecki, P.; Luther, G. W., Low-oxygen and chemical kinetic constraints on the geochemical niche of neutrophilic iron(II) oxidizing microorganisms. Geochim Cosmochim Ac 2008, 72, 3358-3370.

17. Maisch, M.; Lueder, U.; Laufer, K.; Scholze, C.; Kappler, A.; Schmidt, C., Contribution of microaerophilic iron(II)-oxidizers to iron(III) mineral formation. Environ Sci Technol 2019, 53, 8197-8204.

18. Yoshida, S.; Hasegawa, S., The rice root system: its development and function. Drought resistance in crops with emphasis on rice 1982, 10, 97-134.

19. Hoagland, D. R.; Arnon, D. I., The water-culture method for growing plants without soil. Circular. California agricultural experiment station 1950, 347, 1-32.

20. Achtnich, C.; Bak, F.; Conrad, R., Competition for Electron-Donors among Nitrate Reducers, Ferric Iron Reducers, Sulfate Reducers, and Methanogens in Anoxic Paddy Soil. Biol Fert Soils 1995, 19, 65-72.

21. Wang, X. J.; Chen, X. P.; Kappler, A.; Sun, G. X.; Zhu, Y. G., Arsenic Binding to Iron(Ii) Minerals Produced by an Iron(Iii)-Reducing Aeromonas Strain Isolated from Paddy Soil. Environ Toxicol Chem 2009, 28, 2255-2262.

22. Kumada, K.; Asami, T., A new method for determining ferrous iron in paddy soils. Soil Sci Plant Nutr 1957, 3, 187-193.

23. Roden, E. E.; Wetzel, R. G., Organic carbon oxidation and suppression of methane production by microbial Fe(III) oxide reduction in vegetated and unvegetated freshwater wetland sediments. Limnol Oceanogr 1996, 41, 1733-1748.

24. Weiss, J. V.; Emerson, D.; Megonigal, J. P., Rhizosphere iron(III) deposition and reduction in a Juncus effusus L.-dominated wetland. Soil Sci Soc Am J 2005, 69, 1861-1870.

25. Moon, H. K.; Kim, Y. W.; Lee, J. S.; Choi, Y. E., Micropropagation of Kalopanax pictus tree via somatic embryogenesis. In Vitro Cell Dev-Pl 2005, 41, 303-306.

26. Brendel, P. J.; Luther, G. W., Development of a Gold Amalgam Voltammetric Microelectrode for the Determination of Dissolved Fe, Mn, O-2, and S(-Ii) in Porewaters of Marine and Fresh-Water Sediments. Environ Sci Technol 1995, 29, 751-761.

27. Easlon, H. M.; Bloom, A. J., Easy Leaf Area: Automated Digital Image Analysis for Rapid and Accurate Measurement of Leaf Area. Appl Plant Sci 2014, 2: apps. 1400033.

28. Flessa, H.; Fischer, W. R., Plant-Induced Changes in the Redox Potentials of Rice Rhizospheres. Plant Soil 1992, 143, 55-60.

29. Kirk, G., The biogeochemistry of submerged soils. John Wiley & Sons: 2004.

30. Millero, F. J.; Sotolongo, S.; Izaguirre, M., The Oxidation-Kinetics of Fe(II) in Seawater. Geochim Cosmochim Ac 1987, 51, 793-801.

31. Stumm, W.; Lee, G. F., Oxygenation of ferrous iron. Industrial & Engineering Chemistry 1961, 53, 143-146.

32. Lueder, U.; Druschel, G.; Emerson, D.; Kappler, A.; Schmidt, C., Quantitative analysis of O-2 and Fe2+ profiles in gradient tubes for cultivation of microaerophilic Iron(II)-oxidizing bacteria. Fems Microbiol Ecol 2018, 94, fix177.

33. Rentz, J. A.; Kraiya, C.; Luther, G. W.; Emerson, D., Control of ferrous iron oxidation within circumneutral microbial iron mats by cellular activity and autocatalysis. Environ Sci Technol 2007, 41, 6084-6089.

34. Krepski, S. T.; Emerson, D.; Hredzak-Showalter, P. L.; Luther, G. W.; Chan, C. S., Morphology of biogenic iron oxides records microbial physiology and environmental conditions: toward interpreting iron microfossils. Geobiology 2013, 11, 457-471.

35. Kato, S.; Ohkuma, M.; Powell, D. H.; Krepski, S. T.; Oshima, K.; Hattori, M.; Shapiro, N.; Woyke, T.; Chan, C. S., Comparative Genomic Insights into Ecophysiology of Neutrophilic, Microaerophilic Iron Oxidizing Bacteria. Front Microbiol 2015, 6, 1265.

36. Gannon, J. T.; Manilal, V. B.; Alexander, M., Relationship between Cell-Surface Properties and Transport of Bacteria through Soil. Appl Environ Microb 1991, 57, 190-193.

37.   Emerson, D.; Moyer, C., Isolation and characterization of novel iron-oxidizing bacteria that grow at circumneutral pH. Appl Environ Microb 1997, 63, 4784-4792.

38.   Dakora, F. D.; Phillips, D. A., Root exudates as mediators of mineral acquisition in low-nutrient environments. Plant Soil 2002, 245, 35-47.

39.   Hinsinger, P.; Plassard, C.; Tang, C. X.; Jaillard, B., Origins of root-mediated pH changes in the rhizosphere and their responses to environmental constraints: A review. Plant Soil 2003, 248, 43-59.

40.   Begg, C. B. M.; Kirk, G. J. D.; Mackenzie, A. F.; Neue, H. U., Root-Induced Iron Oxidation and Ph Changes in the Lowland Rice Rhizosphere. New Phytol 1994, 128, 469-477.

41.   Yu, T. R., Characteristics of Soil Acidity of Paddy Soils in Relation to Rice Growth. Dev Plant Soil Sci 1991, 45, 107-112.

42.   Savant, N. K.; Kibe, M. M., Influence of Continuous Submergence on Ph, Exchange Acidity and Ph-Dependent Acidity in Rice Soils. Plant Soil 1971, 35, 205-208.

43.   Wang, Z. P.; Lindau, C. W.; Delaune, R. D.; Patrick, W. H., Methane Emission and Entrapment in Flooded Rice Soils as Affected by Soil Properties. Biol Fert Soils 1993, 16, 163-168.

44.   Jensen, C. R., Oxygen diffusion through soil and roots measured with oxygen-18. Retrospective Theses and Dissertations. 1961, https://lib.dr.iastate.edu/rtd/1946, (accessed 07/05/2019).

45.   van Bodegom, P. M.; Groot, T.; van den Hout, B.; Leffelaar, P. A.; Goudriaan, J., Diffusive gas transport through flooded rice systems. J Geophys Res-Atmos 2001, 106, 20861-20873.

46.   Aitken-Christie, J.; Kozai, T.; Smith, M. A. L., Automation and environmental control in plant tissue culture. Springer Science & Business Media Dordrecht: 1995.

47.   Moldrup, P.; Olesen, T.; Gamst, J.; Schjonning, P.; Yamaguchi, T.; Rolston, D. E., Predicting the gas diffusion coefficient in repacked soil: Water-induced linear reduction model. Soil Sci Soc Am J 2000, 64, 1588-1594.

48.   Moldrup, P.; Olesen, T.; Schjonning, P.; Yamaguchi, T.; Rolston, D. E., Predicting the gas diffusion coefficient in undisturbed soil from soil water characteristics. Soil Sci Soc Am J 2000, 64, 94-100.

49. Neira, J.; Ortiz, M.; Morales, L.; Acevedo, E., Oxygen diffusion in soils: Understanding the factors and processes needed for modeling. Chil J Agr Res 2015, 75, 35-44.

50. Gregory, P. J., Roots, rhizosphere and soil: the route to a better understanding of soil science? Eur J Soil Sci 2006, 57, 2-12.

51. van Bodegom, P.; Stams, F.; Mollema, L.; Boeke, S.; Leffelaar, P., Methane oxidation and the competition for oxygen in the rice rhizosphere. Appl Environ Microb 2001, 67, 3586-3597.

52. Walker, T. S.; Bais, H. P.; Grotewold, E.; Vivanco, J. M., Root exudation and rhizosphere biology. Plant Physiol 2003, 132, 44-51.

3.6   Supporting Information

Iron Lung – How Rice Roots induce Iron Redox Changes in the Rhizosphere and create Niches for Microaerophilic Fe(II)-oxidizing Bacteria

Markus Maisch[1], Ulf Lueder[1], Andreas Kappler[1,2], Caroline Schmidt[1]

[1] Geomicrobiology, Center for Applied Geosciences, University of Tübingen, Germany
[2] Department for Bioscience, Aarhus University, Denmark

Number of tables in supporting information: 1
Number of figures in supporting information: 8
Total numbers of pages in supporting information: 11 (including cover page)

Experimental setup: transparent rhizotrons
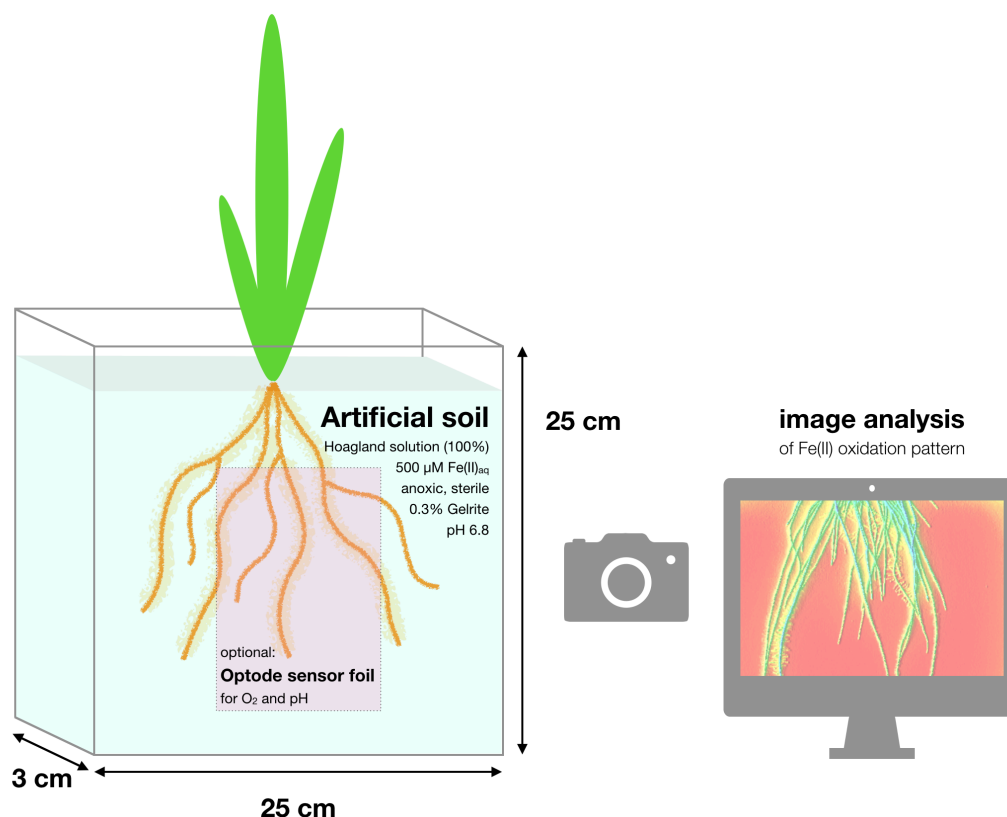
Figure S1. Representation of the experimental setup. Rhizotron dimensions, artificial soil composition, position of optode sensor foils inside the rhizotron for non-invasive mapping of O_2 and pH, and the schematic outline for image analysis of Fe(II) oxidation patterns.

Voltammetric measurements for Fe(II)$_{aq}$. Dissolved ferrous iron (Fe(II)$_{aq}$) concentrations were determined by voltammetric measurements using a three-electrode system hooked onto a DLK-70 web-potentiostat (Analytical Instrument Systems, Flemington, NJ). The working electrode was a lab-constructed glass-encased 100 µm gold amalgam (Au/Hg) electrode.[1] A silver (Ag) wire, coated with AgCl and a platinum (Pt) wire were used as reference and counter electrode, respectively. Calibration for Fe(II)$_{aq}$ was performed applying the pilot ion method[1,2] with Mn(II)$_{aq}$ standards. Cyclic voltammograms for Fe(II)$_{aq}$ and Mn(II)$_{aq}$ were collected by conditioning the electrode at -0.05 V for 2 s and subsequent scanning from -0.05 V to -2 V and reverse with a scan rate of 1000 mV s^{-1}. Prior to each scan, a potential of -0.9 V was applied for 5 s to precondition the electrode surface. Ten scans were run at every measuring position and the final three voltammograms were analyzed using the VOLTINT add-on for Matlab.[3] Measured Fe(II)$_{aq}$ concentrations were measured 5 mm in the artificial soil matrix. For

high-resolution in-situ Fe(II) measurements around individual roots, the spatial resolution between measuring points was 2 mm. Microsensor adjustment was controlled with a 3-D micromanipulator. Abiotic Fe(II) oxidation kinetics and Fe(II) half-life times within the rhizotron were calculated according to Maisch et al., (2019).[4]

Calculation of abiotic Fe(II) oxidation kinetics and Fe(II) half-life times. Abiotic Fe(II) oxidation rates at a specific time point (considering only homogeneous oxidation) and half-life times for Fe(II) were calculated following Maisch et al., 2019[4]. Spatial Fe(II) oxidation rates were determined considering the respective spatial Fe(II) concentration and the corresponding mean O_2 concentration within 2 mm of the measuring point. Measuring conditions (25°C, and corresponding pH conditions at the measuring point) were considered for calculation of Fe(II) oxidation rates and Fe(II) half-life times, respectively.

Non-invasive oxygen and pH mapping using planar optode sensors. For non-invasive O_2 quantification in the rhizotrons, planar optode sensor foils (SF-RPSu4 & SF-HP5R, PreSens, Regensburg, Germany) were used. The monitoring is based on fluorescence ratiometric imaging (FRIM). The sensor foils contain two different fluorophores, an indicator and a reference dye. The ratiometric approach compensates for inhomogeneities in the sensor foil as well as in the excitation light field. Both fluorophores are excited in the blue range of the spectrum, one is emitting in the green, and one in the red range of the spectrum. The reference fluorophores emission is constant whereas the indicator emission is depending on the oxygen concentration. The indicator is a dye composed of transition metal complexes. These show an effect called dynamic luminescence quenching, i.e. their fluorescence intensity as well as the fluorescence lifetime is quenched in the presence of oxygen. The quenching follows the Stern-Volmer relationship: I0/I = 1 + KSV * $[O_2]$. KSV is a known parameter and specific for the respective indicator dye used in the calibration algorithm suggested by the manufacturer. The correlation of the ratiometric imaging is linearly correlated to O_2 concentrations. A two-point calibration allows a reliable non-invasive quantification of O_2 concentrations within a detection uncertainty range of ±0.02 μM O_2 for the setup used in the current study.

The spatial resolution of the VisiSens TD detection unit (12bit) is depending on the field of view (FOV). When using the Big Area Imaging Kit (as we did in the current study) and a FOV of 30 x 18 cm^2, the pixel resolution is about 200 μm. The O_2 sensor foils not only contain molecular components but particles. Hence, the spatial resolution is also depending on the sensor foil. The particles in the sensor foil for O_2 are small enough that the spatial resolution of the detection unit is the limiting factor. The particles in the pH sensor foil are larger and the

lower limit for the spatial resolution on the foil is 100 µm. Using the Big Area Imaging Kit the spatial resolution is limited to 200 µm in the experimental setup.

Image analysis and Fe(II) quantification. Protocols and scripts were calibrated with in-situ Fe(II) microsensor measurements in a blank container with abiotic oxidation patterns and known Fe(II)$_{aq}$/(III) concentrations. Image analysis correlated proportionally to Fe(II) concentrations in a range of 50 – 500 µM Fe(II). Step size for Fe(II) quantification via image analysis was set to 50 µM Fe(II) (and a total range from 50 – 500 µM Fe(II)). Areas outside the measuring range or within the step sizes remained as blank in plots. A rhizotron setup with a plant was sacrificed for a destructive quantification of Fe(III) minerals on roots (see below).

Iron plaque quantification. Root material covered in iron plaque precipitates was collected at the end of the growth experiment and the root cut into sections of 1 cm. Iron minerals were extracted in 2M HCl for 2 hours and dissolved total iron quantified by ferrozine assay[5] as described in Materials and Methods. Collected root sections were referenced to positions in rhizotrons and quantified iron plaque referred to pixel identity of roots in rhizotron.

Oxygen concentration patterns during plant growth
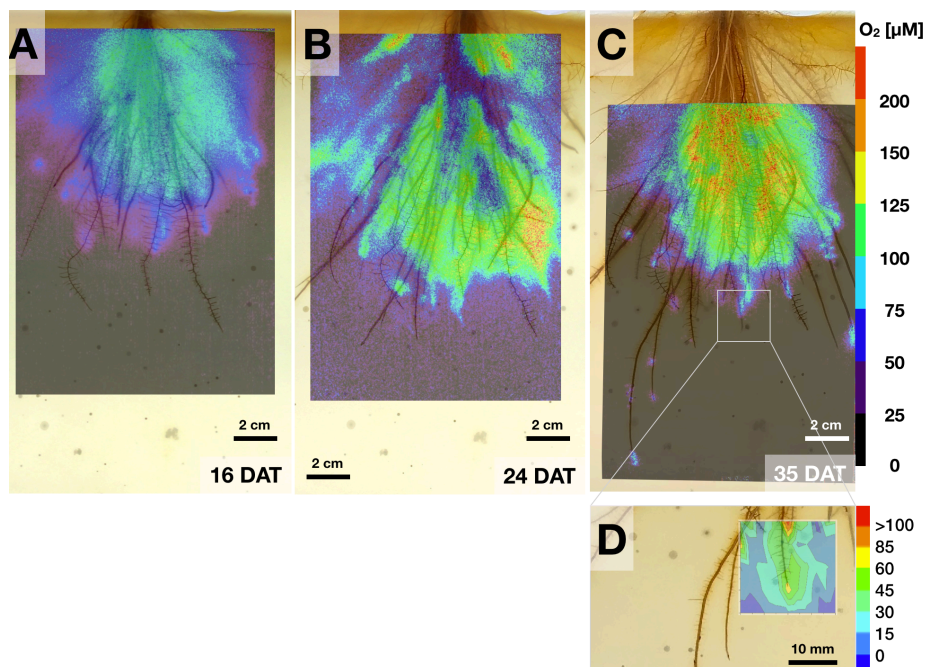
Figure S2. Oxygen concentrations in the rhizosphere. Non-invasive mapping of O$_2$ concentrations at A) 16 DAT, B) 24 DAT and C) 35 DAT (DAT = Days after transfer). D: High-resolution O$_2$ mapping around a single root using O$_2$ microsensors.

Abiotic Fe(II) oxidation kinetics and Fe(II) half-life times along rhizosphere transect
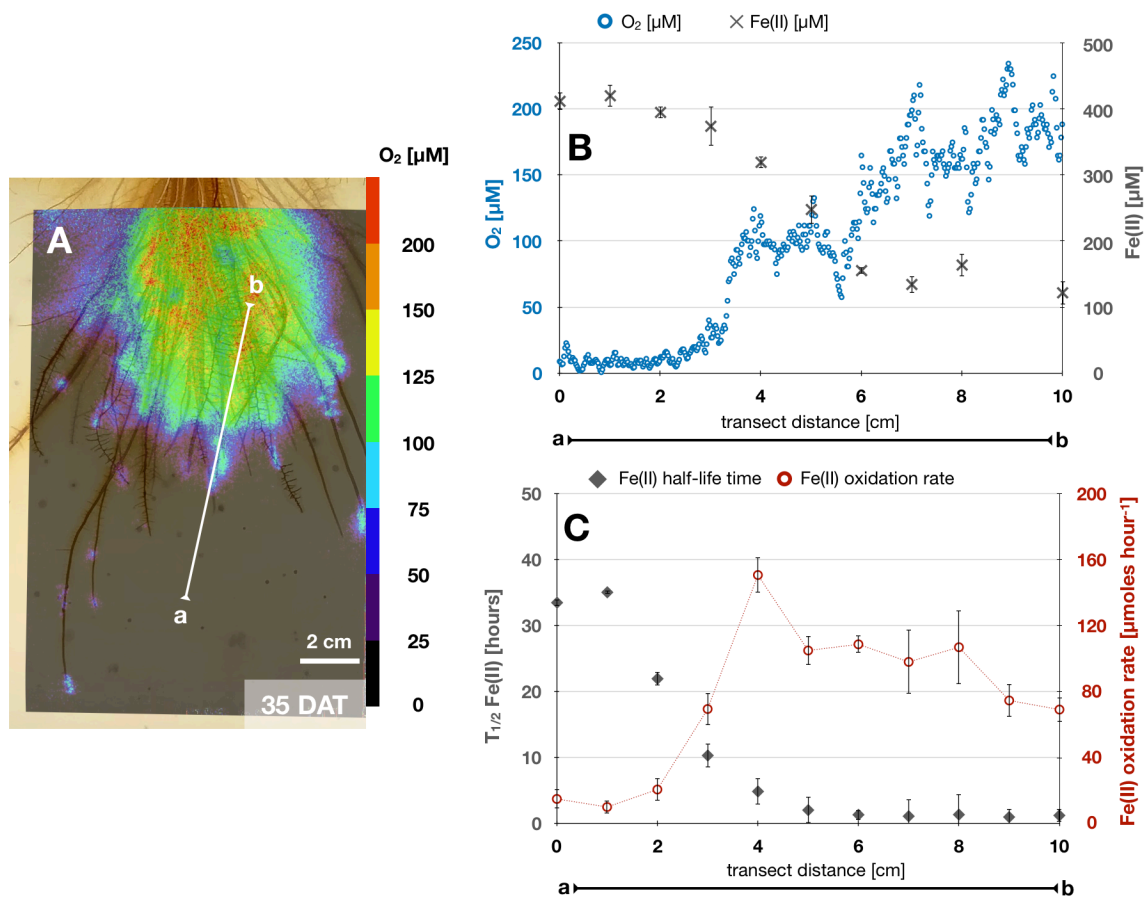
Figure S3. A: Oxygen concentrations within the rhizosphere of a rice plant 35 DAT (= days after transfer) and transect for spatial calculation of Fe(II) oxidation kinetics and Fe(II) half-life times; B: Spatial O_2 and Fe(II) concentrations along transect a–b and C: calculated Fe(II) half-life times and abiotic Fe(II) oxidation rates at specific positions along transect.

Habitable zones for microaerophilic Fe(II)-oxidizing bacteria during plant growth
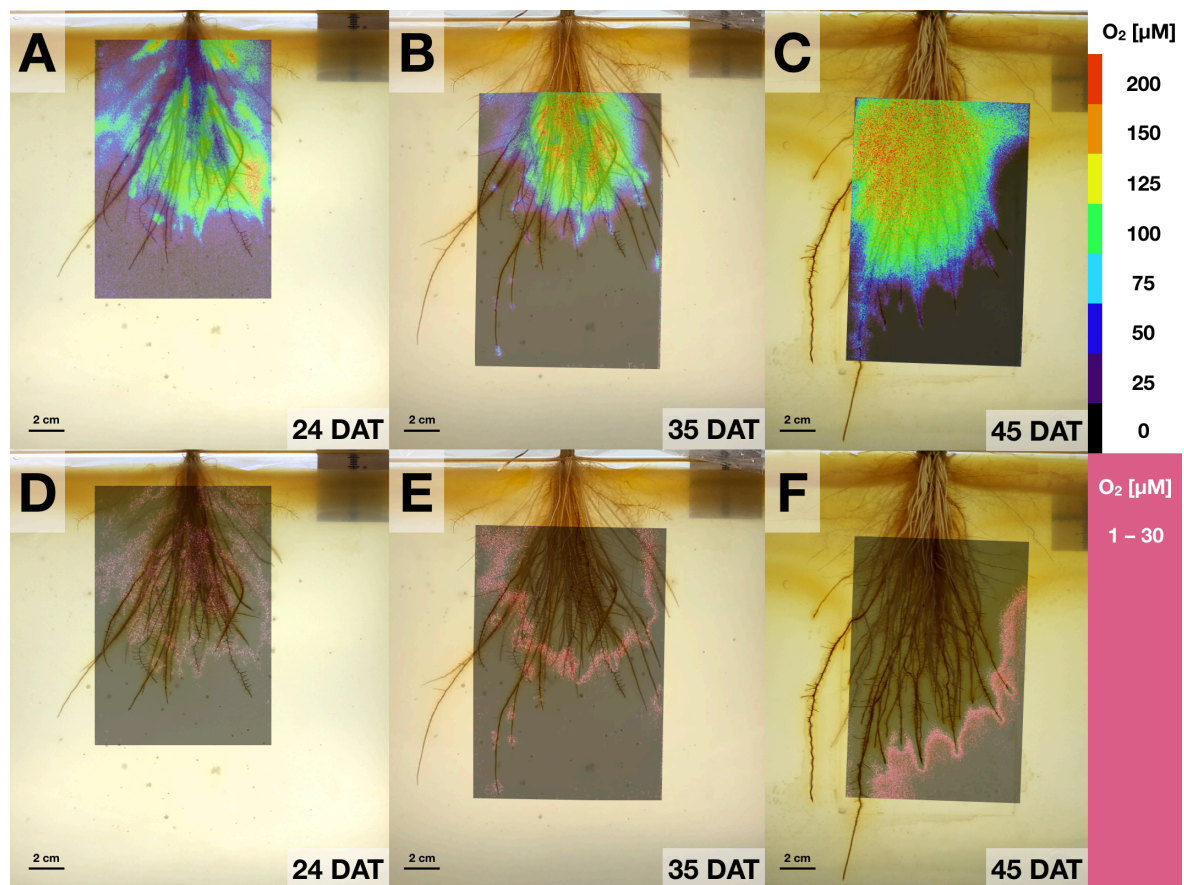
Figure S4. Habitable zones for microaerophilic Fe(II)-oxidizing bacteria. Non-invasively measured O_2 concentrations in the rhizosphere during plant growth (A-C) and identified zones with microoxic conditions (1-30 µM O_2) that provide ideal O_2 concentrations for microFeOx (D-F) over time (DAT = Days after transfer). The relative expansion of this zone increases during root and plant growth from 24 DAT to 45 DAT by more than 30%.

Mössbauer spectroscopy of iron plaque minerals

Sample preparation. Within an anoxic glovebox (100% N_2), root biomass was collected from rhizotrons and dried at constant 30°C. Dried sample material was mortared, and subsequently loaded into Plexiglas holders (area 1 cm^2), forming a thin disc. Prior to analysis, samples were stored anoxically at -20°C to suppress recrystallization processes or microbial activity. Samples were transported to the instrument within airtight bottles which were only opened immediately prior to loading into a closed-cycle exchange gas cryostat (Janis cryogenics) to minimize exposure to air. Spectra were collected at 77 K using a constant acceleration drive system (WissEL) in transmission mode with a ^{57}Co/Rh source. All spectra were calibrated against a 7 μm thick α-^{57}Fe foil that was measured at room temperature. Analysis was carried out using Recoil (University of Ottawa) and the Voigt Based Fitting (VBF) routine.[6] The half width at half maximum (HWHM) was constrained to 0.127 mm/s during fitting.

Results. The spectra collected at 77K showed a dominant narrow doublet (Db) characterized by a low center shift (CS) ranging from CS = 0.47 mm/s and a quadrupole splitting (ΔE_Q) of ΔE_Q = 0.78 mm/s. These hyperfine parameters can be attributed to ferrihydrite as iron(III) mineral phase precipitated on and around the roots.

Table S1. Iron plaque Mössbauer parameters. Hyperfine field parameters of Mössbauer spectrum collected at 77 K.

Sample	Temp (K)	Phase	CS (mm/s)	ΔE_Q (mm/s)	Pop (%)	±	χ^2	Mineral phase
Fe plaque	77	Db	0.47	0.78	100	0.3	0.99	Fh

CS – Center shift, ΔE_Q – Quadrupole splitting, Pop. – relative abundance, χ^2 – goodness of fit, identified mineral phase (Fh – ferrihydrite).
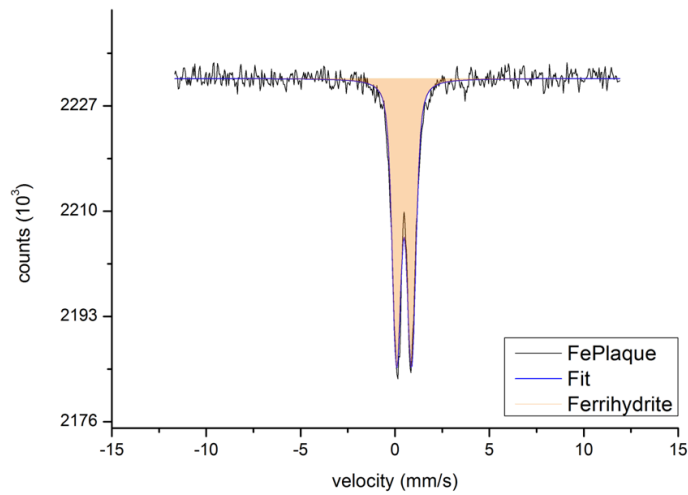
Figure S5. Mössbauer spectrum of iron plaque minerals. Iron plaque minerals were identified by Mössbauer spectroscopy at 77 K. The dominant doublet feature in the spectrum can be attributed to the presence of ferrihydrite as the only identified Fe(III) mineral phase in the sample.

Radial oxygen loss (ROL) and iron plaque formation
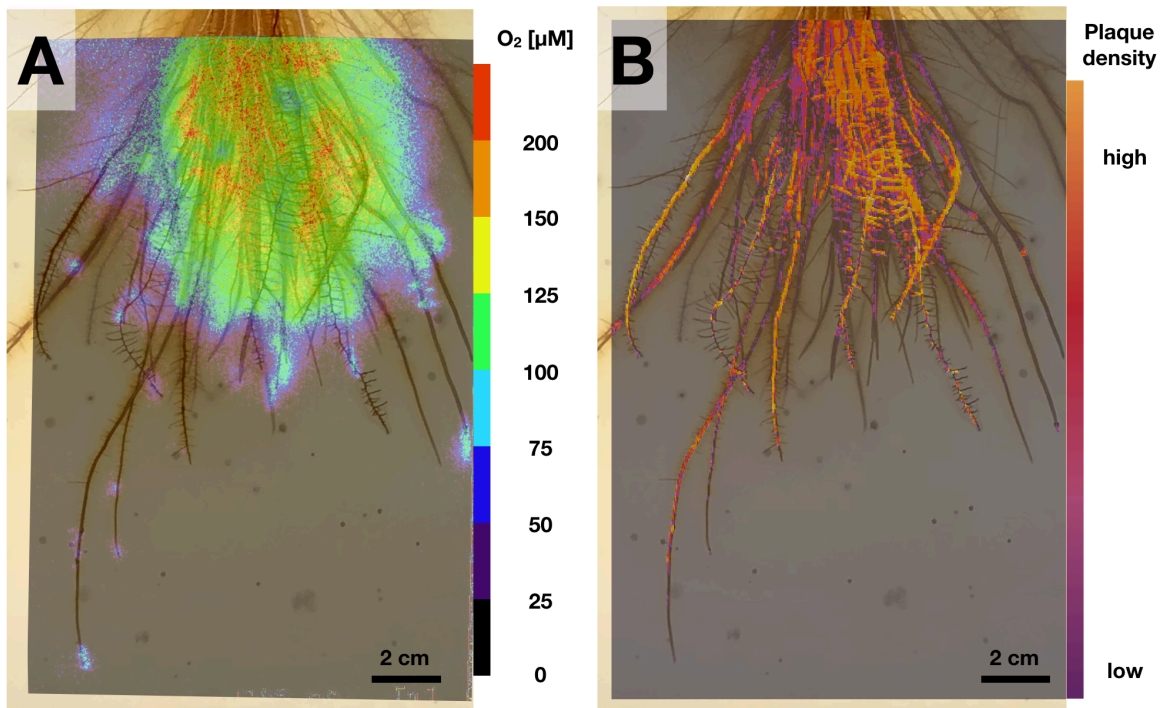
Figure S6. O_2 concentration patterns and identified iron plaque mineral precipitation. A) O_2 concentration measured with optodes. B) Iron plaque precipitation (orange areas) was detected non-invasively via image analysis by pixel thresholding along the roots and correlated with increases in local O_2 concentrations in the rhizosphere before 16 days after transfer.

Quantification of oxidized area in the rhizosphere
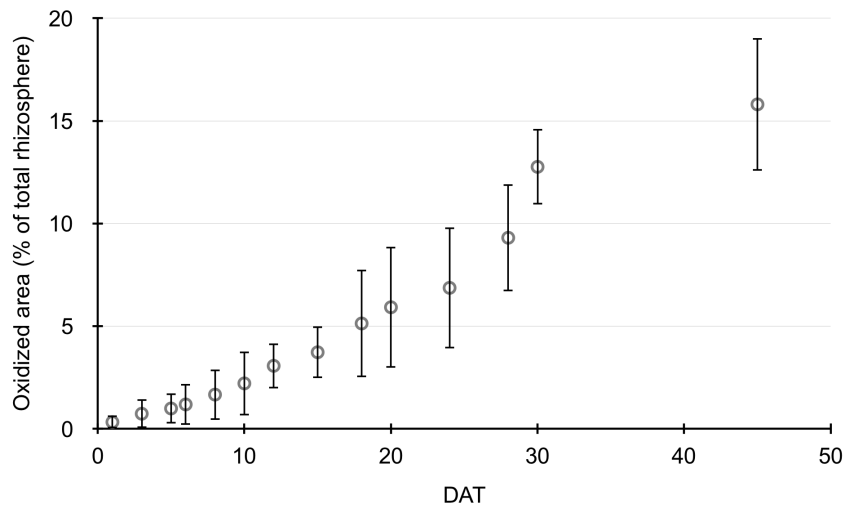
Figure S7. Quantification of oxidized rhizosphere over time. Oxidized zones in the rhizosphere were identified by image analysis and quantified non-invasively. The extension of relative area showing Fe(II) oxidation increased exponentially in all measured replicate plants (n=7) during plant growth. DAT = days after transfer.

Iron plaque formation and pH changes
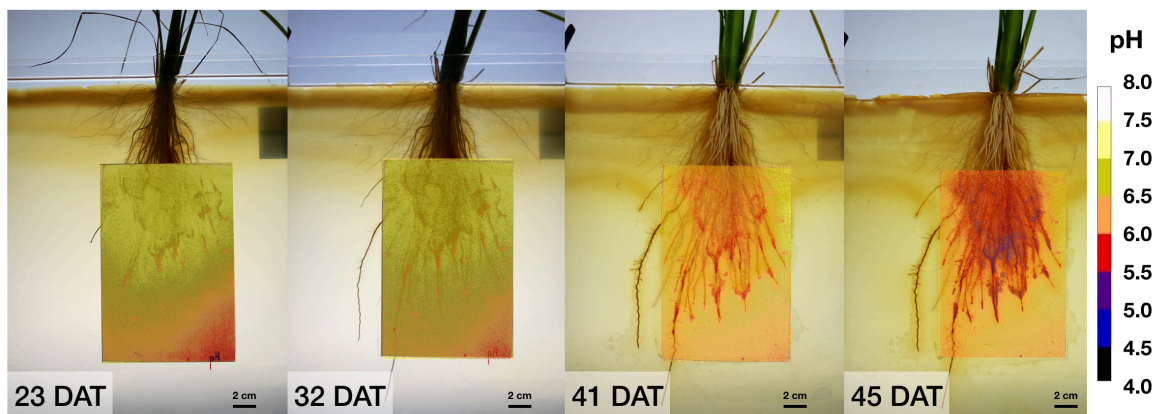
Figure S8. Local pH changes in the rhizosphere during iron plaque formation. Non-invasive mapping of the pH demonstrated that the pH decreased during iron plaque formation: A) 23 DAT, B) 32 DAT, C) 41 DAT, D) 45 DAT. (DAT = days after transfer).

References

1. Brendel, P. J.; Luther, G. W., Development of a Gold Amalgam Voltammetric Microelectrode for the Determination of Dissolved Fe, Mn, O-2, and S(-II) in Porewaters of Marine and Fresh-Water Sediments. *Environ Sci Technol* **1995,** *29*, 751-761.

2. Slowey, A. J.; Marvin-DiPasquale, M., How to overcome inter-electrode variability and instability to quantify dissolved oxygen, Fe(II), mn(II), and S(-II) in undisturbed soils and sediments using voltammetry. *Geochem T* **2012,** *13*.

3. Bristow, G.; Taillefert, M., VOLTINT: A Matlabg (R)-based program for semi-automated processing of geochemical data acquired by voltammetry. *Comput Geosci-Uk* **2008,** *34*, 153-162.

4. Maisch, M.; Lueder, U.; Laufer, K.; Scholze, C.; Kappler, A.; Schmidt, C., Contribution of microaerophilic iron(II)-oxidizers to iron(III) mineral formation. *Environ Sci Technol* **2019,** *53,* 8197-8204..

5. Stookey, L. L., Ferrozine - a New Spectrophotometric Reagent for Iron. *Anal Chem* **1970,** *42*, 779-781.

6. Rancourt, D. G.; Ping, J. Y., Voigt-Based Methods for Arbitrary-Shape Static Hyperfine Parameter Distributions in Mossbauer-Spectroscopy. *Nucl Instrum Meth B* **1991,** *58*, 85-97.

4   From Plant to Paddy — How Rice Root Iron Plaque Can Affect the Paddy Field Iron Cycling

Markus Maisch[1], Ulf Lueder[1], Andreas Kappler[1,2], Caroline Schmidt[1]

[1] Geomicrobiology, Center for Applied Geosciences, University of Tübingen, Germany

[2] Department for Bioscience, Aarhus University, Denmark

Chapter 4

4.1 Abstract

Iron plaque on rice roots represents a sink and source of iron in paddy fields. However, the extent of iron plaque in impacting paddy field iron cycling is not yet fully deciphered. Here, we followed iron plaque formation during plant growth in laboratory-controlled setups containing a transparent soil matrix. Using image analysis, microsensor measurements, and mineral extractions, we demonstrate that radial oxygen loss (ROL) is the main driver for rhizosphere iron oxidation. While O_2 was restricted to the vicinity of roots, root tips showed highest spatio-temporal variation in ROL (<5–50 µM) following diurnal patterns. Iron plaque covered >30% of the total root surface corresponding to 60–180 mg Fe(III) per gram dried root and gradually transformed from low-crystalline minerals (e.g., ferrihydrite) on root tips, to >20% higher-crystalline minerals (e.g., goethite) within 40 days. Iron plaque exposed to an Fe(III)-reducing *Geobacter* spp. culture resulted in 30% Fe(II) remobilization and >50% microbial transformation to Fe(II) minerals (e.g., siderite, vivianite, and Fe–S phases) or persisted by >15% as Fe(III) minerals. Based on the collected data, we estimated that iron plaque formation and reductive dissolution can impact more than 5% of the rhizosphere iron budget which has consequences for the (im)mobilization of soil contaminants and nutrients.

4.2 Introduction

Paddy fields cover more than 6% of arable land surface and represent the basis for cultivation of rice, the major food crop for more than half of the world's population. Most commonly, rice plants are cultivated on flooded paddy fields. Under these water-logged conditions, the submerged soil is typically depleted in oxygen (O_2) and rich in organics—an ideal habitat for Fe(III)-reducing microorganisms.[1] Using Fe(III) minerals as terminal electron acceptor, these bacteria significantly impact the redox state of soil-borne iron minerals and fuel the pool of dissolved $Fe(II)_{aq}$ in the pore water by remobilizing $Fe(II)_{aq}$ from minerals through reductive dissolution. This typically leads to high concentrations of more than a few hundred micromoles of dissolved and phytoavailable Fe(II) in the rhizosphere pore water of paddy fields.[2]

Iron is an essential trace element for photosynthesis.[3,4] However, high concentrations of phytoavailable Fe(II) ultimately lead to an intoxication of the photosystem and leaf bronzing in rice plants.[5] In order to control the uptake of $Fe(II)_{aq}$, rice plants release O_2 from roots by so-called radial oxygen loss (ROL).[6] At circumneutral pH, Fe(II) gets rapidly chemically oxidized by O_2 from ROL to ferric iron (Fe(III)) and precipitates as Fe(III) (oxyhydr)oxides on and around the root surface as iron plaque.[7] These Fe(III) (oxyhydr)oxides represent a highly

reactive mineral fraction in the soil horizons as they not only participate in the immobilization of essential plant nutrients but impact, to a large extent, the sequestration of many other soil components such as contaminants and trace elements.[6,8-11]

It is hypothesized that an enormous variety of microorganisms is involved in iron cycling in the rhizosphere and that they considerably affect the iron redox cycle in water-logged paddy soils.[12] However, it was shown for only a few examples that iron-metabolizing bacteria can find ideal conditions in the paddy field rhizosphere.[13,14] Examples include microaerophilic Fe(II)-oxidizing bacteria which were shown to kinetically contribute to Fe(II) oxidation under microoxic conditions.[15,16] Furthermore, Emerson et al. (1999) provided first evidence that neutrophilic microaerophilic Fe(II)-oxidizing bacteria were often closely associated with roots and root iron plaques in the wetland rhizosphere.[17] Neubauer et al. (2007) demonstrated the potential of these bacteria to enhance iron plaque formation on wetland plant roots and in a recent study the effective habitable zone for microaerophilic Fe(II)-oxidizing bacteria was shown to expand to a large extent throughout the entire rhizosphere during plant growth. [18,19] Congruent with these findings, it is undoubtable that rice plant roots and microaerophilic Fe(II)-oxidizing bacteria in particular play a major role in iron mineralization in the rhizosphere of flooded paddy fields.

In addition to the foregoing role of soil-borne iron to serve as an electron donor, the iron plaque minerals can also serve as an electron acceptor for Fe(III)-reducing bacteria.[20,21] Reduction of iron plaque minerals not only considerably change the sorption capacities of these iron minerals but leads to a re-mobilization of surface-bound contaminants by microbial reductive dissolution.[22,23] Over the last few decades, research interest towards an understanding of root iron plaque formation, retention of contaminants, and the role of bacteria in re-mobilization have slightly increased.[24-28] Investigations on the microbial community level, determining Fe(II) oxidation and Fe(III) reduction rates, partly complemented the knowledge about a dynamic rhizosphere systems in paddy fields on a large scale.[29] Moreover, famous studies proposed the existence of an active rhizosphere iron cycle promoted by the presence of wetland vegetation such as rice plants in paddy fields.[30,31] However, the extent to which Fe(II)-oxidizing and Fe(III)-reducing bacteria might be involved in this redox-active iron cycling around the roots has not been investigated so far.

In the current study, we aim to demonstrate that rice plant roots not only span up a biogeochemical network that creates a narrowly closed iron cycle in the entire rice plant rhizosphere but actively contribute to the cycle by iron mineral (trans)formation. Furthermore, we intended (i) to quantify the ROL-induced iron plaque mineral formation; (ii) to analyze the potential spatio-dynamic impact of microaerophilic Fe(II) oxidation, and (iii) to determine the capability of microbial Fe(III) reduction for iron plaque dissolution and Fe remobilization. By

implementing experimental data from laboratory-controlled incubation and rhizotron studies, we were able to estimate the plant and microbially induced budget for Fe(II) oxidation, while the derivation of rates for Fe(III) reduction are closing the rhizosphere iron cycle on the reductive side. These findings advance the understanding of complex rhizosphere iron redox interactions and help to quantify iron fluxes between dominant iron-reducing and -oxidizing processes in a rice plant rhizosphere during rice plant growth.

4.3   Materials and Methods

Plant Cultivation. Rice seeds (Oryza sativa Nipponbare) were sterilized (0.1 % H_2O_2 rinse, ultrapure water) and seedlings were pre-grown in sterile 50% Hoagland [32] solution at pH 6.8. For rhizotron studies in the growth gel, seedlings were transferred into anoxic and sterile rhizotrons (described in Maisch et al., 2019a and Supporting Information) and consecutively covered with opaque fabric to prevent illumination of the roots. For hydroponic cultivation, pre-grown seedlings were transferred at three-leaf stage into anoxic hydroponic setups with 500 mL of 100% Hoagland solution amended with 500 µM Fe(II)$_{aq}$, buffered (PIPES, 20 mM) at pH 6.8. Setups were wrapped in aluminum foil in order to prevent illumination of the growth solution and the roots. Decline in hydroponic medium by evapotranspiration was replaced by anoxic and sterile 50% Hoagland solution at pH 6.8 and 500 µM Fe(II)$_{aq}$. Plants were kept at temperature-controlled conditions (25–27 °C, 70% rel. humidity) following day (14 h)–night (10 h) cycles illuminated by a high-pressure sodium lamp (10,000–12,000 lx).

Geochemical Measurements and Image Analysis in Rhizotrons. Using planar optode sensor foils, O_2 and pH were measured non-invasively from outside the rhizotrons as described in Maisch et al. (2019a). For the quantification of averaged local O_2 concentrations, designated regions of interests (ROI) with dimensions of 10 × 10 mm (1 cm^2) were defined in recorded images at different time points using the software VisiSens ScientifiCal$^{©}$ (Presens, Regensburg, Germany). In-situ Fe(II)$_{aq}$ concentrations were spatially quantified by Voltammetry (Cu-Au sensors with a Hg-Au alloy surface (100 µm), hooked to a potentiostat (DLK-70, Analytical Instrument Systems, Flemington, NJ, US)). Homogeneous Fe(II) oxidation rates were calculated based on geochemical parameters in the rhizotrons following the method described in Lueder et al. (2018) and Maisch et al. (2019b).[16, 33] Images of the root-zone were recorded following the simulated daylight period with a digital camera (EOS 1200D, Canon) using constant camera settings. Image analysis and quantification of oxidized areas in the rhizosphere were performed on the basis of pixel identity and color thresholding[34-36] as also described in Maisch et al. (2019a). On that basis, particle analysis was performed to

quantify the area of iron plaque on root surfaces at individual time intervals. The surface of root iron plaque minerals was estimated by extrapolating the two-dimensional area of iron plaque formation (A_{image})

$$A_{image} = 2 \times r \times h = d \times h \tag{1}$$

with h (cm) as imaging area height, r (cm) as imaging area radius and d (cm) as imaging area diameter to a three-dimensional outer surface mantle area of ideal cylindrical roots[37] as an approximation for the mineral surface of root iron plaque ($A_{iron\ plaque}$)

$$A_{iron\ plaque} = 2 \times r \times \pi \times h \tag{2}$$

summarized in the following simplified equation as

$$A_{iron\ plaque} = A_{image} \times \pi \tag{3}$$

Iron Plaque Mineral Identification. Roots covered in iron plaque minerals were collected 48 days after plant transplantation under anoxic conditions inside a glovebox (100% N_2) from root tips (young roots), the middle parts of roots (approx. 20 day old roots), and basal root zone (approx. 40 day old roots). Iron minerals were identified using Mössbauer spectroscopy (Supporting Information).

Iron Plaque Reduction in Liquid Culture. After 52 days on hydroponic cultivation, rice plants were removed from Hoagland solution, green biomass was detached and roots were transferred individually into anoxic sterile 500 mL mineral medium [38] buffered (22 mM bicarbonate) at pH 6.8 containing 20 mM Na-acetate as electron donor substrate. A 5% (v/v) inoculum of an Fe(III)-reducing enrichment culture (99.8 % identity to *Geobacter* sp. CD1[39] based on 16S rRNA) isolated from a paddy field (Vercelli, Italy; Supporting Information) was added to each microcosm. In order to inhibit cell activity in abiotic control incubations, 4% paraformaldehyde (PFA) were added to the respective setups. Microcosms were kept in the dark at constant temperature (24 °C) for a total of 8 days.

Iron Plaque Reduction in Rhizotrons. Roots covered in iron plaque were sampled from a 52-day old rice plant which was previously grown on an Fe(II)-rich hydroponic solution. Collected root material was soaked in a cell suspension of an Fe(III)-reducing enrichment culture (see above) and subsequently transferred into a rhizotron that contained warm (35 °C), sterile and anoxic mineral medium,[38] amended with 0.3% Gelrite. After cooling down to room temperature, the mineral medium formed a transparent gel. The rhizotron was kept in the dark at constant temperature (24 °C).

Chapter 4

Iron Plaque Reduction: Geochemical Measurements and Mineral Identity. Liquid samples were collected from microcosm setups under anoxic conditions at different time steps. In order to quantify dissolved $Fe(II)_{aq}$ and particulate Fe(II)/(III), filtered (0.45 µm) and non-filtered samples were acidified (1:2) in 2 M HCl to prevent oxidation at ambient atmosphere and were analyzed by the Ferrozine assay.[40] For iron plaque mineral analysis, roots covered in iron plaque were collected randomly prior to the iron plaque reduction experiment and at the end after 10 days from biotic and inhibited control setups. Samples from the rhizotron iron plaque reduction experiment were collected after 10 days and dried under anoxic conditions (28 °C, 100% N_2). Iron minerals in these samples were identified by Mössbauer spectroscopy as described in the Supporting Information. In order to recalculate the total amount of iron plaque on the root prior to microbial reduction, residual iron plaque minerals at the end of the incubation were extracted in 6 M HCl, while dissolved Fe(total) was quantified by the Ferrozine assay. Dissolved, particulate Fe(II)/(III) and extracted Fe(total) were then added up to recalculate a value for the initial total iron plaque on the root surface.

4.4 Results

Spatio-Temporal Quantification of ROL and the Identification of O_2 Hot Spots. Root growth and O_2 concentrations were followed in transparent rhizotron setups during plant growth (Figure 1A). After 5 days after transfer (DAT), intermittent O_2 was detected in the rhizosphere forming steep gradients ranging from 70 µM O_2 on the surface of first lateral root tips to <5 µM O_2 expanding 6 mm into the anoxic soil matrix. During root growth, O_2 concentrations radially increased in the vicinity of individual roots. On the root surface O_2 concentrations reached values of >100 µM. Towards the anoxic soil matrix, O_2 decreased gradually below the detection limit in a distance of 1.5 ± 0.5 cm away from the root surface. While the basal root zone was continuously dominated by oxidized conditions with O_2 concentrations >50 µM, local oxygenated hot spots with elevated O_2 concentrations formed around young root tips. In contrast to the anoxic soil matrix in which O_2 was constantly below the detection limit, root tips were continuously surrounded by high O_2 concentrations with more than 60 µM of O_2 at the root tip center. Local O_2 concentrations radially expanded around root tips and formed steep O_2 gradients that reached 3–15 mm into the rhizosphere (Figure 1B). This ROL hot spot not only led to an increase in local O_2 concentrations but was also found to accelerate chemical Fe(II) oxidation. Abiotic Fe(II) oxidation kinetics were calculated to reach oxidation rates of up to 20 µM Fe(II) hour^{-1} within the radial vicinity of 5 mm around the root tip center (Figure 1C).
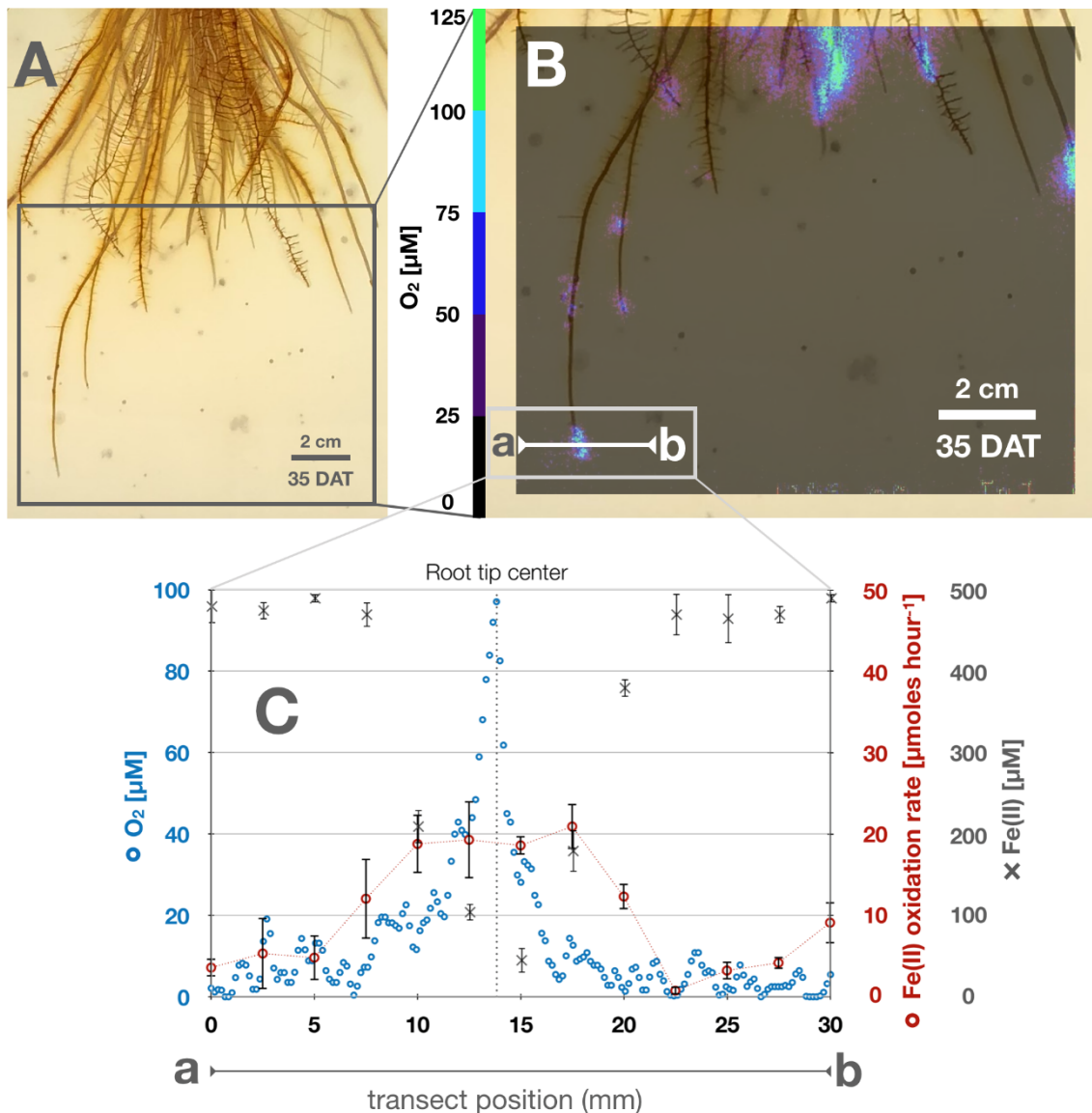
Figure 1. Radial oxygen loss and iron geochemistry at the root–soil interface at the end of light-incubated cycles: (**A**) Rice roots covered in iron plaque. (**B**) Radial oxygen concentrations surrounding root tips 35 DAT (DAT = days after transfer), a-b indicates a transect where O_2 and Fe(II) were measured and Fe(II) oxidation kinetics were calculated. (**C**) Transect a-b: representative concentrations of O_2, Fe(II) and calculated homogeneous Fe(II) oxidation rate along transect.

In order to spatio-temporally quantify changes in local O_2 patterns surrounding root tips, O_2 concentrations were recorded in 5-minute time intervals over a period of 48 h. Local O_2 concentrations were quantified in three designated areas (1 cm^2) (Figure 2A). Within two diurnal cycles of 24 h each, highest local O_2 concentrations surrounding three designated root tips were observed at the end of light incubated cycles (Figure 2A–D). During dark incubated cycles, local O_2 concentrations in the vicinity of root tips remarkably decreased by more than 80% with 2.7 (± 1.0) µM hour^{-1} on average within 10 h of incubation the dark (Figure 2E; Table 1). Examples include O_2 hot spots where local O_2 concentrations of up to 100 µM O_2

and a radial expansion of 5–10 mm in the light decreased to O_2 concentrations of <50 µM and a radial expansion of less than 5 mm in the dark (Figure 1; Figure 2A–D). Repeatedly within 48 h, both the lowest O_2 concentrations and lowest degrees in expansion were measured at the end of the dark-incubated cycles among all root tips (Figure 2). With the initiation of illumination, O_2 loss from root tips was observed to respond within 2 h by an increase in local O_2 concentrations by 2.0 (±1.2) µM hour^{-1} on average measured at three replicate root tips (Figure 2A–D). Similarly, the radial O_2 expansion increased and plateaued between 5–10 mm after 9 h of light incubation before it decreased again with the initiation of the following dark cycle.
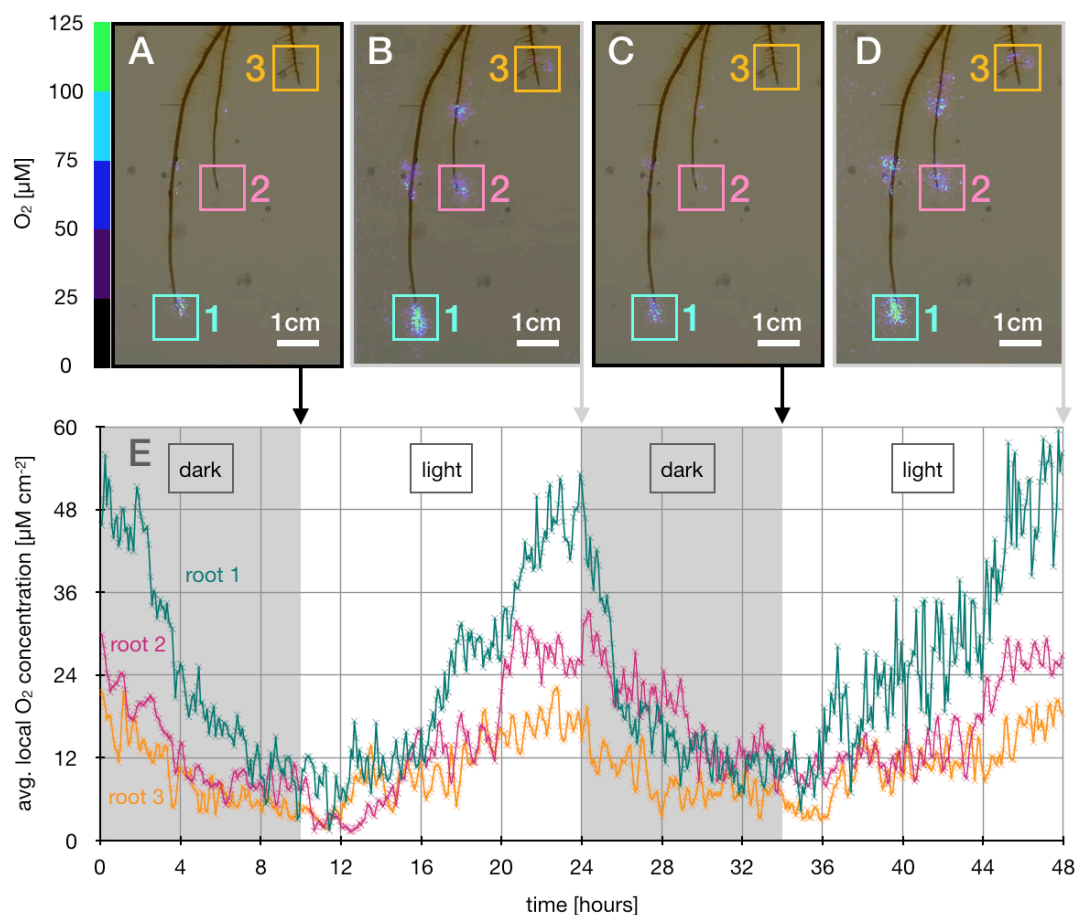
Figure 2. Diurnal changes in local O_2 concentrations at root tips. (**A**)–(**D**) illustrate three root tips and local O_2 concentrations in the range of 0–125 µM O_2 represented as color coded pixels. Colored squares 1–3 represent areas around root tips (1.0 cm^2) where local O_2 concentrations were quantified at the end of dark (10 h) and light (14 h) incubated cycles, respectively. (**E**) displays averaged measured local O_2 concentrations over time, measured in time intervals of 5 min for each root tip area 1–3, respectively.

Table 1. Responses of local root tip O_2 concentrations to diurnal cycles. Changes in local O_2 concentrations ($\Delta\,O_2$ local) at three designated root tips (roots 1–3) and average changes during dark (10 h) and light (14 h) incubation.

$\Delta\,O_2$ Local Concentration at Root Tip	Dark ($\mu M\ hour^{-1}$)	Light ($\mu M\ hour^{-1}$)
Root 1	-3.8 (±0.6)	+3.2 (±0.8)
Root 2	-2.4 (±0.4)	+2.0 (±0.3)
Root 3	-1.9 (±0.3)	+0.9 (±0.2)
Average	-2.7 (±1.0)	+2.0 (±1.2)

Iron Plaque Mineral Formation and Transformation. The release of O_2 from roots lead to the oxidation of Fe(II) and the formation of ferric iron minerals on the root surface across the entire rhizosphere. Following analysis of rhizosphere images, we observed that after 3 DAT freshly precipitated orange-colored iron plaque minerals formed on young roots (Figure S1B–G, Supporting Information). Following root growth and iron plaque mineral formation over 45 days, both the average total root surface area and surface area of root iron plaque increased significantly following a linear trend over time (Figure 3A; Figure S1A, Supporting Information) with an averaged formation of 4.3 cm^2 root surface area ($R^2 = 0.97$) and 1.7 cm^2 iron plaque surface area ($R^2 = 0.98$) precipitating per day. However, among all replicate setups, the ratio of iron plaque covered to non-covered root surface area widely varied within 30 DAT ranging from <15% to more than 50% of the total root surface covered in iron plaque precipitates (Figure 3B). Yet, towards the end of the experiment after 45 DAT, on average 36 (±2.6)% of the total root surface area in all setups were covered in iron plaque minerals which corresponds to an average root iron plaque surface area of 75 (±13.6) cm^2 per plant at the end of the experiment.
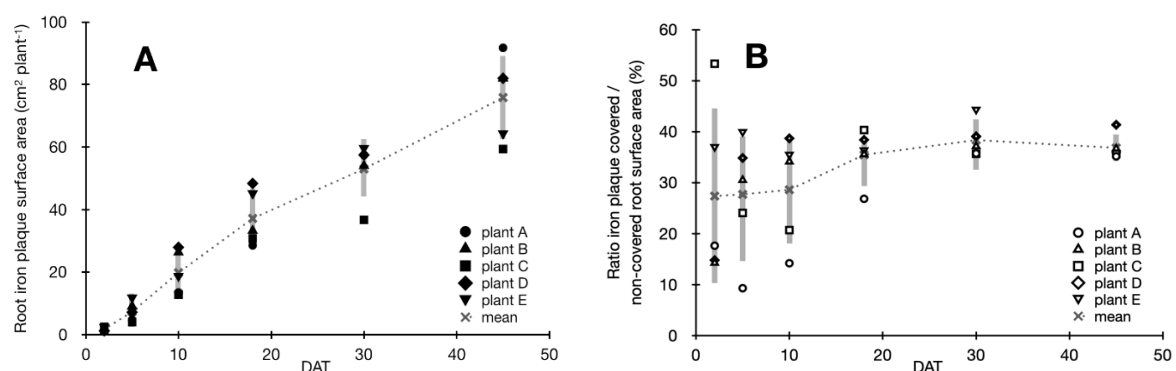
Figure 3. Root iron plaque formation during plant growth. (**A**) Iron plaque mineral surface (cm^2 per plant) on roots during plant growth (DAT = days after transfer) of five replicate plants (filled symbols), mean root iron plaque surface area (cross & punctuated line) and standard deviation (grey bars); (**B**) Ratios of iron plaque-covered to non-covered root surface area (%) in rhizotrons during plant growth over 45 DAT, averaged ratio of all replicates (cross and punctuated line) and standard deviation (grey bars).

Iron plaque minerals collected at the end of the growth experiment from (i) the basal root zone (approx. 40 days old), (ii) the middle part of the root (approx. 20 days old), and (iii) the root tips (freshly formed iron plaque) differed substantially in their mineralogical composition. The oldest root iron plaque minerals showed the highest degree in crystallinity with 15% goethite, approx. 10% lepidocrocite and some resilient ferrihydrite (Figure 4; Figure S2A; Table S1). Root iron plaque minerals collected from the middle part of the root section were composed of 25% lepidocrocite, approx. 70% ferrihydrite and 5% goethite only (Figure 4; Figure S2B; Table S1). Freshly formed iron plaque collected from root tips was dominated by >95% ferrihydrite and a small fraction of approx. 4% potentially sorbed/complexed Fe(II) (Figure 4; Figure S2C; Table S1).
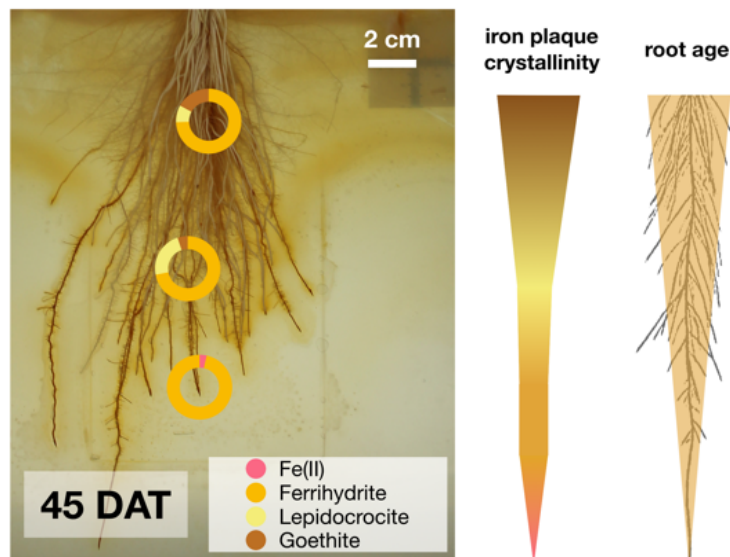
Figure 4. Iron plaque collected from different root sections, young root tip, middle part (approx. 20 days old) and basal root zone (approx. 40 days old) showed increasing iron mineral crystallinity which correlated positively to root age.

Iron Plaque Reduction, Mineral Transformation, and Reductive Dissolution. In order to quantify the extent of iron plaque that can be reduced and remobilized microbially, roots from rice plants that were covered with iron plaque minerals were exposed to an Fe(III)-reducing enrichment culture isolated from a paddy field (Vercelli, Italy; 99.8% identity to *Geobacter* sp. CD1[39] based on 16S rRNA). Within 24 h, iron plaque minerals in biotic setups changed in color from orange to black, while abiotic control incubations remained orange (Figure 5A). In biotic setups, dissolved Fe(II) concentrations increased significantly from initially <10 µM Fe(II) to 730 (±130) µM Fe(II) after 24 h which translates to an Fe(II) remobilization rate of 15 µmoles per hour. In the inhibited control incubation, Fe(II) concentrations remained constant

throughout the experiment with Fe(II) concentrations <50 µM. Following 43 h of incubation, Fe(II) concentrations declined by approx. 15% in biotic incubations and leveled off at constant concentrations of around 550 µM Fe(II) until the end of the incubation after 185 h (Figure 5B).
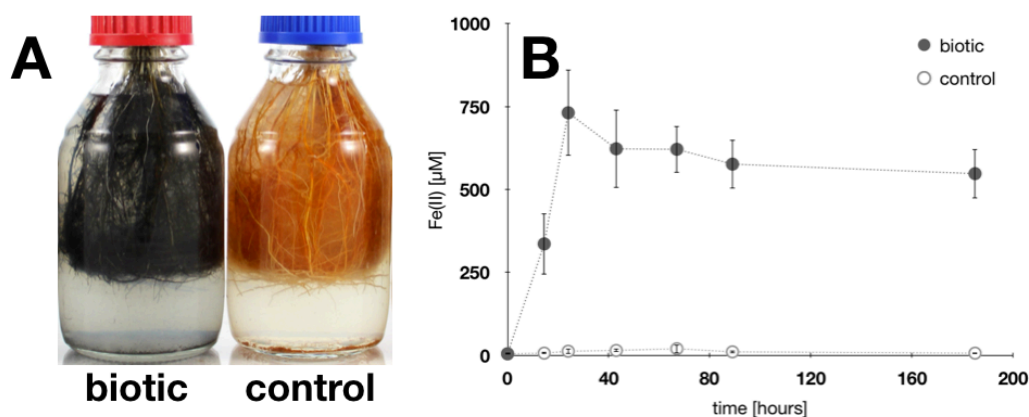
Figure 5. Root iron plaque reduction. (**A**): Root iron plaque exposed for 24 h to an Fe(III)-reducing enrichment culture (99.8% similarity to *Geobacter* spp.). Iron plaque minerals changed from orange (control) to black (biotic) during incubation. (**B**): Dissolved Fe(II) concentrations in medium during iron plaque reduction. Iron(III) plaque minerals were reduced and Fe(II) remobilized through microbial reductive dissolution. Error bars represent experimental standard deviation from six replicate setups.

Table 2. Iron plaque formation, remobilization, and transformation during microbial Fe(II) reduction. Total iron plaque mineral formation on roots was quantified by mineral extraction.

	Total Root Iron Plaque (mg Fe g^{-1} Dry Root Weight, (Mean))	Iron Plaque Remobilization (mg Fe g^{-1} Dry Root Weight (%))	Iron Plaque Fe(II)/Fe(III) Ratio after Incubation (%)
Remobilization Ratio	60.2–189.0 (117.4 ± 23.0)	23.4–58.6 (20–29)	73–85

During microbial reduction, also the iron plaque mineralogy changed considerably. After 185 h, a sample was collected from biotic and control incubations. Mössbauer spectroscopy demonstrated that iron minerals in the control incubation can be identified as 90% ferrihydrite and 10% lepidocrocite (Figure S3A). On the contrary, in active Fe(III)-reducing incubations, more than 80% of the remaining iron plaque on the root surface was composed of Fe(II) minerals (e.g., 70% Fe(II) (oxyhydr)oxides and 10% Fe(II)-sulfur species), while only 20% of the root iron plaque minerals remained as Fe(III) (oxyhydr)oxide identified to be ferrihydrite (Table S2; Figure S3B). Iron mineral extractions after the incubation confirmed that 20–29% of the total initial iron plaque (ranging from 60.2–189.0 mg g^{-1} dry root weight, mean 117.4 (±23.0) mg g^{-1} dry root weight) was remobilized as Fe(II) during microbial incubation (Table 2).

Spatio-Temporal Iron Plaque Reduction, Fe(II) Remobilization, and Rhizosphere Gradients.
Roots covered in iron plaque were exposed to the Fe(III)-reducing enrichment culture and
incubated in transparent growth gel in order to spatio-temporally follow Fe(III)-reduction and
remobilization of Fe(II) from roots. After 3 days, black colored iron plaque was observed in a
heterogeneous pattern and constituted approximately 50% of the total iron plaque on roots
(Figure 6). Changes in color from initially orange minerals to dark phases were previously
demonstrated to indicate Fe(III) reduction and mineral transformation. Over the following
days, black minerals dominated root iron plaque and expanded over the entire root biomass
(Figure 6A–D). After 10 days of incubation, the entire root biomass was fully covered in black
minerals (Figure 6E). Dissolved Fe(II) was measured voltammetrically along a transect through
the rhizosphere to quantify dissolved Fe(II) as a product of reductive dissolution of iron plaque.
Concentrations of Fe(II) varied to a large extent from <500 µM at positions without roots to
high concentrations reaching >1.5 mM Fe(II) close to roots covered in black precipitates
(Figure 6F). Reduced iron plaque minerals were analyzed by Mössbauer spectroscopy as
identified as similar mineral phases (as Fe(III) mineral vivianite, potentially Fe(II)–S phase and
some resilient ferrihydrite) as previously observed in liquid culture iron plaque reduction
experiments (Table S3; Figure S4).
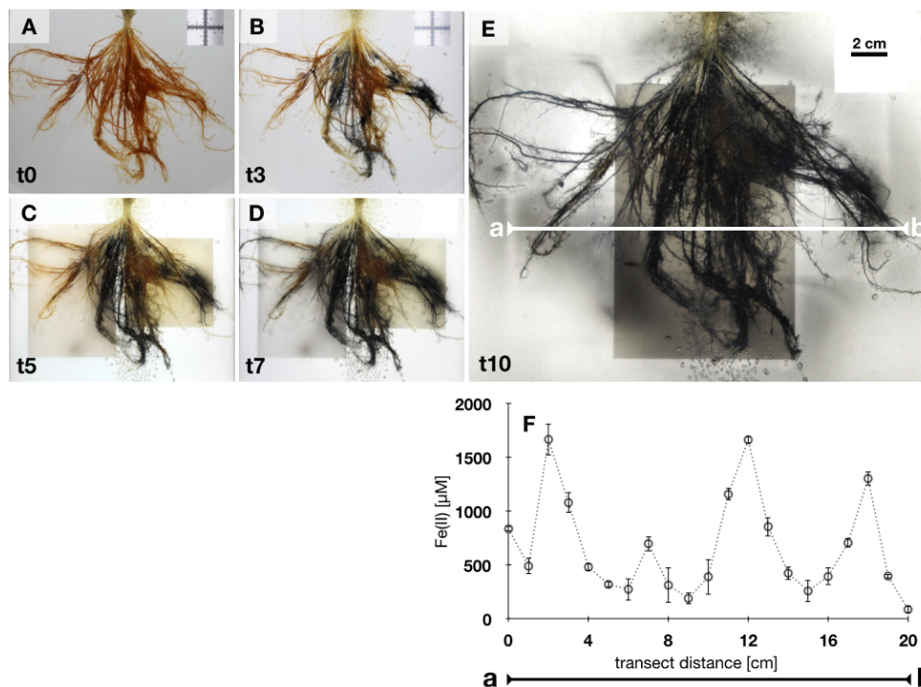
Figure 6. Microbial Fe(III) iron plaque reduction. (**A**)–(**E**): Roots covered with iron plaque minerals
incubated in rhizotron with an Fe(III)-reducing enrichment culture. Iron plaque minerals change in
color over time A, t0: day 0 – E,t10: day 10. (**F**): Voltammetric measurements along transect a-b in
setup of Figure, after 10 days of incubation, detect Fe(II) remobilized from root iron plaque is closely
associated with roots. Error bars represent standard deviation from triplicate voltammograms.

4.5 Discussion

Rice Roots as Initiator for Rhizosphere Iron Mineral Formation and Heavy Metal Immobilization. Research interest in iron plaque on rice roots raised significantly over the last decades.[24-26,28] Numerous studies impressed with estimates derived from laboratory and field observations attempting to explain the sorption of soil components to iron plaque and quantifying the iron plaque immobilization capacity for contaminants.[24-28] The results in the current study aim to complement the understanding of rice roots as an important driver for the formation of soil iron minerals. Here, we found that an averaged total of approx. 75 cm^2 per plant iron plaque surface area was calculated to have formed on the root surface until the end of the growth cycle after 45 DAT (Figure 7). It has been previously observed that root iron plaque can form on roots of rice plants and form a thick layer between 20–40 µm.[41,42] Given the calculated iron plaque surface area and the range of reported iron plaque layer thickness, the resulting volume of iron plaque that can form on the roots until 45 DAT was calculated to reach values between 150 mm^3 to 300 mm^3 per plant. Since ferrihydrite was the most dominant iron mineral species identified in the iron plaque in our setups, the density of ferrihydrite of ρ_{Fh} = 3.8 g/cm^3 [43] was considered as an estimate for the density of all iron minerals that formed as root iron plaque. This estimate results in a total of 570 mg to 1,140 mg of ferrihydrite that can theoretically form on the root surface of one plant within 45 DAT. Considering that ferrihydrite consists of approx. 70 atomic weight % of iron atoms, this results in a net mass of around 400 mg to 800 mg iron that precipitated as iron minerals on the roots of each rice plant within only 45 days. In comparison with the observed linear trend of averaged 1.7 cm^2 root iron plaque surface area being formed per day, which corresponds to a volume of up to 5.1 mm^3 root iron plaque, we estimated that 20 mg ferrihydrite (which represents approx. 14 mg soil-borne iron) can precipitate daily on the root surface of one single rice plant.

Evidently, this large number of iron minerals that can precipitate on the root surface has broad consequences not only for the immobility of soil-borne iron but the biogeochemical cycling of iron in paddy soils. With around 80–100 rice plants conventionally planted per square meter of paddy soil, more than 1.2 g soil-borne iron can precipitate on rice roots within one cubic meter of flooded paddy soil per day. A paddy field in south east Asia, that is commonly characterized by 20–50 g iron per kg wetted soil[14,44] and an averaged bulk density of approx. 1.5 g/cm^3 [45], can contain between 3×10^4–7.5×10^4 g iron per m^3 soil. Following the concept and the constant availability of dissolved Fe(II), rice plants would have the potential to daily affect between 2–5 ppm of the total soil by iron plaque formation. Considering the medium duration of 120–140 days per growing season, the roots of rice

plants would theoretically be able to precipitate 156–182 g iron as root iron plaque minerals per growing season within one cubic meter soil, which represents a maximum of approx. 0.6 % of total iron budget in a paddy soil. Although 0.6 % seems to represent only a small fraction of the total iron budget in a paddy field, the consequences for the retention of dissolved substances, such as nutrients, (cat)ions, or contaminants might be significantly impacted. The total surface area of iron plaque minerals that can form under the hypothesized conditions increases daily by 170 cm^2 per m^3 paddy soil when 100 plants are planted. Ideal ferrihydrite in particular, is dominated by singly-coordinated surface groups with a reported number of 6.0 ± 0.5 nm^{-2}.[43] Consequently, a formation of 170 cm^2 iron plaque surface area provides a total number of 1.02×10^{17} singly-coordinated surface groups where dissolved ions in the pore water, such as phosphate, carbonate, and heavy metals, i.e., arsenite or arsenate can build a Stern layer[46] and form inner-sphere complexes with the root iron (oxyhydr)oxides.

The formation of plant-induced iron (oxyhydr)oxide minerals in the soil horizon could theoretically also impact the retention of other soil constituents and metal(loid)s such as arsenic. In other words, under the theoretic assumption that one dissolved soil-borne ion can bind to one surface group of root plaque ferrihydrite, the observed formation of root iron plaque on the roots of rice plants could provide surface sites for approx. 0.2 μmoles dissolved ions per day within one m^3 of paddy soil. Typically, paddy fields contaminated with arsenic contain up to 150 μg arsenic (=2 μM) per liter pore water. Given an effective soil porosity of 0.25, which is commonly observed in wetted paddy fields,[47] the pore water of 1 m^3 paddy soil can effectively contain 500 μmoles of arsenic ions. Based on these assumptions and the observed root iron plaque formation from the current study, the roots of 100 rice plants on one 1 m^2 paddy field would have the potential to form iron mineral surface sites that can bind and immobilize up to 20 μmoles of arsenic per growing season, which corresponds to approx. 5% of the total dissolved arsenic in 1 m^3 contaminated paddy soil. In addition to one layer of inner-sphere complexes, also outer-sphere adsorption complexes might play an important role in arsenic immobilization and even increase the root iron plaque sorption capacities for arsenic ions.[48] On the contrary, it is worth mentioning that root iron plaque mineral surfaces will not exclusively be occupied by arsenic ions only. A large variety of dissolved and mobile soil components, such as phosphate, magnesium, soil organic matter and other chelating compounds[49] might compete for surface binding sites on the root iron plaque and potentially decrease the net amount of arsenic binding to root iron plaque. Moreover, as ferrous iron concentrations in rice paddies can vary to a large extent, the reported estimates for the formation of root iron plaque minerals potentially only apply for soil parameters with similar, rather elevated, iron concentrations. In paddy soils with a relatively high abundance of clay minerals, dissolved Fe(II) concentrations were reported to be lower, thus diminishing the

formation of root iron plaque minerals. Consequently, our assumptions might represent only a conservative estimate for the potential of root iron plaque to immobilize arsenic from the pore water. However, these findings can help to serve as a guideline for an approximation of contaminant (im)mobility in paddy fields which is lacking so far. Moreover, the estimated extent of roots in forming soil iron minerals by aerobic redox reactions and the capability to immobilize dissolved soil constituents demonstrate the impact rice plants can have on the oxidative side of the iron biogeochemical cycle in paddy fields.
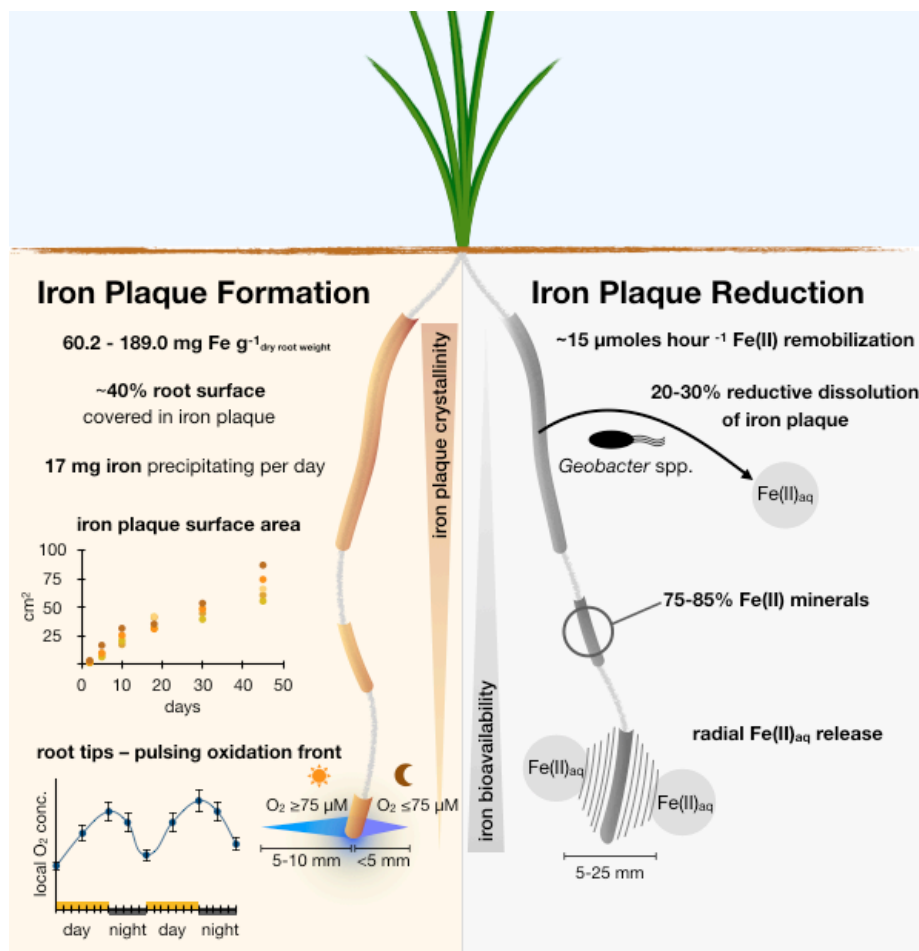
Figure 7. Summary of biogeochemical processes observed in this study that affect the rhizosphere iron cycle at and around rice roots covered in root iron plaque. (**Left**): Oxidative side of the outlined rhizosphere iron cycle with estimates for an immobilization of iron per gram dry weight rice root, root iron plaque coverage, and diurnal changes in ROL at root tips that affect local redox conditions. (**Right**): Reductive side of the proposed rhizosphere iron cycle with observed rates and extent for root iron plaque remobilization through reductive dissolution and reductive mineral transformation by the *Geobacter* spp. culture used in the current study, affecting iron plaque crystallinity and bioavailability, respectively.

Impact of Microaerophilic Fe(II)-Oxidizers on Iron Plaque Formation. Several studies proposed that Fe(II) oxidation and iron mineral formation in wetland soil ecosystems are abiotic processes[50,51] driven by ROL only. However, field studies demonstrated that neutrophilic Fe(II)-oxidizing bacteria are associated with roots covered in iron plaque[17,29,52] and additional studies under laboratory-controlled conditions showed these bacteria can actively contribute to Fe(II) oxidation[33] while others quantified that these bacteria can even enhance root iron plaque formation by up to 40%.[18] Weiss et al. (2003) observed that a low abundance of microaerophilic Fe(II)-oxidizing bacteria co-occurred even with the lowest iron plaque formation on roots of wetland plants.[29] Although complex geochemical dynamics in paddy soils are hard to decipher, we recently showed that the habitats for microaerophilic Fe(II)-oxidizing bacteria in a rice plant rhizosphere are highly dynamic in space and time and that these bacteria find ideal conditions in the entire rice plant rhizosphere.[19] This observation is supported by findings from Weiss at al. 2003 who found that the relative abundance of microaerophilic Fe(II)-oxidizing bacteria in the rhizosphere exceeded the abundance in bulk soil.[29] However, even without a contribution of microaerophilic Fe(II)-oxidizing bacteria, large amounts of ferric minerals formed along the roots and covered more than 30% (Figure 3; Figure S1B) of the root surface with more than 60 mg g^{-1} dry root weight precipitation on the roots. Taking into account the 30% of plant root surface area which was affected by ROL and iron plaque formation, given the reported numbers of microaerophilic Fe(II)-oxidizing bacteria in wetland soils ranging from $7.1 \times 10^2 - 1.1 \times 10^6$ g^{-1} dry weight soil (up to 4.1×10^5 cells cm^{-3} soil)[29] and the reported Fe(II) oxidation rates for a large variety of microaerophilic Fe(II)-oxidizing bacteria ranging from $1.0–8.3\cdot10^{-16}$ mol Fe(II) cell^{-1} hour^{-1},[18,33,53,54] net microaerophilic Fe(II) oxidation can conservatively be estimated to oxidize between 4.1×10^{-11} to 3.4×10^{-10} mol Fe(II) cm^{-3} (0.04 to 0.34 mmol Fe(II) m^{-3}) wetland soil per hour regarding the highest reported cell numbers from paddy fields. This amount of microaerophilically induced iron mineral formation could result in a total of 0.03 to 0.4 g iron mineral precipitation within one m^3 paddy soil per day under optimum conditions. Compared to the finding that more than 1.2 g soil-borne iron that can precipitate on rice roots within one cubic meter of flooded paddy soil per day, the impact of biogenic microaerophilic Fe(II) oxidation can vary to a large extent but has the potential to enhance net total iron mineral formation in the rhizosphere by approx. 3–30%. On the contrary, the microbial oxidation of soil-borne Fe(II) and the sequestration of O$_2$ by these bacteria could potentially reduce abiotic oxidation kinetics and diminish the role of plant-mediated iron plaque formation, suggesting that the net contribution to Fe(II) oxidation can be even more attributed to the microbial activity.

Considering that reported cell numbers for microFeOx were likely underestimated[29] due to the fact that <1% of soil microbial community is cultivatable under laboratory conditions, the

absolute number of microFeOx in the environment might be even higher and the calculated impact underestimated. On the contrary, in the environment numerous other complex biogeochemical processes (e.g., nitrate-dependent Fe(II) oxidation, annamox, oxidizing chelators) can contribute to the oxidative side of the rhizosphere iron cycle, compete with microaerophilic Fe(II) respiration[55] and lower the effective impact of microaerophilic Fe(II) oxidation which cushions their role in iron mineralization. On the contrary, the sequestration of O_2 from ROL by microaerophilic Fe(II)-oxidizing bacteria might diminish local O_2 concentrations surrounding individual roots. Both the production of ferric biominerals, as a product of microbial Fe(II) oxidation, and the depletion in O_2 might create suitable conditions for Fe(III)-reducing microorganisms usually sensitive to O_2. These bacteria could be attracted into the redox-active zone in the vicinity of the roots and conserve metabolic energy by microbially reducing the ferric minerals produced by microaerophilic Fe(II)-oxidizers. However, these assumptions might represent only an ideal and vague estimate. Nevertheless, the reported observations can help to complement the quantitative understanding of the microaerophilic rhizosphere iron cycle and shed light on a yet potentially underestimated plant–microbe interaction that can effectively contribute to iron mineral deposition in flooded paddy fields.

Root Iron Plaque as a Hot Spot for Fe(III) Reduction. In this context, it is worth mentioning that Fe(III) minerals also represent an ideal electron acceptor for numerous Fe(III)-reducing bacteria.[13] Especially poorly crystalline Fe(III) oxides (such as ferrihydrite) that have been observed on the roots of rice and numerous other wetland plants growing in natural settings[7] were speculated to favor the high abundances of Fe(III)-reducing bacteria in wetland rhizospheres.[56,57] In particular, associated with roots, these Fe(III)-reducing microorganisms showed a significantly higher relative abundance in the rhizosphere (>10%) compared to bulk soil.[57] In practice, acetate and plant-derived root exudates are readily bioavailable carbon sources and widely found in the vicinity of roots of numerous wetland plants.[58-60] For such reasons, roots covered in ferric iron minerals also represent an ideal habitat for Fe(III)-reducing bacteria, such as *Geobacter* spp., that can couple the oxidation of these fatty acids and organics to the reduction of root Fe(III) plaque.[57,61] With the current findings, it is now realized that *Geobacter* spp. is capable of remobilizing more than 30% of the iron plaque minerals within a relatively short time (<24 h; Figure 5, Table 2). Given the rate of more than 15 µmoles Fe(II) per hour being released by reductive dissolution, this demonstrates that Fe(III)-reducing bacteria can have a huge impact on the remobilization and transformation of iron plaque minerals. This remobilization by reduction was in focus of a large variety of observations. Historical examples include a study by King and Garey (1999) which is probably one of the first studies that found ecologically relevant reduction of iron from around 4.5 mg Fe per g^{-1}

dry root weight of wetland plants.[56] They observed that iron was only reduced under anoxic conditions and consolidated the importance of microbial Fe(III) reduction for the iron redox cycling in water-logged temperate environments. Presently, our findings showed that microbial Fe(III) reduction can not only contribute significantly to Fe(III) plaque reduction (by up to 70%) but considerably impact Fe(II) remobilization from iron plaque with more than 23 mg Fe(II) being released per plant within less than 48 h (Figure 5). Most remarkable yet was that iron plaque minerals which were found to be microbially reduced showed highest concentrations radially spread in the close vicinity of the root surface and only little mobility (10–25 mm) in the artificial soil matrix (Figure 6). This suggests that the reduction of ferric iron minerals and the remobilization of one-third of the initial iron plaque precipitates as Fe(II) to the vicinity of the root surface can fuel, e.g., microbial Fe(II) oxidation, only in a small redox active microenvironment closely (within 25 mm) surrounding the root surface.

While young roots showed predominantly low-crystalline ferrihydrite as freshly precipitated iron plaque, a relatively high proportion of >20% lepidocrocite and goethite was found on older (approx. 42 days old) roots (Figure 4). These transitions in iron mineralogy suggest that the degree in iron plaque crystallinity correlates positively to root age (Figure 7). Generally, such time-dependent changes in crystallinity are commonly observed to be the result of mineral transformation processes, referred to as Ostwald ripening.[62] Under environmental aspects, these changes in iron plaque mineralogy not only affect surface properties of the iron plaque itself but also decrease sorption capacities for, e.g., nutrients and contaminants. A decrease in sorption capacities, as it was observed for higher crystalline iron minerals, can have drastic negative effects on contaminant retention.[63-65] Moreover, the higher relative abundance of more crystalline iron plaque minerals was demonstrated to decrease the bioavailability for microbial Fe(III) reduction[66,67] and thus the remobilization rate of iron plaque-derived Fe(II). We therefore conclude that, with time, iron plaque minerals are becoming more recalcitrant towards (abiogenic and microbial) Fe(III) reduction and that the microbial bioavailability correlates negatively with root age. In doing so, microbial processes, such as Fe(III) reduction and reductive dissolution, might be inhibited by the abundance of more crystalline iron mineral phases shifting the dominance in impacting the iron plaque reduction to more prevalent abiotically-induced reducing processes, such as by humic acids or other plant-derived complexing compounds. This hypothesis is strongly supported by findings from Roden et al. (1996) and recently from Najem et al. (2016) who observed a significantly lower microbial Fe(III) reduction rate for Fe(III)-reducing bacteria grown on aged or higher-crystalline iron minerals compared to growth on freshly precipitated ferrihydrite.[68, 69] We therefore suspect that while the crystallinity of root iron plaque minerals increases with root age, the availability to serve as a substrate for Fe(III)-reducing bacteria gradually

decreases during plant growth (Figure 7). Under these circumstances, we conclude that young roots (i.e., root tips) may represent a highly dynamic iron redox hot spot. Here, freshly precipitated low-crystalline iron plaque minerals can form which immediately serve as ideal substrate for microbial Fe(III) reduction. Apparently, the bulk root zone is predominantly characterized by more stagnant iron redox conditions due to higher-crystalline iron mineral fractions (Figure 4) and constantly oxygenated conditions which both can inhibit Fe(III) reduction. For such reasons, we suggest that plant induced iron plaque formation, the alteration of minerals, and more importantly, vertical temporal-dynamic iron plaque reduction need to be considered as important parameters for future rhizosphere studies in paddy fields.

Root Tips — The Light Dependent Locomotion for Rhizosphere Redox Changes in Paddy Soils. In addition to the foregoing, we recognized that root tips showed the highest extent in O_2 concentration dynamics. During light-incubated cycles, O_2 concentrations around root tips increased periodically to concentrations $O_2 > 100$ µM expanding the oxidized zones 5–10 mm radially into the anoxic zones. Both, O_2 concentrations and the expansion decreased during dark incubated cycles to O_2 concentrations <50 µM, with a radial expansion of less than 5 mm around root tips. Along with a stagnation in root growth for 1–3 days, dense ferric iron precipitates settled on the root tip forming a rusty cover on the root cap. As soon as root growth proceeded, the root tip broke through the ferric mineral cover and remained free of any mineral cover before O_2 levels increased locally in the following 48 h. The formation of these thick iron plaque covers on the root tips was always accompanied by an increase in ROL from root tip zones, which supports our hypothesis that root tips represent a highly dynamic hot spot for redox reactions such as the oxidation of Fe(II) and formation of low-crystalline iron plaque minerals. Historically, the oxidizing capacity of root tips in anoxic paddy soils was observed by Flessa et al. (1992) who found that rice root tips can radially (1–4 mm) increase local redox conditions.[35] Most surprising yet in the current study was that the oxidizing capacity of these root tips followed a diurnal pattern that correlated to the availability of light. Consequently, in an otherwise anoxic environment, the root tips can be considered as a redox-active precursor for the oxygenation of the rhizosphere and as a main driver for redox changes in soil-borne iron speciation. More importantly, the root tip-induced O_2 availability not only changes iron speciation, but also dominantly affects the soil redox zonation and microbial community shifts throughout the rhizosphere. While the moderate efflux of O_2 from root tips (5 µM < O_2 < 50 µM) (Figure 1) might create optimum conditions for microFeOx,[19,33] also other O_2-dependent (bio)geochemical processes may be triggered by the pulsating ROL from root tips. Exemplarily, it was demonstrated that the temporal availability of O_2 can trigger heterotrophic microorganisms or aerobic methanotrophs. Consequently, this

increase in aerophilic microbial activity can not only increase soil organic carbon turnover, but also decrease CH_4 emissions in and from paddy soils.[70] In contrast, regions in the ferric iron plaque minerals with low (no) O_2 and the presence of plant exudates (such as chelators and short-chained fatty acids) can then trigger Fe(III)-reducing bacteria sensitive to O_2, e.g., *Geobacter* spp. to thrive their metabolic activity by using low-crystalline Fe(III) plaque minerals as electron acceptor (Figure 5). This dynamic heterogeneity in ROL, rapid local changes in Fe speciation on and around root tips and the spatio-dynamic formation of habitable zones for both aerobic Fe(II)-oxidizing and anaerobic Fe(III)-reducing bacteria that are closely involved in iron plaque redox cycling, prove the so far only speculated importance of the root tips as a precursor for plant-induced redox changes in an otherwise anoxic rice paddy.[71]

Environmental Relevance. Biogeochemical iron redox processes that depend on the availability of O_2 are linked to the presence of root related ROL that represents the only supply of O_2 in water-logged paddy fields. In fact, ROL is not only the main parameter that ultimately triggers ferric iron plaque mineral formation but is an essential driver that enables, e.g., neutrophilic microbial microaerophilic Fe(II) oxidation in the rhizosphere.[17] Even so, the availability of O_2 from ROL was demonstrated to shift entire soil microbial community composition structures and energy conservation pathways.[14] Examples include Fe(III)-reducing bacteria (such as *Geobacter* spp.) which are sensitive to O_2,[72] would not be able to conserve energy from root Fe(III) plaque reduction under (micro)oxic conditions as they are prevalent in the close vicinity of the root surface (Figure 1). Microaerophilic Fe(II)-oxidizing bacteria, however, can find their ideal niche conditions in the opposing gradients of soil-borne Fe(II) and O_2 from ROL[15,17] and might even enhance Fe(II) oxidation kinetics[33] and consequently contribute to root iron plaque formation.[18] As shown in the current study, ROL showed extremely high spatial and temporal variation throughout the entire rhizosphere which in turn would shift prevalent conditions favoring (microbial and abiotic) Fe(II) oxidation to Fe(III) reduction and vice versa. Especially during the vegetative growth phase of rice plans, longitudinal O_2 diffusion towards the root apex[73] was shown to promote Fe(II) oxidation kinetics and Fe(III) mineral formation at the root tips (Figure 1A,C), while obligate anoxic Fe(III)-reducing bacteria would be inhibited.

In the paddy soil environment, the total root iron mineral surface area which increased with plant age (Figure 2) can consequently affect the retention of nutrients and has the potential to immobilize heavy metals and contaminants to a relevant extent. Moreover, our results imply that they can impact the soil iron budget to a relatively large extent, which can have consequences for a large variety of soil processes, such as methane emissions from paddy fields,[74,75] and the preservation of soil organic carbon.[76] The reductive side of the iron

redox cycle closes by Fe(III)-reducing reactions that consequently depend on the availability of Fe(III) minerals. These minerals can serve as an electron acceptor for a large variety of microbially-mediated processes such as heterotrophic Fe(III) reduction or abiotically induced Fe(III) reduction by H_2 and other chelating compounds such as plant exudates. Metabolic energy conservation under these conditions is only possible when the pool of Fe(II) and Fe(III) is constantly refueled to serve as a microbial electron source or acceptor either way. These findings strongly support our hypothesis that rice roots can considerably impact the biogeochemical iron cycle in water-logged paddy fields. Not only is the oxidative power of the plant root itself catalyzing numerous iron redox processes, but it also serves as an important conductor for O_2 that spatio-dynamically enables and disables microbial iron redox reactions. Undoubtedly, the current study investigated rhizosphere processes on a rather simplified analogue to a more complex and interacting rice paddy ecosystem containing numerous other key members interacting with the rhizosphere trinity of plant, soil, and bacteria.

However, the current observations extent our understanding in the rhizosphere iron cycling and help to decipher individually that rice plant roots can be one of these key members for both the reductive and oxidative side of the soil-borne iron cycle.[14,58] We suggest future research to include similar approaches, increasing the integrity of biogeochemical interactions to fully decipher potential cross-links in the iron cycle between the enormous variety of participants. One potential step towards an understanding of the iron cycle in a more complex rhizosphere system could be the quantitative spatiotemporal investigation of root iron plaque formation incubated in the presence and absence of different members of iron-cycling bacteria, and the availability of soil-extracted soil organic matter or humic substances as metabolic substrate. Moreover, different irrigation practices could also be simulated in future studies. Soil redox conditions in the current setup were maintained constantly anoxic, representing water-logged paddy field. Periodic draining of paddy fields, however, might switch redox conditions to prevalent oxic conditions, suppressing microbial Fe(III) reduction. All these variable parameters taken together, the understanding of this spatio-dynamic small-scale iron redox rhizosphere system can have a huge impact on large scale observations and should be considered for future investigations of the rhizosphere iron redox cycle in paddy fields.

4.6 References

1. Fredrickson, J. K.; Gorby, Y. A., Environmental processes mediated by iron-reducing bacteria. *Curr Opin Biotech* **1996,** *7*, (3), 287-294.

2. Begg, C. B. M.; Kirk, G. J. D.; Mackenzie, A. F.; Neue, H. U., Root-Induced Iron Oxidation and Ph Changes in the Lowland Rice Rhizosphere. *New Phytol* **1994,** *128*, (3), 469-477.

3. Taylor, S. E.; Terry, N.; Huston, R. P., Limiting Factors in Photosynthesis .3. Effects of Iron Nutrition on the Activities of 3 Regulatory Enzymes of Photosynthetic Carbon Metabolism. *Plant Physiol* **1982,** *70*, (5), 1541-1543.

4. Terry, N., Limiting Factors in Photosynthesis .1. Use of Iron Stress to Control Photo-Chemical Capacity Invivo. *Plant Physiol* **1980,** *65*, (1), 114-120.

5. Becker, M.; Asch, F., Iron toxicity in rice-conditions and management concepts. *Journal of Plant Nutrition and Soil Science* **2005,** *168*, (4), 558-573.

6. Armstrong, W., Oxygen Diffusion from Roots of Rice Grown under Non-Waterlogged Conditions. *Physiol Plantarum* **1971,** *24*, (2), 242-+.

7. Yamaguchi, N.; Ohkura, T.; Takahashi, Y.; Maejima, Y.; Arao, T., Arsenic Distribution and Speciation near Rice Roots Influenced by Iron Plaques and Redox Conditions of the Soil Matrix. *Environ Sci Technol* **2014,** *48*, (3), 1549-1556.

8. Armstrong, W., Radial Oxygen Losses from Intact Rice Roots as Affected by Distance from Apex, Respiration and Waterlogging. *Physiol Plantarum* **1971,** *25*, (2), 192-+.

9. Mendelssohn, I. A.; Kleiss, B. A.; Wakeley, J. S., Factors Controlling the Formation of Oxidized Root Channels - a Review. *Wetlands* **1995,** *15*, (1), 37-46.

10. Wang, Z. P.; Delaune, R. D.; Masscheleyn, P. H.; Patrick, W. H., Soil Redox and Ph Effects on Methane Production in a Flooded Rice Soil. *Soil Sci Soc Am J* **1993,** *57*, (2), 382-385.

11. Yu, T. R., Characteristics of Soil Acidity of Paddy Soils in Relation to Rice Growth. *Dev Plant Soil Sci* **1991,** *45*, 107-112.

12. Liesack, W.; Schnell, S.; Revsbech, N. P., Microbiology of flooded rice paddies. *Ferns Microbiol Rev* **2000,** *24*, (5), 625-645.

13. Hori, T.; Muller, A.; Igarashi, Y.; Conrad, R.; Friedrich, M. W., Identification of iron-reducing microorganisms in anoxic rice paddy soil by C-13-acetate probing. *Isme J* **2010,** *4*, (2), 267-278.

14. Achtnich, C.; Bak, F.; Conrad, R., Competition for Electron-Donors among Nitrate Reducers, Ferric Iron Reducers, Sulfate Reducers, and Methanogens in Anoxic Paddy Soil. *Biol Fert Soils* **1995,** *19*, (1), 65-72.

15. Druschel, G. K.; Emerson, D.; Sutka, R.; Suchecki, P.; Luther, G. W., Low-oxygen and chemical kinetic constraints on the geochemical niche of neutrophilic iron(II) oxidizing microorganisms. *Geochim Cosmochim Ac* **2008,** *72*, (14), 3358-3370.

16. Lueder, U.; Druschel, G.; Emerson, D.; Kappler, A.; Schmidt, C., Quantitative analysis of O-2 and Fe2+ profiles in gradient tubes for cultivation of microaerophilic Iron(II)-oxidizing bacteria. *Fems Microbiol Ecol* **2018,** *94*, (2).

17. Emerson, D.; Weiss, J. V.; Megonigal, J. P., Iron-oxidizing bacteria are associated with ferric hydroxide precipitates (Fe-plaque) on the roots of wetland plants. *Appl Environ Microb* **1999,** *65*, (6), 2758-2761.

18. Neubauer, S. C.; Toledo-Duran, G. E.; Emerson, D.; Megonigal, J. P., Returning to their roots: Iron-oxidizing bacteria enhance short-term plaque formation in the wetland-plant rhizosphere. *Geomicrobiol J* **2007,** *24*, (1), 65-73.

19. Maisch, M.; Lueder, U.; Kappler, A.; Schmidt, C., Iron Lung: How Rice Roots Induce Iron Redox Changes in the Rhizosphere and Create Niches for Microaerophilic Fe(II)-Oxidizing Bacteria. *Environ Sci Tech Let* **2019a,** *6*, (10), 600-605.

20. Urrutia, M. M.; Roden, E. E.; Fredrickson, J. K.; Zachara, J. M., Microbial and surface chemistry controls on reduction of synthetic Fe(III) oxide minerals by the dissimilatory iron-reducing bacterium Shewanella alga. *Geomicrobiol J* **1998,** *15*, (4), 269-291.

21. Langley, S.; Gault, A.; Ibrahim, A.; Renaud, R.; Fortin, D.; Clark, I. D.; Ferris, F. G., A Comparison of the Rates of Fe(III) Reduction in Synthetic and Bacteriogenic Iron Oxides by Shewanella putrefaciens CN32. *Geomicrobiol J* **2009,** *26*, (2), 57-70.

22. Bridge, T. A. M.; Johnson, D. B., Reduction of soluble iron and reductive dissolution of ferric iron-containing minerals by moderately thermophilic iron-oxidizing bacteria. *Appl Environ Microb* **1998,** *64*, (6), 2181-2186.

23. Bennett, B.; Dudas, M. J., Release of arsenic and molybdenum by reductive dissolution of iron oxides in a soil with enriched levels of native arsenic. *J Environ Eng Sci* **2003,** *2*, (4), 265-272.

24. Hansel, C. M.; Fendorf, S.; Sutton, S.; Newville, M., Characterization of Fe plaque and associated metals on the roots of mine-waste impacted aquatic plants. *Environ Sci Technol* **2001,** *35*, (19), 3863-3868.

25. Kirk, G. J. D.; Bajita, J. B., Root-Induced Iron Oxidation, Ph Changes and Zinc Solubilization in the Rhizosphere of Lowland Rice. *New Phytol* **1995,** *131*, (1), 129-137.

26. Wahid, P. A.; Kamalam, N. V., Reductive Dissolution of Crystalline and Amorphous Fe(Iii) Oxides by Microorganisms in Submerged Soil. *Biol Fert Soils* **1993,** *15*, (2), 144-148.

27. Weber, K. A.; Achenbach, L. A.; Coates, J. D., Microorganisms pumping iron: anaerobic microbial iron oxidation and reduction. *Nat Rev Microbiol* **2006,** *4*, (10), 752-764.

28. Yu, H. Y.; Li, F. B.; Liu, C. S.; Huang, W.; Liu, T. X.; Yu, W. M., Iron Redox Cycling Coupled to Transformation and Immobilization of Heavy Metals: Implications for Paddy Rice Safety in the Red Soil of South China. *Advances in Agronomy, Vol 137* **2016,** *137*, 279-317.

29. Weiss, J. V.; Emerson, D.; Backer, S. M.; Megonigal, J. P., Enumeration of Fe(II)-oxidizing and Fe(III)-reducing bacteria in the root zone of wetland plants: Implications for a rhizosphere iron cycle. *Biogeochemistry* **2003,** *64*, (1), 77-96.

30. Garnier, J.; Garnier, J. M.; Vieira, C. L.; Akerman, A.; Chmeleff, J.; Ruiz, R. I.; Poitrasson, F., Iron isotope fingerprints of redox and biogeochemical cycling in the soil-water-rice plant system of a paddy field. *Sci Total Environ* **2017,** *574*, 1622-1632.

31. Roden, E. E.; Wetzel, R. G., Kinetics of microbial Fe(III) oxide reduction in freshwater wetland sediments. *Limnol Oceanogr* **2002,** *47*, (1), 198-211.

32. Hoagland, D. R.; Arnon, D. I., The water-culture method for growing plants without soil. *Circular. California agricultural experiment station* **1950,** *347*, (2nd edit).

33. Maisch, M.; Lueder, U.; Laufer, K.; Scholze, C.; Kappler, A.; Schmidt, C., Contribution of Microaerophilic Iron(II)-Oxidizers to Iron(III) Mineral Formation. *Environ Sci Technol* **2019b,** *53*, (14), 8197-8204.

34. Kirk, G., *The biogeochemistry of submerged soils*. John Wiley & Sons: 2004.

35. Flessa, H.; Fischer, W. R., Plant-Induced Changes in the Redox Potentials of Rice Rhizospheres. *Plant Soil* **1992,** *143*, (1), 55-60.

36. Schmidt, H.; Eickhorst, T.; Tippkotter, R., Monitoring of root growth and redox conditions in paddy soil rhizotrons by redox electrodes and image analysis. *Plant Soil* **2011,** *341*, (1-2), 221-232.

37. Benjamin, J. G.; Nielsen, D. C., A method to separate plant roots from soil and analyze root surface area. *Plant Soil* **2004,** *267*, (1-2), 225-234.

38. Muehe, E. M.; Scheer, L.; Daus, B.; Kappler, A., Fate of Arsenic during Microbial Reduction of Biogenic versus Abiogenic As-Fe(III)-Mineral Coprecipitates. *Environ Sci Technol* **2013,** *47*, (15), 8297-8307.

39. Muehe, E. M.; Obst, M.; Hitchcock, A.; Tyliszczak, T.; Behrens, S.; Schroder, C.; Byrne, J. M.; Michel, F. M.; Kramer, U.; Kapplert, A., Fate of Cd during Microbial Fe(III) Mineral Reduction by a Novel and Cd-Tolerant Geobacter Species. *Environ Sci Technol* **2013,** *47*, (24), 14099-14109.

40. Stookey, L. L., Ferrozine - a New Spectrophotometric Reagent for Iron. *Anal Chem* **1970,** *42*, (7), 779-&.

41. Seyfferth, A. L.; Webb, S. M.; Andrews, J. C.; Fendorf, S., Arsenic Localization, Speciation, and Co-Occurrence with Iron on Rice (Oryza sativa L.) Roots Having Variable Fe Coatings. *Environ Sci Technol* **2010,** *44*, (21), 8108-8113.

42. Blute, N. K.; Brabander, D. J.; Hemond, H. F.; Sutton, S. R.; Newville, M. G.; Rivers, M. L., Arsenic sequestration by ferric iron plaque on cattail roots. *Environ Sci Technol* **2004,** *38*, (22), 6074-6077.

43. Hiemstra, T.; Van Riemsdijk, W. H., A surface structural model for ferrihydrite I: Sites related to primary charge, molar mass, and mass density. *Geochim Cosmochim Ac* **2009,** *73*, (15), 4423-4436.

44. Matsumoto, S.; Kasuga, J.; Makino, T.; Arao, T., Evaluation of the effects of application of iron materials on the accumulation and speciation of arsenic in rice grain grown on uncontaminated soil with relatively high levels of arsenic. *Environ Exp Bot* **2016,** *125*, 42-51.

45. Tan, X. Z.; Shao, D. G.; Liu, H. H.; Yang, F. S.; Xiao, C.; Yang, H. D., Effects of alternate wetting and drying irrigation on percolation and nitrogen leaching in paddy fields. *Paddy Water Environ* **2013,** *11*, (1-4), 381-395.

46. Carlson, J. J.; Kawatra, S. K., Factors Affecting Zeta Potential of Iron Oxides. *Min Proc Ext Met Rev* **2013,** *34*, (5), 269-303.

47. Aimrun, W.; Amin, M. S. M.; Eltaib, S. M., Effective porosity of paddy soils as an estimation of its saturated hydraulic conductivity. *Geoderma* **2004,** *121*, (3-4), 197-203.

48. Stumm, W.; Wehrli, B.; Wieland, E., Surface Complexation and Its Impact on Geochemical Kinetics. *Croat Chem Acta* **1987,** *60*, (3), 429-456.

49. Gu, B. H.; Schmitt, J.; Chen, Z.; Liang, L. Y.; Mccarthy, J. F., Adsorption and Desorption of Different Organic-Matter Fractions on Iron-Oxide. *Geochim Cosmochim Ac* **1995,** *59*, (2), 219-229.

50. Howeler, R. H.; Bouldin, D. R., The Diffusion and Consumption of Oxygen in Submerged Soils1. *Soil Sci Soc Am J* **1971,** *35*, 202-208.

51. Kirby, C. S.; Thomas, H. M.; Southam, G.; Donald, R., Relative contributions of abiotic and biological factors in Fe(II) oxidation in mine drainage. *Appl Geochem* **1999,** *14*, (4), 511-530.

52. Cahyani, V. R.; Murase, J.; Ikeda, A.; Taki, K.; Asakawa, S.; Kimura, M., Bacterial communities in iron mottles in the plow pan layer in a Japanese rice field: Estimation using PCR-DGGE and sequencing analyses. *Soil Sci Plant Nutr* **2008,** *54*, (5), 711-717.

53. Emerson, D.; Moyer, C. L., Neutrophilic Fe-Oxidizing bacteria are abundant at the Loihi Seamount hydrothermal vents and play a major role in Fe oxide deposition. *Appl Environ Microb* **2002,** *68*, (6), 3085-3093.

54. Chan, C. S.; Emerson, D.; Luther, G. W., The role of microaerophilic Fe-oxidizing micro-organisms in producing banded iron formations. *Geobiology* **2016,** *14*, (5), 509-528.

55. Melton, E. D.; Swanner, E. D.; Behrens, S.; Schmidt, C.; Kappler, A., The interplay of microbially mediated and abiotic reactions in the biogeochemical Fe cycle. *Nat Rev Microbiol* **2014,** *12*, (12), 797-808.

56. King, G. M.; Garey, M. A., Ferric Iron Reduction by Bacteria Associated with the Roots of Freshwater and Marine Macrophytes. *Appl Environ Microb* **1999,** *65*, (10), 4393.

57. Weiss, J. V.; Emerson, D.; Megonigal, J. P., Geochemical control of microbial Fe(III) reduction potential in wetlands: comparison of the rhizosphere to non-rhizosphere soil. *Fems Microbiol Ecol* **2004,** *48*, (1), 89-100.

58. Colombo, C.; Palumbo, G.; He, J. Z.; Pinton, R.; Cesco, S., Review on iron availability in soil: interaction of Fe minerals, plants, and microbes. *J Soil Sediment* **2014,** *14*, (3), 538-548.

59. Dannenberg, S.; Conrad, R., Effect of rice plants on methane production and rhizospheric metabolism in paddy soil. *Biogeochemistry* **1999,** *45*, (1), 53-71.

60. Strom, L.; Mastepanov, M.; Christensen, T. R., Species-specific effects of vascular plants on carbon turnover and methane emissions from wetlands. *Biogeochemistry* **2005,** *75*, (1), 65-82.

61. Lovley, D. R.; Giovannoni, S. J.; White, D. C.; Champine, J. E.; Phillips, E. J. P.; Gorby, Y. A.; Goodwin, S., Geobacter-Metallireducens Gen-Nov Sp-Nov, a Microorganism Capable of Coupling the Complete Oxidation of Organic-Compounds to the Reduction of Iron and Other Metals. *Arch Microbiol* **1993,** *159*, (4), 336-344.

62. Cornell, R. M.; Schneider, W.; Giovanoli, R., The Transformation of Ferrihydrite into Lepidocrocite. *Clay Miner* **1989,** *24*, (3), 549-553.

63. Jacob, D. L.; Otte, M. L., Conflicting processes in the wetland plant rhizosphere: metal retention or mobilization? *Water, Air and Soil Pollution: Focus* **2003,** *3*, (1), 91-104.

64. Xu, X.; Mills, G. L., Do constructed wetlands remove metals or increase metal bioavailability? *J Environ Manage* **2018,** *218*, 245-255.

65. Elsner, M.; Schwarzenbach, R. P.; Haderlein, S. B., Reactivity of Fe(II)-bearing minerals toward reductive transformation of organic contaminants. *Environ Sci Technol* **2004,** *38*, (3), 799-807.

66. Bonneville, S.; Van Cappellen, P.; Behrends, T., Microbial reduction of iron(III) oxyhydroxides: effects of mineral solubility and availability. *Chem Geol* **2004,** *212*, (3-4), 255-268.

67. Munch, J. C.; Ottow, J. C. G., Preferential Reduction of Amorphous to Crystalline Iron-Oxides by Bacterial-Activity. *Soil Sci* **1980,** *129*, (1), 15-21.

68. Roden, E. E.; Zachara, J. M., Microbial reduction of crystalline iron(III) oxides: Influence of oxide surface area and potential for cell growth. *Environ Sci Technol* **1996,** *30*, (5), 1618-1628.

69. Najem, T.; Langley, S.; Fortin, D., A comparison of Fe(III) reduction rates between fresh and aged biogenic iron oxides (BIOS) by Shewanella putrefaciens CN32. *Chem Geol* **2016,** *439*, 1-12.

70. Kludze, H. K.; Delaune, R. D.; Patrick, W. H., Aerenchyma Formation and Methane and Oxygen-Exchange in Rice. *Soil Sci Soc Am J* **1993,** *57*, (2), 386-391.

71. Colmer, T. D.; Cox, M. C. H.; Voesenek, L. A. C. J., Root aeration in rice (Oryza sativa): evaluation of oxygen, carbon dioxide, and ethylene as possible regulators of root acclimatizations. *New Phytol* **2006,** *170*, (4), 767-777.

72. Lovley, D. R.; Ueki, T.; Zhang, T.; Malvankar, N. S.; Shrestha, P. M.; Flanagan, K. A.; Aklujkar, M.; Butler, J. E.; Giloteaux, L.; Rotaru, A. E.; Holmes, D. E.; Franks, A. E.; Orellana, R.; Risso, C.; Nevin, K. P., Geobacter: The Microbe Electric's Physiology, Ecology, and Practical Applications. *Adv Microb Physiol* **2011,** *59*, 1-100.

73. Colmer, T. D., Aerenchyma and an inducible barrier to radial oxygen loss facilitate root aeration in upland, paddy and deep-water rice (Oryza sativa L.). *Ann Bot-London* **2003,** *91*, (2), 301-309.

74. Jackel, U.; Schnell, S., Suppression of methane emission from rice paddies by ferric iron fertilization. *Soil Biol Biochem* **2000,** *32*, (11-12), 1811-1814.

75. Furukawa, Y.; Inubushi, K., Effect of application of iron materials on methane and nitrous oxide emissions from two types of paddy soils. *Soil Sci Plant Nutr* **2004,** *50*, (6), 917-924.

76. Cai, A. D.; Feng, W. T.; Zhang, W. J.; Xu, M. G., Climate, soil texture, and soil types affect the contributions of fine-fraction-stabilized carbon to total soil organic carbon in different land uses across China. *J Environ Manage* **2016,** *172*, 2-9.

4.7 Supporting Information

From Plant to Paddy — How Rice Root Iron Plaque Can Affect the Paddy Field Iron Cycling

Markus Maisch[1], Ulf Lueder[1], Andreas Kappler[1,2], Caroline Schmidt[1]

[1] Geomicrobiology, Center for Applied Geosciences, University of Tübingen, Germany

[2] Department for Bioscience, Aarhus University, Denmark

Number of tables in supporting information: 3

Number of figures in supporting information: 4

Total numbers of pages in supporting information: 10 (including cover page)

Plant growth containers. Plant growth containers were made of transparent plexiglass (25 cm × 25 cm × 3 cm i.d.). Under sterile conditions and constant anoxic gas flow (100% N_2) 1.75 cm^3 anoxic Hoagland solution (100%, 35 °C, pH 6.8) amended with 500 μM $Fe(II)_{aq}$ (from $FeCl_2$) and 0.3% Gelrite (Carl Roth, Karlsruhe, Germany) were filled into the containers. When cooling down to room temperature, the solution formed a transparent solid soil matrix. Approximately 100 mL of 20% Hoagland solution was constantly kept on top of the growth gel to prevent desiccation. The growth containers were wrapped in aluminum foil to protect the soil matrix from illumination. The leaf biomass, however, was illuminated by light. These setups were kept in a specifically-designed greenhouse to maintain constant light, temperature and humidity conditions. Penetration of O_2 from the atmosphere into the gel was monitored by microelectrodes and found to be relevant only in the upper 0.7 cm of the growth gel and therefore considered to be neglectable for the investigation of the rhizosphere.

Mössbauer spectroscopy. Within an anoxic glovebox (100% N_2), sampled root biomass was dried at constant 30°C. Dried sample material was mortared, and subsequently loaded into plexiglas holders (area 1 cm^2), forming a thin disc. Prior to analysis, samples were stored anoxically at -20°C to suppress recrystallization processes or microbial activity. Samples were transported to the instrument within airtight bottles which were only opened immediately prior to loading into a closed-cycle exchange gas cryostat (Janis cryogenics) to minimize exposure to air. Spectra were collected at 77 K using a constant acceleration drive system (WissEL) in transmission mode with a $^{57}Co/Rh$ source. All spectra were calibrated against a 7 μm thick α-^{57}Fe foil that was measured at room temperature. Analysis was carried out using Recoil (University of Ottawa) and the Voigt Based Fitting (VBF) routine [1]. The half width at half maximum (HWHM) was constrained to 0.127 mm s^{-1} during fitting.

Isolation of Fe(III)-reducing bacteria from a paddy field rhizosphere. Wet soil was collected from a paddy field located in Vercelli, Italy and transported to the laboratory under cool conditions. In order to enrich Fe(III)-reducing bacteria, soil material was homogenized and aliquots of 1 g were added to 100 mL anoxic and sterile mineral medium[2] amended with 20 mM acetate and 10 mM ferrihydrite. From these Fe(III)-reducing enrichment incubations, dilution series were performed following Muehe et al..[2] Positive tubes were easily identified by a change in color from red to black which indicated the reduction of ferric iron to ferrous iron minerals. A sample from the highest positive dilution was tested for purity by fluorescence microscopy and by 16S rRNA gene cloning and sequencing. This culture was constantly transferred (10 %; v/v) into fresh culture tubes.

Root surface and iron plaque surface area. Root surface area increased over time during plant growth over 45 days (Figure S1a). A simple linear regression was applied to determine the increase in root surface area over time and resulted in a trending increase of approx. 4.3 cm^2 root surface area per day (R^2 = 0.97). Root iron plaque development during plant growth over 45 days was identified by image analysis and shown in one experimental replicate as shown in Figure S1 B-G.
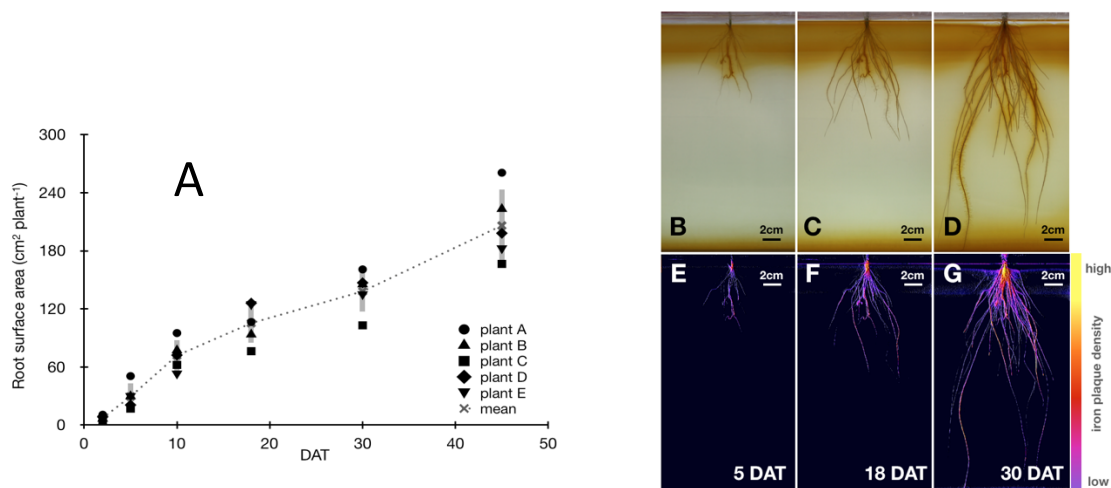
Figures S1. Root surface and iron plaque area. A: Root surface area (cm^2 per plant) in rhizotrons during plant growth (DAT = days after transfer) of five replicate plants (filled symbols), mean root surface area (cross & punctuated line) and standard deviation (grey bars). **B-D: Root growth and iron plaque formation** in rhizotrons 5, 18 and 30 DAT. **E-G: Iron plaque identification** on roots by imaging and pixel analysis 5, 18 and 30 DAT and non-dimensional estimated iron plaque density (legend bar).

Mössbauer spectroscopy on aged root iron plaque minerals. Iron plaque minerals were collected at the end of the growth experiment from (i) the basal root zone (approx. 40 days old), (ii) the middle part of the root (approx. 20 days old), and (iii) from young root tips (approx. 2 days old). Transmission spectra of root iron plaque collected from the basal root zone (Figure S2 A) was dominated by a narrow doublet with a low quadrupole splitting (ΔE_Q). The best-fit model suggested two individual components to be fitted as doublet 1 (Db1) and doublet 2 (Db2) (Table S1). The low ΔE_Q for both doublets suggests the presence of two Fe(III) species. The hyperfine field parameters of Db1 can be attributed to the presence of ferrihydrite as most abundant Fe(III) species, while Db2 likely represents the presence of approx. 8 % lepidocrocite. The presence of a sextet in the spectrum of iron plaque from the basal root zone suggests the presence of an iron species undergoing magnetically ordering at 77 K. Hyperfine field parameters of the best-model fit suggest the presence of goethite in this sample with a relative abundance of approx. 17%.

The fitted components in spectrum of iron plaque collected from 20-days old roots (Figure S2 B) showed similar characteristics as iron plaque from basal roots. However, the relative abundance of lepidocrocite was estimated to be 3-fold higher compared to iron plaque from basal root zone while ferrihydrite remained at the same level with approx. 70 % relative abundance (Table S1). In the background of the spectrum a poorly-developed sextet was visible. The best-fit parameters for the sextet feature suggest a higher-crystalline magnetically ordered mineral phase with a relative abundance of approx. 5 % while hyperfine field parameters are similar to goethite as being detected previously.

The spectrum for freshly-precipitated iron plaque collected from root tips was clearly dominated by a narrow doublet (Figure S2 C). Here, the best-fit model suggests the presence of only one component (Db1). Hyperfine field parameters for Db1 can be attributed to the presence of ferrihydrite as the dominant (>95 %) iron mineral phase in this sample (Table S1). Additionally, a poorly developed wide doublet with a high quadrupole splitting suggests the presence of a high-spin Fe(II) phase. However, the hyperfine field parameters do not allow a clear identification as iron mineral but suggest the presence of potentially adsorbed/complexed Fe(II) in this sample.

Table S1. Mössbauer spectra hyperfine parameters for root iron plaque minerals. CS – Center shift, ΔE_Q – Quadrupole splitting, ε – Quadrupole shift, B_{hf} – Hyperfine field, Pop. – relative abundance, $\chi 2$ – goodness of fit, identified mineral phase (Fh – ferrihydrite, Fe(II) – ferrous iron species, Lep – Lepidocrocite, Gt – Goethite)

Sample	Temp. (K)	Phase	CS (mm/s)	ΔE_Q (mm/s)	ε (mm/s)	B_{hf} (T)	Pop (%)	±	χ^2	Mineral phase
basal roots (45 days old)	77	Db1	0.47	0.75			74.5	0.5	0.60	Fh
		Db2	0.46	0.60			8.5			Lep
		Sxt1	0.45		-0.14	49.7	17			Gt
middle roots (20 days old)	77	Db1	0.46	0.82			72.0	0.6	0.58	Fh
		Db2	0.49	0.64			23.0			Lep
		Sxt1	0.47		-0.16	47.4	5.0			Gt
Root tips (2 days old)	77	Db1	0.47	0.71			96.5	0.3	0.66	Fh
		Db2	1.32	2.10			3.5			Fe(II)
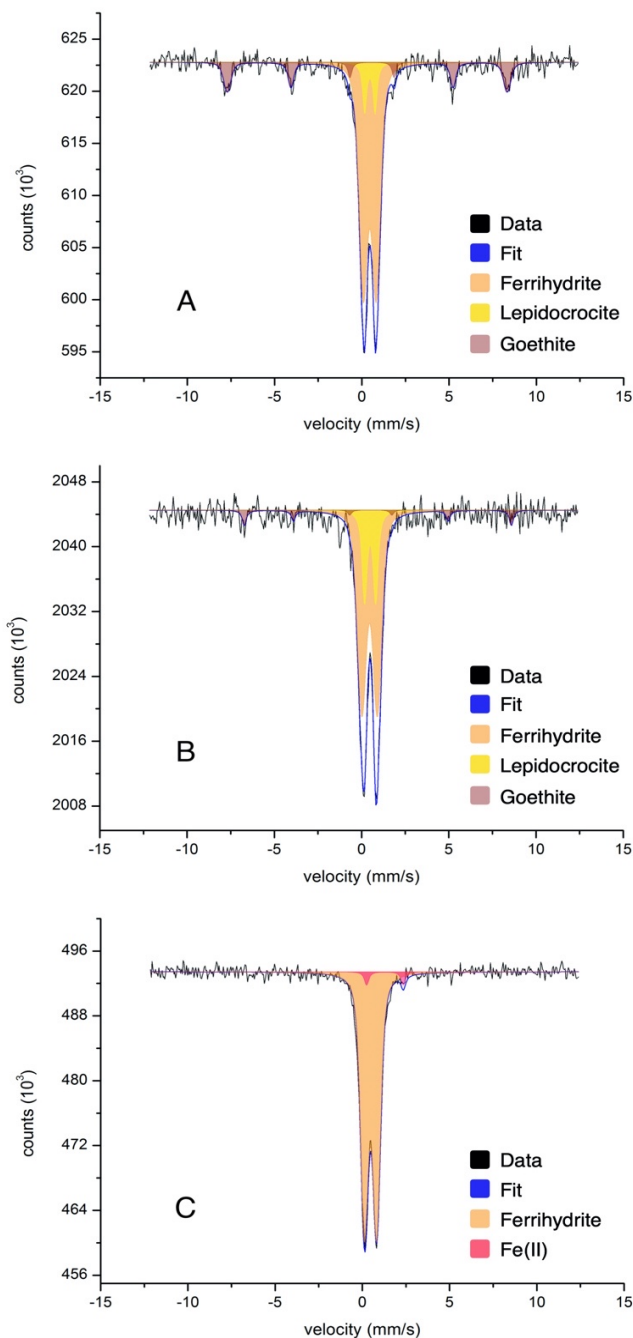
Figures S2. Mössbauer transmission spectra of root iron plaque minerals collected at 77 K. A: Root iron plaque from basal root zone (45 days old) dominated by ferrihydrite (orange) and lepidocrocite (yellow) as fitting components for the narrow doublet (Db) and goethite (brown) as higher-crystalline iron mineral species represented by the magnetically-ordered sextet (Sxt). B: Root iron plaque from middle part of roots (20 days old) composing of ferrihydrite and lepidocrocite as fitting components for the narrow doublet (Db) and a small proportion goethite as higher-crystalline iron mineral species represented by the magnetically-ordered sextet (Sxt). C: Root iron plaque on root tips (2 days old) dominated by ferrihydrite and potentially sorbed Fe(II) (red) detected as wide doublet.

Identification of reduced iron plaque minerals by Mössbauer spectroscopy. Samples collected from experimental setups with root covered in iron plaque minerals which were exposed to an Fe(III)-reducing culture were identified by Mössbauer spectroscopy. The transmission spectrum of abiotic control incubation with inhibited cells showed the presence of a well-defined dominant doublet structure (Figure S3 A). The best-fit model using the VBF fitting routine suggested two individual components to fit the measured data. These components were assigned to a doublet feature Db1 and Db2, respectively. Both, Db1 and Db2 were characterized by a narrow ΔE_Q <0.8 which suggests the presence of a low-spin Fe(III) phase for both doublets. The individual hyperfine field parameters for Db1 likely can be attributed to the presence of ferrihydrite by >80 %, while Db2 suggests lepidocrocite to be abundant by approx. 20 % (Table S2).

The transmission spectrum for the active incubation was dominated by a wide doublet feature (Figure S3 B) with a relatively high ΔE_Q which indicates the presence of a high-spin Fe(II) phase being present in this sample (Db1; Table S2) The other hyperfine field parameters are close to reference parameters of siderite as ferrous iron carbonate being present by approx. 60 % relative abundance. Additionally, a narrow doublet (Db2) with a low quadrupole splitting was overlapping with Db1. The hyperfine field parameters are similar to ferrihydrite, while the fitting model suggests an approx. 20 % relative abundance. Moreover, a poorly defined sextet was observed in the spectrum of this sample (Figure S3 B). The collapsed and low hyperfine field of 27 T only cannot be referenced to any commonly known reference iron phase. However, collapsed feature and the beginning of a magnetic ordering at 77 K suggests the presence of a short-range ordered iron (oxyhydr)oxide. Although this observation does not allow a clear iron phase identification, the corresponding iron mineral extraction data suggests the presence of an Fe(II) compound. Potentially associated with sulfur species which caused the distortions of iron atoms, the resulting sextet feature in the recorded spectrum might represent some sort of Fe(II) sulfur compound as it was observed for other iron sulfur species.[3,4] We therefore assigned the relative abundance of the observed sextet by approx. 10 % to the presence of a yet unknown Fe(II)–S species (Table S2).

Table S2. Mössbauer spectra hyperfine parameters for non/reduced root iron plaque minerals.
CS – Center shift, ΔE_Q – Quadrupole splitting, ε – Quadrupole shift, B_{hf} – Hyperfine field, Pop. – relative abundance, $\chi 2$ – goodness of fit, identified mineral phase (Fh – ferrihydrite, Lep – Lepidocrocite, Sid – Siderite, Fe(II)–S – ferrous iron sulfur species)

Sample	Temp.	Phase	CS	ΔE_Q	ε	B_{hf}	Pop	±	χ^2	Mineral phase
	(K)		(mm/s)	(mm/s)	(mm/s)	(T)	(%)			
non-reduced root iron plaque	77	Db1	0.49	0.78			72.6	0.9	0.71	Fh
		Db2	0.42	0.57			27.4			Lep
reduced root iron plaque	77	Db1	1.35	2.89			63.6	0.4	0.83	Sid
		Db2	0.41	0.83			19.5			Fh
		Sxt1	0.39		-0.01	27.4	16.9			Fe(II)–S
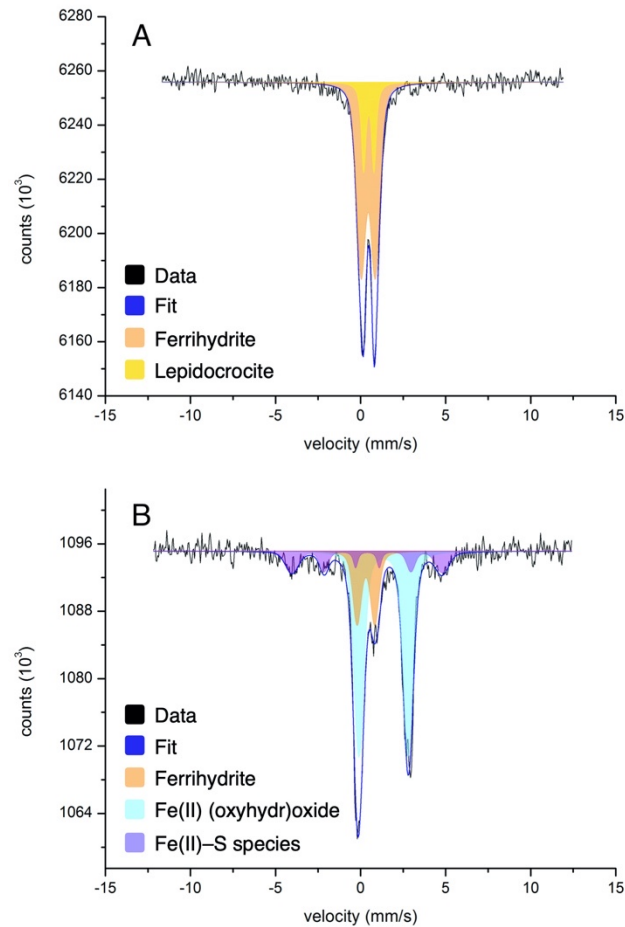
Figure S3. Mössbauer spectra of root iron plaque reduction experiments measured at 77 K. A: Transmission spectrum of non-reduced root iron plaque minerals collected from inhibited control incubations. Mainly ferrihydrite (brown doublet) and lepidocrocite (yellow) were the two main iron phases. B: Transmission spectrum of reduced root iron plaque minerals collected from roots exposed to an Fe(III)-reducing culture. An Fe(II) mineral phase, most likely siderite (light blue), some resilient ferrihydrite (brown) and a collapsing sextet which is potentially representing a short-range ordered yet unknown Fe(II)–S species (purple).

Hyperfine field parameters and Mössbauer spectrum of reduced iron plaque in rhizotron.

Table S3. Mössbauer spectra hyperfine parameters for non/reduced root iron plaque minerals.
CS – Center shift, ΔE_Q – Quadrupole splitting, ε – Quadrupole shift, B_{hf} – Hyperfine field, Pop. –
relative abundance, χ2 – goodness of fit, identified mineral phase (Viv – Vivianite coordination A/B,
Fh – ferrihydrite, Fe(II)–S – ferrous iron sulfur species)

Sample	Temp.	Phase	CS	ΔE_Q	ε	B_{hf}	Pop	±	χ^2	Mineral phase
	(K)		(mm/s)	(mm/s)	(mm/s)	(T)	(%)			
reduced root iron plaque	77	Db1	1.29	3.19			34.6	0.9	0.71	Viv (A)
		Db2	1.32	2.63			19.1			Viv (B)
		Db3	0.46	0.71			22.8			Fh
		Sxt	0.41		-0.02	28.3	23.5			Fe(II)–S
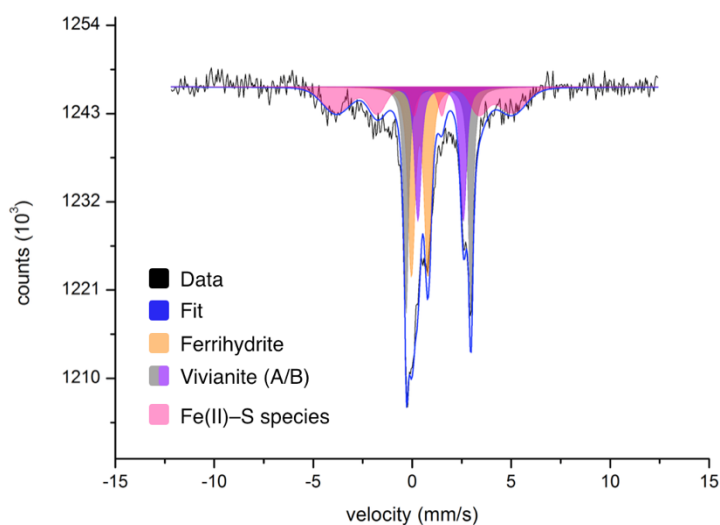
Figure S4. Mössbauer spectrum of root iron plaque reduction experiments in rhizotrons measured at 77 K. Transmission spectrum of reduced root iron plaque minerals collected from rhizotron exposed to an Fe(III)-reducing culture. An Fe(II) mineral phase, most likely vivianite (grey/purple, represent two iron coordination states in vivianite), some resilient ferrihydrite (orange) and a collapsing sextet which is potentially representing a short-range ordered yet unknown Fe(II)–S species (pink).

Chapter 4

References

1. Rancourt, D. G.; Ping, J. Y., Voigt-Based Methods for Arbitrary-Shape Static Hyperfine Parameter Distributions in Mossbauer-Spectroscopy. *Nucl Instrum Meth B* **1991**, *58*, (1), 85-97.

2. Muehe, E. M.; Scheer, L.; Daus, B.; Kappler, A., Fate of Arsenic during Microbial Reduction of Biogenic versus Abiogenic As-Fe(III)-Mineral Coprecipitates. *Environ Sci Technol* **2013**, *47*, (15), 8297-8307.

3. Rao, P. V.; Holm, R. H., Synthetic analogues of the active sites of iron-sulfur proteins. *Chem Rev* **2004**, *104*, (2), 527-559.

4. Zakhvalinskii, V. S.; Piliuk, E. A.; Taran, S. V.; Sklyarova, A.; Matveev, V. V.; Linden, J.; Zakharchuk, I., Fe-57 Mossbauer spectroscopy investigation of La0.7Ca0.3Mn0.5Fe0.5O3. *Results Phys* **2016**, *6*, 1175-1177.

5   The Dark Side of Root Iron Plaque – How Microbial Iron Plaque Reduction Affects the Fate of Arsenic in Contaminated Paddy Fields

Markus Maisch[1], Panunporn Tutiyasarn[1], Carolin Kerl[2], Britta Planer-Friedrich[2], Andreas Kappler[1,3], Caroline Schmidt[1]

[1] Geomicrobiology, Center for Applied Geoscience, University of Tuebingen, Germany

[2] Environmental Geochemistry, Bayreuth Center for Ecology and Environmental Research (BayCEER), University of Bayreuth, Germany

[3] Center for Geomicrobiology, Department of Bioscience, University of Aarhus, Denmark

5.1 Abstract

Iron plaque on rice roots can immobilize As in ferric (Fe(III)) minerals which decreases the uptake into the plant and the mobility in contaminated soils. However, little is known about the role of bacteria in the reduction of As-bearing Fe(III) plaque minerals or the efficiency of reduced iron plaque in As immobilization. Here, we demonstrate the formation of secondary iron minerals (70% siderite, 30% ferrihydrite, Fh & goethite, Gt) during microbial iron plaque reduction, that can immobilize 2.5 times more As than oxidized iron plaque (Fh & Gt). Comparing 3 different As-loads in iron plaque, we found that >1mg per 10 mg iron plaque can negatively affect microbial reduction rates by 50%. During reductive dissolution, As was first remobilized but re-adsorbed onto secondary iron minerals after 7 days. Abiotic reduction of dissolved As(V) occurred on redox-active surfaces of secondary iron plaque minerals and produced >20% As(III) out of the initial As(V) pool. The later immobilization onto secondary iron plaque minerals was selective for As(V) and increased the relative abundance of As(III) in solution. These results help to assess the role of microbial iron plaque reduction and to enumerate the consequences for the fate of As in contaminated paddy fields.

5.2 Introduction

Arsenic (As) is a highly toxic metalloid which is almost omnipresent in paddy soils throughout Southeast Asia, such as Bangladesh and Vietnam. Often of geogenic origin in sulphide compounds in groundwater aquifers (e.g. arsenopyrite: FeAsS), As is being accumulated in paddy fields due to the discharge of groundwater for paddy field irrigation. In these contaminated paddy fields, As concentrations have been observed to reach more than 50 µg per gram soil, or up to 500 µg per litre porewater which exceeds the As limit concentrations of 10 µg per litre recommended by the World Health Organisation (WHO) by far.[1] Rice plants growing on As-contaminated paddy fields showed elevated As concentrations in their biomass and rice grains which possess a potential risk for humans who take up large quantities of rice as their daily nutrition. Perhaps the most important reason for intensive research that has been performed on the arsenic behaviour and translocation from soil pore water into edible rice grains.[2-5]

It is now commonly accepted, that the behaviour of As in the soil environment is strongly controlled by its redox state. The two most relevant oxidation states are arsenite (As(III)) and arsenate (As(V)). In contrast to As(V), as being the more dominant species under oxic conditions, As(III) is more prevalent under reducing conditions, more mobile and significantly more toxic compared to As(V).[6] Additionally, the speciation and mobility of arsenic in soils is strongly influenced by other geochemical conditions, especially soil pH, the soil redox potential (E_h) and the presence of other soil ions. In particular, the presence of ferric

iron minerals can effectively influence the mobility of soil As. Due to their high point of zero charge, surfaces of iron mineral are positively charged under circum-neutral pH conditions, which makes them function as good absorbents for negatively charged compounds such as arsenate (which are predominantly present in soils as $H_2AsO_4^-$ and $HAsO_4^{2-}$) or arsenite (present as H_3AsO_3).[7] The immobilization of As onto these iron minerals can effectively lower the concentration of dissolved As in the soil pore water and reduce the uptake of As into rice plants.[2,8] One phenomenon that significantly lowers the net uptake budget of arsenic from soil pore water into rice plants is the plant-induced root iron plaque formation. By releasing oxygen (O_2) from their roots, the so-called radial oxygen loss (ROL), rice plants oxygenate parts of the rhizosphere and effectively precipitate iron minerals on their root surface.[9-11] This root iron plaque can serve as a physical barrier for As and considerably reduce the As uptake into rice plants.[12,13] Moreover, we recently calculated that root iron plaque formation can not only contribute to the net iron mineral budget in a rice plant rhizosphere, but can theoretically immobilize up to 5% of the pore water As per cubic meter of contaminated paddy soil.[14]

On the contrary, there have been many studies which intensively enumerated processes that lead to a remobilization of As via reductive dissolution of As-bearing iron minerals during microbial Fe(III) mineral reduction.[15-17] Besides the sad prominent example of As-bearing sediments in aquifers,[18] also iron mineral covered roots of wetland plants loaded with As were hypothesized as hot spots for microbial Fe(III) reduction and As remobilization, due to the presence of organic substances, plant exudates or fatty acids which can serve as an electron donor for numerous Fe(III)-reducing bacteria.[19,20] Under dominating reducing conditions, especially at the end of harvesting cycles when plant stubbles are being left in the soil and start to decompose, roots covered in As-loaded iron plaque can turn from a net sink for As into a severe source due to As remobilization during microbial dissimilatory Fe(III) reduction.[17,21,22] Simultaneously, other studies suggest a higher sorption affinity for As on surfaces of secondary minerals that formed during microbial Fe(III)-reducing processes or a co-precipitation of As with newly-formed Fe(II) minerals, thus resulting in a higher net immobilization capacity for As.[23,24] This hypothesis suggests an enhanced immobilization capacity of reduced root iron plaque minerals for As and a net sink for As.

So far, observations from field studies and laboratory investigations still cannot draw a comprehensive conclusion for the fate of As during root iron plaque reduction. Evidently, a holistic understanding for the fate of As during root iron plaque reduction is still lacking. In particular, it is scarcely documented to which extent As is remobilized from root iron plaque minerals during microbial root iron plaque reduction. Further, very little is known about an inhibition of Fe(III)-reducing microorganisms by elevated concentrations of co-precipitated As in iron plaque minerals. Ultimately, the extent of As which can be immobilized on secondarily-

formed root iron plaque minerals and changes in As speciation during adsorption are so far poorly documented.[25] All these processes have a strong impact on both the (im)mobility and toxicity of As in contaminated paddy fields. So far, an enumerative understanding of individual parameters controlling the behaviour of As in the rhizosphere of paddy fields which are undergoing oxic and reductive cycles, is still lacking.

Within this study, we first isolated an Fe(III)-reducing enrichment culture that was capable to grow and actively reduce Fe(III) minerals in the presence of elevated As concentrations. In a next step, we quantitatively followed As immobilization on microbially-reduced and non-reduced root iron plaque and enumerated the speciation of adsorbed and dissolved As. Finally, rates of microbial root iron plaque reduction with three levels of As-load were compared, the mobility and speciation of As and Fe between the solid and the liquid phase were determined during and after microbial reduction. The collected data, an identification of (non-)reduced root iron plaque minerals and the enumerative distribution of As species during microbial As-loaded iron plaque reduction help to decipher physical and biological processes that can severely affect the fate of As in contaminated paddy fields towards the end of the growing season.

5.3   Materials and Methods

Rice plant cultivation and root iron plaque formation. Rice seeds (*Oryza sativa* Nipponbare) were sterilized (0.1% H_2O_2 rinse, ultrapure water) and seedlings were pre-grown in 50% sterile Hoagland[26] solution at pH 6.8. Seedlings were transferred at three-leaf stage into anoxic hydroponic setups with 500 mL 100% Hoagland solution amended with 500 µM Fe(II)$_{aq}$, buffered (PIPES, 20 mM) at pH 6.8. Setups were wrapped in aluminum foil in order to prevent illumination of the growth solution and the roots. Decline in hydroponic medium was replaced by anoxic and sterile 50% Hoagland solution at pH 6.8 and 500 µM Fe(II)$_{aq}$. Plants were kept at temperature-controlled conditions (25-27 °C, 70 % rel. humidity) following day (14 h) – night (10 h) cycles illuminated by a high-pressure sodium lamp (10,000 – 12,000 lx).

Microbial root iron plaque mineral reduction. After 32 days, rice plants were removed from hydroponic cultivation setups, green biomass was detached and roots were individually transferred into 500 mL sterile anoxic mineral medium[24] which was buffered (22 mM bicarbonate) at pH 6.8. Na-acetate, as an electron-donor substrate, was added to a final concentration of 20 mM. A 5% (v/v) inoculum of an Fe(III)-reducing culture (99.8% identity to *Geobacter* sp. CD1[27] based on 16S rRNA) isolated from a paddy field (Vercelli, Italy) was added to each microcosm. To inhibit cell activity in abiotic control setups, 4% PFA were added to the respective setups. Microcosms were incubated in the dark at constant

temperature (24°C). Biotic and abiotic incubations were performed in 6 experimental replicates, respectively.

Experimental setup I – As immobilization. Roots from inactivated control setups with non-reduced iron plaque and root iron plaque exposed to an Fe(III)-reducing culture were collected under anoxic conditions inside a glovebox (100 % N_2). Roots were transferred individually into 500 mL fresh anoxic and sterile mineral medium. To inhibit cell activity in setups with roots which were previously exposed to an Fe(III)-reducing culture, 4% PFA were added to setups with reduced iron plaque, respectively. Setups were stored for 24 hours at 4°C to reach equilibrium conditions between root iron plaque and dissolved iron concentrations and to fully inhibit cell activity. An anoxic and sterile As(V) solution was added to experimental setups to reach final concentrations for As(V) of 2 µM and 10 µM, respectively. Experiments were performed in triplicate setups for each treatment. Setups were kept in the dark at constant temperature (24°C) and samples for a quantification of total As, As(III) and As(V) were collected as following. At the end of the experiment, root iron plaque minerals were dissolved in 6 M HCl to quantify total Fe on root and As incorporated into root iron plaque.

Experimental setup II – microbial Fe(III) reduction of As-loaded iron plaque. Plants were grown in sterile and anoxic hydroponic setups on 500 mL Hoagland solution buffered (20 mM PIPES) at pH 6.8 as previously described. To produce As-loaded iron plaque minerals on roots, setups were spiked with an anoxic and sterile As(V) solution to aim at final concentrations of 250 µM As (referred to as low [+]), 500 µM As (referred to as medium [++] and 1,000 µM As (referred to as high [+++]), respectively. Setups without As addition served as control treatment. Each treatment (+,++,+++) was performed in 4 experimental replicates, the control experiment without As addition was performed in one setup only. After 14 days to As exposure, plants were removed from hydroponic solution, green biomass was detached and roots were dried under anoxic conditions (100% N_2; 30°C) for 48 hours. Dried root material was individually transferred to sterile and anoxic mineral medium (pH 6.8) amended with 22 mM Na-Acetate as electron donor substrate. A 5% (v/v) inoculum of the Fe(III)-reducing culture was added to each microcosm. To create abiotic control treatments, 4% PFA was added to one setup containing As-loaded roots to inhibit cell activity, respectively. Microcosms were incubated in the dark at constant temperature (24°C). Samples for a quantification of total As, As(III) and As(V) were collected as following. At the end of the experiment, root iron plaque minerals were dissolved in 6 M HCl to quantify total Fe on root and As incorporated into root iron plaque.

Sampling and analytical methods. Samples for an identification of iron minerals by Mössbauer spectroscopy in reduced and non-reduced iron plaque was collected from roots under anoxic conditions (100 N_2). Collected root material was dried under anoxic conditions, mortared, remaining root material was removed and iron plaque mineral particles collected for sample preparation (as described in Supporting Information). Samples were stored frozen (-20°C) under anoxic conditions until analysis.

Samples for Fe(II)/(III) quantification were collected under anoxic and sterile conditions. Particulate Fe(II)/(III) was analysed in non-filtered samples, while samples for dissolved Fe(II)/(III)$_{aq}$ were syringe-filtered (0.45 µm). All samples were acidified in 1 M HCl (20:80) to prevent chemical Fe(II) oxidation at ambient atmosphere. Particulate and dissolved Fe(II)/(III) was quantified by following the ferrozine assay[28] on 96-well plates measured in transmission mode on a photometer (Multiskan FC Microplate Photometer; Thermo Scientific).

Samples for total As were collected under anoxic and sterile conditions, stabilized with 2.5 % 7 M HNO_3 and subsequently analyzed for total As by ICP-MS (XSeries2, Thermo Scientific) using oxygen as the reaction cell gas (AsO+, m/z 91). Arsenic species were separated by IC (Dionex ICS-3000) using an AS16 column (Dionex AG/AS16 IonPac, 2.5–100 mM NaOH, flow rate 1.2 mL/min)[29] and quantified by ICP–MS (XSeries 2, Thermo Scientific) as AsO^+ (*m/z* 91) using oxygen as reaction cell gas.[30]

5.4   Results

Microbial root iron plaque reduction and mineral transformations.

Roots covered in iron plaque minerals were incubated with an Fe(III)-reducing culture to produce microbially-reduced iron plaque minerals. Setups with root iron plaque and PFA-inhibited cells serve as a control setup for non-reduced iron plaque minerals. Following 2 days of inoculation, root iron plaque minerals changed in biotic setups from orange to black which indicated Fe(III) mineral reduction (Figure 1). Simultaneously, samples from liquid medium showed elevated Fe(II)/Fe$_{total}$ ratios after 2 days (Figure S1), confirming the production of Fe(II) as a result of microbial Fe(III) reduction. After 7 days of incubation Fe(II)/Fe$_{total}$ ratios plateaued between 80-100% indicating the highest extent in microbial Fe(III) reduction of root iron plaque. Inhibited control setups did not show a significant change in color and remained orange until the end of the incubation after 15 days (Figure 1). Likewise, Fe(II)/Fe$_{total}$ ratios remained constantly low until the end of the incubation (Figure S1).
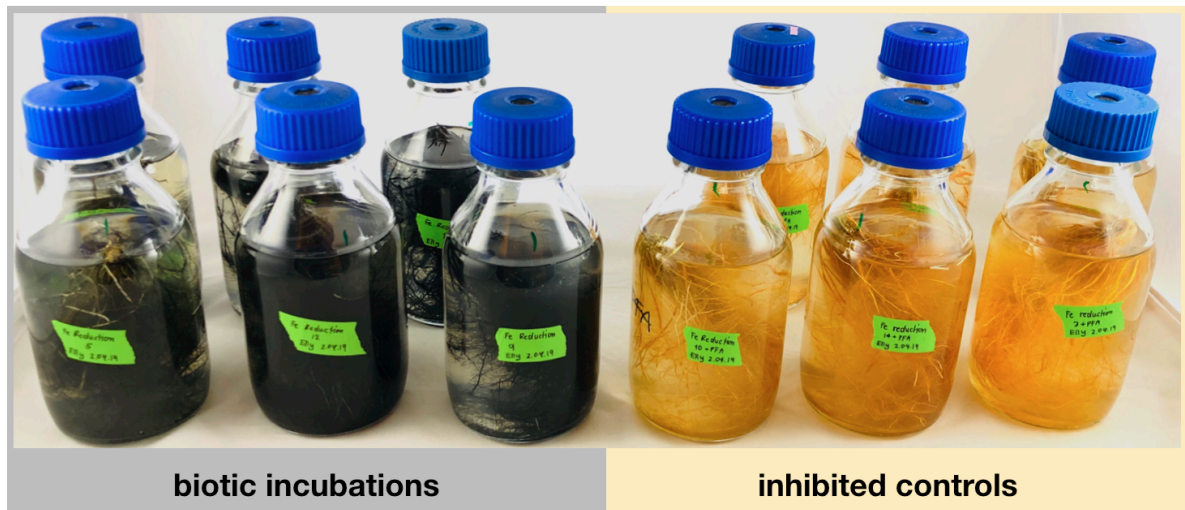
Figure 1. Microbial root iron plaque reduction. Root iron plaque incubated with an Fe(III)-reducing culture (left) and control incubations with inhibited cells (right). Changes in color from orange to black indicate the reduction of iron plaque minerals.

Mössbauer spectroscopy on reduced root iron plaque minerals showed the presence of an Fe(II) mineral phase similar to siderite (Supporting Information). With a relative abundance of more than 70%, this Fe(II) mineral represents the dominant iron mineral phase in reduced root iron plaque (Figure 2). Additionally, ferrihydrite with a relative abundance of 23% and residual goethite (approx. 5%) were detected as remaining Fe(III) mineral phases. On the contrary, root iron plaque in inhibited controls was dominated by Fe(III) minerals, such as ferrihydrite (90 % rel. abundance) and a minor fraction of goethite (approx. 10 %).
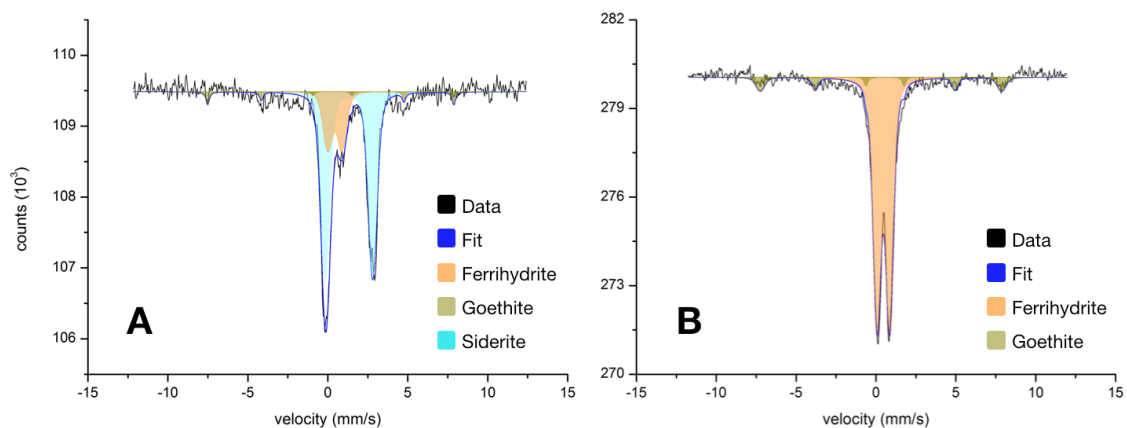
Figure 2. Mössbauer spectra of microbially-reduced and non-reduced root iron plaque minerals. A: The spectrum of the microbially-reduced iron plaque minerals indicated the presence of siderite as an additional Fe(II) mineral forming as a product of Fe(III) reduction with residual ferrihydrite and goethite. **B**: Non-reduced iron plaque minerals showed ferrihydrite and a small fraction of goethite as main components.

Iron quantification in liquid incubation and iron mineral extractions at the end of the experiment demonstrated that more than 50% of the initially produced root iron plaque minerals were remobilized from the root surface and remained in solution (Table 1). A total Fe(II) content of more than 70% was detected in the iron plaque minerals while less than 30% that remained present as Fe(III). Non-reduced control incubations showed less than 5% iron remobilization from root iron plaque and were predominantly characterized by 100% Fe(III) as main species in the iron plaque minerals.

Table 1. Iron speciation and mineral phases in microbially-reduced and non-reduced root iron plaque and iron remobilization from iron plaque.

	Fe speciation in iron plaque [mineral phase]		Iron remobilization from root iron plaque
	Fe(III) (%)	Fe(II) (%)	Fe_{total} (%)
microbially-reduced	28.1 (±1.3) [ferrihydrite & goethite]	71.9 (±2.7) [siderite]	54.5 (±3.9)
non-reduced	100.0 [ferrihydrite & goethite]	0.0 [–]	3.2 (±0.9)

Effect of secondary-formed root iron plaque minerals on the fate of As. In order to quantify the extent in arsenic immobilization onto reduced and non-reduced root iron plaque minerals, microbially-reduced and non-reduced root iron plaque was exposed to high (approx. 2 µM) and low (approx. 10 µM) As(V) concentrations, respectively. In setups containing microbially-reduced root iron plaque and high initial As concentrations, dissolved As concentrations decreased considerably to less than 8 µM within 6 hours. Reduced setups spiked with low initial As decreased to less than 1.5 µM As in solution within this time (Figure 3A). In both, the high and low As treatment, the decrease in As concentrations equals more than 25% of the total initial As which was immobilized on reduced root iron plaque within 6 hours only (Table 2). Towards the end of the incubation after 48 hours, the highest extent in As immobilization was observed in setups containing low As concentrations. More than 50% of the initial As was immobilized in the reduced setups containing low As concentrations, while a maximum of approx. 40% As was immobilized on reduced root iron plaque containing high initial As concentrations (Figure 3B, Table 2). Setups containing non-reduced root iron plaque showed significantly less As immobilization during the incubation. In these setups, total dissolved As concentrations remained relatively stable with only a slight decrease of 10-15% towards the end of the incubation (Figure 3C). After 48 hours, more than 80% of the initial As still remained in solution while a maximum of 15% As was immobilized

on non-reduced root iron plaque containing low initial As concentrations (Figure 3D, Table 2). Setups with high initial As concentrations showed <10% As immobilization on non-reduced root iron plaque.

Moreover, during the exposure of root iron plaque to low and elevated As(V) concentrations, the formation of As(III) was observed in all treatments within the initial 6 hours. In setups with reduced root iron plaque, more than 20% of the initial As(V) was reduced to As(III) at the end of the incubation and remained dissolved in solution both for the low and high As treatment (Figure 3A, Table 2). In contrast to that, setups with non-reduced root iron plaque showed less As(III) formation (Figure 3C). With <5% As(III) for the high As and <12% As(III) formation for the low As treatment, the relative proportion of As(III) in setups with non-reduced root iron plaque remained constantly lower compared to setups with microbially-reduced root iron plaque (Table 2).
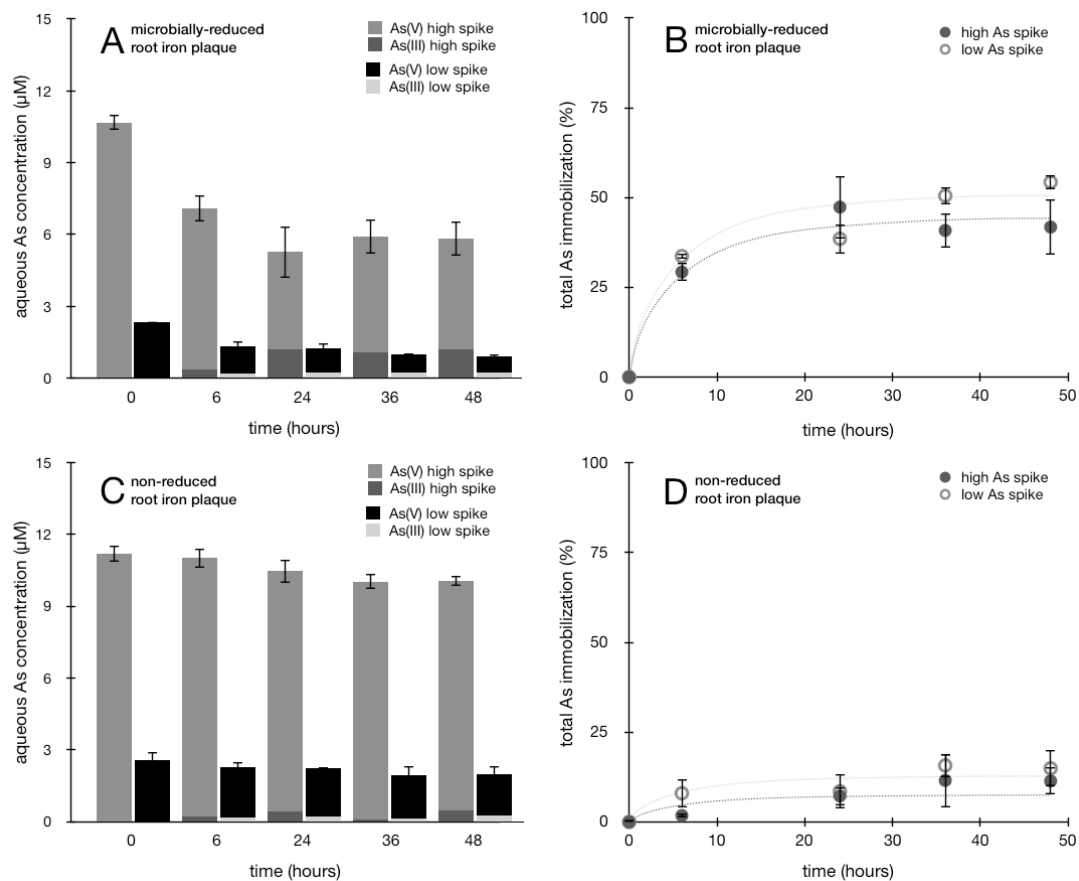
Figure 3. Arsenic concentrations, speciation and extent in arsenic immobilization in setups with **A:** microbially-reduced root iron plaque, exposed to high As(V) (left bars per time step) and low As(V) (right bars per time step) and respective As(III)/(V) proportion in solution (dark/light grey). **B:** Extent in As immobilization in setups with microbially-reduced root iron plaque at high (filled circles) and low (open circles) initial As concentrations. **C:** As concentrations in setups with non-reduced root iron plaque over time, exposed to high (left bars per time step) and low (right bars at time step) and respective As(III)/(V) proportion in solution (dark/light grey). **D:** Extent in As immobilization in setups with non-reduced root iron plaque at high (filled circles) and low (open circles) initial As concentrations.

Table 2. Arsenic speciation in solution and immobilization in setups with microbially-reduced and non-reduced root iron plaque exposed to high and low initial As concentrations.

	As speciation in solution		As immobilization on iron plaque
	As(V) (%)	As(III) (%)	As_{total} (%)
microbially-reduced (high As spike)	79.6 (±4.9)	20.4 (±2.9)	41.8 (±7.6)
non-reduced (high As spike)	95.6 (±1.3)	4.4 (±0.4)	11.4 (±3.8)
microbially-reduced (low As spike)	74.9 (±2.3)	25.1 (±0.9)	54.3 (±1.9)
non-reduced (low As spike)	88.4 (±1.6)	11.6 (±1.4)	14.9 (±5.1)

The effect of As in root iron plaque minerals on microbial iron plaque reduction. In order to identify whether As influences the rate and extent of microbial root iron plaque reduction, As-loaded root iron plaque (3 different elevated concentrations of As) was exposed to an Fe(III)-reducing culture. Over the course of the incubation, the concentration and speciation for iron and arsenic in solution was quantitatively monitored. Mineral extractions at the end of the incubation complement the collected data by an overall mass balance for precipitated and remobilized iron and arsenic during microbial root iron plaque reduction.

In all biotic incubations with As-bearing root iron plaque, the formation of aqueous Fe(II) indicated the microbial activity and Fe(III) reduction of root iron plaque (Figure S2). Fe(II) concentrations increased gradually after 2 days in all treatments. Incubations containing low (+) and no As showed fastest Fe(III) reduction rates compared to the other two treatments with medium (++) and high (+++) co-precipitated As in root iron plaque. In particular, biotic incubations with highest As concentrations showed a 50% slower increase in Fe(II) concentrations compared to treatments with lower As concentrations. While Fe(II)/Fe_{total} ratios were almost identical at around 95% for treatments with no, low (+) and medium (++) As concentrations after 12 days, Fe(II)/Fe_{total} ratios in treatments with high As (+++) reached only <75% at this time. Setups with inactivated cells showed a treatment-independent increase in Fe(II)/Fe_{total} ratios over the course of the incubation (Figure 4B). However, the extent in Fe(II) formation did not exceed 25% during the experiment.

Table 3. Iron speciation in root iron plaque and remobilized iron from roots during microbial reduction of iron plaque with different As loads.

treatment	Fe speciation in iron plaque		Iron remobilization from root iron plaque
	Fe(III) (%)	Fe(II) (%)	Fe_{total} (%)
no As	28.1 (±1.3)	71.9 (±2.7)	54.5 (±3.9)
+++	41.3 (±6.2)	58.7 (±6.2)	28.8 (±10.3)
+++ (inhibited)	95.9 (±0.9)	4.1 (±0.9)	18.0 (±2.7)
++	30.7 (±7.6)	69.3 (±7.6)	34.4 (±5.7)
++ (inhibited)	92.4 (±4.5)	7.6 (±4.5)	16.0 (±3.1)
+	24.4 (±24.9)	75.6 (±24.9)	40.3 (±4.3)
+ (inhibited)	89.0 (±2.7)	11.0 (±2.7)	12.4 (±2.1)

The speciation of iron in iron plaque and the extent in iron remobilization during microbial reduction of As-loaded root iron plaque was determined at the end of the incubations. The highest extent in iron remobilization from root iron plaque during microbial Fe(III) reduction was observed in incubations without As amendment. More than 50% of the initially precipitated total iron was observed to be remobilized by microbial reductive dissolution (Table 3). The remaining iron minerals on the rice roots showed an average Fe(II) content of approx. 70%, while residual Fe(III) minerals showed a relative abundance of approx. 30%. Similar ratios have been observed for iron plaque reduction with low (+) As concentrations. On average, around 40% of the initial iron plaque minerals were remobilized during microbial reduction, whereas remaining iron plaque minerals were dominated by 75% Fe(II) and 25% Fe(III) content. Less iron plaque remobilization was observed for roots exposed to higher As concentrations. While approx. 35% iron was remobilized from roots with medium As content (++), the lowest extent in iron remobilization was monitored for roots with highest As content (+++). Only around 29% iron was remobilized from root iron plaque with highest As treatment which is significantly less compared to iron remobilization from treatments with low (+) and no As. Similar trends were observed in the iron speciation of the remaining iron plaque minerals. The relative proportion of Fe(II) gradually decreased from more than 75% Fe(II) in root iron plaque with low As (+) to less than 60% in treatments with high (+++) As concentrations (Table 3). Inhibited control incubations showed less iron remobilization with general ratios of <20% iron remobilization independent from treatment conditions (Table 3).

Congruent with a remobilization of iron from root iron plaque, also As was remobilized from roots into solution during microbial iron plaque reduction. At the beginning of the incubation, no As was being detected in solution. After 2 days of incubation As concentrations increased considerably in all treatments and reached highest concentrations after 5-7 days (Figure 4B). Highest As concentrations were detected during the reduction of iron plaque with high As (+++) loads (Figure 4B) with total As concentrations of more than 70 µM in solution after 1 week of incubation. Treatments with lower As loads in iron plaque reached highest concentrations of approx. 50 µM and 25 µM after 5 days for the medium (++) and low (+) As conditions, respectively. Interestingly, As concentrations in solution declined after 7 days of incubation in all treatments, most significantly for the medium As amendment (++; Figure 4B). Here, As concentrations in solution decreased significantly by more than 50% to <20 µM at the end of the incubation.

During the formation of root iron plaque, a total of approx. 2 mg As, 1.3 mg As and 0.3 mg As was being co-precipitated in setups high (+++), medium (++) and low As amendments, respectively (Table 4). In the high As (+++) and low As (+) treatment, more than 40% of the initially co-precipitated As was being remobilized into the culturing solution during microbial iron plaque reduction. In the medium As treatment (++), the amount of As in solution equaled an As remobilization rate of <20% only (Table 4). This observation is also being reflected in the low As concentrations in the aqueous phase as observed at the end of the incubation (Figure 4B).
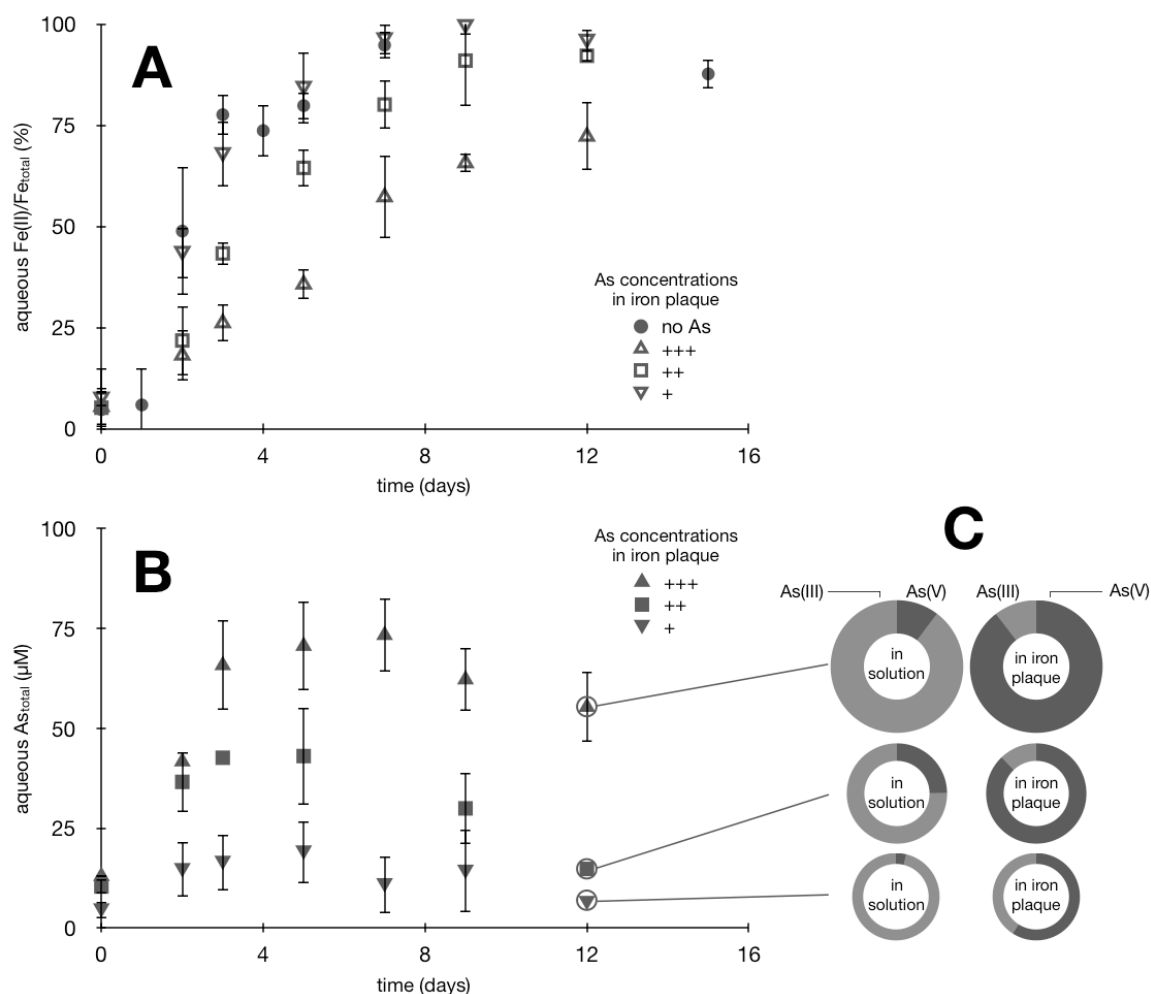
Figure 4. Iron and arsenic remobilization during microbial reduction of As-bearing root iron plaque. A: Fe(II)/Fe$_{total}$ ratio in setups containing active cells of an Fe(III)-reducing *Geobacter* spp. culture and root iron plaque with no (filled circles), low (open triangle, +), medium (open square, ++) and high (open pyramid, +++) co-precipitated arsenic. **B:** As$_{total}$ concentrations in solution in respective setups with low (+), medium (++) and high (+++) As-loaded root iron plaque. **C:** Illustration of relative proportions of As(III) and As(V) in solution and in remaining root iron plaque minerals in treatments with high, medium and low As-loaded root iron plaque. Dimensions of circles represent the relative amount of total As concentrations found in each treatment, respectively. Errors in data plots represent propagated standard deviation from triplicate experiments.

Table 4. Arsenic speciation and relative abundance in root iron plaque and in solution remobilized from roots during microbial reduction of iron plaque at different As loads.

	▲ +++			■ ++			▼ +		
	As(V) (µmol)	As(III) (µmol)	As total (µg)	As(V) (µmol)	As(III) (µmol)	As total (µg)	As(V) (µmol)	As(III) (µmol)	As total (µg)
in solution	11.3 (±2.4)	98.8[a] (±16.6)	826.1 (±36.1)	7.3[b]	22.2[a,b]	221.5 (±20.1)	0.5[b]	12.4[a,b]	96.9 (±17.8)
in iron plaque	130.2 (±21.3)	15.2 (±16.8)	1090.5 (±45.7)	128.5 (±35.9)	17.9 (±8.5)	1097.6 (±78.2)	16.8 (±12.9)	11.7 (±7.4)	213.8 (±32.6)

[a] including the detection of thioarsenate (<10 %).

[b] measurement only from one replicate due to sample loss.

The speciation of As in the remaining root iron plaque minerals differed substantially from As speciation in solution. The predominant As speciation in remaining root iron plaque minerals was observed to be the oxidized form As(V) (Figure 4C). Among all treatments, more than 60% of the iron plaque-bound As was abundant as As(V). Only a small fraction of 10-30% was present as As(III) (Table 4). In contrast to that, As in solution was constantly present mainly as As(III) which represented more than 75% of the total As found in liquid phase. A noticeable maximum of approx. 25% As(V) in solution was only detected in the medium As (++) treatment (Figure 4C). It needs to be highlighted that this treatment was generally characterized by a relatively low As remobilization from root iron plaque and a high root iron mineral-bound fraction for total As of more than 80% (Table 4).

5.5 Discussion

Secondary mineral formation during microbial iron plaque reduction enhances As immobilization. So far, it has been recognized by numerous studies that root iron plaque formation can decrease the uptake of As into rice plants by binding As to the hydroxyl surface groups of Fe(III) (oxyhydr)oxide minerals on the root surface[7,31] or by forming ternary complexes with organic matter.[32] Consequently, As was reported to be sequestered on Fe(III) (oxyhydr)oxide minerals and its mobility in the paddy field rhizosphere was observed to diminish with an increasing number of rhizosphere Fe(III) (oxyhydr)oxides.[8] On the contrary, it has been validated that a complete dissolution of these Fe(III) (oxyhydr)oxides can significantly enhance the remobilization of As by reductive dissolution of Fe(III) (oxyhydr)oxides as it was commonly observed for studies with As-bearing iron minerals and Fe(III)-reducing microorganisms.[15-18] The intermediate scenario, which has not been investigated intensively, is the effect of microbial Fe(III) reduction of root Fe(III) (oxyhydr)oxide minerals and the formation of secondary iron minerals on the root surface.[25] In particular, the fate of As under conditions at which secondary iron minerals are being formed in paddy fields during microbial root iron plaque reduction is scarcely documented.

Here, our results imply that an incomplete reduction and dissolution of root iron plaque minerals not necessarily lead to an intensification in As remobilization from the root surface. Moreover, the significantly enhanced As sorption capacity of microbially-reduced root iron plaque over pristine oxidized root iron minerals, as it is summarized in Figure 3, suggests that the formation of secondary root iron plaque minerals considerably increases net As immobilization per plant. Although a considerable amount of up to 50% root iron plaque by mass was undergoing reductive dissolution during microbial iron reduction (Table 1), secondary mineral formation had a dramatic effect on As immobilization and increased sorption capacities by more than 100%. With more than 80% of the initial As spike was

demonstrated to remain in solution when oxidized iron plaque minerals where present, more than 40% of the initial As was immobilized on reduced root iron plaque. Similar effects have been investigated during the formation of secondary iron minerals, such as siderite, in previous studies.[23] However, sorption behavior of contaminants, such as As, onto secondarily-formed iron minerals on root surfaces has been rarely investigated.[33] Interestingly, the extent in As immobilization was being observed to be concentration-independent. Both, the high As-spiked (10 µM) and low As-spiked (2 µM) setups containing reduced root iron plaque showed a rather similar extent in As immobilization of 42-54%, respectively. Similar trends were validated for non-reduced root iron plaque, however with only 11-15% immobilization, As sequestration was significantly lower compared to reduced root iron plaque (Figure 3, Table 2).

In this context, our results suggest that an incomplete microbial Fe(III) reduction can form secondary minerals on root iron plaque which ultimately increased the extent in As immobilization more than 100% compared to non-reduced iron plaque. These findings imply that microbial reduction of Fe(III) minerals not necessarily turn the roots of rice plants into an As source but have the potential to increase the net performance to serve as a sink for dissolved As species in contaminated soils. It is clear that in the environment, a large number of other soil components, such as organic matter, humic substances and other ions might compete with sorption sites on the reduced iron plaque. However, the current results may help to increase our enumerative understanding on the impact of root iron plaque reduction on contaminant retention in paddy fields.

As-loads on root iron plaque inhibit microbial iron plaque reduction. The remobilization of As from Fe(III) (oxyhydr)oxides during microbial dissimilatory iron reduction has been widely studied for a large variety of environmental settings, such as contaminated sediments, aquifers or rhizosphere systems.[15,17,18,33] Numerous reported the formation of secondary iron minerals followed by a complete dissolution of mineral surfaces which resulted in the release of iron mineral surface-bound contaminants during microbial Fe(III) reduction. However, only a few studies considered a potential toxic effect of these contaminants on microbially-active organisms inhibiting the performance and efficiency in microbial iron mineral reduction.[27,34] So far, to the best of our knowledge studies which are investigating an inhibitory effect of As on microbial root iron plaque reduction are still lacking.

In this context, our observations demonstrate that the concentration of As in root iron plaque has an inhibiting effect on the Fe(III)-reducing culture used in the current study and can suppress microbial Fe(III) reduction rates. Root iron plaque without As load was efficiently reduced and showed the highest extent in dissolved Fe(II) within 3 days only. Root iron plaque

with medium (++) and high (+++) As loads, however, showed a delay of 7-12 days, respectively to reach a similar extent in dissolved Fe(II) concentrations (Figure 4A). Similar trends were observed in the net iron plaque which was remobilized over the course of the incubations. At the end of the experiment after 12 days (14 days for iron plaque without As loads) significantly less total iron was remobilized from As-loaded iron plaque compared to non-contaminated roots. Moreover, the extent in iron remobilization during microbial reduction correlated negatively with increasing As loads (Table 3). In other words, the more As was present in the iron plaque minerals, the less microbial iron plaque remobilization was being observed. Similar trends were reported for other *Geobacter* species during Fe(III) reduction of cadmium-doped iron minerals. Gradually elevated concentrations of cadmium were negatively correlated with microbial Fe(III) reduction rates which was interpreted as an inhibitory effect of Cd on microbial activity.[27] In the case of As, all of the *Geobacter* genomes were reported to have the genetic ability to express the arsenic detoxification machinery (*ars* genes) which is generally described to detoxify the cells by enzymatically reducing As(V) to As(III). The more mobile species (As(III)) can then be excreted from the cell by the Acr3 transmembrane antiporter[35] to lower the intracellular As concentration. Often, this enzymatic arsenic detoxification in *Geobacter* was reported to delay or inhibit the microbial activity in Fe(III) mineral reduction.[34] The current data suggests that this effect is also true for the microbial reduction of As-loaded root iron plaque. Interestingly, the highest extent in iron remobilization from iron plaque is congruent to the highest Fe(II)/(III) ratio in the remaining solid iron plaque on the roots. This trend likely reflects the enhanced formation of secondary Fe(II) minerals under certain geochemical conditions when high microbial Fe(III) reduction rates have been observed.[36] Under these conditions, also here, the Fe(II)/Fe(III) speciation in the remaining iron plaque also negatively correlates with As loads in the iron plaque regarding the highest and lowest loads (Table 3). These observations support our hypothesis that higher loads of As in root iron plaque can negatively affect microbial iron plaque reduction, microbial reductive dissolution of iron minerals, and thus the formation of secondary minerals.

In the environment, this observation in turn can negatively impact the formation of secondary iron minerals and thus decrease the positive net effect on As immobilization onto reduced root iron plaque. Moreover, iron plaque containing high loads of As can lead to sustaining changes in the microbial community which might not only negatively impact the ecosystem functioning but increase the bioavailability of dissolved As species for plants and microorganisms. The extensive accumulation in plants and uptake into edible rice grains consequently impacts food quality and possesses a potential threat to human health. For such reasons, the effect of As-loads on microbial Fe(III) reduction of root iron plaque needs

to be further considered to fully decipher the fate of As in the rhizosphere biogeochemical cycling in contaminated paddy fields.

Rescission of As remobilization during iron plaque reduction and the formation of secondary iron minerals. The mobility of Arsenic during microbial iron plaque reduction turned out to be more complex than initially expected. First, the remobilization of As from root iron plaque into solution correlated positively to the observed ratios in dissolved $Fe(II)/Fe_{total}$ (Figure 4A & B). The relative net extent in As remobilization within the first 5 days resembled the total initial As loads on roots in the three different treatments with high (+++), medium (++) and low As (+) loads. However, in a second phase, following 7 days of incubation, dissolved As was constantly removed from solution in all treatments until the end of the incubation (Figure 4B). Considering the collected data on the iron speciation in solution (Figure 4A), the mineral identification of microbially-reduced iron plaque (Figure 2) and the iron mineral extraction at the end of the incubation (Table 3), we hypothesize that the remobilization of As within the initial 5 – 7 days was mainly caused by the reductive dissolution of the poorly crystalline iron minerals, such as ferrihydrite. The sequestration of As into solid phases was potentially due to the adsorption on secondarily-formed iron minerals, as it was already observed in experiment 1. A similar behavior including a remobilization during reductive dissolution of As-bearing sedimentary iron minerals has been described before for groundwater aquifers in Southeast Asia.[18] Depending on geochemical conditions, however, it has been reported that the microbial reductive dissolution can cause the formation of secondary iron minerals that either co-precipitate with As or incorporate As from solution by adsorption processes.[24,36]

The mobility of contaminants such as arsenic can severely impact the ecosystem dynamics and can negatively affect the long-term functioning.[37] In paddy fields, a sudden rise in dissolved and bioavailable As during As-loaded iron plaque reduction can not only diminish the abundance and diversity of the microbial community, but also increase the short term translocation of As into the rice plant and the grains. This again increases the risk for humans partaking rice as a major food stock. On the long term, the rescission of As remobilization and the sequestration onto secondary iron minerals may reduce local concentrations of dissolved As which can result in a lower bioavailability in contaminated paddy fields, and thus relieve the ecosystem of a toxic stressor. Right for this very reason, the constant monitoring of rhizosphere and plant parameters during rice plant growth are decisive to know when reducing conditions around the rice roots develop, microbial iron plaque reduction initiates which ultimately triggers the release of As.

Redox transformation of As(V) on the surface of reduced iron plaque minerals increases its mobility and toxicity. In both experiments, with As(V) and reduced root iron plaque minerals, we observed the production of significant amounts of reduced As(III). In the first set of abiotic experiments with microbially reduced iron plaque, a net proportion of 20 – 25% of the total As in solution was found to be As(III) at the end of the sorption experiment after 48 hours. The As(III) in these setups formed relatively fast and was being detected within the first samples collected after 6 hours already (Figure 3). Since all cell activity in these setups was inhibited, we concluded that the redox transformation from As(V) to As(III) occurred abiotically.

Similar observations have been made in experiment 2. Although most of the total As was found to remain associated with the iron plaque minerals, a significant amount of up to 40% was being remobilized from iron plaque during microbial reduction. From this fraction, more than 75% were present as As(III). Remaining As associated with (secondarily-formed) root iron plaque minerals was dominated to the largest extent by As(V) (Figure 4, Table 4) due to the relatively high sorption affinity of As(V) to iron mineral surfaces [38]. The production of dissolved As(III) in the latter experiment can be the result of the As detoxification machinery in *Geobacter* spp., the intracellular enzymatic reduction of As(V) to As(III) and the release through transmembrane antiporters to lower the intracellular As concentration.[35] Observations from the previous experiment, however, suggest that the formation of more than 20% As(III) was a product of abiotic redox-reactions of As(V) with secondary-formed iron plaque minerals (Figure 3, Table 2). Similar observations have been made by Muehe et al. (2013), who observed between 30-40% As(V) reduction during the microbial reduction of As-loaded Fe(III) (oxyhydr)oxides.[24] They suggested that surface-bound Fe(II), which was produced during microbial Fe(III) reduction, activated the mineral surface and initiated the electron transfer to As(V)[39] as it was already observed for a variety of other contaminants, including chromate(IV)[40] and uranium(VI).[41] As a result, the reduced As(III) was released into solution due to the lower sorption affinity to iron minerals such as siderite[24] and remained present in the aqueous phase. Moreover, the presence of As(III) in the solid phase suggests that approx. 20% of the produced As(III) was re-precipitated or adsorbed onto remaining Fe(III) minerals, which is in line with the respective speciation of the solid state iron minerals found on the root surface at the end of the incubation (Table 3). The here-observed higher extent in total As(III) formation in experiment 2 compared to experiment 1, are potentially the combined net effect of i) abiotically catalyzed redox-reactions of As(V) with secondary-formed mineral surfaces, which accounted for approx. 20% total As(V) reduction and ii) 10-30% total As(V) reduction which can be attributed to the biological As(V) reduction by *Geobacter* spp. cells.

The abiotic reduction of As(V) on reduced secondary-formed root iron plaque minerals can severely affect the fate of contaminants in the paddy field rhizosphere. Since As(III)

represents the more mobile and toxic species, the horizontal mass transfer of As across the rhizosphere could significantly increase when microbially-reduced root iron plaque becomes the dominant species in the rhizosphere. Previously surface-bound As, undergoing a chemical reduction to As(III) has a higher affinity to remain in solution instead of re-adsorbing on secondary-formed iron plaque minerals. There is evidence that the incorporation of As onto secondary-formed root iron plaque, as it was reported in this study, is selective for As(V) due to the higher surface affinity to iron minerals.[38] As a consequence, less mobile As(V) can be efficiently immobilized while more mobile and toxic As(III) is being produced at reduced iron plaque minerals. Clearly, the abiotic reduction of As(V) on reduced iron plaque needs to be investigated under more environmentally-relevant conditions, such as in the presence of humic substances, organic matter or plant exudates which were shown to affect the speciation and mobility of As(III). However, the current results demonstrate that the role of microbially-reduced root iron plaque and its capability to chemically produce 20% more mobile and toxic As(III) need to be considered for an enumerative understanding of contaminant mobility in paddy fields and to determine when root iron plaque can turn from an As sink into as source for As(III).

5.6 References

1. Roberts, L. C.; Hug, S. J.; Voegelin, A.; Dittmar, J.; Kretzschmar, R.; Wehrli, B.; Saha, G. C.; Badruzzaman, A. B. M.; Ali, M. A., Arsenic Dynamics in Porewater of an Intermittently Irrigated Paddy Field in Bangladesh. *Environ Sci Technol* **2011,** *45*, (3), 971-976.

2. Abedin, M. J.; Cotter-Howells, J.; Meharg, A. A., Arsenic uptake and accumulation in rice (Oryza sativa L.) irrigated with contaminated water. *Plant Soil* **2002,** *240*, (2), 311-319.

3. Garnier, J. M.; Travassac, F.; Lenoble, V.; Rose, J.; Zheng, Y.; Hossain, M. S.; Chowdhury, S. H.; Biswas, A. K.; Ahmed, K. M.; Cheng, Z.; van Geen, A., Temporal variations in arsenic uptake by rice plants in Bangladesh: The role of iron plaque in paddy fields irrigated with groundwater. *Sci Total Environ* **2010,** *408*, (19), 4185-4193.

4. Li, R. Y.; Zhou, Z. G.; Zhang, Y. H.; Xie, X. J.; Li, Y. X.; Shen, X. H., Uptake and Accumulation Characteristics of Arsenic and Iron Plaque in Rice at Different Growth Stages. *Commun Soil Sci Plan* **2015,** *46*, (19), 2509-2522.

5. Dittmar, J.; Voegelin, A.; Maurer, F.; Roberts, L. C.; Hug, S. J.; Saha, G. C.; Ali, M. A.; Badruzzaman, A. B. M.; Kretzschmar, R., Arsenic in Soil and Irrigation Water Affects Arsenic Uptake by Rice: Complementary Insights from Field and Pot Studies. *Environ Sci Technol* **2010,** *44*, (23), 8842-8848.

6. Oremland, R. S.; Stolz, J. F., Arsenic, microbes and contaminated aquifers. *Trends Microbiol* **2005,** *13*, (2), 45-49.

7. Dixit, S.; Hering, J. G., Comparison of arsenic(V) and arsenic(III) sorption onto iron oxide minerals: Implications for arsenic mobility. *Environ Sci Technol* **2003,** *37*, (18), 4182-4189.

8. Chen, Z.; Zhu, Y. G.; Liu, W. J.; Meharg, A. A., Direct evidence showing the effect of root surface iron plaque on arsenite and arsenate uptake into rice (Oryza sativa) roots. *New Phytol* **2005,** *165*, (1), 91-97.

9. Maisch, M.; Lueder, U.; Kappler, A.; Schmidt, C., Iron Lung: How Rice Roots Induce Iron Redox Changes in the Rhizosphere and Create Niches for Microaerophilic Fe(II)-Oxidizing Bacteria. *Environ Sci Tech Let* **2019,** *6*, (10), 600-605.

10. Kirby, C. S.; Thomas, H. M.; Southam, G.; Donald, R., Relative contributions of abiotic and biological factors in Fe(II) oxidation in mine drainage. *Appl Geochem* **1999,** *14*, (4), 511-530.

11. Flessa, H.; Fischer, W. R., Plant-Induced Changes in the Redox Potentials of Rice Rhizospheres. *Plant Soil* **1992,** *143*, (1), 55-60.

12. Moyer, C. E.; Tappero, R.; Bais, H.; Sparks, D. L., Role of iron plaques in immobilizing arsenic in the rice-root environment. *Abstr Pap Am Chem S* **2012,** *244*.

13. Yamaguchi, N.; Ohkura, T.; Takahashi, Y.; Maejima, Y.; Arao, T., Arsenic Distribution and Speciation near Rice Roots Influenced by Iron Plaques and Redox Conditions of the Soil Matrix. *Environ Sci Technol* **2014,** *48*, (3), 1549-1556.

14. Maisch, M.; Lueder, U.; Kappler, A.; Schmidt, C., From Plant to Paddy—How Rice Root Iron Plaque Can Affect the Paddy Field Iron Cycling. *Soil Systems* **2020,** *4*, (2).

15. Islam, F. S.; Gault, A. G.; Boothman, C.; Polya, D. A.; Charnock, J. M.; Chatterjee, D.; Lloyd, J. R., Role of metal-reducing bacteria in arsenic release from Bengal delta sediments. *Nature* **2004,** *430*, (6995), 68-71.

16. Qiao, J. T.; Li, X. M.; Li, F. B., Roles of different active metal-reducing bacteria in arsenic release from arsenic-contaminated paddy soil amended with biochar. *J Hazard Mater* **2018,** *344*, 958-967.

17. Cummings, D. E.; Caccavo, F.; Fendorf, S.; Rosenzweig, R. F., Arsenic mobilization by the dissimilatory Fe(III)-reducing bacterium Shewanella alga BrY. *Environ Sci Technol* **1999,** *33*, (5), 723-729.

18. Fendorf, S.; Michael, H. A.; van Geen, A., Spatial and Temporal Variations of Groundwater Arsenic in South and Southeast Asia. *Science* **2010,** *328*, (5982), 1123-1127.

19. King, G. M.; Garey, M. A., Ferric Iron Reduction by Bacteria Associated with the Roots of Freshwater and Marine Macrophytes. *Appl Environ Microb* **1999,** *65*, (10), 4393.

20. Kusel, K.; Chabbi, A.; Trinkwalter, T., Microbial processes associated with roots of bulbous rush coated with iron plaques. *Microbial Ecol* **2003,** *46*, (3), 302-311.

21. Lukasz, D.; Liwia, R.; Aleksandra, M.; Aleksandra, S., Dissolution of Arsenic Minerals Mediated by Dissimilatory Arsenate Reducing Bacteria: Estimation of the Physiological Potential for Arsenic Mobilization. *Biomed Res Int* **2014**.

22.   Wang, X.; Huang, R.; Li, L.; He, S. X.; Yan, L.; Wang, H.; Wu, X.; Yin, Y. L.; Xing, B. S., Arsenic removal from flooded paddy soil with spontaneous hygrophyte markedly attenuates rice grain arsenic. *Environ Int* **2019,** *133*.

23.   Hansel, C. M.; Benner, S. G.; Neiss, J.; Dohnalkova, A.; Kukkadapu, R. K.; Fendorf, S., Secondary mineralization pathways induced by dissimilatory iron reduction of ferrihydrite under advective flow. *Geochim Cosmochim Ac* **2003,** *67*, (16), 2977-2992.

24.   Muehe, E. M.; Scheer, L.; Daus, B.; Kappler, A., Fate of Arsenic during Microbial Reduction of Biogenic versus Abiogenic As-Fe(III)-Mineral Coprecipitates. *Environ Sci Technol* **2013,** *47*, (15), 8297-8307.

25.   Wang, X. J.; Chen, X. P.; Kappler, A.; Sun, G. X.; Zhu, Y. G., Arsenic Binding to Iron(Ii) Minerals Produced by an Iron(Iii)-Reducing Aeromonas Strain Isolated from Paddy Soil. *Environ Toxicol Chem* **2009,** *28*, (11), 2255-2262.

26.   Hoagland, D. R.; Arnon, D. I., The water-culture method for growing plants without soil. *Circular. California agricultural experiment station* **1950,** *347*, (2nd edit).

27.   Muehe, E. M.; Obst, M.; Hitchcock, A.; Tyliszczak, T.; Behrens, S.; Schroder, C.; Byrne, J. M.; Michel, F. M.; Kramer, U.; Kapplert, A., Fate of Cd during Microbial Fe(III) Mineral Reduction by a Novel and Cd-Tolerant Geobacter Species. *Environ Sci Technol* **2013,** *47*, (24), 14099-14109.

28.   Stookey, L. L., Ferrozine - a New Spectrophotometric Reagent for Iron. *Anal Chem* **1970,** *42*, (7), 779-&.

29.   Wallschlager, D.; London, J., Determination of methylated arsenic-sulfur compounds in groundwater. *Environ Sci Technol* **2008,** *42*, (1), 228-234.

30.   Kerl, C. F.; Ballaran, T. B.; Planer-Friedrich, B., Iron Plaque at Rice Roots: No Barrier for Methylated Thioarsenates. *Environ Sci Technol* **2019,** *53*, (23), 13666-13674.

31.   Tessier, A.; Rapin, F.; Carignan, R., Trace-Metals in Oxic Lake-Sediments - Possible Adsorption onto Iron Oxyhydroxides. *Geochim Cosmochim Ac* **1985,** *49*, (1), 183-194.

32.   Tessier, A.; Fortin, D.; Belzile, N.; DeVitre, R. R.; Leppard, G. G., Metal sorption to diagenetic iron and manganese oxyhydroxides and associated organic matter: Narrowing the gap between field and laboratory measurements. *Geochim Cosmochim Ac* **1996,** *60*, (3), 387-404.

33. Kocar, B. D.; Herbel, M. J.; Tufano, K. J.; Fendorf, S., Contrasting effects of dissimilatory iron(III) and arsenic(V) reduction on arsenic retention and transport. *Environ Sci Technol* **2006,** *40*, (21), 6715-6721.

34. Chow, S. S.; Taillefert, M., Effect of arsenic concentration on microbial iron reduction and arsenic speciation in an iron-rich freshwater sediment. *Geochim Cosmochim Ac* **2009,** *73*, (20), 6008-6021.

35. Dang, Y.; Walker, D. J. F.; Vautour, K. E.; Dixon, S.; Holmes, D. E., Arsenic Detoxification by Geobacter Species. *Appl Environ Microb* **2017,** *83*, (4).

36. Kappler, A.; Straub, K. L., Geomicrobiological cycling of iron. *Rev Mineral Geochem* **2005,** *59*, 85-108.

37. Borch, T.; Kretzschmar, R.; Kappler, A.; Van Cappellen, P.; Ginder-Vogel, M.; Voegelin, A.; Campbell, K., Biogeochemical Redox Processes and their Impact on Contaminant Dynamics. *Environ Sci Technol* **2010,** *44*, (1), 15-23.

38. Babechuk, M. G.; Weisener, C. G.; Fryer, B. J.; Paktunc, D.; Maunders, C., Microbial reduction of ferrous arsenate: Biogeochemical implications for arsenic mobilization. *Appl Geochem* **2009,** *24*, (12), 2332-2341.

39. Amstaetter, K.; Borch, T.; Larese-Casanova, P.; Kappler, A., Redox Transformation of Arsenic by Fe(II)-Activated Goethite (alpha-FeOOH). *Environ Sci Technol* **2010,** *44*, (1), 102-108.

40. Williams, A. G. B.; Scherer, M. M., Kinetics of Cr(VI) reduction by carbonate green rust. *Environ Sci Technol* **2001,** *35*, (17), 3488-3494.

41. Liger, E.; Charlet, L.; Van Cappellen, P., Surface catalysis of uranium(VI) reduction by iron(II). *Geochim Cosmochim Ac* **1999,** *63*, (19-20), 2939-2955.

5.7 Supporting Information

The Dark Side of Root Iron Plaque – How Microbial Iron Plaque Reduction Affects the Fate of Arsenic in Contaminated Paddy Fields

Markus Maisch[1], Panunporn Tutiyasarn[1], Carolin Kerl[2], Britta Planer-Friedrich[2], Andreas Kappler[1,3], Caroline Schmidt[1]

[1] Geomicrobiology, Center for Applied Geoscience, University of Tuebingen, Germany

[2] Environmental Geochemistry, Bayreuth Center for Ecology and Environmental Research (BayCEER), University of Bayreuth, Germany

[3] Center for Geomicrobiology, Department of Bioscience, University of Aarhus, Denmark

Number of tables in supporting information: 1

Number of figures in supporting information: 2

Total numbers of pages in supporting information: 4 (including cover page)

Mössbauer spectroscopy

Sample preparation. Within an anoxic glovebox (100% N_2), root biomass was collected and dried at constant 30°C. Dried sample material was mortared, and subsequently loaded into Plexiglas holders (area 1 cm^2), forming a thin disc. Prior to analysis, samples were stored anoxically at -20°C to suppress recrystallization processes or microbial activity. Samples were transported to the instrument within airtight bottles which were only opened immediately prior to loading into a closed-cycle exchange gas cryostat (Janis cryogenics) to minimize exposure to air. Spectra were collected at 77 K using a constant acceleration drive system (WissEL) in transmission mode with a $^{57}Co/Rh$ source. All spectra were calibrated against a 7 µm thick α-^{57}Fe foil that was measured at room temperature. Analysis was carried out using Recoil (University of Ottawa) and the Voigt Based Fitting (VBF) routine.[1] The half width at half maximum (HWHM) was constrained to 0.127 mm/s during fitting.

Microbial Fe(III) reduction of root iron plaque minerals
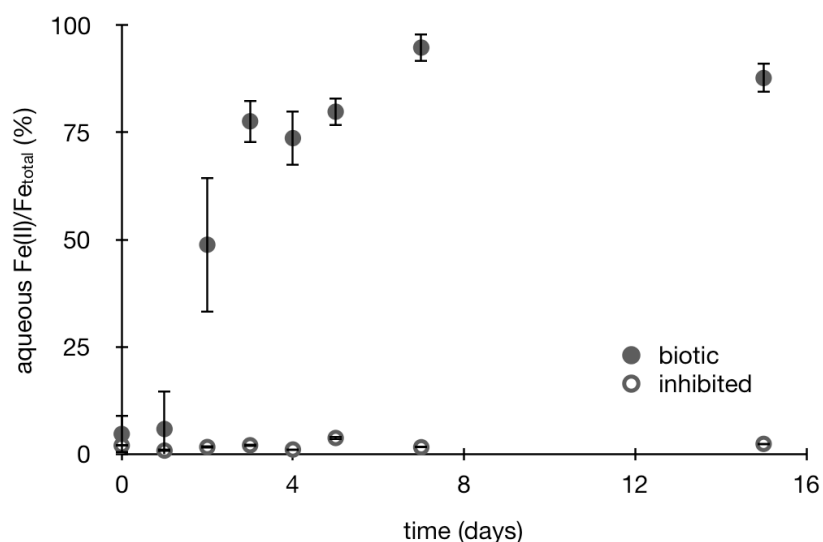
Figure S1. Fe(II)/Fe$_{total}$ ratios in liquid incubation medium during microbial reduction of root iron plaque (filled symbols) and in inhibited controls (empty symbols). Standard deviation is derived from six replicates for each treatment.

Iron mineral identification in reduced and non-reduced root iron plaque

Table S1. Mössbauer spectra hyperfine parameters for root iron plaque minerals. CS – Center shift, ΔE_Q – Quadrupole splitting, ε – Quadrupole shift, B_{hf} – Hyperfine field, Pop. – relative abundance, $\chi 2$ – goodness of fit, identified mineral phase (Fh – ferrihydrite, Sid – Siderite, Gt – Goethite)

Sample	Temp.	Phase	CS	ΔE_Q	ε	B_{hf}	Pop	±	χ^2	Mineral phase
	(K)		(mm/s)	(mm/s)	(mm/s)	(T)	(%)			
microbially-reduced	77	Db1	0.45	0.80			23.3	1.3	0.90	Fh
		Db2	1.32	2.96			71.9			Sid
		Sxt1	0.48		-0.19	49.5	4.8			Gt
non-reduced	77	Db1	0.47	0.77			89.7	0.9	0.6	Fh
		Sxt1	0.49		-0.23	49.8	10.3			Gt
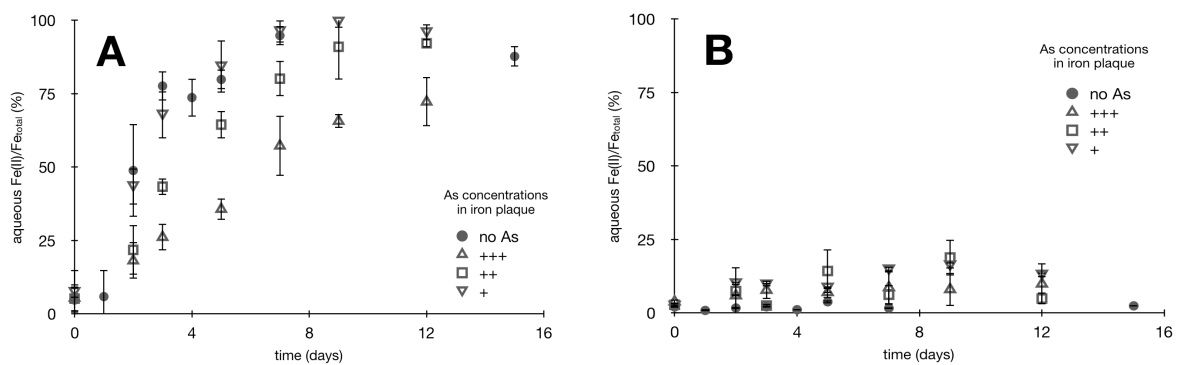
Figure S2. Fe(II)/Fe₍ₜₒₜ₎ ratios during microbial reduction of As-loaded root iron plaque in setups with **A:** active cells of an Fe(III)-reducing *Geobacter* spp. culture and root iron plaque with no (filled circles), low (open triangle, +), medium (open square, ++) and high (open pyramid, +++) co-precipitated arsenic. **B:** Control incubations with inhibited cells and root iron plaque with no (filled circles), low (open triangle, +), medium (open square, ++) and high (open pyramid, +++) co-precipitated arsenic.

Chapter 5

References

1.   Rancourt, D. G.; Ping, J. Y., Voigt-Based Methods for Arbitrary-Shape Static Hyperfine Parameter Distributions in Mossbauer-Spectroscopy. *Nucl Instrum Meth B* **1991**, *58*, (1), 85-97.

6 Summary, General Discussion and Outlook

Iron is an essential nutrient for all forms of life. Besides representing an important element for metabolic enzymes, Fe further plays a key role in sustaining functions of environmental systems by serving as both electron acceptor and donor for numerous chemical processes or biological redox reactions for energy conservation.[1] The speciation of iron, the mineralogy of iron minerals and interactions between rice plants and the microbial community are key for the functioning of paddy fields as ecosystems and substantial for the quality of rice as a major staple food as all of these factors can determine the fate of heavy metals in contaminated paddy fields.[2] However, the iron cycle in paddy soils and interactions between iron-cycling soil bacteria, the plant physiology and physico-chemical soil parameters are scarcely documented. In particular, the role of rice plants and their influence on iron cycling by forming root iron plaque minerals, the consequences of ROL and root iron plaque on the microbial soil community and vice versa are poorly understood. To date, the exact niches for neutrophilic microaerophilic Fe(II)-oxidizing bacteria in the rice plant rhizosphere, where they find optimum growth conditions, were rather hypothesized than precisely identified.[3-5] Due to this lack of knowledge, multiple processes in paddy soils and the rice plant rhizosphere still remain invisible, thus obfuscating the clear picture of what is really happening within the iron cycle in the underground of rice paddies. With regards to the rhizosphere as potential bottle neck for contaminant translocation from field to grain, the understanding of the rhizosphere iron cycling, the role of iron plaque and iron-cycling bacteria and their impact on contaminant translocation, retention and mobility deserve increasing attention.

The motivation for this PhD project was to quantitatively visualize yet invisible processes and biological interactions between root iron plaque and iron-cycling bacteria in the rhizosphere of rice plants growing on water-logged paddy soils. By developing new experimental approaches and a method for the quantification of biological Fe(II) oxidation rates of microaerophilic Fe(II)-oxidizing bacteria, their contribution to total Fe(II) oxidation under different microoxic O_2 levels (**chapter 2**) and the impact on the oxidative side of the iron cycle could be deciphered. By identifying and quantifying geochemical parameters, such as pH and O_2, that considerably affect Fe(II) oxidation kinetics in the rice plant rhizosphere on an extremely high spatial (mm) and temporal (mins) resolution, it became possible to not only estimate the impact of rice plants on iron mineral formation in anoxic paddy soils but to extrapolate consequences for the iron biogeochemistry in the rice paddy rhizosphere during the life cycle of a rice plant (**chapter 3**) .

Additional experiments with Fe(III)-reducing bacteria and the determination of consequences for root iron plaque minerals and the fate of arsenic, as a model heavy metal in contaminated paddy fields, complemented the results and allowed estimates on a rhizosphere iron cycle that deciphered i) the role of rice plants and their extent in participating in the paddy soil iron cycling, ii) the potential contribution of microaerophilic Fe(II)-oxidizing bacteria to the overall iron (oxyhydr)oxide formation and iii) the impact of Fe(III)-reducing bacteria on the reductive side of the iron cycle by remobilizing root iron plaque by reductive dissolution or mineral transformation (**chapter 4**). Ultimately, the identification of consequences for the fate of arsenic during root iron plaque reduction and a quantification of (im)mobilization capacities of microbially reduced root iron plaque illustrate the need for further research on microbial interactions with root iron plaque to fully understand the paddy field iron cycling (**chapter 5**).

6.1 Rice plants as a precursor for the oxygenation of water-logged paddy soils and their role in the biogeochemical iron cycle.

Traditionally, rice plants are grown on water-logged paddy soils. These water-logged soil bodies are typically depleted in in O_2 due to the activity of heterotrophic bacteria that couple the degradation of organic substrates to the reduction of O_2 and reduced soil compounds that abiotically reduce O_2, such as humic substances.[6] Under these fully anoxic conditions, numerous metals which are abundant in paddy soils can persist in their reduced form – such as Fe(II).[7] With the initiation of root growth, rice plants can emit O_2 from their roots by ROL which precipitates Fe(III) (oxyhydr)oxides as iron plaque on the root surface.[8] This effect regulates the iron uptake and thus prevents an iron intoxication and was observed in a large variety of wetland plants.[9] However, rice plants not only contribute to the paddy soil iron cycle by forming root iron plaque. The release of O_2 from roots can significantly impact and trigger uncountable other biogeochemical processes in the paddy soil rhizosphere that are either directly or indirectly involved in the paddy soil iron cycle.[10-13] However, the spatio-temporal identification and the enumerative quantification of consequences for other biogeochemical processes related to the dynamic ROL during rice plant growth remained scarcely documented so far.

Prior to the transplantation of young rice plant seedlings into future rice fields, water-logged paddy soils remain fully anoxic with predominantly reducing conditions in the entire soil horizon (Figure 1). But already in the early stages of young rice plants, young roots release significant amounts of O_2 via ROL into the formerly anoxic paddy soil (**chapter 3**). In most of the plants observed in this PhD study, ROL and the formation of root iron plaque correlated positively. Within a relatively short period of time of only a few weeks, large parts of the initially

anoxic rhizosphere became locally enriched by root-excreted O_2. Besides ROL and the formation of Fe(III) (oxyhydr)oxides on the root surface of young roots, the pH of the surrounding soil was correlatively dropped with the formation of iron plaque minerals. Likely as a result of the abiotic Fe(II) oxidation by O_2, the hydration of the formed Fe(III) and the resulting formation of protons (H^+), the drop in pH can be attributed to the oxidation of ferrous iron and the formation of root iron plaque to some extent [14-16]. However, also the release of plant exudates, which was commonly observed in wetland plants can result in a decrease of soil pH.[17,18] A spatio-temporal correlation of an acidification of paddy soils and the oxidation of Fe(II), however, remained speculative so far and was hypothesized to occur homogeneously distributed along the anoxic/oxic interface of water-logged paddy soils only.[19]
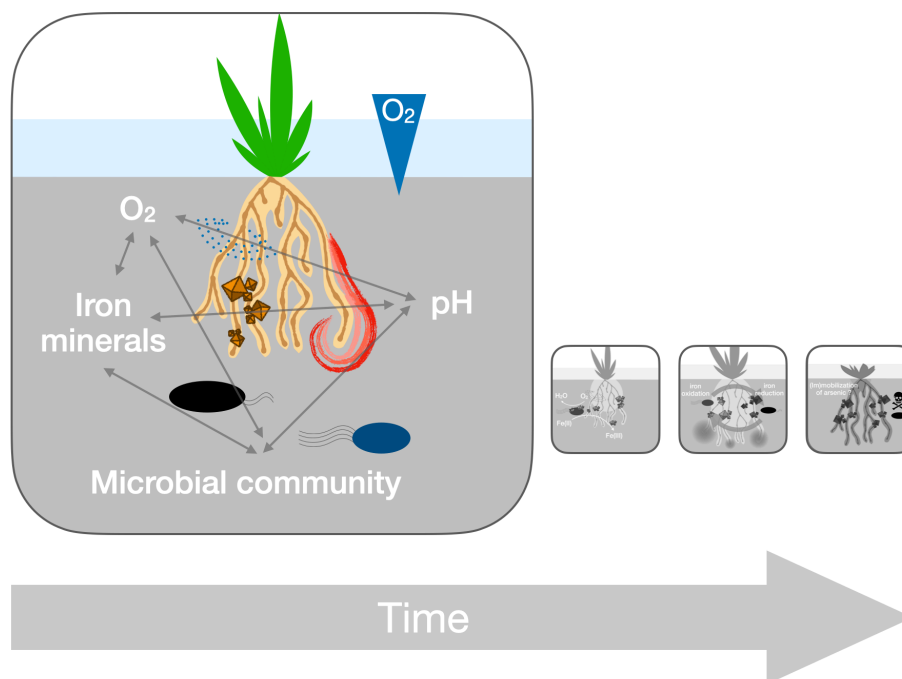
Figure 1. Interactions between rice plants and soil parameters that influence the biogeochemical iron cycle in water-logged paddy soils.

Impact of pH changes on paddy soil iron biogeochemistry. Both, O_2 and pH are very closely interlinked in determining the redox reactivity of numerous other redox active elements in paddy soils.[20-22] During plant and root growth, the local drop in pH by more than 2 units, which affected a radial area of up to 25 mm surrounding individual rice roots, can significantly enhance dissolution kinetics of mineral-bound nutrients and enhance their uptake into the plant via the root tissues (**chapter 3**). But also the speciation and the solubility of metals and metalloids were found to be severely influenced by pH changes driven by the release of plant exudates or ferrous iron oxidation.[23,24] In doing so, the redox speciation of these (heavy)

metals, their physicochemical forms and associations, e.g. sorption with soil constituents or root iron plaque, ultimately affect their toxicity and mobility.[25,26] It was found that even a small decrease in local pH conditions by units of <2 significantly increases the solubility of (heavy) metals such as Cd, Pb, Zn and As and consequently enhances their solubility in the liquid phase.[27] In doing so, their (bio)availability to be chemically or microbially reduced increases drastically which often turn these metal(oid)s from a less mobile and toxic contaminant to a highly mobile and severely toxic substance in water-logged soils.[28,29] For the most part, the acidification of the soil pH was also found to increase the uptake of these contaminants into the plant, by hampering the re-adsorption onto iron plaque oxides that formed during Fe(II) oxidation.[9,30,31] In other words, the observed decrease in local pH conditions during root iron plaque formation might diminish the sorption capacity of root iron plaque to act as a physico-chemical barrier for metal(loid)s. This can potentially enhance the translocation of contaminants from soil to rice grain exceeding the uptake loads which were so far expected, even at neutral bulk soil pH. With respect to the observations in this PhD study, the local changes in pH which were very narrowly associated with the root surface on the mm-scale during the entire growth period of the rice plants, are an absolute necessity to be considered for future studies to fully assess contaminant translocation from field to grain.

But also for the soil-borne iron redox kinetics, ambient pH conditions are one of the main parameters that ultimately determine the chemical redox reaction rates of e.g. Fe(II) with O_2. A decrease in pH from 7 to 6, for instance, decelerates the abiotic Fe(II) oxidation rates by a factor of 100 at constant O_2 conditions.[32,33] This drop in local pH conditions, in turn, can increase the persistence of Fe(II), enhance the local bioavailability for e.g. microaerophilic Fe(II)-oxidizing bacteria which were shown to find suitable conditions in the rhizosphere of a rice plant (**chapter 2**). The decrease in pH that spatiotemporally correlated to ROL might subsequently act as a feedback loop for microaerophilic Fe(II)-oxidizing bacteria increasing their capability to compete with the abiotic oxidation reactions for Fe(II).[34] On the contrary, humic substances and other soil organic matter (SOM) was demonstrated to be significantly less soluble at pH 6 compared to pH 7.[35] Consequently, not only the mobility of SOM but also the bioavailability of organic substrates to e.g. heterotrophic and Fe(III)-reducing might drastically vanish by the root- and ROL-induced acidification of the soil matrix narrowly surrounding the rice roots. The excretion of O_2 from active roots, the ferrous iron oxidation and the resulting acidification of the soil pH in the immediate vicinity of rice roots might therefore initiate a self-sustaining process for ferric root iron plaque minerals by suppressing heterotrophic bacteria that can indirectly reduce Fe(III) by using humic substances as a reducing shuttle[36] or by inhibiting Fe(III) bacteria that directly reduce Fe(III) minerals[37,38]

Impact of ROL on soil iron biogeochemistry. Not only in this context, but also for a large number of other biogeochemical redox processes, involved in the rhizosphere iron cycle, plant-induced ROL is the most relevant source of O_2 in water logged-paddy soils.[1] In this role, rice roots can act as a "lung" for numerous aerobic iron-cycling rhizosphere processes that can laterally expand throughout the soil horizon spatio-temporally connected to plant and root growth (**chapter 3**).

One important side reaction related to the chemical oxidation of soil-borne Fe(II) by ROL is the formation of highly reactive oxygen species (ROS). Physiologically, rice plants have the capability to internally produce ROS that act as a scavenger for bacterial pathogens or are an enzymatic product of stress reactions.[39-41] However, these ROS can also abiotically build up in zones with high Fe(II) oxidation rates and start a cascade of other geochemical reactions which has tremendous implications on other biogeochemical processes such as manganese reduction or damage to the plant tissue.[42] Findings from this PhD study now allow, for the first time, to spatio-temporally identify zones with high Fe(II) oxidation rates in which the production of ROS might potentially occur.[43] Such observations were so far only demonstrated for the rhizosphere of salt marsh system.[44] Further testing is required, however, to evidently prove the formation of ROS in the rice plant rhizosphere fueled by opposing gradients of ROL and Fe(II).

Moreover, the dynamic oxygenation of the paddy soil rhizosphere impacts also variable microbial processes directly and indirectly involved in the paddy soil iron cycle. Generally, it was observed that the microbial community and metabolic pathways in the rhizosphere of wetland plants significantly differ from bulk soil.[45] In this context, it has often been speculated that the capability of wetland plants to excrete O_2 by ROL might suppress obligate anaerobic bacteria while favoring aerobic metabolisms.[1] Indeed, obligate anaerobic microorganisms, such as methanogens or nitrate-reducing bacteria were demonstrated to be negatively affected in their metabolic activity by the presence of even small concentrations of O_2.[1,46,47] Considering the large number of O_2 that was found to accumulate in the rhizosphere during plant growth, it seems undoubtable that ROL has the potential to directly inhibit the activity and colonization of obligate anaerobic methanogenic and nitrate-reducing microorganisms in the direct surrounding of rice roots. In doing so, root ROL has the potential both to indirectly suppress the formation of CH_4 in the rhizosphere and to enhance the availability of O_2 as potential electron acceptor for other bacteria.[48,49] Methanotrophic bacteria, for instance, could couple the reduction of root-released O_2 to the oxidation of CH_4.[50] Ideally, ROL and the indirect microbial process might then even more contribute to a decomposition one of the most abundant greenhouse gases emitted from paddy fields.[47,49]

On the contrary, the application of nitrate fertilizers is a standard procedure in rice cultivation which increases levels of nitrate in the soil. Amended nitrate can then serve as electron acceptor for anaerobic nitrate-dependent Fe(II)-oxidizing bacteria, a further microbial pathway within the paddy soil iron cycle.[51] Moreover, under constantly anoxic conditions, nitrate can be fully decomposed to N_2 by denitrification and degas into the atmosphere.[52] However, it has been shown that the presence of O_2 can interrupt the complete microbial denitrification.[53,54] This often results in the formation of intermediate product species, such as nitrous oxide (N_2O), an additional highly effective greenhouse gas emitted from paddy fields.[55] Rice roots, acting as a conductor for O_2 into the otherwise anoxic paddy soil, in this case, would directly have the potential to enhance N_2O formation.

In this context, it is noteworthy to mention that both, methanotrophic and nitrate reducing bacteria, can closely interact with the root iron plaque minerals. In particular during the intermittent absence of root-excreted O_2, nitrite that forms as intermediate product during microbial (de)nitrification, can act as an oxidant for Fe(II) which allows nitrate-reducing bacteria to indirectly contribute to Fe(II) oxidation.[56] On the other hand, a process has recently been proposed that microbial CH_4 oxidation can be linked to the reduction of Fe(III) minerals.[57] With respect to geochemical conditions in paddy soils, typically rich in nitrate and CH_4, it is very likely that these processes closely interact with the iron cycle within the rice root rhizosphere ultimately governed by highly dynamic ROL from rice roots.[1]

Although numerous studies increased the knowledge in understanding the role of rice plants and root-related ROL in interacting with microbial metabolisms in the rhizosphere iron cycle, intensive research needs to be performed to fully decipher individual key members and processes that are affected by the roots of rice plants acting as "lung" for paddy fields to see the full picture of all processes involved on the oxidative side of the iron cycle. In particular, when water-logged paddy soils are temporarily drained and redox-conditions turn from fully reduced to fully oxidized, the increasing redox potential and the availability of O_2 have dramatic consequences for the redox zonation around rice roots and the (im)mobility of numerous soil constituents which should be considered for future studies as well.

Impact of root iron plaque on paddy soil iron biogeochemistry. Rice plants not only fuel the oxidative side of the rhizosphere iron cycle. In particular, towards the end of a rice plant life cycle, when ROL diminishes and a significant amount of root iron plaque minerals were formed, the presence of ferric iron (oxyhydr)oxides and the excretion of organic root exudates (such as carbohydrates and amino acids) strongly drive the establishment of a redox gradient by fueling heterotrophic metabolisms or the Fe(III)-reducing microbial community. The observed heterogeneity in iron plaque formation and root biomass within the rhizosphere thus

establishes geochemical variations on a very small scale (μm). Besides ammonia-oxidizing or methane-oxidizing (aerobic methane oxidation) bacteria, also a large number of sulfate- and Fe(III)-reducing bacteria[1] were demonstrated to find suitable conditions in the rhizosphere of rice plants when ROL is minimum but root iron plaque minerals present (**chapter 3**). The substantial formation of ROL-induced root iron plaque within only 45 days (**chapter 4**) provides sufficient ferric metabolic substrate to serve as potential electron acceptor for e.g. dissimilatory Fe(III)-reducing bacteria such as *Geobacter sulfurreducens.*[58] However, besides dissimilatory Fe(III)-reducing bacteria, numerous other species had been described to indirectly reduce Fe(III) minerals. Examples include bacteria that couple the oxidation of organic substrates or H_2 to the reduction of humic substances.[36] Reduced humic substances, in turn, have the capability to chemically reduce Fe(III) allowing a large variety of bacteria to indirectly participate in Fe(III) reduction.[59]

Despite the capability of rice roots to directly exert strong control over geochemical redox conditions in the rhizosphere, also geochemical properties of the iron plaque itself can determine the biogeochemical interactions with Fe(III) reducing bacteria. Within the framework of this PhD study, it could be shown for the first time, that *time* can significantly impact the crystallinity of root iron plaque minerals. While poorly-crystalline ferrihydrite was the predominant iron mineral phase on pristine young roots, more crystalline phases clearly indicate mineral ripening with time during rice plant growth. It has been shown that the crystallinity of Fe minerals determines the rate and extent of microbial Fe(III) reduction.[60,61] By providing more low-crystalline iron mineral phases at young roots, microbially-catalyzed Fe(III) reduction is presumably enhanced compared to older root sections.

This observed positive correlation of root iron plaque crystallinity with root age (**chapter 3**) suggests that time and iron mineral transformation by Ostwald ripening[62] are additional dominant variables that exert control over the availability of iron plaque to serve as metabolic ferric substrate for Fe(III)-reducing bacteria which had been overlooked so far. In particular with regards to the reductive side of the rhizosphere iron cycle, the influence of time on the bioavailability of root iron plaque minerals needs to be considered for future research studies.

6.2   Role of microaerophilic Fe(II)-oxidizing bacteria in rice paddies.

Microaerophilic Fe(II)-oxidizing bacteria represent an additional group of Fe(II)-oxidizing bacteria that were found in a large variety of environments where Fe(II) is abundant and O_2 at microoxic concentrations. Examples include environmental settings, such as sediments or hydrothermal vents, with opposing gradients of Fe(II) and O_2.[5,63,64] One of the first

microaerophilic Fe(II)-oxidizing strains was isolated with a novel technique resembling these opposing gradients found in nature[65] – commonly called gradient tube (Figure 2).

A few studies suggested that wetlands, such as water-logged paddy soils, should theoretically represent optimum habitats for microaerophilic Fe(II)-oxidizing bacteria, due to low concentrations of O_2 and the oversupply of soil-borne Fe(II).[33,66] However, even less studies reported that this type of bacteria is evidently associated with ferric precipitates on the roots of wetland plants.[67,68] Moreover, reports on microaerophilic Fe(II)-oxidation rates in paddy soils are evidently hard to find.

Generally, gradient tubes are an excellent tool for successfully isolating microaerophilic Fe(II)-oxidizing bacteria from various environments.[65,69-71] Using this culturing technique, with Fe(II) supply from the bottom and O_2 from the top space, microaerophilic Fe(II)-oxidizers grow and inhabit the niche within the opposing gradients of Fe(II) and O_2, where they find sufficient Fe(II) and where O_2 concentrations are low enough to retard the abiotic Fe(II) oxidation.[72] In this niche, they form rather indicative growth bands (Figure 2), which proves that their enzymatic biological Fe(II) oxidation can compete for Fe(II) with the otherwise rapid abiotic oxidation of Fe(II) at circumneutral pH and ambient O_2 concentrations.[73]

Figure 2. Enrichment of microaerophilic Fe(II)-oxidizing bacteria associated with a root of a rice plant in a gradient tube. A root of a rice plant was inoculated in a gradient tube with opposing gradients of Fe(II) from the iron sulfide (FeS) bottom layer and O_2 from the headspace. Orange bands (grey triangles) forming along this gradients likely represent microaerophilic Fe(II)-oxidizing bacteria growing in the niche with individual optimum concentrations for O_2 and Fe(II). Each band likely represents an individual species of microaerophilic Fe(II)-oxidizer.

However, an easy quantification of microaerophilic Fe(II) oxidation rates using gradient tubes remained rather challenging, due to abiotic Fe(II) oxidation kinetics concurrently proceeding with the biological oxidation. Moreover, the pseudo-first order surface-catalyzed heterogeneous Fe(II) oxidation kinetics complicated the deciphering of the homogeneous and heterogeneous oxidation from microbial Fe(II) oxidation.[32,74] So far, only a few studies reported general estimates on microaerophilic Fe(II) oxidation rates[69,70,75,76] – none of them estimating precise oxidation rates on microaerophilic Fe(II)-oxidizers in paddy fields.

By isolating microaerophilic Fe(II)-oxidizing bacteria from a paddy soil in gradient tubes and by implementing a novel technique that mimics the exact geochemical conditions of pH, O_2 and Fe(II) which were found at the position of the growth band within the gradient tube, allowed the precise quantification of microaerophilic Fe(II) oxidation rates (**chapter 2**). Moreover, the simplification of the geochemical boundary conditions by acid-washing the inoculum prior to inoculation reduced the presence of initial Fe(III) (bio)minerals, and potential surface sites for the heterogeneous Fe(II) oxidation[74], and allowed the quantification of the homogeneous Fe(II) oxidation, the heterogeneous oxidation rate that depends on the presence of iron minerals and the distinction from biological Fe(II) oxidation.

The observation that microaerophilic Fe(II)-oxidizing bacteria isolated from the rhizosphere of a paddy soil can substantially contribute to the overall oxidation of Fe(II) by up to 40% (**chapter 2**) suggests that these bacteria might be regarded as one of the microbial key members in the rhizosphere iron cycle (Figure 3).[45,77] However, their contribution was found to be largely limited to a narrow range of O_2 levels from 5-30 µM, that can ultimately determine the extent of these microaerophiles in participating in total Fe(II) oxidation. In this context, it was Neubauer et al. who reported that microaerophilic Fe(II)-oxidizing bacteria are able to contribute total Fe(II) oxidation rates. In fact, they demonstrated that microaerophilic Fe(II) oxidation was able to enhance the formation of root iron plaque on the roots of wetland plants.[77] In all these, they suspected that ROL from roots could serve as a source of O_2 at micromolar concentrations in a system oversupplied with Fe(II) which favors the activity of microaerophilic Fe(II) oxidation.
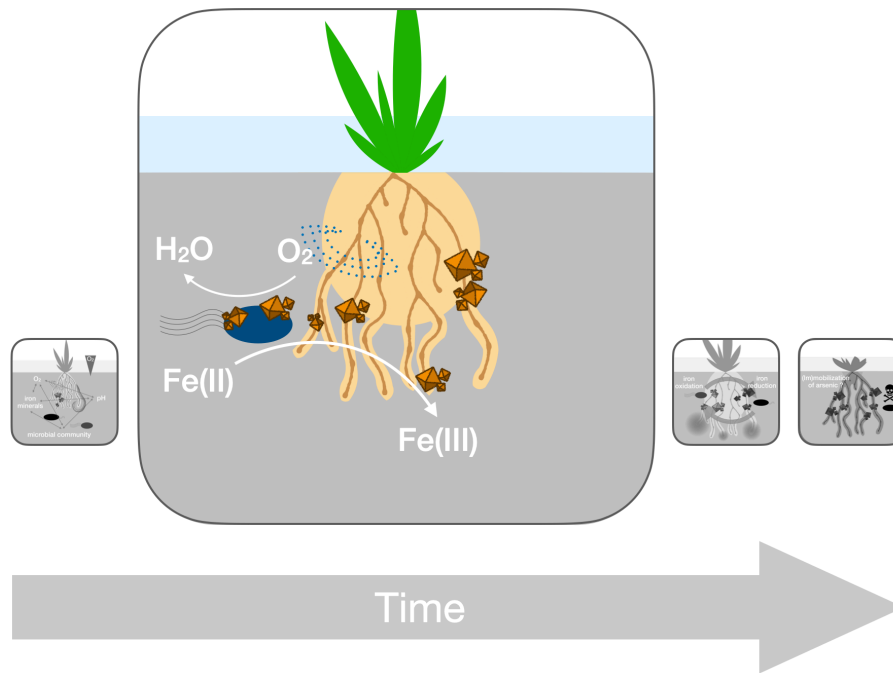
Figure 3. The rhizosphere of rice plants serves as habitat for microaerophilic Fe(II)-oxidizing bacteria which can contribute to the oxidation of soil-borne Fe(II).

More surprising yet was that the rhizosphere of a rice plant indeed provides ideal geochemical conditions for microaerophilic Fe(II)-oxidizing bacteria. Observations from **chapter 3** clearly indicate for the first time, that root-related ROL from rice plant roots can establish a narrow zone with opposing gradients of ROL-related O_2 and soil-borne Fe(II) – ideal conditions for microaerophilic Fe(II)-oxidizers. The high spatiotemporal resolution mapping of geochemical parameters, such as O_2 and Fe(II), revealed that suitable conditions for microaerophilic Fe(II) oxidation were found to be widely spread throughout the entire rhizosphere than being limited to the root surface. In contrast to rather stationary geochemical gradients, such as in sediments,[78,79] biofilms[80] or water columns,[81] the relative expansion of suitable zones for microaerophilic Fe(II)-oxidizers was found to increase with rice plant growth. Consequently, the impact of microaerophilic Fe(II)-oxidizing bacteria on total Fe(II) oxidation can increase considerably with root and rice plant growth. This suggests an increasing importance of microaerophilic Fe(II) oxidation in the rhizosphere correlating positively to plant age with ROL as the initiator enabling the metabolic activity of microaerophilic Fe(II)-oxidizing bacteria in an otherwise anoxic paddy soil.

Moreover, the demonstrated tight interconnection of root-related ROL and the expansion of niches suitable for microaerophilic Fe(II)-oxidizing bacteria during plant growth explain reports from Weiss et al. (2003), who reported a higher abundance of microaerophilic Fe(II)-oxidizers that correlated positively to the presence of wetland plant roots.[45] Taking together

microaerophilic Fe(II) oxidation rates for representatives isolated from a paddy soil rhizosphere (**chapter 2**) while considering the expansion of suitable niches for these bacteria in the rhizosphere of a rice plant (**chapter 3**) and reported numbers for microaerophilic Fe(II)-oxidizers, their direct impact on the total iron budget in water-logged paddy soils was estimated to reach up to 0.3% (**chapter 4**). In fact, 0.3% appears to be only a low impact on the total paddy soil iron cycle. However, this value represents a rather conservative estimate, since reported cell numbers were likely underestimated.[45] Nonetheless, these findings demonstrate that root growth and ROL from rice plants can directly and positively influence rather specialized species of Fe(II)-oxidizing bacteria.

The enhanced activity of microaerophilic Fe(II)-oxidizing bacteria, in turn, can indirectly influence a large variety of microbial community members typically interacting with O_2 and soil organic substrates. The dominant microaerophilic activity in the vicinity of the rice roots has the potential to limit the availability of root-excreted O_2 by coupling it to the enzymatic Fe(II) oxidation.[69] This sequestration can limit the diffusion of O_2 from ROL and diminishes fluxes of O_2 into the anoxic rhizosphere.[73] This microaerophilically-induced O_2 limitation might also influence numerous heterotrophic soil bacteria that couple the oxidation of their metabolic substrates to the reduction of O_2.[47,78,82] Thus, microaerophilic Fe(II)-oxidizing bacteria potentially share the microoxic niche around rice roots with heterotrophic bacteria in competition for O_2. On the contrary, obligate anaerobic Fe(III)-reducing bacteria, such as *Geobacter* spp., that are highly abundant and active in paddy soils[83,84] might significantly benefit from the sequestration of ROL by microaerophilic Fe(II)-oxidizing (and heterotrophic) bacteria and the narrowing of the oxygenated zone around roots.

In particular the formation of low-crystalline biominerals (e.g. ferrihydrite) as a product of microaerophilic Fe(II) oxidation (**chapter 2**) and plant exudates as metabolic substrates for *Geobacter* spp. could then enhance the activity and abundance of otherwise strictly anaerobic Fe(III)-reducing bacteria.[61] In addition to that, Sobolev and Roden (2001) and Roden et al. (2004) have both demonstrated that biologically formed Fe(III) (oxyhydr)oxides in wetland sediments may be directly recycled by Fe(III)-reducing bacteria living in close proximity to Fe(II)-oxidizing bacteria. [85,86] This suggests that microaerophilic Fe(II)-oxidizers can not only enhance soil Fe(II) oxidation by utilizing O_2 from ROL to a larger extent than previously expected but indirectly enhance microbial Fe(III) reduction by providing freshly-formed iron biominerals as ideal ferric metabolic substrate for the Fe(III)-reducing community in the rhizosphere of rice plants.[60] Finding from Weiss et al., (2004) support exactly this hypothesis demonstrating significant evidence that a large number of Fe(III)-reducing bacteria is rather associated with the rhizosphere of wetlands than abundant within the bulk soil.[87] This

suggests that the formation of a microoxic niches and the activity of microaerophilic Fe(II)-oxidizers around rice roots can indirectly impact the activity and abundance of other soil microorganisms which can lead to a zonation of microbial activity within this dynamic micro niche around rice roots. Hence, the formation of microbial hot-spots in the rhizosphere iron cycle in paddy soils is strongly controlled by the growth, activity and ROL of rice plants.

6.3 Hot spots in the biogeochemical iron cycling in the paddy field rhizosphere.

The rice paddy rhizosphere represents a complex interplay of numerous biogeochemical reactions narrowly interacting with each other governed by the overarching trinity of the plant, the microbial community and soil parameters. The key members in the microbial paddy soil iron cycle can not only use Fe(III) from root iron plaque as ferric metabolic substrate but also metabolize ferrous iron and ROL-derived O_2 via Fe(II) oxidation (**chapter 3, 4 & 5**). Weiss et al.,[45] already suggested a dynamic iron cycling in the entire rhizosphere of wetlands involving a broad community of iron-cycling bacteria. However, only the highly-resolved spatio-dynamic localization and quantification of geochemical gradients allowed now for the first time, the identification of geochemical hotspots (Figure 4) that fluctuate in local redox conditions following extremely dynamic patterns (**chapter 4**). These dynamic changes in local redox conditions ultimately dictate which microbial community members might favor from local redox conditions and who is better turning into a temporary dormant state.[88]
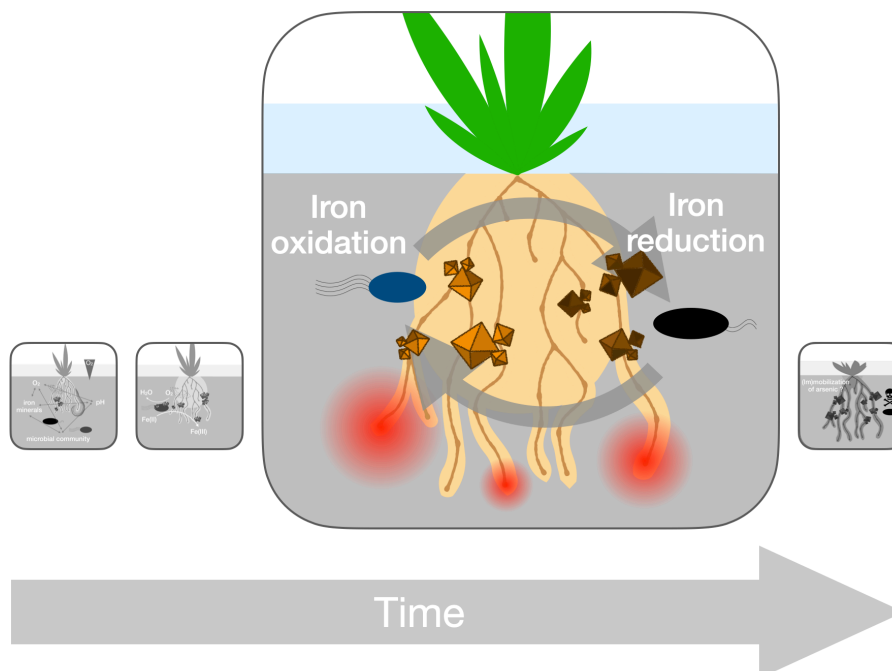
Figure 4. Biogeochemical hot spots at the root tips of rice roots suggest a closely interlinked cycling of microaerophilic Fe(II) oxidation and microbial Fe(III) reduction in water-logged paddy soils.

Classically, the gradual availability of O_2 results in the formation of zoned patterns in most environmental systems, in which distinct microbially or chemically mediated iron redox reactions are dominating, governed by the respective Gibb's free energy that thermodynamically constraints certain microbial niches.[89] In a highly dynamic and heterogeneous redox environment such as a paddy soil rhizosphere, these distinct biological and chemical iron redox-cycling reactions are no longer distributed in space but more often in time, controlled by the respective local redox conditions.[90] One of these stationary but highly redox dynamic geochemical hot spots is located at the root tips of rice plants (**chapter 4**). Correlating to the illumination of the plants, root tips excreted significantly more O_2 by ROL compared to cycles in the dark. Local O_2 concentrations followed this diurnal pattern and fluctuated by more than 150% from 0-70 µM O_2. Such rapid changes in local redox conditions were typically found in the subsurface of freshwater and marine sediments.[78,79] There, changes in sun availability ultimately triggers the photosynthetic activity of oxygenic phototrophs at the sediment surface, thus producing O_2 which shifts the local negative redox potential towards positive.[91] These light-driven dependencies were suggested to spatio-dynamically control the niche formation of the Fe(II)-oxidizing community members in the sediment column and to shift the distribution of microbial habitats along a vertical redox gradient.[88]

With regards to observations in this study, it is proposed that a similar mechanism exists in the paddy field at the geochemical hot spot of a rice root tip. Light-driven ROL provides sufficient O_2 for microaerophilic Fe(II)-oxidizing bacteria to conserve metabolic energy by coupling the reduction of O_2 to the oxidation of soil-borne Fe(II) (**chapter 2**). Assuming an average reported cell number for microaerophilic Fe(II)-oxidizing bacteria in 1 cm^3 water-saturated wetland soil of 4.21×10^5 cells cm^{-3} soil,[45] the averaged calculated biotic Fe(II) oxidation rate per cell of around 3.5×10^{-16} moles cell^{-1} hour^{-1} and an abiotic Fe(II) oxidation rate of 5.1×10^{-10} moles cm^{-3} hour^{-1} (at an O_2 concentration of 20 µM, 500 µM initial Fe(II) and a dominant heterogeneous Fe(II) oxidation of 75% relative contribution as boundary conditions (**chapter 2**)),[69,73] the total Fe(II) oxidation rate within 1 cm^3 of paddy soil surrounding the root apex, can be estimated to 6.5×10^{-10} moles Fe(II) cm^{-3} hour^{-1} (0.65 nanomoles Fe(II) cm^{-3} hour^{-1}). Within 12 hours of illumination, a total of approx. 7.8 nanomoles Fe(II) can be oxidized by microaerophilic Fe(II)-oxidizing bacteria to Fe(III) within one cm^3 around the root tip, not considering the paddy soil density.

Obligate anaerobic Fe(III)-reducing bacteria, such as the activity of most *Geobacter* spp. remain inhibited during that time, due to the presence of O_2 in the root tip area.[92] With the initiation of dark cycles, local O_2 concentrations decline to a minimum due to microbial and chemical processes that consume O_2, providing optimum conditions for Fe(III)-

reducing bacteria to conserve metabolic energy by oxidizing cell-derived polysaccharides, plant exudates (fatty acids) and other organic substrates coupled to the reduction of mainly easily accessible freshly-formed, low crystalline iron (bio)minerals (Figure 5). For *Geobacter sulfurreducens*, one typical representative of dissimilatory Fe(III)-reducing bacteria found in paddy fields, a maximum Fe(III) reduction rate of up to 2.25×10^{-13} moles cell^{-1} day^{-1} has been reported[93] which translates to 9.0×10^{-15} moles Fe(III) that can be reduced per cell within one hour. Considering averaged reported cell numbers of approx. 8.9×10^5 cells cm^{-3} soil^{-1} for *Geobacteraceae* capable of Fe(III) reduction,[94] a total microbial Fe(III) reduction rate, which can be attributed to the activity of *Geobacter* spp., was estimated to reduce a maximum of 8.01×10^{-9} moles Fe(III) cm^{-3} hour^{-1} (8.01 nanomoles Fe(II) cm^{-3} hour^{-1}). Within a dark cycle of 12 hours, no O_2 present at the root apex and no substrate limitation for *Geobacter* spp. cells, the microbial Fe(III) reduction would then be capable of reducing more than 95 nanomoles Fe(III) cm^{-3} water-logged paddy soil.

Under these conceptualized conditions, microbial Fe(III) reduction would have the potential to reduce 12-times more Fe(III) than being produced by microaerophilic Fe(II)-oxidizing bacteria or mediated by ROL during light cycles. Consequently, all of the iron plaque (bio)minerals could undergo microbial reduction in this scenario. In doing so, dissolved Fe(II) and secondary-formed minerals as end products of microbial Fe(III) reduction, would then provide the ferrous metabolic substrate for the microaerophilic oxidative side of the iron cycle leading to a day/night driven Fe recycling at the tips of rice roos in anoxic paddy soils (Figure 5)[86] This proposed closely-interlinked and rapid cycling of reduced and oxidized Fe not only demonstrates the importance of temporally highly-resolved measurement techniques but illustrates the formation of extremely dynamic microniches at the tips of rice roots that ultimately can determine the activity of dominant key players in the rhizosphere iron cycle. Given the large number of individual roots per rice plant estimated to reach more than 100 towards the end of a rice plant life cycle,[95] the formation of a biogeochemical hot spot that is capable of impacting the iron cycle at each root apex shows that the importance of rice root tips, as drivers for highly dynamic and changing redox conditions in their close vicinity, was not sufficiently considered so far. Now, that root tips are identified as a highly-dynamic redox microenvironment, more research is necessary to fully understand their role in functioning as a light-driven precursor for the oxygenation of an otherwise anoxic rhizosphere, which ultimately can control microbial activity and the behavior of numerous other soil constituents.
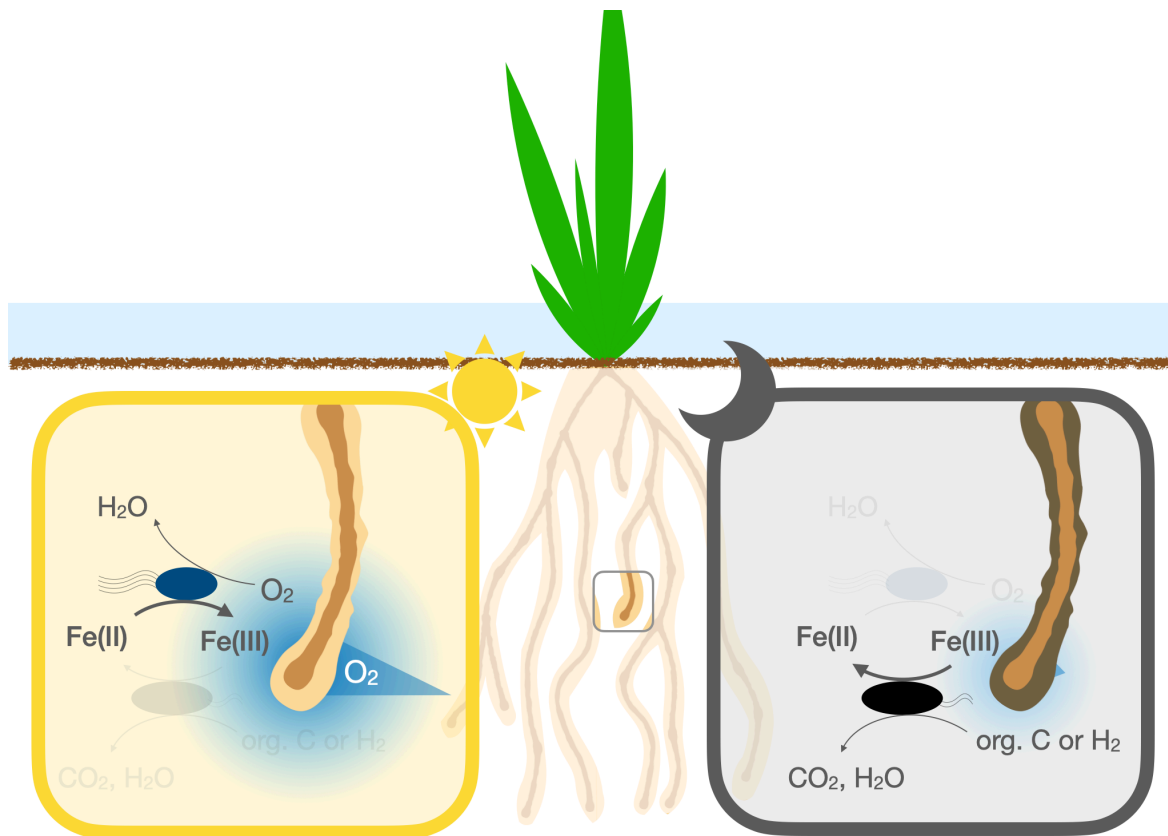
Figure 5. Root tips as light-driven biogeochemical hot spot in the paddy soil iron cycling. During light-illuminated cycles (left), radial oxygen loss (ROL) from root tips radially increases local O_2 concentrations creating ideal niches for microaerophilic Fe(II)-oxidizing bacteria (blue) that couple the oxidation of soil-borne Fe(II) to the reduction of O_2 from ROL. During night cycles, ROL diminishes and local O_2 concentrations decrease to almost 0 µM. Obligate anaerobic Fe(III)-reducing bacteria (black) find suitable conditions and couple the oxidation of H_2, plant- or cell biomass-derived organic substrates to the reduction of low crystalline iron (bio)minerals, fueling the pool of reduced Fe(II).

6.4 Impact of microbial root iron plaque reduction and consequences for the fate of As.

Much is known about the role of iron plaque on the roots of rice plants and their functioning as adsorbent for contaminant immobilization in paddy fields. Current knowledge benefited from numerous studies focusing on the investigation of complexation or adsorption processes of contaminants on these iron minerals.[9,31,96] The fate of metals and metalloids in aqueous systems and sorption behavior is well understood for a large number of heavy metals, such as cadmium (Cd)[97], zink (Zn)[98], lead (Pb)[99] and arsenic (As)[100]. Especially the immobilization of As on iron (oxyhydr)oxide minerals is well investigated and it is now commonly accepted that root iron plaque minerals represent a good adsorbent for negatively charged and more toxic As(V) species in contaminated rice paddies.[13,101] This role makes iron

plaque acting as a net sink for As and as a physico-chemical barrier for As preventing the translocation from soil to grain.

However, with the beginning of the flowering stage, ROL diminishes and fades completely towards the end of rice plant life-cycle.[12] In water-logged paddy soils, the loss in vertical O_2 transport by ROL typically leads to anoxic conditions and to a re-establishment of anoxic conditions in the rhizosphere.[102,103] In the absence of O_2 around plant roots, reductive dissolution of iron minerals during microbial Fe(III) reduction plays a dominant role in the iron cycle of water-logged paddy soils.[87,104] Belatedly, the remobilization of As from As-loaded root iron plaque was shifted into focus with the ultimate goal to investigate the role of As-loaded iron plaque minerals as a source of As.[105-107] The adsorption of As onto secondary iron minerals, formed during microbial Fe(III) reduction, however, was considered only by a minority of studies.[28,108-110] Scarcely documented so far remained the fate of As in the presence of microbially-reduced root iron plaque minerals and the extent of As in negatively affecting microbial Fe(III) mineral reduction (Figure 6).[111]
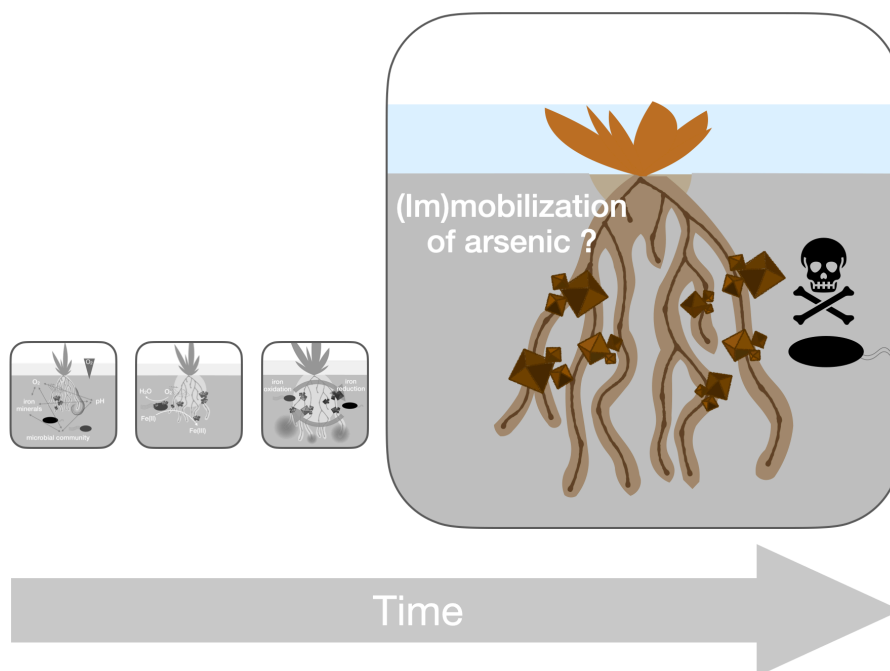
Figure 6. Microbial root iron plaque reduction can turn iron plaque minerals from a sink of arsenic(V) into a temporary source of arsenic(III), while As loads negatively affect microbial Fe(III) reduction

In this context, experiments in this PhD study found that microbially reduced root iron plaque minerals are capable to immobilize twice as much As compared to fully oxidized root iron plaque (**chapter 5**). Likely, the enhanced immobilization capacities are a result of changes in mineral surface properties e.g. surface charge, surface site densities and adsorption affinity going along with mineral transformations during microbial reduction.[112,113]

Similar observations have been made by Muehe et al. (2013) who found significantly more As(V) immobilized on secondary minerals formed during microbial reduction of iron (bio)minerals.[28] Moreover, they observed significant changes in the As speciation during the adsorption reactions which was also observed during the immobilization of As onto reduced root iron plaque minerals observed in this PhD study. Also in here, a surprisingly high fraction of more than 20% remaining As in solution was present in its reduced form as As(III). Apparently, this observation very likely represents the result of abiotic redox reactions at the mineral surface, since any cell activity was inhibited. Similar observations have been made during the adsorption of other contaminants on reduced iron minerals.[112,114,115] suggested to be the consequence of mineral surface-bound Fe(II) that initiated electron transfer from mineral to metal ligands. A similar effect is conceivable on the surface of microbially reduced root iron plaque loaded with electrons.

Moreover, As-bearing root iron plaque was found to decelerate microbial Fe(III) reduction by more than 50% at high As levels, suggesting a toxic effect of As at high concentrations.[111] However, the reduced microbial Fe(III) reduction in the presence of high As concentrations is contradictory to other findings[116] showing enhanced microbial Fe(III) reduction in the presence of As. This was explained by the fact, that present As ions hampered the formation of higher crystalline Fe minerals, thus leaving less crystalline and more bioavailable Fe(III) (oxyhydr)oxides for microbial Fe(III) reduction, and by the development of a suggested resistance towards As in the strain they used.

A breakthrough in understanding the role of microbial Fe(III) reduction of As-loaded root iron plaque was the observation that the mobility of As can be divided into two phases. Within phase 1, during microbial Fe(III) reduction and the reductive dissolution of As-bearing root iron plaque, aqueous As(V) concentrations increased rapidly remobilizing significant amounts of As into solution. Within phase 2, during the formation of secondary formed iron minerals, a significant number of As was re-immobilized by sorption onto secondarily-formed root iron plaque minerals and total As concentrations in solution declined again. Since most of the remaining As in solution was present as As(III), with a significantly lower affinity to adsorb onto iron minerals compared to As(V),[27,113] it can be concluded that the microbial reduction of As-loaded root iron plaque leads to a preferential remobilization of As(III) into solution but increases net adsorption capacities for As(V), acting as a net selective sink for oxidized As species in paddy soils.

With regards to the environment of water-logged paddy soils, the functioning of microbially reduced root iron plaque as a net sink for As needs to be considered as a sequence of different biogeochemical processes, that is, microbial Fe(III) reduction, root Fe(III) mineral dissolution, secondary iron plaque mineral formation, As(V) adsorption, As(V)

reduction and As(III) remobilization into solution. In an alternative scenario with As(V) initially associated with root iron plaque, As(V) is remobilized during microbial iron plaque reduction, As(V) partially reduced on the reactive Fe(II)/Fe(III) surface of newly formed secondary minerals, but only As(V) can selectively be immobilized again onto newly formed secondary root iron plaque minerals while As(III) remains in solution. This clearly demonstrates that Fe(III)-reducing bacteria are not only involved to a large extent in the rhizosphere iron cycling in water-logged paddy fields but that they can be key members in altering the geochemical properties of root iron plaque minerals which in turn affects the fate of contaminants such as As in rice paddies.

More importantly, these dynamic processes observed in this PhD project, evidently show that direct or indirect microbial root iron plaque reduction needs to be considered to impact the fate of a large variety of other soil contaminants such as Cd, Zn and Pb occasionally present in paddy soils. Apparently, the capability of root iron plaque to selectively immobilize oxidized species of As turns secondary-formed root iron plaque minerals into a net sink for As in contaminated paddy soils. The functioning to act as an abiotic reductant for As(III) formation, the more mobile and toxic As species, however, clearly indicates the potential hidden threat to act as a selective source for more harmful As species.

In particular towards the end of the growing season, when ROL diminishes and more reducing conditions re-establish within the rice paddy rhizosphere, the attentive monitoring of microbial interactions with root iron plaque can help to decide whether to use root plaque as a tool for bioremediation or to turn it into a source of toxic arsenic (Figure 6). Hence, future research not only has to expand the understanding in the rhizosphere trinity of rice plant, bacteria and soil parameters but is in charge of visualizing the full picture of all rhizosphere processes that can affect the fate of contaminants in one of the most precious environments for food stock production – paddy soils.

6.5 Motivational outlook for future experiments.

With regards to the motivation of this PhD study to visualize so far invisible biogeochemical processes that interact with root iron plaque in the rice plant rhizosphere, a quite large number of new findings could be uncovered. Besides the development of a new approach to quantify Fe(II) turnover rates of microaerophilic Fe(II)-oxidizing bacteria, a concept for the characterization of ROL-induced iron mineral formation, the consequences for paddy soil biogeochemistry, and the contribution of typical representatives of iron-cycling bacteria to the paddy soil iron cycling could be derived. For that, the high spatiotemporally resolution of measurements was key to identify these processes in the highly dynamic rhizosphere system. Ultimately, new insights into the effect of arsenic, as a model contaminant in paddy soils, on

the microbial reduction of root iron plaque and vice versa could be gained. Nevertheless, these findings, by far, do not represent the end of the line. Despite the foregoing findings, I hypothesize that a large variety of yet invisible processes wait to be uncovered.

First, the large microbial community of microaerophilic Fe(II)-oxidizing bacteria differs significantly in their physiological needs and requirements to conserve energy at their metabolic optimum. One possible aspect for future studies might be the natural abundance of multiple strains of microaerophilic Fe(II)-oxidizing bacteria and the characterization of their optimum niche conditions. Knowing about their preferences for environmental conditions would allow predictions when and where individual representatives of microaerophilic Fe(II)-oxidizing bacteria might be abundant and active. The incubation conditions using the newly-developed incubation method (**chapter 2**) could be adapted to more complex environmental systems, such as including complexed forms of Fe(II), associated with humic substances or natural organic matter. Moreover, the motivation for future studies could be the simulation of the hypothesized narrowly interlinked rhizosphere iron cycle around the root tips. In a co-culture of a microaerophilic Fe(II)-oxidizing culture and an obligate anaerobic Fe(III)-reducing strain, Fe(III)-reducing bacteria will be inhibited by adjusting microoxic conditions through O_2 injection. Microoxic geochemical conditions then favor the activity of microaerophilic Fe(II)-oxidizing bacteria and catalyze the enzymatic and chemical Fe(II) oxidation. Oxygen will be sequestered during Fe(II) oxidation which ultimately leads to anoxic conditions, thus favoring microbial Fe(III) reduction again that can utilize highly bioavailable low crystalline Fe(III) (bio)minerals as ferric metabolic substrate. Such investigations can help to decipher the role of and the competition between microbial Fe(III) reduction and microaerophilic Fe(II) oxidation in the rhizosphere iron cycling under dynamically-varying geochemical conditions.

Secondly, the visualized strong control that rice plants exert over biogeochemical conditions in paddy soils should be further investigated. With respect to the enormous complexity of paddy soils, the simplified rhizotrons filled a with nutrient-amended growth gel, could be adapted to more environmental conditions. The introduction of calcareous mineral particles in the soil matrix, for instance, would naturally buffer strong declines in the local pH as it was observed in this PhD study (**chapter 3**). Additionally, the amendment of organic matter would serve as a natural O_2 sequester via heterotrophic microbial activity, potentially limit the O_2 concentrations and expansion of wide redox gradients around the individual roots. Theoretically, this would narrow the habitable niche for microaerophilic Fe(II)-oxidizing bacteria, which in turn could shift the prevalent contribution of the biological Fe(II) oxidation in the microoxic rhizosphere and visualize a more close-to-nature view on biogeochemical processes which would help to estimate the relevance of microaerophilic Fe(II) oxidation in the rhizosphere. In this context, the developed methodological approach could also serve as

a non-invasive instrument to follow microbial Fe(III) reduction over the vegetative development of a rice plant and quantitatively identify a correlation of ROL and the effect on the in/activity of Fe(III)-reducing bacteria. Quantitative estimates on the extent of microbial Fe(III) reduction in participating in the iron plaque dissolution and Fe(II) remobilization from iron plaque could then help to optimize the timing for harvesting and drainage practices by periodically oxidizing the rhizosphere to suppress microbial Fe(III) reduction and the remobilization of contaminants.

Third, the remaining roots (and microbially reduced) root iron plaque could be used as tool for remediating contaminated fields. It was shown that microbially-reduced root iron plaque minerals can serve as efficient adsorbent for e.g. As(V) species (**chapter 5**). After harvesting rice grains and surface biomass, iron-mineral coated roots could deliberately be exposed to water-logging conditions again creating a (microbially) reducing environment. Under these conditions, it could be investigated whether microbial Fe(III) reduction efficiently transforms root iron plaque minerals to secondary minerals which can subsequently be serve as adsorbent for numerous (heavy) metals. By identifying the exact timing of highest contaminant immobilization rates on secondary formed root iron plaque minerals, the removal of heavy metal-bearing roots from contaminated paddy soils could be used as sustainable bioremediation technique to successively free paddy soils from major pollutants.

Chapter 6

References

1. Liesack, W.; Schnell, S.; Revsbech, N. P., Microbiology of flooded rice paddies. *Fems Microbiol Rev* **2000,** *24*, (5), 625-645.

2. Garnier, J.; Garnier, J. M.; Vieira, C. L.; Akerman, A.; Chmeleff, J.; Ruiz, R. I.; Poitrasson, F., Iron isotope fingerprints of redox and biogeochemical cycling in the soil-water-rice plant system of a paddy field. *Sci Total Environ* **2017,** *574*, 1622-1632.

3. Achtnich, C.; Bak, F.; Conrad, R., Competition for Electron-Donors among Nitrate Reducers, Ferric Iron Reducers, Sulfate Reducers, and Methanogens in Anoxic Paddy Soil. *Biol Fert Soils* **1995,** *19*, (1), 65-72.

4. Kusel, K.; Chabbi, A.; Trinkwalter, T., Microbial processes associated with roots of bulbous rush coated with iron plaques. *Microbial Ecol* **2003,** *46*, (3), 302-311.

5. Vollrath, S.; Behrends, T.; Van Cappellen, P., Oxygen Dependency of Neutrophilic Fe(II) Oxidation by Leptothrix Differs from Abiotic Reaction. *Geomicrobiol J* **2012,** *29*, (6), 550-560.

6. Lynch, J. M.; Whipps, J. M., Substrate Flow in the Rhizosphere. *Plant Soil* **1990,** *129*, (1), 1-10.

7. Gotoh, S.; Patrick, W. H., Transformation of Iron in a Waterlogged Soil as Influenced by Redox Potential and Ph. *Soil Sci Soc Am J* **1974,** *38*, (1), 66-71.

8. Armstrong, W., Radial Oxygen Losses from Intact Rice Roots as Affected by Distance from Apex, Respiration and Waterlogging. *Physiol Plantarum* **1971,** *25*, (2), 192-+.

9. Yamaguchi, N.; Ohkura, T.; Takahashi, Y.; Maejima, Y.; Arao, T., Arsenic Distribution and Speciation near Rice Roots Influenced by Iron Plaques and Redox Conditions of the Soil Matrix. *Environ Sci Technol* **2014,** *48*, (3), 1549-1556.

10. Colmer, T. D.; Cox, M. C. H.; Voesenek, L. A. C. J., Root aeration in rice (Oryza sativa): evaluation of oxygen, carbon dioxide, and ethylene as possible regulators of root acclimatizations. *New Phytol* **2006,** *170*, (4), 767-777.

11. Manzur, M. E.; Grimoldi, A. A.; Insausti, P.; Striker, G. G., Radial oxygen loss and physical barriers in relation to root tissue age in species with different types of aerenchyma. *Funct Plant Biol* **2015,** *42*, (1), 9-17.

12. Wang, X.; Yao, H. X.; Wong, M. H.; Ye, Z. H., Dynamic changes in radial oxygen loss and iron plaque formation and their effects on Cd and As accumulation in rice (Oryza sativa L.). *Environ Geochem Hlth* **2013,** *35*, (6), 779-788.

13. Liu, W. J.; Zhu, Y. G.; Hu, Y.; Williams, P. N.; Gault, A. G.; Meharg, A. A.; Charnock, J. M.; Smith, F. A., Arsenic sequestration in iron plaque, its accumulation and speciation in mature rice plants (Oryza sativa L.). *Environ Sci Technol* **2006,** *40*, (18), 5730-5736.

14. Taylor, G. J.; Crowder, A. A.; Rodden, R., Formation and Morphology of an Iron Plaque on the Roots of Typha-Latifolia L Grown in Solution Culture. *Am J Bot* **1984,** *71*, (5), 666-675.

15. Cornell, R. M.; Schwertmann, U., *The iron oxides: structure, properties, reactions, occurrences and uses*. John Wiley & Sons: 2003.

16. Mendelssohn, I. A.; Kleiss, B. A.; Wakeley, J. S., Factors Controlling the Formation of Oxidized Root Channels - a Review. *Wetlands* **1995,** *15*, (1), 37-46.

17. Begg, C. B. M.; Kirk, G. J. D.; Mackenzie, A. F.; Neue, H. U., Root-Induced Iron Oxidation and Ph Changes in the Lowland Rice Rhizosphere. *New Phytol* **1994,** *128*, (3), 469-477.

18. Hinsinger, P.; Plassard, C.; Tang, C. X.; Jaillard, B., Origins of root-mediated pH changes in the rhizosphere and their responses to environmental constraints: A review. *Plant Soil* **2003,** *248*, (1-2), 43-59.

19. Yu, H. Y.; Li, F. B.; Liu, C. S.; Huang, W.; Liu, T. X.; Yu, W. M., Iron Redox Cycling Coupled to Transformation and Immobilization of Heavy Metals: Implications for Paddy Rice Safety in the Red Soil of South China. *Advances in Agronomy, Vol 137* **2016,** *137*, 279-317.

20. Kirk, G. J. D.; Bajita, J. B., Root-Induced Iron Oxidation, Ph Changes and Zinc Solubilization in the Rhizosphere of Lowland Rice. *New Phytol* **1995,** *131*, (1), 129-137.

21. Harter, R. D., Effect of Soil-Ph on Adsorption of Lead, Copper, Zinc, and Nickel. *Soil Sci Soc Am J* **1983,** *47*, (1), 47-51.

22. Zhang, C. H.; Ge, Y.; Yao, H.; Chen, X.; Hu, M. K., Iron oxidation-reduction and its impacts on cadmium bioavailability in paddy soils: a review. *Front Env Sci Eng* **2012,** *6*, (4), 509-517.

23. Charlatchka, R.; Cambier, P., Influence of reducing conditions on solubility of trace metals in contaminated soils. *Water Air Soil Poll* **2000,** *118*, (1-2), 143-167.

24. Marin, A. R.; Masscheleyn, P. H.; Patrick, W. H., Soil Redox-Ph Stability of Arsenic Species and Its Influence on Arsenic Uptake by Rice. *Plant Soil* **1993,** *152*, (2), 245-253.

25. Ouimet, R.; Moore, J. D.; Duchesne, L., Effects of experimental acidification and alkalinization on soil and growth and health of Acer saccharum Marsh. *Journal of Plant Nutrition and Soil Science* **2008,** *171*, (6), 858-871.

26. Vanbreemen, N.; Mulder, J.; Driscoll, C. T., Acidification and Alkalinization of Soils. *Plant Soil* **1983,** *75*, (3), 283-308.

27. Borch, T.; Kretzschmar, R.; Kappler, A.; Van Cappellen, P.; Ginder-Vogel, M.; Voegelin, A.; Campbell, K., Biogeochemical Redox Processes and their Impact on Contaminant Dynamics. *Environ Sci Technol* **2010,** *44*, (1), 15-23.

28. Muehe, E. M.; Scheer, L.; Daus, B.; Kappler, A., Fate of Arsenic during Microbial Reduction of Biogenic versus Abiogenic As-Fe(III)-Mineral Coprecipitates. *Environ Sci Technol* **2013,** *47*, (15), 8297-8307.

29. Colombo, C.; Palumbo, G.; He, J. Z.; Pinton, R.; Cesco, S., Review on iron availability in soil: interaction of Fe minerals, plants, and microbes. *J Soil Sediment* **2014,** *14*, (3), 538-548.

30. Zhang, X. K.; Zhang, F. S.; Mao, D. R., Effect of iron plaque outside roots on nutrient uptake by rice (Oryza sativa L.). Zinc uptake by Fe-deficient rice. *Plant Soil* **1998,** *202*, (1), 33-39.

31. Garnier, J. M.; Travassac, F.; Lenoble, V.; Rose, J.; Zheng, Y.; Hossain, M. S.; Chowdhury, S. H.; Biswas, A. K.; Ahmed, K. M.; Cheng, Z.; van Geen, A., Temporal variations in arsenic uptake by rice plants in Bangladesh: The role of iron plaque in paddy fields irrigated with groundwater. *Sci Total Environ* **2010,** *408*, (19), 4185-4193.

32. Sung, W.; Morgan, J. J., Kinetics and Product of Ferrous Iron Oxygenation in Aqueous Systems. *Environ Sci Technol* **1980,** *14*, (5), 561-568.

33. Neubauer, S. C.; Emerson, D.; Megonigal, J. P., Life at the energetic edge: Kinetics of circumneutral iron oxidation by lithotrophic iron-oxidizing bacteria isolated from the wetland-plant rhizosphere. *Appl Environ Microb* **2002,** *68*, (8), 3988-3995.

34. Ehrenfeld, J. G.; Ravit, B.; Elgersma, K., Feedback in the plant-soil system. *Annu Rev Env Resour* **2005,** *30*, 75-115.

35. Curtin, D.; Peterson, M. E.; Anderson, C. R., pH-dependence of organic matter solubility: Base type effects on dissolved organic C, N, P, and S in soils with contrasting mineralogy. *Geoderma* **2016,** *271*, 161-172.

36. Lovley, D. R.; Fraga, J. L.; Blunt-Harris, E. L.; Hayes, L. A.; Phillips, E. J. P.; Coates, J. D., Humic substances as a mediator for microbially catalyzed metal reduction. *Acta Hydrochimica Et Hydrobiologica* **1998,** *26*, (3), 152-157.

37. Roden, E. E.; Urrutia, M. M.; Mann, C. J., Bacterial reductive dissolution of crystalline Fe(III) oxide in continuous-flow column reactors. *Appl Environ Microb* **2000,** *66*, (3), 1062-1065.

38. King, G. M.; Garey, M. A., Ferric Iron Reduction by Bacteria Associated with the Roots of Freshwater and Marine Macrophytes. *Appl Environ Microb* **1999,** *65*, (10), 4393.

39. Liu, X. M.; Williams, C. E.; Nemacheck, J. A.; Wang, H.; Subramanyam, S.; Zheng, C.; Chen, M. S., Reactive Oxygen Species Are Involved in Plant Defense against a Gall Midge. *Plant Physiol* **2010,** *152*, (2), 985-999.

40. Vaidyanathan, H.; Sivakumar, P.; Chakrabarty, R.; Thomas, G., Scavenging of reactive oxygen species in NaCl-stressed rice (Oryza sativa L.) - differential response in salt-tolerant and sensitive varieties. *Plant Sci* **2003,** *165*, (6), 1411-1418.

41. Tsukagoshi, H., Control of root growth and development by reactive oxygen species. *Curr Opin Plant Biol* **2016,** *29*, 57-63.

42. Cakmak, I., Tansley review No. 111 - Possible roles of zinc in protecting plant cells from damage by reactive oxygen species. *New Phytol* **2000,** *146*, (2), 185-205.

43. Lueder, U.; Jorgensen, B. B.; Kappler, A.; Schmidt, C., Fe(III) Photoreduction Producing Fe-aq(2+) in Oxic Freshwater Sediment. *Environ Sci Technol* **2020,** *54*, (2), 862-869.

44. Dias, D. M. C.; Copeland, J. M.; Milliken, C. L.; Shi, X. M.; Ferry, J. L.; Shaw, T. J., Production of Reactive Oxygen Species in the Rhizosphere of a Spartina-Dominated Salt Marsh Systems. *Aquat Geochem* **2016,** *22*, (5-6), 573-591.

45. Weiss, J. V.; Emerson, D.; Backer, S. M.; Megonigal, J. P., Enumeration of Fe(II)-oxidizing and Fe(III)-reducing bacteria in the root zone of wetland plants: Implications for a rhizosphere iron cycle. *Biogeochemistry* **2003,** *64*, (1), 77-96.

46. Fetzer, S.; Bak, F.; Conrad, R., Sensitivity of Methanogenic Bacteria from Paddy Soil to Oxygen and Desiccation. *Fems Microbiol Ecol* **1993,** *12*, (2), 107-115.

47. van Bodegom, P.; Stams, F.; Mollema, L.; Boeke, S.; Leffelaar, P., Methane oxidation and the competition for oxygen in the rice rhizosphere. *Appl Environ Microb* **2001,** *67*, (8), 3586-3597.

48. Roden, E. E.; Wetzel, R. G., Organic carbon oxidation and suppression of methane production by microbial Fe(III) oxide reduction in vegetated and unvegetated freshwater wetland sediments. *Limnol Oceanogr* **1996,** *41*, (8), 1733-1748.

49. Conrad, R., Microbial ecology of methanogens and methanotrophs. *Advances in Agronomy, Vol 96* **2007,** *96*, 1-63.

50. Zheng, Y.; Zhang, L. M.; Zheng, Y. M.; Di, H. J.; He, J. Z., Abundance and community composition of methanotrophs in a Chinese paddy soil under long-term fertilization practices. *J Soil Sediment* **2008,** *8*, (6), 406-414.

51. Ratering, S.; Schnell, S., Nitrate-dependent iron(II) oxidation in paddy soil. *Environ Microbiol* **2001,** *3*, (2), 100-109.

52. Yoshida, M.; Ishii, S.; Fujii, D.; Otsuka, S.; Senoo, K., Identification of Active Denitrifiers in Rice Paddy Soil by DNA- and RNA-Based Analyses. *Microbes Environ* **2012,** *27*, (4), 456-461.

53. Veraart, A. J.; de Klein, J. J. M.; Scheffer, M., Warming Can Boost Denitrification Disproportionately Due to Altered Oxygen Dynamics. *Plos One* **2011,** *6*, (3).

54. Oh, J.; Silverstein, J., Acetate limitation and nitrite accumulation during denitrification. *J Environ Eng-Asce* **1999,** *125*, (3), 234-242.

55. Islam, S. M. M.; Gaihre, Y. K.; Biswas, J. C.; Singh, U.; Ahmed, M. N.; Sanabria, J.; Saleque, M. A., Nitrous oxide and nitric oxide emissions from lowland rice cultivation with urea deep placement and alternate wetting and drying irrigation. *Sci Rep-Uk* **2018,** *8*.

56. Klueglein, N.; Zeitvogel, F.; Stierhof, Y. D.; Floetenmeyer, M.; Konhauser, K. O.; Kappler, A.; Obst, M., Potential Role of Nitrite for Abiotic Fe(II) Oxidation and Cell Encrustation during Nitrate Reduction by Denitrifying Bacteria. *Appl Environ Microb* **2014,** *80*, (3), 1051-1061.

57. Cai, C.; Leu, A. O.; Xie, G. J.; Guo, J. H.; Feng, Y. X.; Zhao, J. X.; Tyson, G. W.; Yuan, Z. G.; Hu, S. H., A methanotrophic archaeon couples anaerobic oxidation of methane to Fe(III) reduction. *Isme J* **2018,** *12*, (8), 1929-1939.

58. Methe, B. A.; Nelson, K. E.; Eisen, J. A.; Paulsen, I. T.; Nelson, W.; Heidelberg, J. F.; Wu, D.; Wu, M.; Ward, N.; Beanan, M. J.; Dodson, R. J.; Madupu, R.; Brinkac, L. M.; Daugherty, S. C.; DeBoy, R. T.; Durkin, A. S.; Gwinn, M.; Kolonay, J. F.; Sullivan, S. A.; Haft, D. H.; Selengut, J.; Davidsen, T. M.; Zafar, N.; White, O.; Tran, B.; Romero, C.; Forberger, H. A.; Weidman, J.; Khouri, H.; Feldblyum, T. V.; Utterback, T. R.; Van Aken,

S. E.; Lovley, D. R.; Fraser, C. M., Genome of Geobacter sulfurreducens: Metal reduction in subsurface environments. *Science* **2003,** *302*, (5652), 1967-1969.

59. Kappler, A.; Benz, M.; Schink, B.; Brune, A., Electron shuttling via humic acids in microbial iron(III) reduction in a freshwater sediment. *Fems Microbiol Ecol* **2004,** *47*, (1), 85-92.

60. Hansel, C. M.; Benner, S. G.; Nico, P.; Fendorf, S., Structural constraints of ferric (hydr)oxides on dissimilatory iron reduction and the fate of Fe(II). *Geochim Cosmochim Ac* **2004,** *68*, (15), 3217-3229.

61. Cutting, R. S.; Coker, V. S.; Fellowes, J. W.; Lloyd, J. R.; Vaughan, D. J., Mineralogical and morphological constraints on the reduction of Fe(III) minerals by Geobacter sulfurreducens. *Geochim Cosmochim Ac* **2009,** *73*, (14), 4004-4022.

62. Voorhees, P. W., The Theory of Ostwald Ripening. *J Stat Phys* **1985,** *38*, (1-2), 231-252.

63. Chan, C. S.; Fakra, S. C.; Emerson, D.; Fleming, E. J.; Edwards, K. J., Lithotrophic iron-oxidizing bacteria produce organic stalks to control mineral growth: implications for biosignature formation. *Isme J* **2011,** *5*, (4), 717-727.

64. Emerson, D.; Moyer, C. L., Neutrophilic Fe-Oxidizing bacteria are abundant at the Loihi Seamount hydrothermal vents and play a major role in Fe oxide deposition. *Appl Environ Microb* **2002,** *68*, (6), 3085-3093.

65. Emerson, D.; Moyer, C., Isolation and characterization of novel iron-oxidizing bacteria that grow at circumneutral pH. *Appl Environ Microb* **1997,** *63*, (12), 4784-4792.

66. MacDonald, D. J.; Findlay, A. J.; McAllister, S. M.; Barnett, J. M.; Hredzak-Showalter, P.; Krepski, S. T.; Cone, S. G.; Scott, J.; Bennett, S. K.; Chan, C. S.; Emerson, D.; Luther, G. W., Using in situ voltammetry as a tool to identify and characterize habitats of iron-oxidizing bacteria: from fresh water wetlands to hydrothermal vent sites. *Environ Sci-Proc Imp* **2014,** *16*, (9), 2117-2126.

67. Emerson, D.; Weiss, J. V.; Megonigal, J. P., Iron-oxidizing bacteria are associated with ferric hydroxide precipitates (Fe-plaque) on the roots of wetland plants. *Appl Environ Microb* **1999,** *65*, (6), 2758-2761.

68. Weiss, J. V.; Rentz, J. A.; Plaia, T.; Neubauer, S. C.; Merrill-Floyd, M.; Lilburn, T.; Bradburne, C.; Megonigal, J. P.; Emerson, D., Characterization of neutrophilic Fe(II)-oxidizing bacteria isolated from the rhizosphere of wetland plants and description of Ferritrophicum radicicola gen. nov sp nov., and Sideroxydans paludicola sp nov. *Geomicrobiol J* **2007,** *24*, (7-8), 559-570.

69. Druschel, G. K.; Emerson, D.; Sutka, R.; Suchecki, P.; Luther, G. W., Low-oxygen and chemical kinetic constraints on the geochemical niche of neutrophilic iron(II) oxidizing microorganisms. *Geochim Cosmochim Ac* **2008,** *72*, (14), 3358-3370.

70. Hädrich, A.; Taillefert, M.; Akob, D. M.; Cooper, R. E.; Litzba, U.; Wagner, F. E.; Nietzsche, S.; Ciobota, V.; Rösch, P.; Popp, J.; Küsel, K., Microbial Fe(II) oxidation by Sideroxydans lithotrophicus ES-1 in the presence of Schlöppnerbrunnen fen-derived humic acids. *Fems Microbiol Ecol* **2019,** *95*, (4).

71. Li, X. M.; Mou, S.; Chen, Y. T.; Liu, T. X.; Dong, J.; Li, F. B., Microaerobic Fe(II) oxidation coupled to carbon assimilation processes driven by microbes from paddy soil. *Sci China Earth Sci* **2019,** *62*, (11), 1719-1729.

72. Stumm, W.; Lee, G. F., Oxygenation of ferrous iron. *Industrial & Engineering Chemistry* **1961,** *53*, (2), 143-146.

73. Lueder, U.; Druschel, G.; Emerson, D.; Kappler, A.; Schmidt, C., Quantitative analysis of O-2 and Fe2+ profiles in gradient tubes for cultivation of microaerophilic Iron(II)-oxidizing bacteria. *Fems Microbiol Ecol* **2018,** *94*, (2).

74. Tamura, H.; Kawamura, S.; Hagayama, M., Acceleration of the Oxidation of Fe-2+ Ions by Fe(Iii)-Oxyhydroxides. *Corrosion Science* **1980,** *20*, (8-9), 963-971.

75. Emerson, D.; Scott, J. J.; Leavitt, A.; Fleming, E.; Moyer, C., In situ estimates of iron-oxidation and accretion rates for iron-oxidizing bacterial mats at Loihi Seamount. *Deep-Sea Res Pt I* **2017,** *126*, 31-39.

76. Chan, C. S.; Emerson, D.; Luther, G. W., The role of microaerophilic Fe-oxidizing micro-organisms in producing banded iron formations. *Geobiology* **2016,** *14*, (5), 509-528.

77. Neubauer, S. C.; Toledo-Duran, G. E.; Emerson, D.; Megonigal, J. P., Returning to their roots: Iron-oxidizing bacteria enhance short-term plaque formation in the wetland-plant rhizosphere. *Geomicrobiol J* **2007,** *24*, (1), 65-73.

78. Laufer, K.; Nordhoff, M.; Roy, H.; Schmidt, C.; Behrens, S.; Jorgensen, B. B.; Kappler, A., Coexistence of Microaerophilic, Nitrate-Reducing, and Phototrophic Fe(II) Oxidizers and Fe(III) Reducers in Coastal Marine Sediment. *Appl Environ Microb* **2016,** *82*, (5), 1433-1447.

79. Melton, E. D.; Stief, P.; Behrens, S.; Kappler, A.; Schmidt, C., High spatial resolution of distribution and interconnections between Fe- and N-redox processes in profundal lake sediments. *Environ Microbiol* **2014,** *16*, (10), 3287-3303.

80. Chan, C. S.; McAllister, S. M.; Leavitt, A. H.; Glazer, B. T.; Krepski, S. T.; Emerson, D., The Architecture of Iron Microbial Mats Reflects the Adaptation of Chemolithotrophic Iron Oxidation in Freshwater and Marine Environments. *Front Microbiol* **2016,** *7*.

81. Maisch, M.; Wu, W. F.; Kappler, A.; Swanner, E. D., Laboratory Simulation of an Iron(II)-rich Precambrian Marine Upwelling System to Explore the Growth of Photosynthetic Bacteria. *Jove-J Vis Exp* **2016**, (113).

82. Frenzel, P.; Bosse, U.; Janssen, P. H., Rice roots and methanogenesis in a paddy soil: ferric iron as an alternative electron acceptor in the rooted soil. *Soil Biol Biochem* **1999,** *31*, (3), 421-430.

83. Ding, L. J.; Su, J. Q.; Xu, H. J.; Jia, Z. J.; Zhu, Y. G., Long-term nitrogen fertilization of paddy soil shifts iron-reducing microbial community revealed by RNA-C-13-acetate probing coupled with pyrosequencing. *Isme J* **2015,** *9*, (3), 721-734.

84. Hori, T.; Muller, A.; Igarashi, Y.; Conrad, R.; Friedrich, M. W., Identification of iron-reducing microorganisms in anoxic rice paddy soil by C-13-acetate probing. *Isme J* **2010,** *4*, (2), 267-278.

85. Sobolev, D.; Roden, E. E., Characterization of a neutrophilic, chemolithoautotrophic Fe(II)-oxidizing beta-proteobacterium from freshwater wetland sediments. *Geomicrobiol J* **2004,** *21*, (1), 1-10.

86. Roden, E. E.; Sobolev, D.; Glazer, B.; Luther, G. W., Potential for microscale bacterial Fe redox cycling at the aerobic-anaerobic interface. *Geomicrobiol J* **2004,** *21*, (6), 379-391.

87. Weiss, J. V.; Emerson, D.; Megonigal, J. P., Geochemical control of microbial Fe(III) reduction potential in wetlands: comparison of the rhizosphere to non-rhizosphere soil. *Fems Microbiol Ecol* **2004,** *48*, (1), 89-100.

88. Melton, E. D.; Swanner, E. D.; Behrens, S.; Schmidt, C.; Kappler, A., The interplay of microbially mediated and abiotic reactions in the biogeochemical Fe cycle. *Nat Rev Microbiol* **2014,** *12*, (12), 797-808.

89. Schmidt, C.; Behrens, S.; Kappler, A., Ecosystem functioning from a geomicrobiological perspective - a conceptual framework for biogeochemical iron cycling. *Environ Chem* **2010,** *7*, (5), 399-405.

90. Revsbech, N. P.; Pedersen, O.; Reichardt, W.; Briones, A., Microsensor analysis of oxygen and pH in the rice rhizosphere under field and laboratory conditions. *Biol Fert Soils* **1999,** *29*, (4), 379-385.

91. Melton, E. D.; Schmidt, C.; Kappler, A., Microbial iron(II) oxidation in littoral freshwater lake sediment: the potential for competition between phototrophic vs. nitrate-reducing iron(II)-oxidizers. *Front Microbiol* **2012,** *3*.

92. Straub, K. L.; Schink, B., Ferrihydrite reduction by Geobacter species is stimulated by secondary bacteria. *Arch Microbiol* **2004,** *182*, (2-3), 175-181.

93. Ishii, S.; Watanabe, K.; Yabuki, S.; Logan, B. E.; Sekiguchi, Y., Comparison of Electrode Reduction Activities of Geobacter sulfurreducens and an Enriched Consortium in an Air-Cathode Microbial Fuel Cell. *Appl Environ Microb* **2008,** *74*, (23), 7348-7355.

94. Yi, W. J.; You, J. H.; Zhu, C.; Wang, B. L.; Qu, D., Diversity, dynamic and abundance of Geobacteraceae species in paddy soil following slurry incubation. *Eur J Soil Biol* **2013,** *56*, 11-18.

95. Yoshida, S.; Bhattacharjee, D. P.; Cabuslay, G. S., Relationship between Plant Type and Root-Growth in Rice. *Soil Sci Plant Nutr* **1982,** *28*, (4), 473-482.

96. Khan, N.; Seshadri, B.; Bolan, N.; Saint, C. P.; Kirkham, M. B.; Chowdhury, S.; Yamaguchi, N.; Lee, D. Y.; Li, G.; Kunhikrishnan, A.; Qi, F.; Karunanithi, R.; Qiu, R.; Zhu, Y. G.; Syu, C. H., Root Iron Plaque on Wetland Plants as a Dynamic Pool of Nutrients and Contaminants. *Advances in Agronomy, Vol 138* **2016,** *138*, 1-96.

97. Jacob, D. L.; Yellick, A. H.; Kissoon, L. T. T.; Asgary, A.; Wijeyaratne, D. N.; Saini-Eidukat, B.; Otte, M. L., Cadmium and associated metals in soils and sediments of wetlands across the Northern Plains, USA. *Environ Pollut* **2013,** *178*, 211-219.

98. Yang, Q. W.; Lan, C. Y.; Shu, W. S., Copper and Zinc in a paddy field and their potential ecological impacts affected by wastewater from a lead/zinc mine, P. R. China. *Environ Monit Assess* **2008,** *147*, (1-3), 65-73.

99. Hamid, Y.; Tang, L.; Wang, X. Z.; Hussain, B.; Yaseen, M.; Aziz, M. Z.; Yang, X. O., Immobilization of cadmium and lead in contaminated paddy field using inorganic and organic additives. *Sci Rep-Uk* **2018,** *8*.

100. Deng, H.; Ye, Z. H.; Wong, M. H., Accumulation of lead, zinc, copper and cadmium by 12 wetland plant species thriving in metal-contaminated sites in China. *Environ Pollut* **2004,** *132*, (1), 29-40.

101. Seyfferth, A. L.; Webb, S. M.; Andrews, J. C.; Fendorf, S., Arsenic Localization, Speciation, and Co-Occurrence with Iron on Rice (Oryza sativa L.) Roots Having Variable Fe Coatings. *Environ Sci Technol* **2010,** *44*, (21), 8108-8113.

102. Flessa, H.; Fischer, W. R., Plant-Induced Changes in the Redox Potentials of Rice Rhizospheres. *Plant Soil* **1992,** *143*, (1), 55-60.

103. Schmidt, H.; Eickhorst, T.; Tippkotter, R., Monitoring of root growth and redox conditions in paddy soil rhizotrons by redox electrodes and image analysis. *Plant Soil* **2011,** *341*, (1-2), 221-232.

104. Jackel, U.; Schnell, S., Role of microbial iron reduction in paddy soil. *Non-Co2 Greenhouse Gases: Scientific Understanding, Control and Implementation* **2000**, 143-144.

105. Qiao, J. T.; Li, X. M.; Li, F. B., Roles of different active metal-reducing bacteria in arsenic release from arsenic-contaminated paddy soil amended with biochar. *J Hazard Mater* **2018,** *344*, 958-967.

106. Babechuk, M. G.; Weisener, C. G.; Fryer, B. J.; Paktunc, D.; Maunders, C., Microbial reduction of ferrous arsenate: Biogeochemical implications for arsenic mobilization. *Appl Geochem* **2009,** *24*, (12), 2332-2341.

107. Roberts, L. C.; Hug, S. J.; Voegelin, A.; Dittmar, J.; Kretzschmar, R.; Wehrli, B.; Saha, G. C.; Badruzzaman, A. B. M.; Ali, M. A., Arsenic Dynamics in Porewater of an Intermittently Irrigated Paddy Field in Bangladesh. *Environ Sci Technol* **2011,** *45*, (3), 971-976.

108. Hansel, C. M.; Benner, S. G.; Neiss, J.; Dohnalkova, A.; Kukkadapu, R. K.; Fendorf, S., Secondary mineralization pathways induced by dissimilatory iron reduction of ferrihydrite under advective flow. *Geochim Cosmochim Ac* **2003,** *67*, (16), 2977-2992.

109. Tufano, K. J.; Reyes, C.; Saltikov, C. W.; Fendorf, S., Reductive Processes Controlling Arsenic Retention: Revealing the Relative Importance of Iron and Arsenic Reduction. *Environ Sci Technol* **2008,** *42*, (22), 8283-8289.

110. Yamaguchi, N.; Nakamura, T.; Dong, D.; Takahashi, Y.; Amachi, S.; Makino, T., Arsenic release from flooded paddy soils is influenced by speciation, Eh, pH, and iron dissolution. *Chemosphere* **2011,** *83*, (7), 925-932.

111. Chow, S. S.; Taillefert, M., Effect of arsenic concentration on microbial iron reduction and arsenic speciation in an iron-rich freshwater sediment. *Geochim Cosmochim Ac* **2009,** *73*, (20), 6008-6021.

112. Amstaetter, K.; Borch, T.; Larese-Casanova, P.; Kappler, A., Redox Transformation of Arsenic by Fe(II)-Activated Goethite (alpha-FeOOH). *Environ Sci Technol* **2010,** *44*, (1), 102-108.

113. Dixit, S.; Hering, J. G., Comparison of arsenic(V) and arsenic(III) sorption onto iron oxide minerals: Implications for arsenic mobility. *Environ Sci Technol* **2003,** *37*, (18), 4182-4189.

114. Liger, E.; Charlet, L.; Van Cappellen, P., Surface catalysis of uranium(VI) reduction by iron(II). *Geochim Cosmochim Ac* **1999,** *63*, (19-20), 2939-2955.

115. Williams, A.; Scherer, M., Kinetics of Cr(VI) reduction by carbonate green rust. *Abstr Pap Am Chem S* **2001,** *222*, U433-U433.

116. Hohmann, C.; Winkler, E.; Morin, G.; Kappler, A., Anaerobic Fe(II)-Oxidizing Bacteria Show As Resistance and Immobilize As during Fe(III) Mineral Precipitation. *Environ Sci Technol* **2010,** *44*, (1), 94-101.

Statement of personal contribution

The conceptual background of this project was designed by Dr. C. Schmidt. Prof. Andreas Kappler was the main supervisor throughout the project and Dr. David Emerson was the second supervisor. Unless otherwise stated, the experiments were either conceptualized by myself or together with Dr. C. Schmidt and/or Prof. A. Kappler. All experiments were performed by myself with assistance of Dr. Ulf Lüder and assisting B.Sc. and M.Sc. students. The discussion and analysis of the obtained results, as well as the writing of all manuscripts, were completed in cooperation with Dr. C. Schmidt. Chapters 2,3 & 4 were written with additional contribution of Prof. A. Kappler and Dr. U. Lüder. Experimental analyses for chapter 5 were performed in cooperation with Dr. Carolin Kerl and Prof. Britta Planer-Friedrich. Details on the individual contribution of all people named are stated below:

Field work: In November, 2017 Dr. C. Schmidt and myself travelled to the Experimental Institute for Cereal Research – Rice Research Unit, in Vercelli, Italy. On site, Dr. Giampiero Valè coordinated our field sampling strategy and assisted with helpful discussions on sample processing and transport. Dr. C. Schmidt and myself performed the sampling of paddy soil and transported sample material back to the host laboratory in Tübingen.

Chapter 2: Dr. U. Lüder assisted with the modelling of oxidation reaction kinetics. Dr. C. Schmidt, Prof. A. Kappler, Dr. Katja Laufer and Caroline Scholze revised the manuscript.

Chapter 3: Dr. C. Schmidt helped with the experimental design and, together with Prof. A. Kappler, assisted with data analysis and revising the manuscript. Dr. U. Lüder assisted with voltammetric measurements. Lars Lüder helped with image data analysis and assisted in the development of 2 non-invasive mapping techniques. Dr. Daniela Obermaier (PreSens) assisted with technical support on non-invasive measuring techniques used to obtain results for this chapter.

Chapter 4: Dr. C. Schmidt helped with the evaluation and interpretation of the data and, together with Prof. A. Kappler, revised the manuscript. Dr. U. Lüder assisted with voltammetric measurements.

Chapter 5: Dr. C. Schmidt assisted with the experimental design. Panunporn Tutiyasarn assisted with performing the experiment and data analysis. Dr. C. Kerl and Prof. B. Planer-Friedrich helped with sample analysis and data interpretation.

I state hereby that I have not plagiarized nor copied any of the text. Chapter 2-4 have been published in scientific journals. Chapter 5 is prepared for submission to a scientific journal and might be published in a slightly modified version elsewhere in the future.

Curriculum Vitae
Markus Maisch

markus.maisch@uni-tuebingen.de

orcid.org/0000-0002-4275-4957

Center for Applied Geoscience (ZAG)

Eberhard-Karls-University Tuebingen

Sigwartstrasse 10, 72076 Tuebingen, Germany

ACADEMIC EDUCATION

Ph.D. in Umweltnaturwissenschaften, Eberhard Karls Universität Tübingen, Germany
since 04/2016

Ph.D. thesis title: *Rusty rice – Unravelling rice plant and microbial interactions in the paddy soil iron cycle*

Supervisors: Prof. Dr. Andreas Kappler, Dr. David Emerson
Workgroup Geomicrobiology, Center for Applied Geoscience, Eberhard Karls Universität Tübingen, Germany

M.Sc. in Geoecology, Eberhard Karls Universität Tübingen, Germany
2014 – 2016

Master thesis title: *Design and development of a laboratory flow-through column to simulate a Precambrian upwelling system and explore the growth of photosynthetic bacteria in an iron(II) upwelling system*

Supervisors: Prof. Dr. Elizabeth Swanner, Prof. Dr. Andreas Kappler
Workgroup Geomicrobiology, Center for Applied Geoscience, Eberhard Karls Universität Tübingen, Germany; Geochemistry & Geobiology Laboratory, Department of Geological & Atmospheric Sciences, Iowa State University, Iowa, USA

B.Sc. in Geoecology, Eberhard Karls Universität Tübingen, Germany
2010 – 2014

Bachelor thesis title: *Die Effekte von Pestiziden auf den biologischen Blattabbau in ackerbaulich geprägten Fließgewässern*

Supervisors: Dr. Polina Orlinsky, Prof. Dr. Heinz-R. Köhler
Workgroup System Ecotoxicology, Department for Bioenergy and System Ecotoxicology, Helmholtz Center for Environmental Research (UFZ) Leipzig, Germany

Professional Appointments

2014-2016 Field and Research Assistant for Dr. E.D. Swanner, Geomicrobiology, University of Tübingen / Geochemistry & Geobiology Laboratory, Department of Geological & Atmospheric Sciences, Iowa State University, Iowa, USA.

2013-2014 Field and Research Assistant for Dr. P. Orlinskiy and Prof. Dr. Matthias Liess, Department for Bioenergy and System ecotoxicology, UFZ Leipzig.

2011-2014 Research Assistant for Dr. E.D. Swanner, Geomicrobiology, University of Tübingen.

2009-2011 Research Assistant for Dr. M.C. Bilton., Vegetational Ecology, University of Tübingen.

Students Supervised

2019 Panunporn Tutiyasarn, M.Sc. student (Applied & Env. Geosciences)

2018 Barbara Kurz, B.Sc. student (Geoecology)

2017 Louis Rees, M.Sc. student (Applied & Env. Geosciences)

2017 Klaus Röhler, Scientific practice student (Applied & Env. Geosciences)

Teaching Experience

2016-2018 Geomicrobiology Lab course, University of Tübingen; Teaching basic cultivation methods and analytical skills in geomicrobiology for M.Sc. students from different fields. Leading and supervising short research projects with specific research questions in geomicrobiology.

Campus Talks

2018 Science Slam at TÜFFF (Tübinger Fenster für Forschung) – Rice plants do form rust & why that is good for us, University of Tübingen.

2017 Biogeochemical interactions in the rhizosphere of paddy soils and effects on rice plant physiology, Center for Plant Molecular Biology (ZMBP), University of Tübingen.

2016 Biogeochemical gradients in the rice plant rhizosphere and consequences for iron plaque formation, Center for Plant Molecular Biology (ZMBP), University of Tübingen.

Selected Awards

2018 PreSens, Regensburg, Germany: Winner of PreSens VisiSens TD competition.

2018 University of Tübingen, Poster award for Ph.D. thesis outline, Quenstedt Symposium.

2016 University of Tübingen, Poster award for M.Sc. thesis, Quenstedt Symposium.

Training Experience

Training in building microsensors/-electrodes for voltammetric and amperometric analyses in aquatic systems by Prof. Dr. Gregory K. Druschel, IUPUI, Indianapolis, USA

Establish and develop infrastructure for a geochemistry & geobiology Laboratory, Prof. Dr. Elizabeth Swanner, Department of Geological & Atmospheric Sciences, Iowa State University, Iowa, USA

Research Contributions

Journal Articles

2020   **Maisch, M.**, Lueder, U., Kappler, A., Schmidt, C. (2020) From plant to paddy – how rice root iron plaque can affect the paddy field iron cycling. Soil Systems 4, 28.
> *Contribution*: Experimental outline, performance of experiments, sample analysis, interpretation and discussion, writing the manuscript

2020   Lueder, U., **Maisch, M.**, Laufer, K., Jørgensen, B.B., Kappler, A., Schmidt, C. (2020) Influence of physical perturbation on Fe(II) supply in coastal marine sediments. Environmental Science and Technology 54, 3209-3218.
> *Contribution*: Discussion on experimental outline, Mössbauer spectroscopy and XRD analysis on samples, sample preparation, data interpretation and discussion for manuscript, writing parts of manuscript

2020   Yang, Z., Sun, T., Subdiga, E., Obst, M., Haderlein, S.B., **Maisch, M.**, Kretzschmar, R., Angenent, L., Kappler, A. (2020) Aggregation-dependent electron transfer via redox-active biochar particles stimulates microbial ferrihydrite reduction. Science of the Total Environment 703, 135515.
> *Contribution*: Mössbauer spectroscopy and XRD analysis on samples, sample preparation, data interpretation and discussion for manuscript, writing parts of manuscript

2019   **Maisch, M.**, Lueder, U., Kappler, A., Schmidt, C. (2019) Iron Lung – How rice roots induce iron redox changes in the rhizosphere and create niches for microaerophilic Fe(II)-oxidizing bacteria. Environmental Science & Technology Letters 6, 600-605.
> *Contribution*: Experimental outline, performance of experiments, sample analysis, interpretation and discussion, writing the manuscript

2019   **Maisch, M.**, Lueder, U., Laufer, K., Scholze, C., Kappler, A., Schmidt, C. (2019) Contribution of microaerophilic iron(II)-oxidizers to iron(III) mineral formation. Environmental Science and Technology 53, 8197-8204.
> *Contribution*: Experimental outline, performance of experiments, sample analysis, interpretation and discussion, writing the manuscript

2019   Boylan, A.A., Perez-Mon, C., Guillard, L., Burzan, N., Loreggian, L., **Maisch, M.**, Kappler, A., Byrne, J.M., Bernier-Latmani, R. (2019) H_2-fulled microbial metabolism in Opalinus Clay. Applied Clay Science 174, 69-76.
> *Contribution*: Mössbauer spectroscopy on samples, sample measurements, sample analysis, data interpretation and discussion for manuscript, writing parts of manuscript

2018 Otte, J., Blackwell, N., Soos, V., Rughoeft, S., **Maisch, M.**, Kappler, A., Kleindienst, S., Schmidt, C. (2018) Sterilization impacts on marine sediment - Are we able to inactivate microorganisms in environmental samples? FEMS Microbiology Ecology, 94, 12

> *Contribution*: Mössbauer spectroscopy on samples, sample measurements, sample analysis, data interpretation and discussion for manuscript, writing parts of manuscript

2018 Swanner, E.D. **Maisch, M.**, Wu, W., Kappler, A., (2018) Oxic Fe(III) reduction could have generated Fe(II) in the photic zone of Precambrian seawater. Scientific Reports, 8, 4238.

> *Contribution*: Development of experimental outline, performance of experiments, sample preparation, analysis and interpretation, research discussion and writing parts of manuscript

2017 Cao, M.J., Qin, K., Li, G.M., Evans, N.J., Hollings, P., **Maisch, M.**, Kappler, A. (2017) Mineralogical evidence for crystallization conditions and petrogenesis of ilmenite-serise I-type granitoids at the Baogutu reduced porphyry Cu deposit (Western Junggar, NW China): Mössbauer spectroscopy, EPM and LA-(MC)-ICPMS analyses. Ore Geology Reviews, 86, 382-403.

> *Contribution*: Mössbauer spectroscopy on samples, sample measurements, sample analysis and data interpretation for manuscript

2016 **Maisch, M.**, Wu, W., Kappler, A., Swanner, E.D. (2016) Laboratory simulation of an iron(II)-rich late Archean marine upwelling system to explore the growth of photosynthetic bacteria. Journal of Visualized Experiments, 113, e54251.

> *Contribution*: Development of the experimental outline, performance of measurements, sample analysis and interpretation, writing the manuscript and preparation for submission

Submitted

2020 Laufer, K., Michaud, A.B., **Maisch, M.**, Byrne, J.M., Kappler, A., Patterson, M.O., Røy, H., Jørgensen, B.B.. Bioavailable iron produced through benthic cycling in glaciated Arctic fjords (Svalbard). *Submitted to Nature Geoscience*

> *Contribution*: Mössbauer spectroscopy and XRD analysis on samples, sample preparation, data interpretation and discussion for manuscript, writing parts of manuscript

Selected Conference Abstracts

2019 **Maisch, M.**, Lueder, U., Kappler, A., Schmidt, C. Rice roots form microniches in paddy soils that control arsenic (im)mobilization, Goldschmidt conference, Barcelona, August 18-23.

2018   **Maisch, M.**, Muehe, M., Kappler, A., Schmidt, C. Iron plaque on rice roots – A sink or source for arsenic? Goldschmidt conference, Boston, August 12-17.

2017   **Maisch M.**, Kappler, A., Schmidt, C. In-situ mapping of biogeochemical gradients in the rhizosphere of rice plants (Oryza sp.) and consequences for iron plaque formation. Goldschmidt conference, Paris, August 13-18.

2017   Schmidt, C., **Maisch, M.**, Lueder, U., Druschel, G., Emerson, D., Kappler, A. Microaerophilic iron(II) oxidation: An experimental approach to quantify microbial iron(II) oxidation rates. Goldschmidt conference, Paris, August 13-18.

2016   **Maisch, M.**, Kappler, A., Schmidt, C., Approach to follow redox gradients and iron plaque formation in-situ over the vegetative development of a rice plant. SOMmic workshop, Helmholtz Centre for Environmental Research, UFZ Leipzig, November 9-11.

2015   **Maisch M.**, Wu, W., Kappler, A., Swanner, E. Laboratory-scale simulation of Precambrian ocean Fe(II)-rich upwelling: implications for cyanobacteria and oxygen production. GEOBio conference, Indiana University Bloomington, October 9-11.

2015   **Maisch M.**, Wu, W., Kappler, A., Swanner, E. A laboratory-scale column to investigate microbial processes in Fe(II)-rich upwelling systems. Goldschmidt conference, Prague, August 16-21.

Appendix

Cover art design for **Environmental Science & Technology Letters 2019 6 (10)**

Acknowledgements

In the first place, I would like to thank Dr. Caroline Schmidt for asking me in my early Bachelor studies to become a research assistant in the Geomicrobiology group. With that, a whole cascade of great, exciting and entertaining years in the laboratory full of knowledge and new experiences started off. She was the one who ultimately led me to the step of doing this PhD project, which I am more than thankful for. Her endless support and creativity motivated me to work on yet unsolved problems and to never stop exploring. After all these years we spent together, I know I can count on you as a friend.

Furthermore, I would like to acknowledge Prof. Andreas Kappler. Being a member in his working group for almost 10 years, I do not want to miss a single day in it. I especially am thankful for Andreas' motivational character, not only as a professor, lecturer and esteemed colleague, but as human. Uncountable are the facts that I learned from him in the field of geochemistry, paper writing and celebrating events with a good barbecue, family and friends. I am excitingly looking forward into another period working together with him during my postdoc.

My thanks also go to Dave Emerson. I was always looking up on you when it came to my favorite iron(II)-oxidizers – the microaerophiles. I will always remember when we had the scientific meeting on the corridor in Bigelow with the view right onto the seaside.

Absolutely not to be forgotten is Betsy. She was the one who started making me to an early scientist already during my Bachelors. Working together with you was encouraging me enormously in becoming an ambitious scientist, never too shy to be stopped by problems. Working with you was life-changing for two reasons: First, I will never forget my time at the Iowa State University setting up your laboratory, enjoying the field trips and making friends. Second, it was at your lab bench in Tübingen where I first met my beloved wife Sophie – you called that love bench from that day on. Thanks for everything!

One of the biggest thanks goes to a group of scientists and technicians that I do not count as colleagues but as wonderful friends. Ulf Lüder is probably the most loyal person I know. If you need to rely on someone, when things get dicey, he is there to help. It is not only his clever mind, but the huge heart he has which makes him unique. I appreciate that very much, thank you very much for your friendship. The angles in the lab, Ellen Röhm and Lars Grimm, not only deserve a thank you, but an applause. They rock the lab and create the atmosphere in which everyone feels comfortable and happy to follow their research passion. If there is an

issue, they solve it before it happens. Moreover, it was the countless discussions with Julian Sorwat that my research and scientific understanding benefitted from. With his grumpy sincerity, he always helped without asking why. Great to have you as a (lab) neighbor and friend. I am also thankful for having Elif Köksoy as lab mate. She always had the right timing for a laughter to brighten up the daily lab life. Thanks go to Monique Patzner, Manuel Schad and Franziska Schädler for being great mates to talk to and get support between lab bench and office door. It is all of you who lighten up the daily lab life by a warm coffee or cold beer after work.

There are countless other helpful people I could rely on. Dr. James Byrne introduced me into to the field of Mössbauer Spectroscopy. From the first day on, this technique fascinated me, eagerly motivated and taught me to dive into other research topics to understand complex iron mineral interactions. Thanks for that opportunity James. Dr. Marie Mühe always inspired me by interpreting results from a different perspective. Her talent in overlooking the even most complex interactions motivated me in critically reviewing my own research. Prof. Britta Planer-Friedrich and Carolin Kerl were a great help in critically discussing the research that involved arsenic. It was always great to meet you for chats on conferences, in Bayreuth or Tübingen. Everyone connected to the Geomicrobiology group, who is not specifically mentioned by name, please feel that your help is very much appreciated. I benefited tremendously from intensive discussions, presentations and quick chats in the coffee kitchen with each of you.

In particular, I want to thank my family, who always supported me and created the fundament for my career as a research scientist. Already in the early days at the university, I always could feel the substantial encouragement from my family. Especially thanks to my brother who had to do these nerdy conversations with me.

Finally, I want to thank my wife Sophie. She was the one who maintained our proper work-life balance and kept me grounded when I could not find the way out of the lab. She fully respects my fire for geomicrobiology and science in general but thankfully reminds me that there are other things in life that also deserve attention.

<center>Thank you.</center>